SYNTHESIS, REACTIVITY, AND COORDINATION CHEMISTRY RELEVANT TO THE COPOLYMERIZATION OF CO_2 AND EPOXIDES BY FIRST ROW TRANSITION METAL SCHIFF BASE COMPLEXES

A Dissertation

by

ERIC BENJAMIN FRANTZ

Submitted to the Office of Graduate Studies of
Texas A&M University
in partial fulfillment of the requirements for the degree of

DOCTOR OF PHILOSOPHY

August 2008

Major Subject: Chemistry

SYNTHESIS, REACTIVITY, AND COORDINATION CHEMISTRY RELEVANT TO THE COPOLYMERIZATION OF CO_2 AND EPOXIDES BY FIRST ROW TRANSITION METAL SCHIFF BASE COMPLEXES

A Dissertation

by

ERIC BENJAMIN FRANTZ

Submitted to the Office of Graduate Studies of
Texas A&M University
in partial fulfillment of the requirements for the degree of

DOCTOR OF PHILOSOPHY

Approved by:

Chair of Committee,	Donald J. Darensbourg
Committee Members,	Abraham Clearfield
	Edward D. Harris
	Francois P. Gabbai
Head of Department,	David H. Russell

August 2008

Major Subject: Chemistry

ABSTRACT

Synthesis, Reactivity, and Coordination Chemistry Relevant to the Copolymerization of CO_2 and Epoxides by First Row Transition Metal Schiff Base Complexes.

(August 2008)

Eric Benjamin Frantz, B.S., University of Houston

Chair of Advisory Committee: Dr. Donald J. Darensbourg

Excepting agricultural based products, which themselves require a great deal of energy to produce, our supply of natural resources such as minerals, metal ore, fresh water, coal, oil and natural gas are all limited in supply. The depletion of these substances is imminent and this knowledge weighs heavily on humankind. The utilization of CO_2 for the production of polycarbonates is one attempt at exploiting a profoundly abundant and renewable resource. The importance of research in this and similar fields justifies the detailed study of the chemicals and procedures involved with this chemistry. This current work concentrates on the fundamental study of transition metal Schiff base complexes that have shown a great deal of promise in their ability to catalyze the copolymerization of CO_2 and epoxide to form aliphatic polycarbonates.

A new chromium(III) Schiff base complex has been synthesized and evaluated for its ability to catalyze the formation of polymer. The ligand employed bears an N_2O_2 coordination sphere identical to the widely utilized chromium(III) and cobalt(III) salen catalysts. This complex was shown to be active towards the copolymerization of CO_2

and cyclohexene oxide. Although the activity was less than that seen with chromium(III) salen complex, the study demonstrates that new ligand systems are available beyond salen and deserve further attention.

A class of manganese(III) Schiff base complexes was also synthesized and evaluated as catalysts. Although crystallographic data has shown that these complexes are structural analogs to chromium(III) salens, the difference in metal center leads to a nearly complete elimination of catalytic activity. Such a marked difference has been taken advantage of by using this very low activity to study the ring-opening of epoxide in the initial step of the copolymerization both mechanistically and kinetically. It has also been utilized in an evaluation of the coordination chemistry of the polymerization process. This has led to some valuable conclusions about the nature and role of the metal center that previously have not been studied. Manganese(III) salen complexes were also synthesized and evaluated in an effort to compare these important ligands to other Schiff bases and confirm the findings mentioned above.

DEDICATION

I dedicate this dissertation to the two women who have and always will be the most important people in my life. My sister has always led the way for me, be it in art, music, education, profession or life. She has set the standard for me and at all times has never hesitated to share what she knows and to treat me as a person of value and worth, even when so few others have. My mother has always been the foundation of my life. She has taught me that the ability to think independently is the greatest and most important gift an individual has. She has also taught me that a Godly life is the only life worth living. Central to her teaching is the knowledge that our stay on earth is short and only fools spend their time like lottery winnings, easy come, easy go, and that an hour watching meaningless TV is like rebuffing God and his gift of thought and breath and love.

ACKNOWLEDGEMENTS

Since my diagnosis in the 4th grade my life has been dominated by one word; dyslexia. I have eaten, drank and slept with this malodorous word foremost in my mind for too long. It has embarrassed me a countless number of times, given me mistakes where there shouldn't have been any and made me confused and frightened where I shouldn't have been and it, most of all, has kept me away from associating with other talented and intelligent people that should have been my companions all my life. And now, as I leave graduate school some eight years older than my cohorts, roughened, aged and grizzled from my long war with this condition I can finally say, "Veni, Vidi, Vici".

In truth, I struggle on, just as I always will, and without the help and patience of some very important people I would not have been able to complete my graduate education. First and foremost, I must thank my advisor and committee chair Professor Donald J. Darensbourg. He has supported me both as a teacher and as an employer for five long years and I hope has been rewarded for the unreasonable amount of time and patience he has given me. I'd like to thank Professors Marcetta Y. Darensbourg, Abraham Clearfield, Edward D. Harris, Francois P. Gabbai, and Steven A. Miller for also being involved in my education, attending my presentations and serving on my committee. My thanks also goes to Dr. Joseph H. Reibenspies and Dr. Nattamai Bhuvanesh (Bhuv) for their enduring patience with the 13 crystal structures I present in this work and the countless ones that never quite made it out of the refinement, data collection or crystal mounting stages of fruition. And of course, my thanks must go out

to my colleague and friend Susan Winters. It would take a plate full of cookies who knows how many stories high to express my gratitude for the help she has given me on the countless number of annoying and should-be-obvious issues I have had.

Now I must embark on thanking those comrades who have stood with me side-by-side though my time here at Texas A&M. Firstly, I'd like thank those Darensbourgers who came before and mentored me, namely, Drs. Rosario Mejia-Rodriquez, Melissa L. Golden, Joey Chiang, Jesse Tye, Marilyn Rampersad, Stephen Jeffery, Jody Rodgers, Ryan Mackiewicz, Damon Billodeaux, and Andrea Phelps. I want to give special thanks to the two DJD students who later preceded me, my good friends Poulomi Ganguly and Wonsook Choi. They not only paved the way immediately in front of me, but encouraged me and instilled in me an appreciation of scientists from other nations. Next, I thank the current DJD and MYD group members Mike Singleton, Roxanne Jenkins, Elky Almaraz, William Foley, Jen Hess, Dr. Kayla Green, Dr. Christine Thomas, Tianbiao "Leo" Liu, Scott Brothers, Adriana Moncada, Osit "Pop" Karroonnirun, Ross Poland, Shawn Fitch, and Jeremy Andreatta. Particular thanks goes to Adriana, Jeremy and Shawn for listening to my ramblings about chemistry and helping me with my many presentations, papers and other materials. I honesly do proff red my writting beforhand, beleave it or knot. Also, I want to express my gratitude to Scott and Jen for joining the group, being my friends and making life as a Darensbourger a heck of a lot more fun. And lastly, I want to thank two exceptionally talented and hard working women who have aided me immensely over the time I've known them. Chris, you have helped guide me over the last two years and acted both as

a friend and deputy advisor at times. Kayla, you are a great listener, colleague and friend (and cook). Both of you will kick butt in your field and I look forward to hearing of your many successes.

TABLE OF CONTENTS

CHAPTER Page

LIST OF FIGURES

FIGURE Page

FIGURE Page

LIST OF TABLES

CHAPTER I

INTRODUCTION

Statement About Green Chemistry

Numerous sources indicate that the amount of human induced CO_2 creation has increased dramatically since the industrial age.[1] Global warming has been, in part, attributed to this increase in CO_2 (a greenhouse gas), and much debate centers around what might be done to decrease production of this industrial byproduct and remove existing quantities. The role which industry-utilized CO_2 might play in reducing these high concentrations is under debate. Of the 25.7 Gt of CO_2 produced by human activities, only 0.128 Gt is in turn consumed by industry.[2] Clearly, even a 10 fold increase in utilization would not lend appreciably to a reduction in greenhouse gas levels. For this reason, applications of CO_2 must originate from the benefits it can potentially provide as a chemical feedstock and not from attempts to curb global warming. Fortunately, CO_2 does possess useful qualities. Apart from its chemical reactivity, it is inexpensive, nontoxic, and, unlike oil, natural gas or coal, renewable.[3] The copolymerization of CO_2 and epoxides to yield useful polycarbonates (PC) is an example of a chemical process that, if brought to commercial use, could take advantage

---

This dissertation follows the format and style of *Inorganic Chemistry*.

of these desirable attributes while at the same time circumventing the use of toxic starting materials and degradation products. In this way the research of the Darensbourg group can be said to be "green" in nature, even though the eventual ends of our efforts will not likely lead to a reduction in global warming.

Commercial Utilization of Polycarbonates

In the late 50's D. W. Fox and H. Schnell independently discovered the synthesis of poly(bisphenol A carbonate) (BPA-PC) while looking for an alternative to polyethylene terephthalate (PET).[4] Since then both aliphatic and aromatic polycarbonates have gained significant usage throughout our society as a specialty engineering thermoplastic. Depending on specific composition, they have many applications, some of which are given in Table 1-1. BPA-PC is still the most widely used aromatic polycarbonate and is marketed as Makrolon® by Bayer and Lexan® by SABIC Innovative Plastics. Apart from its excellent transparency, it offers mechanical properties competitive to other engineering plastics (Table 1-2).[5] The most outstanding feature is impact strength, which, depending on the type of PC can exceed 900 J/m.

Industrial scale production of BPA-PC is accomplished through two major processes outlined in Figure 1-1.[6] The first is an interfacial reaction involving CH_2Cl_2, aqueous NaOH, bisphenol A (BPA) and phosgene gas. The caustic environment leads to formation of the disodium phenoxide salt which reacts with phosgene to form one unit of PC with a chloroformate end group. This species can react with another BPA monomer and so on. For high molecular weights tertiary amines can be added to catalyze the

Table 1-1. Properties and Applications of Polycarbonates.[4]

Area	Properties	Applications
Consumer Products	• transparent • tough • strong and stiff • dimensionally stable • easy to mold • easy to paint, decorate, or finish • flame resistance • heat resistance • sterile	• compact discs • CD-ROMs, DVDs • refrigerator crisper trays • lighting fixtures • automotive head lamps • automotive moon roofs • automotive side windows • prescription eyeglasses • safety face shields • aircraft windows • aircraft canopies • bullet-resistant glass • architectural window glazing
Medical Devices	• transparent to X-rays • light weight • high impact strength • high elongation • biocompatibility • sterile	• syringes • cardiovascular devices • catheters • solution delivery devices • surgical instruments

Table 1-2. Comparison of BPA-PC with Other Engineering Plastics.[5]

Engineering Plastic	Tensile Strength (MPa)	Flexural Modulus (MPa)	Notched Izod Impact Strength (J/m)
BPA-PC (Lexan®131)	62	2340	908
PBT (neat)	54	2250	35
PEI (Ultem®)	110	2516	57
PPE (PX0844)	50	2240	235
PPS (unfilled)	90	3500	50
Poly(amide-imide) (4303L)	192	5000	142
Poly(acetal)	72	3000	90
ABS resin	45	2550	~400

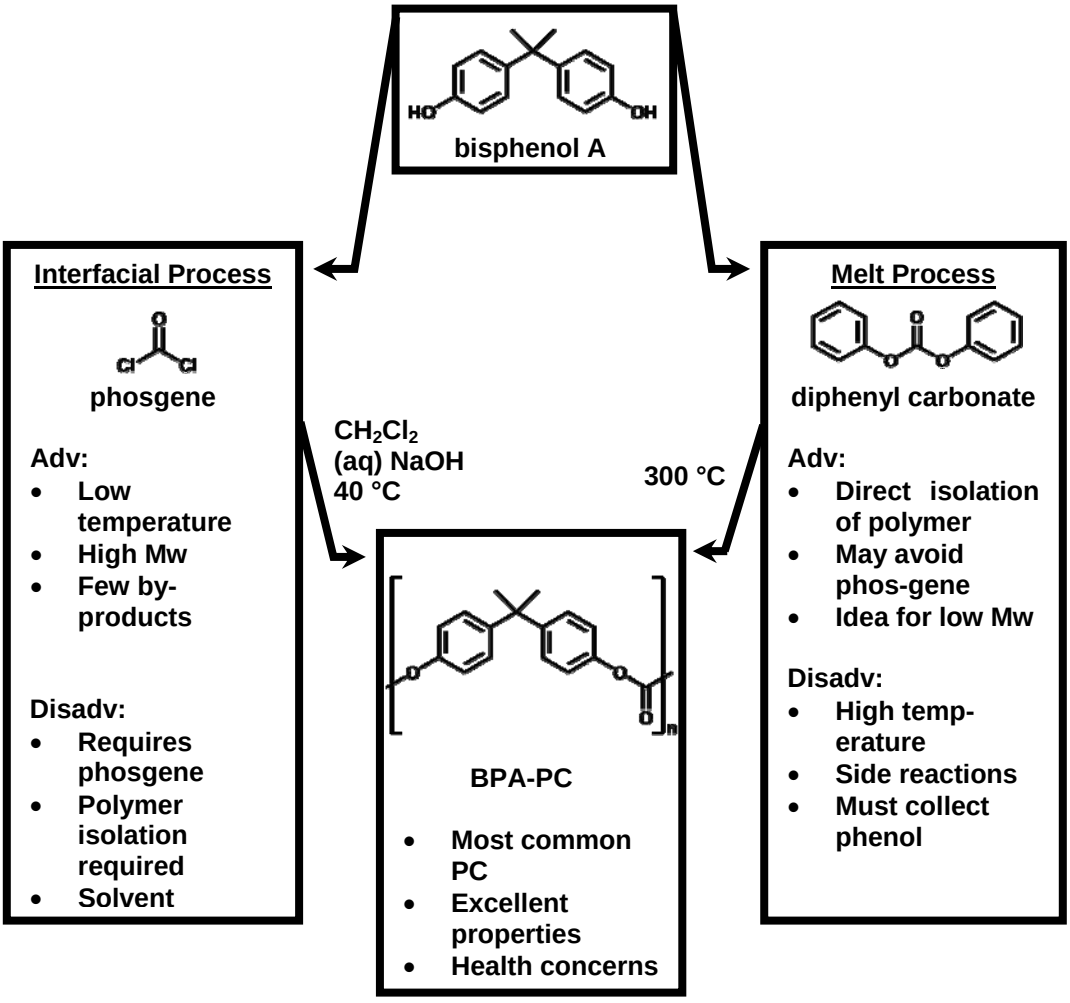

Figure 1-1. The two industrial processes for the production of BPA-PC.[6]

substitution reaction of an incoming polycarbonate chain possessing a chloroformate group.

The second process is a melt polymerization involving the transesterification of diphenyl carbonate with BPA to produce PC and phenol as a byproduct. In this process the use of solvent is avoided and low molecular weight PC is easily achieved. However,

high molecular weights are more difficult to obtain because chain propagation is dependent on the removal of phenol, a process that becomes more difficult as the polymer melt becomes more viscous. In both processes the major area of concern is the use of phosgene gas, a well known chemical weapon. Diphenyl carbonate offers an alternative, but it too is frequently synthesized from phosgene gas and phenol. In addition, the safety of BPA-PC has been under scrutiny in recent years.[7] Laboratory tests on rodents have shown that BPA, leaching from water bottles, can lead to a number of reproductive and neurological ailments at levels typical of human exposure.

The potential governmental regulation of BPA would be devastating to the plastics industry and would doubtlessly lead to stigmatization of PC in much the same way as poly(vinyl chloride) PVC. Health concerns also present significant technical challenges to polymer scientists whose job it will be to develop safe alternatives. Much of the research centered on improving the efficiency and safety of PC production has centered on elimination of phosgene gas. BPA, on the other hand, has not received the same type of attention and virtually every commercially produced PC relies upon this or derivatives thereof. These concerns clearly indicate the need for new polycarbonates that have useful properties, safe starting materials and harmless degradation products. Endeavors to obtain these new materials are currently underway.

Synthesis of Polycarbonate from CO_2 and Epoxide

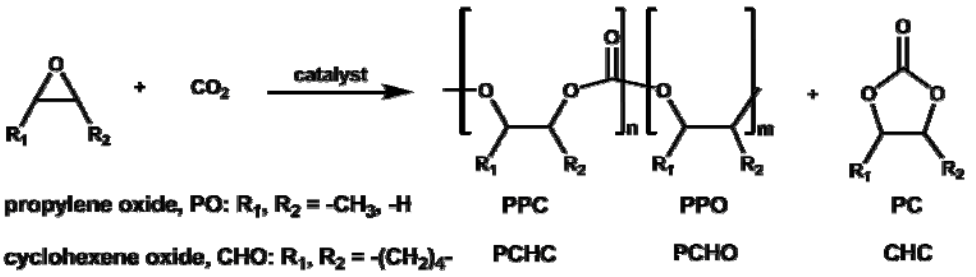

(1-1)

As already mentioned the utilization of CO_2 as a chemical feedstock would be highly desirable considering its low cost, nontoxic nature and renewability. Equation 1-1 illustrates the general reaction of CO_2 and epoxide in the presence of a catalyst to give *n* units of polycarbonate. The most commonly used monomers are cyclohexene oxide (CHO) and propylene oxide (PO), with others being employed to a much lesser extent.[8,9] Frequently accompanying the formation of polycarbonate are linkages of poly(alkyl oxide) (polyether). This is the result of consecutive insertions of epoxides during polymer change propagation. Another byproduct is the formation of five-membered cyclic carbonates that occur through a back-biting mechanism of a dissociated polymer chain.

In 1969 Inoue produced poly(propylene carbonate) (PPC) from CO_2 and propylene oxide with a zinc catalyst derived from $Zn(Et)_2$ treated in water.[10] From this discovery, many heterogeneous, zinc based catalyst were employed for the synthesis of PPC.[11] The typical system involves a metal source such as $ZnEt_2$, $Zn(OAc)_2$, $Zn(OH)_2$, or ZnO reacted with either a trihydroxy phenol or one of a variety of carboxylic acids.

During the 90's, homogeneous zinc catalysts were developed with the most notable being Darensbourg's zinc bis(phenoxide) and Coates' zinc *β*-diimine catalysts (Figure 1-2).[12] Both catalysts are highly active towards the synthesis of poly(cyclohexene carbonate) (PCHC) with Coates' catalyst providing turn over frequencies in upwards of 2000 h^{-1}. (TOF = TON/h, TON = moles epoxide consumed/mole catalyst).

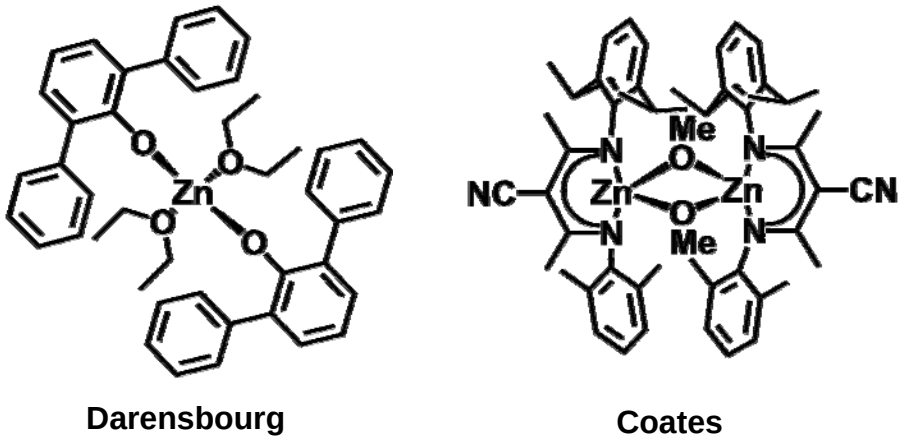

Figure 1-2. Examples of Darensbourg's zinc bis(phenoxide) catalyst and Coates' zinc *β*-diimine catalyst.

Macrocyclic catalysts were also developed including Inoue's (TPP)AlCl and the $scCO_2$ soluble complex (TFPP)CrCl developed by Mang and Holmes (Figure 1-3).[13] With the use of chromium, a transition metal based catalyst, a new type of reactive metal center was introduced and a new approach away from the Zn based systems was conceived.

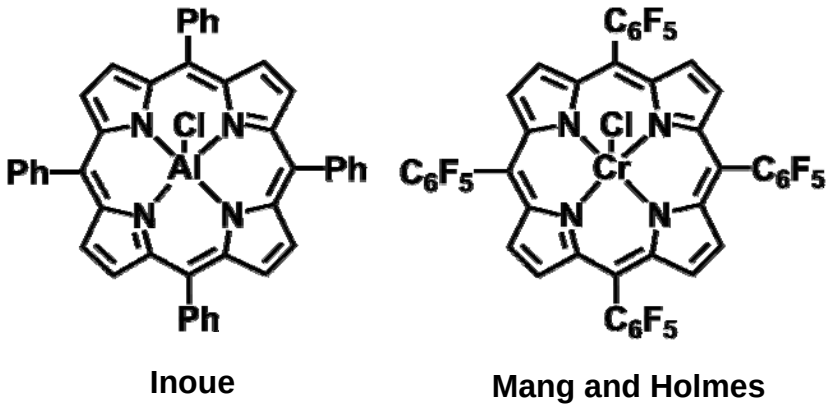

Figure 1-3. Porphyrin based catalysts developed by Inoue, Mang and Holmes.

Salen-Based Catalytic Systems

The work of E. N. Jacobsen has propelled the use of the salen ligand (salen = *N, N*'- bis(3,5-di-*tert*-butylsalicylidene)-1,2-ethylenediimine) to the forefront in several areas of synthetic chemistry.[14] In fact, salen can now be safely described as a "privileged" ligand as it is easy to make, easy to derivatize, chemically stable and, if required, chiral. Salient to the chemistry of polycarbonates is Jacobsen's work with first-row transition metal salen catalysts and epoxides. Scheme 1-1 outlines the three paths in which epoxides are synthesized, kinetically resolved or ring-opened, depending on the metal center. The salen ligand employed is (1R,2R)-*N*,*N*'-bis(3,5-di-*tert*-butylsalicylidene)-1,2-cyclohexenediimine, a chiral ligand that can undergo metallation with synthetic ease. Manganese(III) salen complexes are asymmetric epoxidation catalysts for bulky di- and tri- substituted olefins.[15] The mechanism involves the oxidation of manganese(III) to manganese(V) with an oxidant, such as NaOCl, followed

Scheme 1-1.

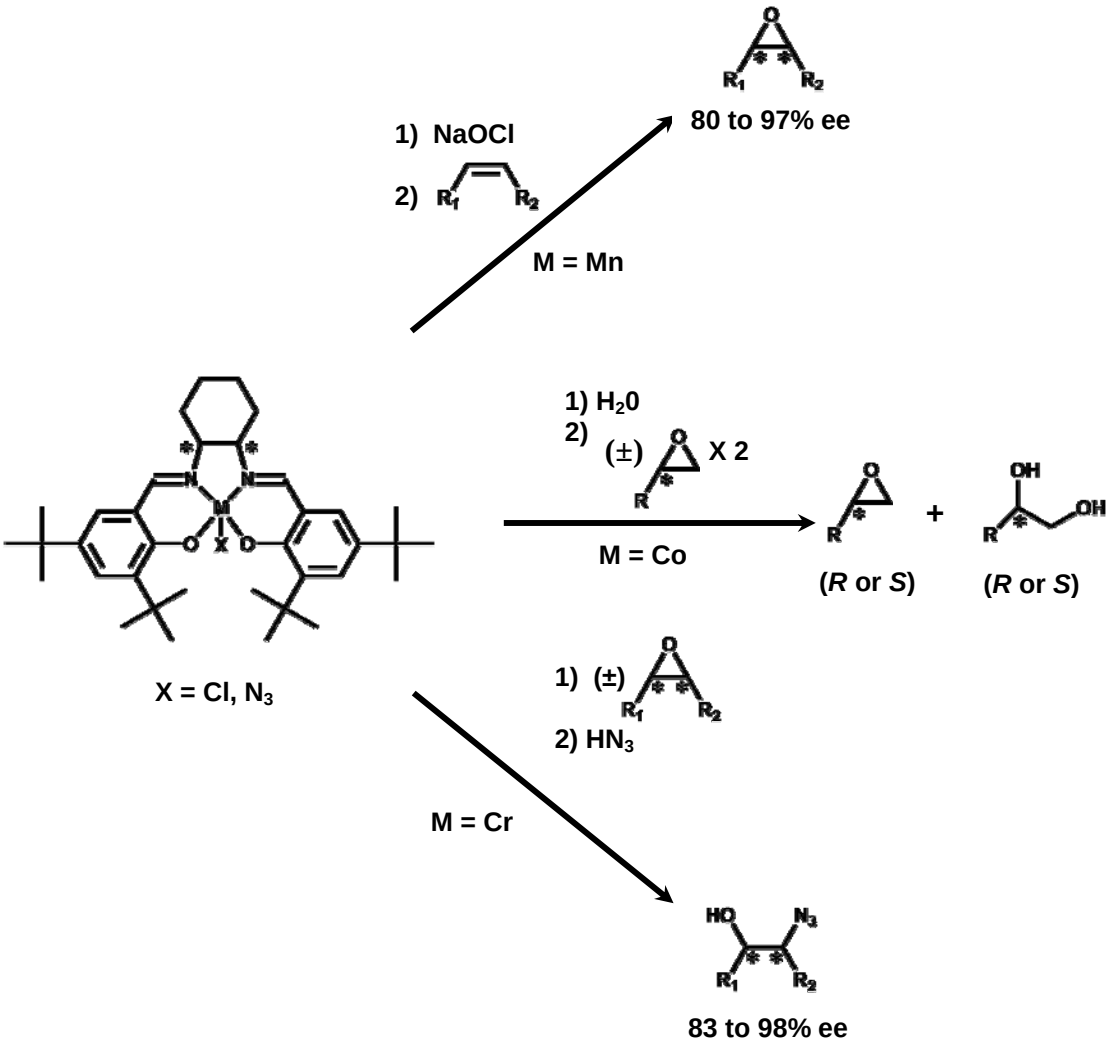

by the non-concerted addition of oxygen across the olefin bond. The metal is reduced the manganese(IV) through a free radical pathway followed by ring-closure and a final reduction to regenerate manganese(III).

The hydrolytic kinetic resolution (HKR) of terminal epoxides can be carried out with the use of cobalt(III) salen complexes.[16] High enantioselectivity can be achieved

for either the *R* or *S* enantiomers of terminal epoxides from a racemic mixture, depending on whether the (*R*, *R*) or (*S*, *S*) version of the chiral salen is used. Accompanying the resolution of epoxide is the ring-opening of the epoxide of opposite chirality to yield a diol. This is facilitated through a bimetallic ring-opening of a metal bound epoxide by a hydroxide of an adjacent metal complex which is the hydrolysis product of the starting anion (Cl^-, OAc^-, OBz^-, OPh^-, etc.).

The third reaction, given in Scheme 1-1, also involves a bimetallic intermediate. Chromium(III) salen complexes are capable of ring-opening both terminal and *meso* epoxides with high emanitomeric excess.[17] As will be explained later, ring-opening of a metal bound, activated epoxide plays a key role in the synthesis of polycarbonates from CO_2. The reaction mechanism described by Jacobsen is outlined in Scheme 1-2. An epoxide binds to the open coordination site of the chromium(III) center to form an octahedral complex. The α-carbon of the epoxide is then nucleophilically attacked by the azide of another metal complex forming a neutral, bimetallic transition state. Then, through anion exchange, the azide is transferred to the attacking complex to regenerate the octahedral epoxide-bound species. To cleave the metal-alkoxide bond and produce the azido alcohol, hydrogen azide is added.

Scheme 1-2

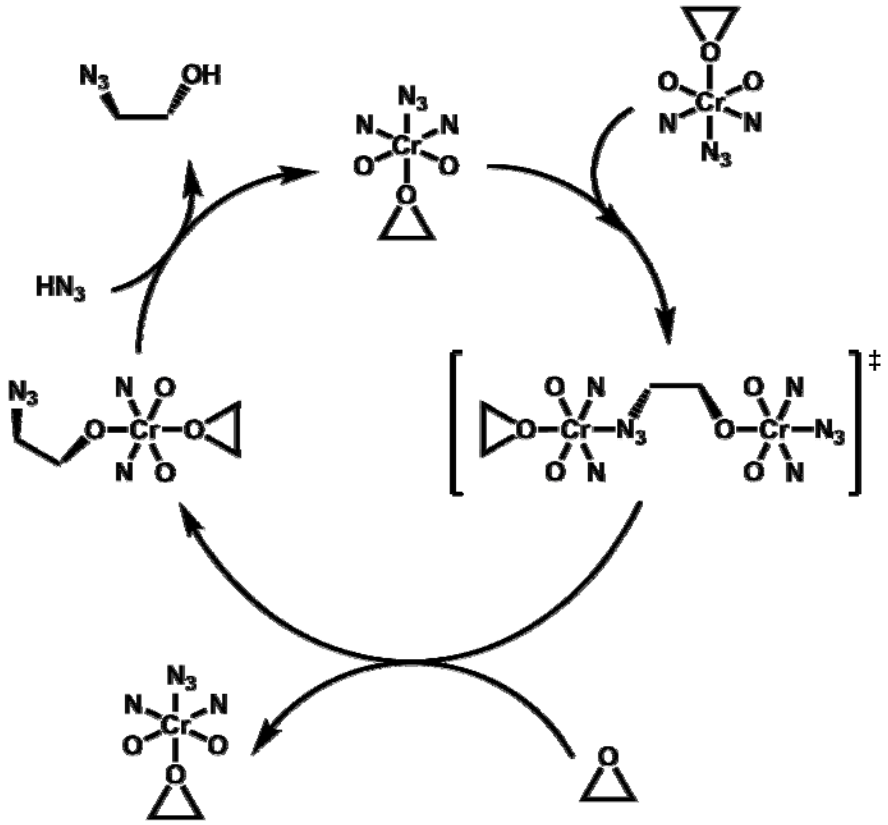

Application of Salen Complexes Towards Polycarbonate Synthesis

In an attempt to synthesize sterioselective polycarbonates, Darensbourg and Yarbrough combined a chiral chromium(III) salen chloride catalyst with a Lewis basic cocatalyst, *N*-methyl imidazole (*N*-MeIm) (Figure 1-4).[18] Although sterioregular copolymer was not achieved, PCHC was attained with a TOF of 88.2 h^{-1} with 5 equiv *N*-MeIm and 24 hours of reaction time. Additional studies with chromium(III) salen complexes and *N*-MeIm aided in optimization of the catalyst system (Table 1-3).[19]

Comparing Entries 1 and 2 demonstrates that an increase in TOF from 36 h^{-1} to 47 h^{-1} is gained by switching the initiator from chloride to azide. When moving to a more electron donating substituent in the 5 position of the phenyl ring, (Entry 3), an increase in TOF from 36 h^{-1} to 57 h^{-1} is achieved. When phenylene and cyclohexylene backbones are employed (Entries 4 and 5) no appreciable increase in activity is observed. From this series it is apparent that azide initiator is more effective and a more electron donating ligand, and thus a more electron-rich metal center, facilitates greater catalytic activity.

Entries 6 to 8 examine the influence of cocatalysts variation.[20] Entry 6 illustrates the ability of tricyclohexylphosphine to act as a Lewis base type cocatalyst. Another class of cocatalysts currently being utilized is derived from ionic sources such as the Cl^- and N_3^- salts of PPN^+ and $(^nBu)_4N^+$ [PPN = bis(triphenylphospheramylidene) ammonium]. These large, non-interacting, cations allow coordination of the anion to the metal, effectively providing an additional initiator for the polymerization process. Entries 7 and 8 illustrate the significant improvement in activity that is obtained when anionic cocatalysts are employed. Entry 8 represents the culmination of an effort to fully optimize catalytic activity combining a highly donating ligand, azide initiator, and $PPNN_3$ as an ionic cocatalyst. The consequent TOF of 1153h^{-1} is the highest reported for any epoxide with a chromium(III) salen based catalyst.

The synthesis of poly(propylene carbonate) from the copolymerization of CO_2 and propylene oxide has also received extensive attention in the area of transition metal salen catalysis. The concomitant formation of cyclic propylene carbonate with polymer formation is a well established drawback to the use of terminal epoxides. It has been

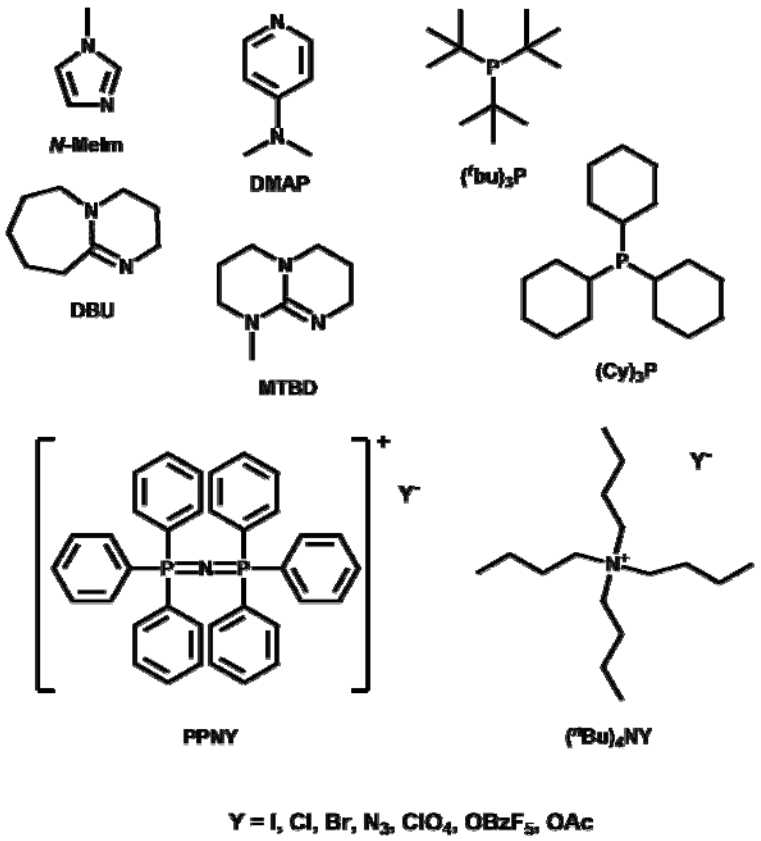

Figure 1-4. Cocatalyst suitable for the copolymerization of CO_2 and epoxide.

determined that the difference in activation energy between polymer and cyclic carbonate formation is some 2.5 times less for PO compared to CHO.[21] In other words, the barrier going from polymer to cyclic formation, the thermodynamic sink, is less for PO. In structural terms, the greater ring strain exerted on the five-membered carbonate ring by the closed cyclohexyl ring of cyclohexene carbonate discourages its formation, relative to that of propylene carbonate.

Table 1-3. Summary of the Copolymerization of CO_2 and CHO by (salen)CrX Complexes.[19,20]

Entry[a]	R_1	R_2	R_3	X	CO_2 (bar)	Cocatalyst (equiv)	TON[d]	TOF (h^{-1})[e]
1[b]	H	H	^{t}Bu	Cl	54	*N*-MeIm (2.25)	857	36
2[b]	H	H	^{t}Bu	N_3	54	*N*-MeIm (2.25)	1126	47
3[b]	H	H	OCH_3	Cl	54	*N*-MeIm (2.25)	1360	57
4[b]	-C_4H_4-		^{t}Bu	Cl	54	*N*-MeIm (2.25)	868	36
5[b]	(1R, 2R)-C_4H_8-		^{t}Bu	Cl	54	*N*-MeIm (2.25)	851	36
6[c]	H	H	^{t}Bu	N_3	34	Cy_3P (3)	1002	251
7[c]	(1R, 2R)-C_4H_8-		OCH_3	N_3	34	PPNCl (1)	2462	1056
8[c]	(1R, 2R)-C_4H_8-		OCH_3	N_3	34	$PPNN_3$ (1)	2686	1153

[a] reaction conditions: 50 mg cat., 80 ºC, 20 mL CHO (0.198 mol). [b] reaction time = 24 h.
[c] reaction time = 4 h. [d] TON = (moles epoxide consumed/moles cat). [e] TOF = TON/h

Scheme 1-3.

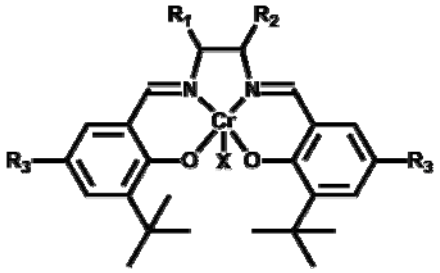

X = Cl, N_3

Scheme 1-4.

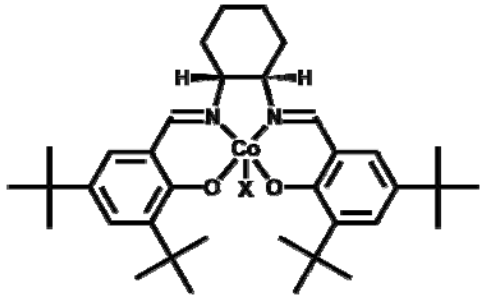

X = Cl, Br, I, N_3, $OBzF_5$, OAc, $OPh(NO_2)_2$, ClO_4

Darensbourg and Phelps applied chromium salen catalysts with various backbones and cocatalysts to the copolymerization of CO_2 and PO.[22] No regio- or sterioselectivity was obtained; however, cyclic formation was suppressed to less than 10% total product conversion with greater than 90% conversion to polymer. The catalyst system most favorable towards both higher activity and polymer conversions was obtained when a phenylene backbone and either Cy_3P or PPNCl were employed as cocatalyst.

Great advances have been made by Coates and Lu in the synthesis of regio and sterioregular PPC with cobalt(III) salen complexes (Scheme 1-4).[23] Under mild reaction conditions (22 ºC and 13.8 bar) the chiral catalyst (*R*,*R*)-(salcy)CoOBzF_5 (OBzF_5 = pentafluorobenzoate) coupled with PPNCl gives a TOF of over 600 h^{-1} with selectivity for PPC formation > 99%.[24] For the same system, regioregular polymer is synthesized with head-to-tail linkages of greater than 90%. Regioregular, syndio-enriched PPC can be achieved when a racemic mixture of PO is used in conjunction with *rac*-(salcy)CoBr. With that same catalyst, regioregular isotactic PPC is obtained starting from 100% (*R*)-PO as monomer. Higher TOF's are noted by Lu with the catalyst (*R*,*R)*-(salcy)Co(OPh(NO_2)$_2$), which, when coupled with PPNCl, gives a TON of 1400 h^{-1} at moderate reaction conditions (45 ºC, 20 bar).

Mechanism of the Copolymerization Process

A mechanistic picture of the copolymerization of CO_2 and epoxides by transition metal salen complexes has been under development by several researchers.[25,26] The prevailing picture of both the initiation and propagation steps in the process revolves around the two coordination sites of the metal center *trans* to each other in a stable, octahedral geometry that also includes the planar ligand arrangement of the salen ligand. Scheme 1-5 outlines the general copolymerization process. In instances where cocatalyst is employed Y will coordinate *trans* to X in complex **1**. Ionic cocatalysts will provide an anion Y that may or may not be identical to X. Thus, an anionic species such as complex **3** may be a diazide, dichloride, mixed azide/chloride, or some other combination of anions. When Lewis-basic type cocatalysts are employed, the identity of X and Y is unclear. Recent evidence suggests that *N*-heterocyclic amines such as DMAP or *N*-MeIm in the presence of CO_2, epoxide, and a Lewis-acidic metal center, can undergo a complex transformation to form a Zwitterionic species that will coordinate to the open site of the metal center and facilitate copolymerization in a fashion identical to ionic cocatalysts.[27]

This transformation is slow and the delayed formation accounts for induction periods witnessed with these procurers. It is also suggested that when phosphines are employed as cocatalysts Zwitterionic species can be formed from the nucleophilic attack of a bound epoxide to give a ring-opened phosphonium alkoxide species capable of acting as a metal-bound anion. During such polymerization processes it is likely that the more nucleophilic species such as Cl^-, or N_3^- will be involved in polymer initiation and

thus the identities of X and Y in Scheme 1-5 may be reversed in these cases. There is also the possibility that polymer chain growth will take place from both *trans* positions of the metal center resulting in two different polymer end groups being present.

After ring-opening, an anionic species such as **4** is obtained containing a metal bound alkoxide that can in turn be involved in CO_2 insertion. From this point the alternating insertions of epoxide and CO_2 leads to the propagation of the growing polymer chain. Complex **4** is also accessible through a bimetallic pathway identical to Jacobsen's mechanism (Scheme 1-2). This situation arises when no cocatalyst is utilized. The ring-bound epoxide is nucleophilically attacked by X (or Y) from another equivalent of complex. This will lead to an ionic pair between **4** and a cationic metal salen complex (not shown). Ion exchange of X^- to the cation leads to complex **5** and the reformation of **2**. Catalytic activity for systems without the use of a cocatalyst is exceptionally low and this may be accounted for by observing that **5** lacks a strong donor group *trans* to the alkoxide. Therefore, the complex lacks activation of the metal-alkoxide bond and the result is a decreased nucleophilicity towards additional monomers.

Scheme 1-5

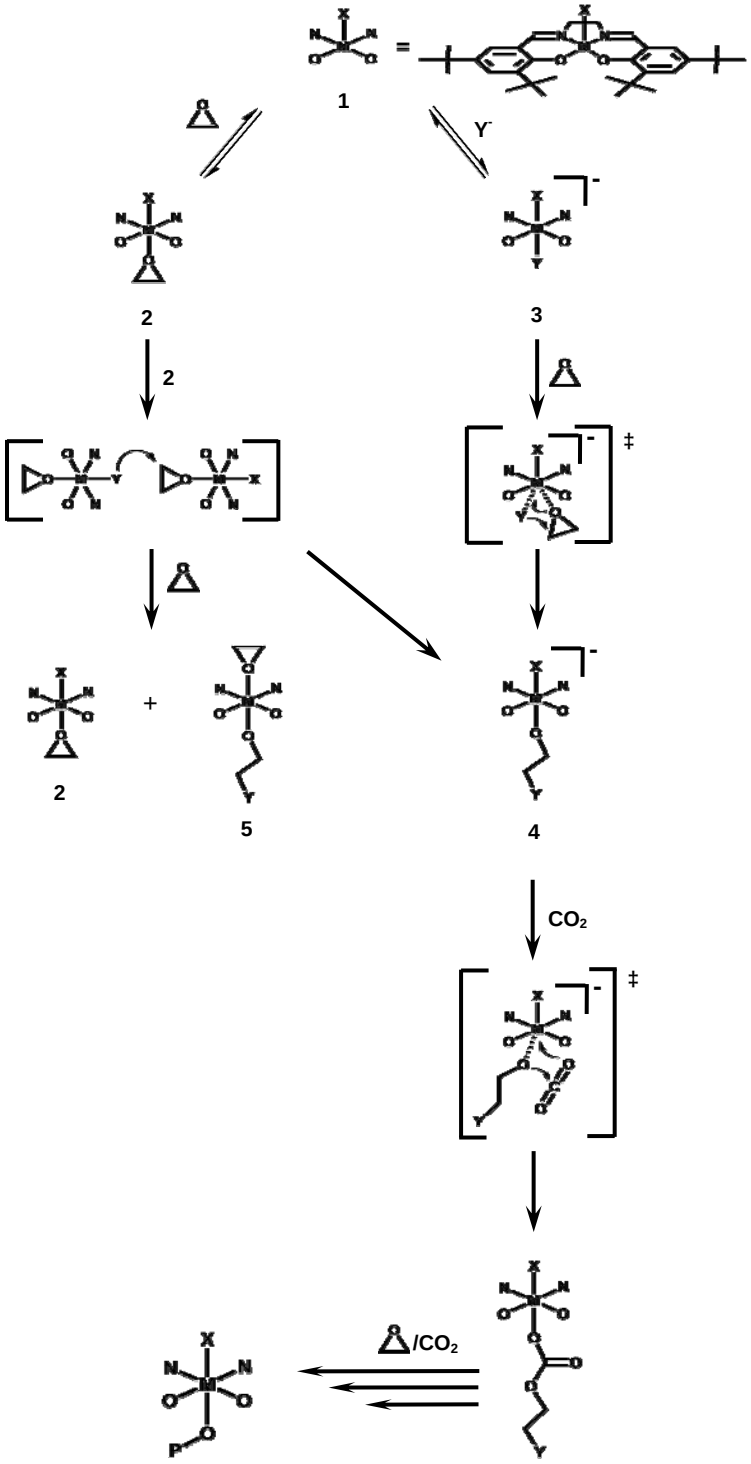

CHAPTER II

THE COPOLYMERIZATION OF CYCLOHEXENE OXIDE AND CARBON DIOXIDE CATALYZED BY A CHROMIUM ACACEN COMPLEX*

Introduction

The robust and versatile salen complexes of chromium(III) and cobalt(III) have proven very potent catalytic systems for the production of poly(cyclohexene carbonate) and poly(propylene carbonate) from epoxides and carbon dioxide (see Equation 1-1).[23,24,26,27,28] This observation has prompted examination of the catalytic efficacy of other $N_2O_2^{2-}$ ligands bound to Cr(III)X (X = Cl^- or N_3^-) for carrying out these processes and in particular, ligands which are sterically less encumbering than salen derivatives. To this end, presented here are results utilizing a metal complex containing such a ligand, namely, *N,N′*-bis(*tert*-butylacetylacetone)-1,2-ethylene diimine (*t*-butylacacenH_2) (see Figure 2-1).[29,30] This ligand is a modification of acacen (*N,N′*-bis(acetylacetone)-1,2-ethylene diimine), a well known Schiff base with a N_2O_2 coordination sphere. The

---

* Reproduced in part with permission from Darensbourg, D. J.; Frantz, E. B.; Andreatta, J. R. *Inorganica Chimica Acta* **2007**, *360*, 523-528. Copyright 2007 Elsevier Science.

primary difference from salen is the lack of phenylene rings along the enolate moiety of the "arms" of acacen. In place of two methyl groups of acacen, the two *t*-butyl groups of (*t*-butylacacen)H_2 have been added in order to enhance solubility and increase electron donation to the chromium center.

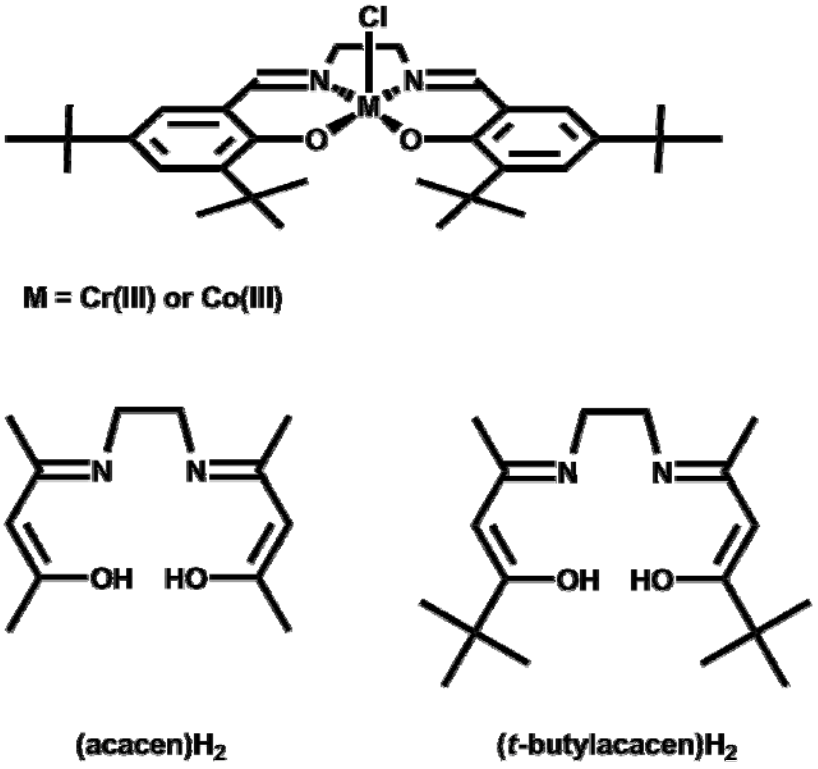

Figure 2-1. Schematic outline of chromium(III) or cobalt(III) salen chloride catalysts, (acacen)H_2 and (*t*-butylacacen)H_2.

Experimental

Method and Materials. Unless otherwise specified, all syntheses and manipulations were carried out on a double-manifold Schlenk vacuum line under an atmosphere of argon or in an argon-filled glovebox. Cyclohexene oxide (Lancaster) was freshly distilled from CaH_2. Bone dry carbon dioxide supplied in a high-pressure cylinder equipped with a liquid dip-tube was purchased from Scott Specialty Gases. The starting materials 3,5-Di-*tert*-butylsalicylaldehyde and 5,5'-dimethylhexane-2,4-dione were synthesized as described in the literature[31,32] or, optionally, the latter can be purchased from Lancaster Synthesis, Inc. Unless otherwise stated, all other reagents were used without further purification. Infrared spectra were recorded on a Mattson 6021 FTIR spectrometer equipped with DTGS and MCT detectors.

Synthesis of *N,N*'-Bis(3,5-di-*tert*-butylsalicylidene)-1,2-ethylenediimine. Ethylenediamine, 3,5-di-*tert*-butylsalicylaldehyde, and a few drops of aqueous formic acid were dissolved in methanol and heated to reflux for 2 h. The precipitated product was filtered and washed with small aliquots of cold methanol, producing a yellow solid (~60 % purified yield).

Synthesis of *N,N*'-Bis(*tert*-butylacetylacetone)-1,2-ethylenediimine [(*t*-butylacacen)H_2]. The synthesis of (*t*-butylacacen)H_2 was adapted from a literature procedure.[33] Ethylenediamine (0.463 g, 7.70 mmol) was added drop-wise to a solution of 5,5'-dimethylhexane-2,4-dione (2.00 g, 14.1 mmol) in 20 mL diethyl ether and heated to reflux for 30 minutes. The solution was then cooled in ice water for one hour and poured into an evaporation disk. After solvent evaporation an off-white solid was

collected (1.17 g, 26.9 % yield). ^{1}H NMR (C_6D_6, 300 MHz): δ 11.06 (s, 2H), 5.15 (s, 2H), 3.41 (m, 4H), 1.91 (s, 6H), 1.11 (s, 18H). ^{13}C {^{1}H} NMR (C_6D_6, 75 MHz): δ 204.8, 163.9, 91.61, 43.75, 41.62, 28.12, 19.40.

Synthesis of (*t*-butylacacen)CrCl (2-1). $CrCl_3(THF)_3$ (0.250 g, 0.667 mmol) and (*t*-butylacacen)H_2 (0.206 g, 0.667 mmol) were dissolved in 20 mL of THF. This solution was then heated to 40º C for 18 hours, in which time the color changed from purple to dark brown. THF was removed by vacuum and 20 mL of diethyl ether added. The reaction mixture was briefly stirred before the dark brown produce solution was extracted by cannulation. Ether was then removed by vacuum to give a hard, glassy dark brown solid (45 mg, 17.1 %). No further purification was performed. Anal. Calcd. for $C_{18}H_{30}N_2O_2CrCl$: C, 54.89; H, 7.68. Found: C, 50.01; H, 7.76.

Crystals of [(*t*-butylacacen)CrOH]$_2$ (**2-2**) were grown by slow vapor deposition of pentane (outer vial) into a dichloromethane solution containing (*t*-butylacacen)CrCl (**2-1**) (inner vial). Both inner and outer vials were meticulously dried before use by Bunsen burner and sealed under argon with the outer vial being caped by a septum. Red-brown colored crystals suitable for X-ray diffraction were collected off the sides of the inner specimen vial after two months storage in a freezer kept at a constant temperature of -19º C. At this time it appeared that the pentane had fully diffused from the outer vial into the inner vial containing the dichloromethane solution and the resultant solvent mixture had partially evaporated leaving behind the crystals in question.

Synthesis of [*N*,*N*'-Bis(3,5-di-*tert*-butylsalicylidene)-1,2-ethylenediimine] Chromium(III) Hydroxide dimer [(Etsalen)Cr(OH)]$_2$ (2-3).[34] Cr(Etsalen)Cl[19] (2.01 g, 3.47 mmol) was weighed and placed into a 50 mL Schlenk flask. $AgClO_4$ (0.717 g, 3.45 mmol) was similarly weighed into a 100 mL Schlenk flask that was covered with aluminum foil and fitted with a slow addition funnel (***NOTE****: perchlorate salts are potentially explosive and should not be used with fritted filters*). Each compound was dissolved in 15 mL of acetonitrile, and the Cr(Etsalen)Cl solution was cannulated into the slow addition funnel and added dropwise to the $AgClO_4$ solution. After mixing was complete, the funnel was rinsed twice with 5 mL of acetonitrile and added to the reaction mixture. The solution was stirred overnight in a dark environment. The resulting Cr(Etsalen)ClO_4 solution was quickly filtered through a Büchner funnel onto sodium methoxide and stirred overnight. Acetonitrile was removed *in vacuo* and the resulting solid was dissolved in dichloromethane. The resultant solution was then washed three times with 20 mL of distilled water, dried with sodium sulfate, filtered through a pad of celite, and dried under vacuum to yield 0.383 g (19.7 %) of a dark brown solid. Crystals appropriate for X-ray diffraction were obtained by vapor diffusion of pentane into a concentrated dichloromethane solution of the product over an extended time. Anal. Calcd (%) for $C_{64}H_{94}Cr_2N_4O_6$: C, 68.67; H, 8.46. Found: C, 67.98; H, 8.37.

Copolymerization of Cyclohexene Oxide and CO_2. High pressure measurements of the copolymerization processes were carried out using a stainless steel Parr autoclave modified with a SiComp window to allow for attenuated total reflectance spectroscopy using infrared radiation (ASI ReactIR 1000 *in situ* probe). After the

autoclave was dried *in vacuo* overnight at 80ºC, 10 mL of neat epoxide was loaded *via* the injection port. After the background solvent reached 80ºC, a single 128-scan background spectrum was collected. The catalyst and cocatalyst were dissolved in 10 mL of neat epoxide and injected into the autoclave followed by immediate charging with 35 bar CO_2 pressure. With a reaction temperature of 80ºC being maintained, a single 128-scan spectrum was collected every 3 min during a reaction period of 10-24 hrs. Profiles of the absorbance at 1750 cm^{-1}(polycarbonate) vs. time were recorded after baseline correction. After cooling and venting in a fume hood, the polymer was extracted as a dichloromethane solution and dried overnight under vacuum at 100ºC. The collected polycarbonate was analyzed by ^1H NMR, where the amount of ether linkages were determined by integrating the peaks corresponding to the methine protons of polyether at ~3.45 ppm and polycarbonate at ~4.6 ppm. Isolated copolymer yields were employed in determining TON and TOF's. Molecular weight determinations (M_w and M_n) were carried out in THF solutions at the New Jersey Center for Biomaterials, Rutgers University.

X-ray Structural Studies. A Bausch and Lomb 10× microscope was used to identify suitable crystals from a representative sample of crystals from the same habit. The representative crystal was coated with a cryogenic protectant (i.e., mineral oil, paratone, or apezon grease) and fixed on a nylon loop. The mounted crystals were placed in a cold nitrogen stream (Oxford) maintained at 110K on a Bruker SMART 1000 three circle goniometer.[35] The X-ray data were collected on a Bruker CCD diffractometer and covered more than a hemisphere of reciprocal space by a combination

of three sets of exposures; each exposure set had a different φ angle for the crystal orientation, and each exposure cover 0.3º in ω. Crystal data and details on collection parameters are give in Table 2-1. The crystal-to-detector distance was 4.9 cm. The space group was determined on the basis of systematic absences and intensity statistics.[36] The structures were solved by direct methods and refined by full-matrix least squares on F^2. All non-H atoms were refined with anisotropic displacement parameters. All H atoms attached to C atoms were placed in idealized positions and refined using a riding model with aromatic C–H = 0.96Å, methyl C–H = 0.98Å, and fixed isotropic displacement parameters equal to 1.2 (1.5 for methyl H atoms) times the equivalent isotropic displacement parameter of the atom to which they were attached. The methyl groups were allowed to rotate about their local 3-fold axis during refinement.

Programs for all structures: data reduction, SAINTPLUS (Bruker[36]); structure solution, SHELXS-86 (Sheldrick[37]); structure refinement, SHELXL-97 (Sheldrick[38]); molecular graphics and preparation of material for publication, SHELXTL-Plus version 5.0 (Bruker[39]). Space-filling models were obtained using X-Seed software (1999).[40]

Results and Discussion

The synthesis of (*t*-butylacacen)CrCl(**2-1**) was accomplished by allowing $CrCl_3(THF)_3$ to react with one equivalent of (*t*-butylacacen)H_2 in THF. In an attempt to grow single crystals, pentane was allowed to slowly diffuse into a dichloromethane solution of **2-1** maintained at -19ºC over a period of two months. Instead of obtaining single crystals of **2-1**, red-brown crystals of the dimer [(*t*-butylacacen)CrOH]$_2$ (**2-2**),

which resulted from hydrolysis of **2-1,** were isolated and subjected to X-ray structure analysis.

Table 2-1. X-ray Crystallographic Data for Complexes **2-2** and **2-3**.

	2-2	**2-3**
Empirical Formula	$C_{18.5}H_{32}ClCrN_2O_3$	$C_{70}H_{114}ClCr_2N_4O_9$
Formula Wt. (g/mol)	417.91	1295.10
Space Group	P1(bar)	P1(bar)
Z	2	2
Volume, Å^3	1078.1(6)	4060.3(16)
Crystal System	triclinic	triclinic
a, Å	9.730(4)	14.449(4)
b, Å	10.607(4)	17.727(4)
c, Å	11.275(4)	18.625(4)
α, deg.	72.606(13)	115.598(11)
β, deg.	76.207(15)	107.087(13)
γ, deg.	87.307(14)	90.567(14)
D_{calcd} (g/cm^3)	1.287	1.059
Temperature (K)	110(2)	110(2)
Wavelength (Å)	0.71073	0.71073
Absorption coefficient (mm^{-1})	5.655	2.888
Goodness of fit on F^2	1.083	1.022
R^a (%)	6.74	8.58
$R_w{}^b$ (%)	13.11	19.02

[a] $R = \Sigma \parallel F_o \mid - \mid F_c \parallel \Sigma F_o$. [b] $R_w = \{[\Sigma w (F_o^2 - F_c^2)^2]/[\Sigma w(F_o^2)^2]\}^{1/2}$

For the sake of comparison, the X-ray structure of a similar dimer, $[(salen)CrOH]_2$ (**2-3**), was obtained upon prolonged crystallization of a purported sample of $[(salen)CrOMe]_2$ and is described as well.[34] Table 2-1 lists crystal data and details of data collection. Selected bond distances and bond angles are summarized in Tables 2-2 and 2-3, with Figures 2-2 and 2-3 depicting thermal ellipsoid representations of the two closely related structures.

Table 2-2. Selected Bond Distances (Å) and Bond Angles (deg) of Complex **2-2**.

Cr(1)···Cr(1)$^{\#}$	3.05(1)	Cr(1)–O(2)	1.947(5)
Cr(1)–O(3)	1.992(4)	Cr(1)–N(1)	2.014(5)
Cr(1)–O(3)$^{\#}$	1.993(5)	Cr(1)–N(2)	2.001(6)
Cr(1)–O(1)	1.953(5)		
O(3)–Cr(1)–O(3)$^{\#}$	79.9(2)	N(2)–Cr(1)–O(1)	98.5(2)
O(1)–Cr(1)–O(3)	89.94(19)	N(2)–Cr(1)–N(1)	79.8(2)
O(1)–Cr(1)–O(3)$^{\#}$	169.83(19)	O(2)–Cr(1)–O(3)	93.15(18)
N(1)–Cr(1)–O(3)	97.7(2)	O(2)–Cr(1)–O(3)$^{\#}$	92.68(19)
N(1)–Cr(1)–O(3)$^{\#}$	93.8(2)	O(2)–Cr(1)–O(1)	88.68(19)
N(1)–Cr(1)–O(1)	86.7(2)	O(2)–Cr(1)–N(1)	168.2(19)
N(2)–Cr(1)–O(3)	171.0(2)	O(2)–Cr(1)–N(2)	90.1(2)
N(2)–Cr(1)–O(3)$^{\#}$	91.6(2)	Cr(1)–O(3)–Cr(1)$^{\#}$	100.1(2)

Table 2-3. Selected Bond Distances (Å) and Bond Angles (deg) of Complex **2-3**.

Cr(1)···Cr(2)	3.09(1)	Cr(2)–O(3A)	1.998(6)
Cr(1)–O(3A)	1.973(6)	Cr(2)–O(3B)	1.962(6)
Cr(1)–O(3B)	1.981(6)	Cr(2)–O(1B)	1.942(6)
Cr(1)–O(1A)	1.935(6)	Cr(2)–O(2B)	1.923(6)
Cr(1)–O(2A)	1.936(6)	Cr(2)–N(1B)	1.987(8)
Cr(1)–N(1A)	2.032(7)	Cr(2)–N(2B)	2.089(8)
Cr(1)–N(2A)	2.021(8)		
O(3A)–Cr(1)–O(3B)	77.3(2)	O(3A)–Cr(2)–O(3B)	77.1(2)
O(1A)–Cr(1)–O(3A)	92.5(2)	O(1B)–Cr(2)–O(3A)	92.8(2)
O(1A)–Cr(1)–O(3B)	168.4(2)	O(1B)–Cr(2)–O(3B)	98.7(3)
O(3A)–Cr(1)–N(2A)	162.7(3)	O(3A)–Cr(2)–N(2B)	88.3(3)
O(3A)–Cr(1)–N(1A)	101.1(3)	O(3A)–Cr(2)–N(1B)	93.0(3)
O(3A)–Cr(1)–O(2A)	92.1(3)	O(3A)–Cr(2)–O(2B)	171.0(2)
O(3B)–Cr(1)–O(2A)	96.6(3)	O(3B)–Cr(2)–O(2B)	94.6(3)
O(3B)–Cr(1)–N(1A)	91.0(3)	O(3B)–Cr(2)–N(1B)	167.9(3)
O(3B)–Cr(1)–N(2A)	85.4(3)	O(3B)–Cr(2)–N(2B)	90.6(3)
N(2A)–Cr(1)–N(1A)	79.1(3)	N(2B)–Cr(2)–N(1B)	82.0(3)
O(1A)–Cr(1)–N(1A)	85.5(3)	O(1B)–Cr(2)–N(1B)	88.6(3)
O(1A)–Cr(1)–N(2A)	104.8(3)	O(1B)–Cr(2)–N(2B)	170.6(3)
N(2A)–Cr(1)–O(2A)	89.7(3)	N(2B)–Cr(2)–O(2B)	88.3(3)
O(2A)–Cr(1)–O(1A)	89.2(3)	O(2B)–Cr(2)–O(1B)	91.9(3)
O(2A)–Cr(1)–N(1A)	166.0(3)	O(2B)–Cr(2)–N(1B)	94.8(3)
Cr(1)–O(3A)–Cr(2)	102.3(3)	Cr(1)–O(3B)–Cr(2)	103.3(3)

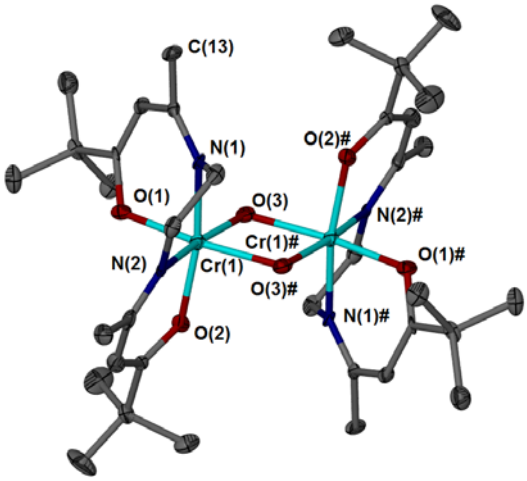

Figure 2-2. Thermal ellipsoid representation of complex **2-2**, [(*t*-butylacacen)CrOH]$_2$.

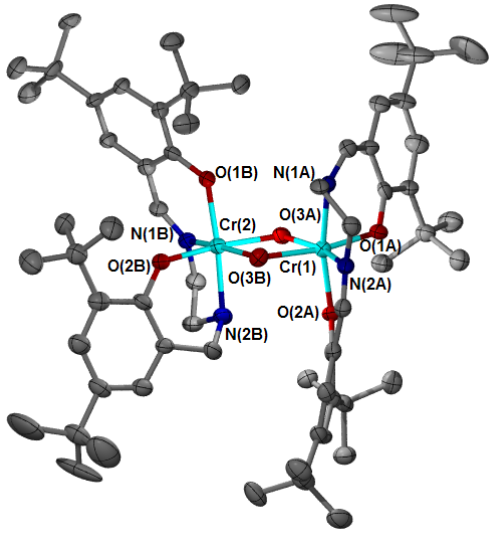

Figure 2-3. Thermal ellipsoid representation of complex **2-3**, [(salen)CrOH]$_2$.

The structural representation for complexes **2-2** and **2-3** is best described in line drawing illustrated in Figure 2-4, where the octahedral coordination polyhedra around

the chromium centers are similarly distorted. That is, several of the angles deviate significantly from 90º. For example, the N–Cr–N and HO–Cr–OH angles in complex

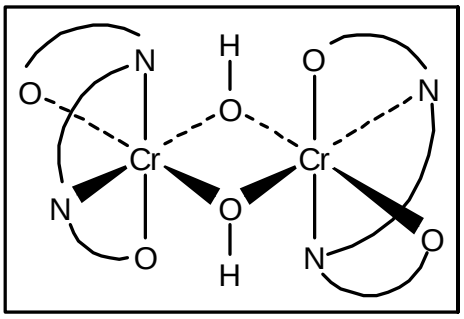

Figure 2-4. Structural representation of [(*t*-butylacacen)CrOH]$_2$ (**2-2**) and (salen)CrOH]$_2$ (**2-3**).

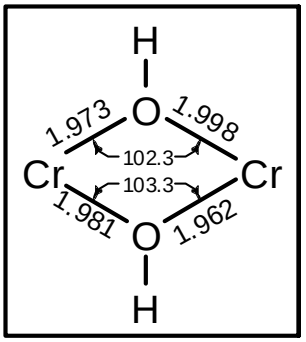

Figure 2-5. Symmetric bridging unit in complexe **2-3**.

2-2 exhibit the largest deviations with values of 79.8(2) and 79.9(2) degrees, respectively. Similar distortions are seen as well in complex **2-3**. The Cr–OH–Cr angles in complex **2-2** are 100.1(2)º, whereas, the corresponding angles in complex **2-3** are 102.3(3)º and 103.3(3)º. In both dimers the bridging unit, shown in Figure 2-5 is quite

symmetric, with Cr···Cr distances of 3.05(1) and 3.09(1) in **2-2** and **2-3**, respectively. Metric parameters similar to those observed for complex **2-3** have been reported in the literature for the dimeric tetrahydrosalen analog of Cr(III) fluoride.[41]

Some preliminary copolymerization reactions have been performed with cyclohexene oxide and carbon dioxide catalyzed by complex **2-1**, (*t*-butylacacen)CrCl, along with three equivalents of PCy_3. The reaction was carried out in a stainless steel reactor at 80ºC under 35 bar of CO_2 for 20 hours with a catalyst loading of 0.058%. Under these reaction conditions 16.1 g of purified copolymer was isolated from a reaction with 19.4 g (20 mL) of cyclohexene oxide. This translates into a TON of 988 (moles of epoxide consumed per mole of catalyst) and a TOF of 49.4 h^{-1}. Figure 2-6 contains the reaction profile for this process where the polycarbonate infrared absorption at 1750 cm^{-1} is monitored as a function of time. This profile clearly reveals an initiation period prior to reaching the maximum reaction rate. On the other hand, for an identical process performed instead in the presence of one equivalent of an ionic initiator, [PPN][Cl], the reaction exhibited *no* initiation period, thereby initially producing copolymer at a faster rate. In this instance the TOF was estimated to be 150 h^{-1} or three times faster than in the presence of a phosphine cocatalyst. The poly(cyclohexylene carbonate) produced in the presence of PCy_3 contained >99% carbonate linkages and displayed a bimodal molecular weight distribution of M_n = 11,000 (PDI = 1.08) and M_n = 26,000 (PDI = 1.06) as determined by GPC in tetrahydrofuran.

A major goal of this study was to assess the relative catalytic activity of complex **2-1** *versus* its (salen)CrCl analog for the copolymerization of cyclohexene oxide and

carbon dioxide. From this cursory study it is apparent that the chromium salen derivative in Figure 2-1 is more catalytically active than its acacen counterpart by a factor of three when activated by [PPN][Cl], however, in the presence of PCy_3 cocatalyst the (salen)CrCl derivative is approximately six times more active. That is, the (salen)CrN_3 analog in the presence of three equivalents of PCy_3 under identical conditions to those employed herein led to a TON of 1318 for a four hour run or a TOF of 329 h^{-1}. Similarly, (salen)CrCl along with one equivalent of [PPN][Cl] afforded a TON of 1977 and a TOF of 494 h^{-1} with a M_n value of 10,000 (PDI = 1.26).[27]

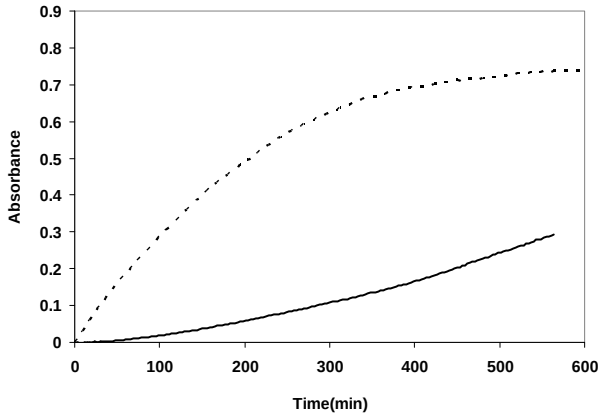

Figure 2-6. *In situ* infrared profile of the polycarbonate peak at 1750 cm^{-1} for the copolymerization of CO_2 and cyclohexene oxide utilizing (*t*-butylacacen)CrCl as catalyst with [PPN][Cl] (dotted line) or PCy_3 (solid line) as cocatalyst.

Scheme 2-1

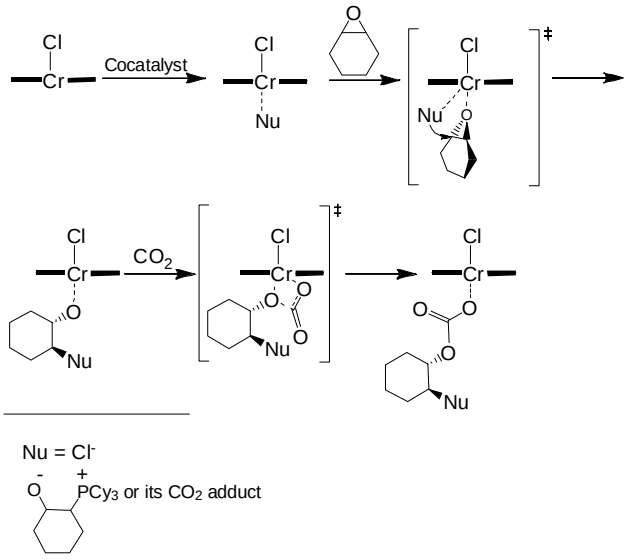

Recently, the mechanistic aspects associated with the role of [PPN][Cl] and PCy_3 as cocatalysts in the initiation step of the copolymerization process involving (salen)CrX catalysts have been reported.[27] The (*t*-butylacacen)CrCl catalyst appears to behave in complete similarity to its (salen)CrX counterpart. In either instance the initial ring-opening of the metal activated epoxide substrate occurs *via* nucleophilic addition by the chloride ion or the zwitterion resulting from phosphine ring-opening of the epoxide, i.e., Scheme 2-1. This latter process is believed responsible for the initiation period observed in the case of phosphine cocatalysts (see Figure 2-6).

Conclusions

A new hydroxo-bridged dimer of [(*t*-butylacacen)CrOH]$_2$ has been isolated from the hydrolysis of the corresponding (*t*-butylacacen)CrCl by the adventitious presence of water during a prolonged recrystallization attempt. It has been structurally and synthetically compared to [(salen)CrOH]$_2$ which has been isolated from the hydrolysis of (salen)CrOMe during attempts to grow single crystals. These derivatives were structurally characterized by X-ray crystallography and shown to be similar in structural details.

Reaction profiles for polycarbonate production, as monitored by *in situ* infrared spectroscopy, from cyclohexene oxide and carbon dioxide in the presence of (*t*-butylacacen)CrCl and the cocatalysts, PCy_3 or [PPN][Cl] are quite similar to data observed for analogous reactions with (salen)CrCl. Although, the mechanistic aspects of the process catalyzed by the two metal systems appear to be the same, the catalytic activity of the (*t*-butylacacen)CrCl species is diminished by a factor of 3-6 depending on cocatalyst. This reduction in catalytic activity is assumed to be due to a less electron-donating acacen ligand.

CHAPTER III

MANGANESE(III) ACACEN COMPLEXES: CHEMISTRY RELEVANT TO THE COPOLYMERIZATION OF EPOXIDES AND CARBON DIOXIDE*

Introduction

With the success of chromium and cobalt salen systems, the investigation of other suitable metals could potentially be valuable. The need for improved catalyst properties justifies such a line of investigation. In particular, polycarbonates of higher molecular weight and greater regio- and sterioselectivity are needed in addition to an expansion of the number of epoxide monomers that can be activated and incorporated into new and valuable copolymers. Logically, other first role transition metals such as iron and manganese may hold some similar catalytic characteristics to chromium and cobalt. Darensbourg and workers synthesized (salen)FeOPh and (salen)Fe(acac) in an effort to develop a series of iron salen catalysts.[42] However, these complexes failed to catalyze the formation of PCHC, yielding only trace amounts of cyclic carbonate.

Manganese(II) cyclen (1,4,7,10-tetraazacyclododecane) complexes have been applied to the synthesis of propylene carbonate (PC) and epichlorohydrin carbonate with [Mn(Me_4cyclen)(NO_3)](ClO_4) being the most active for epichlorohydrin with a TOF of 449 h^{-1} under somewhat harsh condition (120º C, 6.9 bar).[43] Inoue has successfully applied the manganese porphyrin complex (tpp)MnOAc to the formation of PCHC under moderate conditions (80 º C, 51 bar) with a TOF of 16.3 h^{-1}.[44] This polymer had a M_n = 6700, PDI = 1.3 and 99% carbonate linkages. The catalyst was not effective for the formation of PPC from propylene oxide and CO_2, producing only cyclic propylene carbonate. Pertinent to our research, a manganese salen complex (salophen)MnOAc was applied in the same study to the copolymerization of CHO and CO_2 but only resulted in the formation of polyether.

Presented here is a fundamental study of the coordination chemistry of manganese Schiff base complexes as it relates to the copolymerization of CO_2 and epoxides. The ligand system selected for study is that of manganese acacen (acacen = *N*,*N*' –bis(acetylacetone)-1,2-ethylenediimine). These complexes are easily synthesized and exhibit a propensity for providing X-ray-suitable crystals for structural analysis. Boucher and Day have prepared several of these complexes with a wide variety of axial ligands and provided magnetic susceptibility data.[30] Scheme 3-1 summarizes the complexes employed in this study.

Each complex was characterized by X-ray crystallography and (excluding **3-2**) presented here together with their extended macrostructures. A FT-IR study has been undertaken in order to evaluate the extent which these five-coordinate manganese

species bind various substrates of relevance to the copolymerization process. Fundamental differences in behavior between manganese and chromium Schiff base complexes will be described.

Scheme 3-1

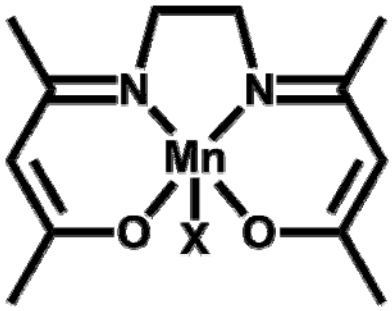

3-1: X = OAc
3-2: X = Cl
3-3: X = N_3
3-4: X = NO_3

Experimental

Methods and Materials. Unless otherwise stated, all synthesis and manipulations discussed were carried out on a double-manifold Schlenk vacuum line under an argon atmosphere or in an argon filled glovebox. Methanol, benzene, diethyl ether, dichloromethane, and pentane were freshly purified by a MBraun Manual Solvent Purification System packed with Alcoa F200 activated alumina desiccant. Ethanol was freshly distilled from Mg/I_2. Cyclohexene oxide was purchased from TCI America and freshly distilled from CaH_2. Chloroform (EMD Chemicals Inc.), ethylenediamine (Aldrich), 2-4 pentanedione (Acros Organics), sodium azide (Lancaster Synthesis Inc.), 4-(Dimethylamino)pyridine (DMAP, Aldrich), $AgNO_3$ (Spectrum Chemical Mgf.

Corp.), 1,8-Diazabicyclo[5.4.0]undec-7-ene (DBU, Acros Organics) and $Mn(OAc)_3•2H_2O$ (Strem Chemicals Inc.) were all used as received without further purification. Bone dry carbon dioxide was purchased from Scott Specialty Gases equipped with a liquid dip-tube.

The synthesis of *N*,*N*'-Bis(acetylacetone)-1,2-ethylenediimine[$(acacen)H_2$], [*N*,*N*'-Bis(acetylacetone)-1,2-ethylenediimine]manganese(III) acetate diaqua [$(acacen)MnOAc•2H_2O$] (**3-1•2H$_2$O**) and [*N*,*N*'-Bis(acetylacetone)-1,2-ethylenediimine]manganese(III) chloride [(acacen)MnCl] (**3-2**) were adapted from literature procedures.[30,33] An alternative route to the synthesis of [*N*,*N*'-Bis(acetylacetone)-1,2-ethylenediimine]manganese(III) azide [$(acacen)MnN_3$] (**3-3**) employing $AgNO_3$ was developed and is reported. Elemental analysis was provided by the Rudiger Laufhutte Microanalysis Laboratory of the School of Chemical Sciences, University of Illinois, Urbana-Champaign. All infrared spectra were recorded using a Mattson 6021 FT-IR spectrometer with DTGS and MCT detectors. All ^{1}H NMR were acquired using Unity+ 300 MHz and VXR 300 MHz superconducting NMR spectrometers.

Synthesis of *N*,*N*'-bis(acetylacetone)-1,2-ethylenediimine[$(acacen)H_2$]. A 125-mL three-necked round-bottom flask was charged with 25 g of 2,4-pentanedione (0.250 mol) along with a Teflon coated stir bar, placed in an oil bath, and equipped with a short-path distillation apparatus. To this flask was added, drop wise, 6.75g of ethylenediamine (0.1125 mol) over the course of 10 minutes. At this point, the solution noticeably heated and resultant water condensation was observed. After 30 minutes

stirring, the solution was slowly heated to 105 ºC and reacted for 24 hours. The resulting red-orange mixture was cooled to room temperature and the crude off-white colored product was collected by filtration in air. The product was then dissolved in 250 mL CH_2Cl_2, dried over 10 g Na_2SO_4, and filtered. Solvent was removed *in vacuo* and an off-white solid was obtained after being recrystallized twice from a CH_2Cl_2/pentane mixture. Yield 17.26 g (67.2%). ^{1}H NMR ($CDCl_3$, 300 MHz): δ 10.88 (s, 2H) , 4.97 (s, 2H), 3.41 (t, 4H), 1.98 (s, 6H), 1.88 (s, 6H).

Synthesis of [*N*,*N*'-bis(acetylacetone)-1,2-ethylenediimine]manganese(III) acetate diaqua [(acacen)MnOAc•2H_2O] (3-1•2H_2O). A 125-mL Schlenk flask was charged with 0.200 g acacenH_2 (0.892 mol), 0.200 g $Mn(OAc)_3$•2H_2O (0.746 mol) and 25 mL MeOH. This mixture was stirred under argon for 10 hrs. The MeOH was then removed *in vacuo* and 50 mL of distilled H_2O was added and the solution mixed for 1 hour before unreacted Mn was removed by filtration in air. The filtered solution was poured into a 500-mL separatory funnel and unreacted ligand was extracted with 50 mL of $CHCl_3$. The product was then isolated by removal of H_2O *in vacuo*, redissolved in 100 mL of CH_2Cl_2 and dried with 2 g $MgSO_4$. The final product was isolated by removal of CH_2Cl_2 *in vacuo* with heat (60 ºC) for 16 hrs to give 70 mg (25.1% yield) of a dark-brown microcrystalline powder. Single crystals suitable for X-ray diffraction were obtained by slow diffusion of pentane into a saturated CH_2Cl_2 solution of the complex. Anal. Calcd. for $C_{14}H_{25}N_2O_6Mn$: C, 45.17; H, 6.77; N, 7.52. Found C, 46.85; H, 6.69; N, 7.65.

Synthesis of [*N,N*'-bis(acetylacetone)-1,2-ethylenediimine]manganese(III) chloride [(acacen)MnCl] (3-2). A 200-mL Schlenk flask was charged with 5.00 g acacenH_2 (22.3 mmol), 5.00 g $Mn(OAc)_3$•$2H_2O$ (18.6 mmol) and 150 mL MeOH. This mixture was stirred under argon for 18 hrs. The MeOH was then removed *in vacuo* and 200 mL of distilled H_2O was added and the solution mixed for 1 h before unreacted Mn was removed by filtration in air. The filtered solution was poured into a 1000-mL separatory funnel and unreacted ligand was extracted with 200 mL of $CHCl_3$. The aqueous solution of (acacen)MnOAc was then treated with 50 g of NaCl and shaken vigorously. Product was then extracted with 5 x 200 mL of $CHCl_3$, separated from the aqueous phase and reextracted from the organic phase with 200 mL of distilled H_2O. To this solution 50 g of NaCl was added and shaken vigorously followed by extraction of the product with 7 x 200 mL of $CHCl_3$. The solution was then reduced in volume to 250 mL *in vacuo* and dried with Na_2SO_4 followed by complete removal of solvent to isolated solid product. Recrystallization of the final product was obtained from 50 mL of benzene and 500 mL of diethyl ether. This yielded 3.28 grams (56.4 %) of a dark-brown microcrystalline powder.

Synthesis of [*N,N*'-bis(acetylacetone)-1,2-ethylenediimine]manganese(III) azide [(acacen)MnN_3] (3-3). A 125-mL round-bottom flask was charged with 0.300 g **2** (0.959 mmol), 0.178 g $AgNO_3$ (1.06 mmol) and 30 mL distilled H_2O. A heavy, white precipitant immediately formed and was filtered from the aqueous solution after 30 minutes mixing. The solution was transferred to a 500-mL separatory funnel, treated with 6.50 g NaN_3, and vigorously shaken. The product was extracted with 100 mL

$CHCl_3$, dried by Na_2SO_4, filtered and rinsed with an additional 30 mL $CHCl_3$. Solution volume was reduced to ~15 mL volume *in vacuo* and the final product was recrystallized by the addition of 300 mL diethyl ether. A fine, dark brown microcrystalline solid was collected by filteration and dried in air. Yield 146 mg (47.3 %). Single crystals suitable for X-ray diffraction were obtained by slow diffusion of pentane into a saturated CH_2Cl_2 solution of the complex. Anal. Calcd. for $C_{12}H_{18}N_5O_2Mn$: C, 45.15; H, 5.68; N, 21.94. Found C, 44.62; H, 5.61; N, 21.19.

Synthesis of [*N*,*N*'-bis(acetylacetone)-1,2-ethylenediimine]manganese(III) nitrate ethanol [(acacen)$MnNO_3$(EtOH)] (3-4). A 125-mL round-bottom flask was charged with 0.200 g **3-2** (640 mmol), 0.120 g $AgNO_3$ (704 mmol), and 25 mL distilled H_2O. After 60 minutes mixing a heavy, white precipitant was remove by filtration. The final product was obtained by removal of H_2O *in vacuo* (24 h) and azeotrope of benzene to give 153 mg (70.5%) of a fine brown powder. Single crystals suitable for X-ray diffraction were obtained by slow diffusion of diethyl ether into a saturated EtOH solution of the complex.

Infrared Equilibrium and Binding Studies. Equilibrium studies were carried out by use of a Beer's Law plot obtained through measuring absorption versus concentrations of **3-3** in chloroform at 0.0188 M, 0.015 M, 0.0113 M, 0.0108 M, 0.0075 M. A 0.0188 M chloroform solution of **3-3** was then used in conjunction with 10, 12.5, 15, 17.5, and 20 equivalents of DMAP to determine concentration of both five- and six-coordinate species under varying conditions. Binding studies with other cocatalyst were

performed in a similar manner through the use of a 0.0188 M chloroform solution of **3-3** with varying equivalents (5 to 100) of the species under study.

Copolymerization Reactions. Polymerization experiments were performed using a 300-mL Parr autoclave heated to 80 ºC overnight while under vacuum. Reaction mixtures were prepared by dissolving 50 mg of catalyst and the appropriate amount of cocatalyst in neat cyclohexene oxide and then added to the reactor by injection port. Typical reactions were run at 80ºC under 35 bar CO_2 pressure for 24 hours. Following each reaction the contents of the reactor was dissolved in CH_2Cl_2 and analyzed by FT-IR to ascertain the presence of cyclic carbonate and polycarbonate.

X-Ray Structural Studies. Single crystals of **3-3', 3-3''·(3-3·DMAP)**, and **3-3·pyr** suitable for X-Ray diffraction were obtained by slow diffusion of pentane into an (acacen)MnN_3/CH_2Cl_2 solution containing 20 equivalents of Ph_3P, 10 equivalents DMAP and a solution of **3-3** in pyridine, respectively. For all reported structures a Leica IC A, MZ 75 microscope was used to identify suitable crystals of the same habit. Each crystal was coated in paratone, affixed to a Nylon loop and placed under streaming nitrogen (110K) in a Bruker SMART 1000 CCD or Bruker-D8 Adv GADDS diffractometer. Space group determination was made on the basis of systematic absences and intensity statistics. Crystal structures were solved by direct methods (for **3-3**, **3-3''•(3-3•DMAP)**, and **3-3•pyr**) or DIRDIF (for **3-1•2H_2O, 3-3'**, and **3-4•EtOH)**) and refined by full-matrix least squares on F^2. Except in the cases of water and ethanol, all H atoms were placed in idealized positions with fixed isotropic displacement parameters equal to 1.5 times (1.2 for methyl protons) the equivalent isotropic

displacement parameters of the atom to which they are attached. Water and ethanol protons were located by Fourier difference maps. All non hydrogen atoms were refined using anisotropic displacement parameters.

Programs used: data collection and cell refinement, SMART WNT/2000 Version 5.632[45] or FRAMBO Version 4.1.05 (GADDS)[46]; data reductions, SAINTPLUS Version 6.63[36]; absorption correction, SADABS[47]; structural solutions, SHELXS-97[38]; DIRDIF-99.2[48] and WinGX Version 1.70.01[49]; structural refinement, SHELXL-97[38]; graphics and publication materials, SHEXTL Version 6.14[39] and X-Seed Version 1.5.[40]

Results and Discussion

Synthesis and Structural Characterization of (acacen)MnX Complexes. The synthesis of several five-coordinate, square pyramidal complexes of the general formula (acacen)MnX have been well-developed, thereby providing a reliable route to numerous derivatives.[30] The procedure reported, however, is rather cumbersome as it requires the formation of (acacen)MnCl (**3-2**) from (acacen)Mn(OAc) (**3-1**), which was previously isolated from the reaction of $Mn(OAc)_3$ and H_2acacen in methanol. That is, the recovery of (acacen)MnCl from the aqueous solution involves several extractions of the complex with copious quantities of chloroform. Furthermore, the anion exchange reaction of (acacen)MnCl with a NaX salt requires multi-step, lengthy extraction processes. A more convenient preparation of the desired azide analog was achieved by the *in situ* formation of the intermediate (acacen)$MnNO_3$ (**3-4**) derivative by Equation 3-1. Direct reaction of the aqueous solution of complex **3-4** with NaN_3 followed by a one-step extraction with a

minimum quantity of chloroform led to an acceptable yield (47.3%) of (acacen)MnN_3 (**3-3**). Presumably, this variation is a general method for the synthesis of (acacen)MnX derivatives from complex **3-4** and NaX.

(3-1)

Numerous examples of manganese(III) Schiff base complexes have been reported exhibiting both monomeric and extended polymeric coordination modes. In the former case both five- and six-coordinate complexes have been crystallographically described, with (acacen)MnCl and (bzacen)MnCl[50] (bzacen = *N,N′-bis*(benzoylacetone)-1,2-ethylenediimine) remaining five-coordinate. Six-coordinate complexes have been structurally characterized as both cations, e.g., [(bzacen)Mn$(MeOH)_2$]ClO_4,[51] or neutral species such as (bzacen)Mn(NCS)(pyrimidine)[52] or (salphen)Mn(NCS)(MeOH).[53] One-dimensional polymeric coordination complexes containing an apical ligand capable of forming a bridge to an adjacent metal center in the solid state have been reported and include, (acacen)Mn$N(CN)_2$,[54] (bzacen)MnOAc,[55] and (bzacen)MnN_3[56]. Other related Schiff base complexes exhibiting a similar propensity in the solid state are (salen)MnOAc,[57] (salpn)MnN_3,[58,59] and (2-OH-salpn)MnOAc.[60] An azide-bridged polymer chain has also been reported for $(acac)_2MnN_3$.[61] Crystallographic data pertaining to all complexes structurally characterized in this study are provided in Table 3-1.

Table 3-1. Crystallographic Data for (Acacen)MnX Derivatives.

	3-1•2H_2O	**3-3**	**3-3'**	**3-4•EtOH**	**3-3''•(3•DMAP)**	**3-3•Pyr**
empirical formula	$C_{14}H_{24}MnN_2O_{5.5}$	$C_{12}H_{18}MnN_5O_2$	$C_{24}H_{36}Mn_2N_{10}O_4$	$C_{14}H_{24}MnN_3O_6$	$C_{31}H_{48}Mn_2N_{12}O_4$	$C_{17}H_{23}MnN_6O_2$
fw	363.29	319.25	638.51	385.30	762.69	398.35
temp(K)	110(2)	110(2)	110(2)	110(2)	110(2)	110(2)
cryst. system	Monoclinic	Monoclinic	Orthorhombic	Monoclinic	Monoclinic	Monoclinic
space group	P2/c	$P2_1/c$	Pcan	$P2_1/n$	$P2_1/c$	P2(1)
a (Å)	17.165(2)	10.2639(11)	13.778(10)	8.1727(5)	8.7824(9)	6.5564(5)
b (Å)	6.7320(9)	13.5749(15)	19.679(15)	17.1898(11)	13.9008(14)	14.10006(11)
c (Å)	14.886(2)	11.3173(11)	20.056(15)	12.3854(8)	28.352(3)	10.0027(8)
β (deg)	109.339(2)	112.173(6)		94.7680(10)	90.793(2)	93.029(4)
V ($Å^3$)	1623.1(4)	1460.2(3)	5438(7)	1733.97(19)	3461.0(6)	923.45(12)
D(calcd)(g/cm^3)	1.487	1.452	1.560	1.476	1.464	1.433
Z	4	4	8	4	4	2
abs. coeff. (mm^{-1})	0.841	7.441	0.980	0.796	0.785	6.019
obs. relfcns	10674	10112	36076	16375	19090	7612
unique relfcns [$I > 2\sigma(I)$]	2790	2238	4657	3952	6101	2707
restraints/params	12/209	0/185	204/361	0/222	0/452	1/239
goodness-of-fit on F^2	1.058	1.004	1.022	0.989	1.057	1.005
R, [a] [$I > 2\sigma(I)$]	0.0557	0.0488	0.0793	0.0689	0.0497	0.0471
R_w, [b] [$I > 2\sigma(I)$]	0.1361	0.1013	0.1902	0.1622	0.1231	0.0950

[a] $R = \Sigma||F_o| - |F_c||/\Sigma|F_o|$ [b] $R_w = \{[\Sigma w(F_o^2 - F_c^2)^2]/[\Sigma w(F_o^2)^2]\}^{1/2}$, $w = 1/[\sigma^2(F_o^2) + (aP)^2 + bP$, where $P = [\max(F_o^2),0) + 2(F_c^2)]/3$.

The X-ray structure of one member of the series of (acacen)MnX derivatives discussed herein, (acacen)MnCl (**3-2**), has previously been reported.[30] Crystals of the acetate (**3-1**) and azide (**3-3**) analogs suitable for X-ray diffraction were grown by the slow diffusion of pentane into a concentrated dichloromethane solution of the respective complexes. Perspective thermal ellipsoid drawings of **3-1** and **3-3** are provided in Figures 3-1 and 3-2, along with a depiction of the resulting metal bridged polymeric chain. In each case, distortion of the ligand is presumed to be the result of steric interactions between bridged metal complexes. In **3-1•2H$_2$O** the acetates provide a near linear bridge between adjacent manganese centers with a Mn(1)–O(3)–O(4) bond angle of 171.12º (Table 3-2). This complex exhibits greater linearity than the analogous angle of 166.1º measured in (bzacen)MnOAc.[55] In addition, least-square plane calculations

Table 3-2. Selected Bond Distances and Angles for **3-1•2H$_2$O**, **3-3**, **3-3'**, **3-3"·(3-3·DMAP), 3-4·EtOH** and **3-3·pyr.**

		3-1•2H$_2$O	
N_2O_2 plane			
Mn(1)-O(1)	1.904(2)	Mn(1)-N(1)	1.977(3)
Mn(1)-O(2)	1.898(2)	Mn(1)-N(2)	1.985(3)
O(2)-Mn(1)-O(1)	91.71(10)	O(1)-Mn(1)-N(1)	91.77(11)
O(2)-Mn(1)-N(2)	92.62(11)	N(1)-Mn(1)-N(2)	83.92(12)
acetate bridge			
Mn(1)-O(3)	2.2414(18)	Mn(1)-O(4)	2.2887(19)
O(1)-Mn(1)-O(3)	90.56(7)	Mn(1)-O(4)-C(13)	144.7(2)
O(1)-Mn(1)-O(4)	88.96(7)	Mn(1)-O(3)-O(4)	171.25(9)
Mn(1)-O(3)-C(13)	147.2(2)		
metal-to-metal			
Mn-Mn (polymeric)	6.73(2)		
		3-3	
N_2O_2 plane			
Mn(1)-O(1)	1.909(3)	Mn(1)-N(1)	1.982(4)
Mn(1)-O(2)	1.917(3)	Mn(1)-N(2)	1.978(3)
O(2)-Mn(1)-O(1)	93.22(12)	O(1)-Mn(1)-N(1)	90.92(13)

Table 3-2. Continued.

3-3, Continued			
O(2)-Mn(1)-N(2)	92.55(13)	N(1)-Mn(1)-N(2)	83.31(14)
azide bridge, $\mu_{1,3}$			
Mn(1)-N(3)	2.284(4)	Mn(1)-N(5)	2.299(4)
O(1)-Mn(1)-N(3)	87.95(13)	Mn(1)-N(3)-N(4)	120.2(3)
O(1)-Mn(1)-N(5)	91.88(13)	Mn(1)-N(5)-N(4)	123.9(3)
metal-to-metal			
Mn-Mn (polymeric)	5.66(4)		
3-3'			
N_2O_2 plane			
Mn(1)-O(1)	1.921(5)	Mn(2)-O(3)	1.900(4)
Mn(1)-O(2)	1.901(4)	Mn(2)-O(4)	1.911(4)
Mn(1)-N(1)	1.978(5)	Mn(2)-N(3)	1.959(5)
O(2)-Mn(1)-O(1)	93.6(2)	O(4)-Mn(2)-O(3)	92.54(19)
O(2)-Mn(1)-N(2)	91.1(2)	O(4)-Mn(2)-N(4)	91.5(2)
O(1)-Mn(1)-N(1)	92.0(2)	O(3)-Mn(2)-N(3)	91.9(2)
N(1)-Mn(1)-N(2)	83.1(2)	N(3)-Mn(2)-N(4)	83.9(2)
azide bridge, $\mu_{1,3}/\mu_{1,1}$			
Mn(1)-N(5)	2.326(5)	Mn(2)-N(8)	2.375(4)
Mn(2)-N(5)	2.328(5)	Mn(1)-N(10A)	2.320(6)
O(1)-Mn(1)-N(5)	93.5(2)	O(3)-Mn(2)-N(8)	88.14(19)
O(3)-Mn(2)-N(5)	92.40(19)	O(1)-Mn(1)-N(10A)	86.6(2)
Mn(1)-N(5)-N(6)	110.6(4)	Mn(2)-N(8)-N(9)	114.9(4)
Mn(2)-N(5)-N(6)	110.6(4)	Mn(1)-N(10A)-N(9)	128.6(5)
Mn(1)-N(5)-Mn(2)	138.8(3)		
metal-to-metal			
Mn(1)-Mn(1) (poly.)	10.03(3)	Mn(1)-Mn(2) (EE)	6.05(8)
Mn(1)-Mn(2) (EO)	4.35(6)		
3-3•DMAP			
N_2O_2 plane			
Mn(1)-O(1)	1.9160(19)	Mn(1)-N(1)	1.966(2)
Mn(1)-O(2)	1.9226(18)	Mn(1)-N(2)	1.988(2)
O(2)-Mn(1)-O(1)	92.27(8)	O(1)-Mn(1)-N(1)	91.84(9)
O(2)-Mn(1)-N(2)	92.93(9)	N(1)-Mn(1)-N(2)	82.58(9)
apical ligands			
Mn(1)-N(3)	2.214(3)	N(3)-N(4)	1.164(4)
Mn(1)-N(6)	2.388(2)	N(4)-N(5)	1.171(4)
O(1)-Mn(1)-N(3)	94.61(9)	O(1)-Mn(1)-N(6)	85.30(8)
Mn(1)-N(3)-N(4)	142.1(2)		
3-3"			
N_2O_2 plane			
Mn(2)-O(3)	1.8951(18)	Mn(2)-N(15)	1.972(2)
Mn(2)-O(4)	1.8952(19)	Mn(2)-N(16)	1.967(2)
O(4)-Mn(2)-O(3)	88.83(8)	O(3)-Mn(2)-N(15)	91.42(8)

Table 3-2. Continued.

3-3", Continued			
O(4)-Mn(2)-N(16)	91.22(9)	N(15)-Mn(2)-N(16)	83.86(9)
apical ligands			
Mn(2)-N(17)	2.084(2)	N(18)-N(19)	1.164(4)
N(17)-N(18)	1.175(3)		
O(3)-Mn(2)-N(17)	98.50(9)	Mn(2)-N(17)-N(18)	143.3(2)
3-4•EtOH			
N_2O_2 plane			
Mn(1)-O(1)	1.892(2)	Mn(1)-N(1)	1.973(2)
Mn(1)-O(2)	1.906(2)	Mn(1)-N(2)	1.965(2)
O(2)-Mn(1)-O(1)	91.45(9)	O(1)-Mn(1)-N(1)	92.76(9)
O(2)-Mn(1)-N(2)	91.34(9)	N(1)-Mn(1)-N(2)	84.48(10)
apical ligands			
Mn(1)-O(3)	2.308(2)	N(3)-O(4)	1.258(3)
Mn(1)-O(6)	2.254(2)	N(3)-O(5)	1.232(3)
N(3)-O(3)	1.265(3)		
O(1)-Mn(1)-O(3)	95.56(8)	O(1)-Mn(1)-O(6)	89.15(8)
Mn(1)-O(3)-N(3)	134.01(19)	Mn(1)-O(6)-C(13)	120.44(18)
3-3•Pyr			
N_2O_2 plane			
Mn(1)-O(1)	1.898(3)	Mn(1)-N(1)	1.986(4)
Mn(1)-O(2)	1.918(4)	Mn(1)-N(2)	1.962(4)
O(2)-Mn(1)-O(1)	91.03(15)	O(1)-Mn(1)-N(1)	92.75(16)
O(2)-Mn(1)-N(2)	92.14(16)	N(1)-Mn(1)-N(2)	83.52(18)
apical ligands			
Mn(1)-N(3)	2.220(5)	N(3)-N(4)	1.193(6)
Mn(1)-N(6)	2.432(4)	N(4)-N(5)	1.168(6)
O(1)-Mn(1)-N(3)	92.05(16)	O(1)-Mn(1)-N(6)	87.72(15)
Mn(1)-N(3)-N(4)	127.3(4)		

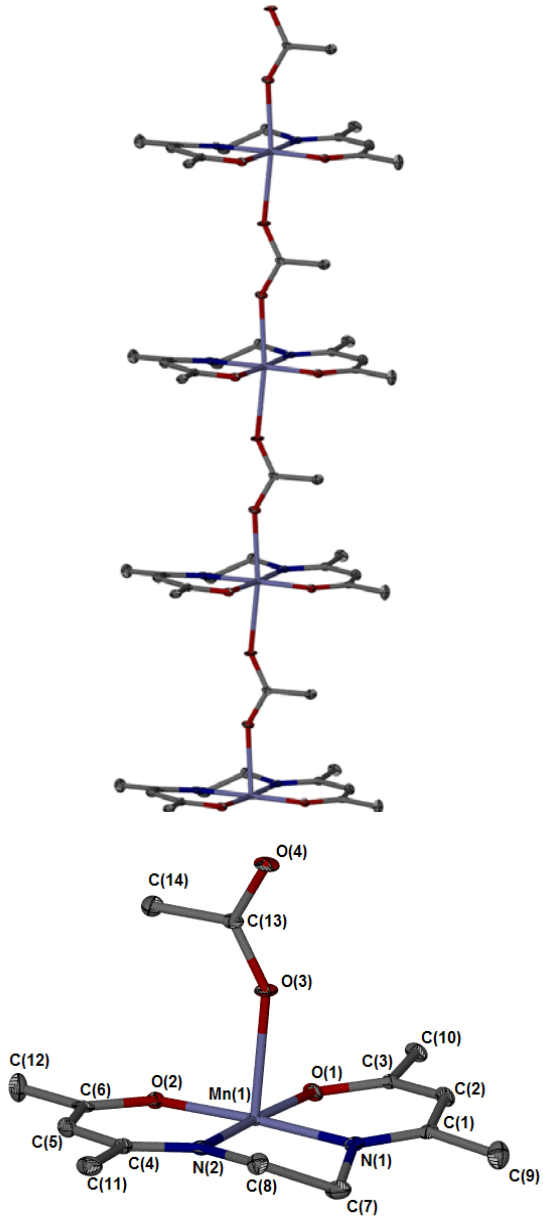

Figure 3-1. Thermal ellipsoid plot of **3-1•2H$_2$0** at 50% probability. Waters are omitted for clarity. The polymer chain viewed along the *b* axis.

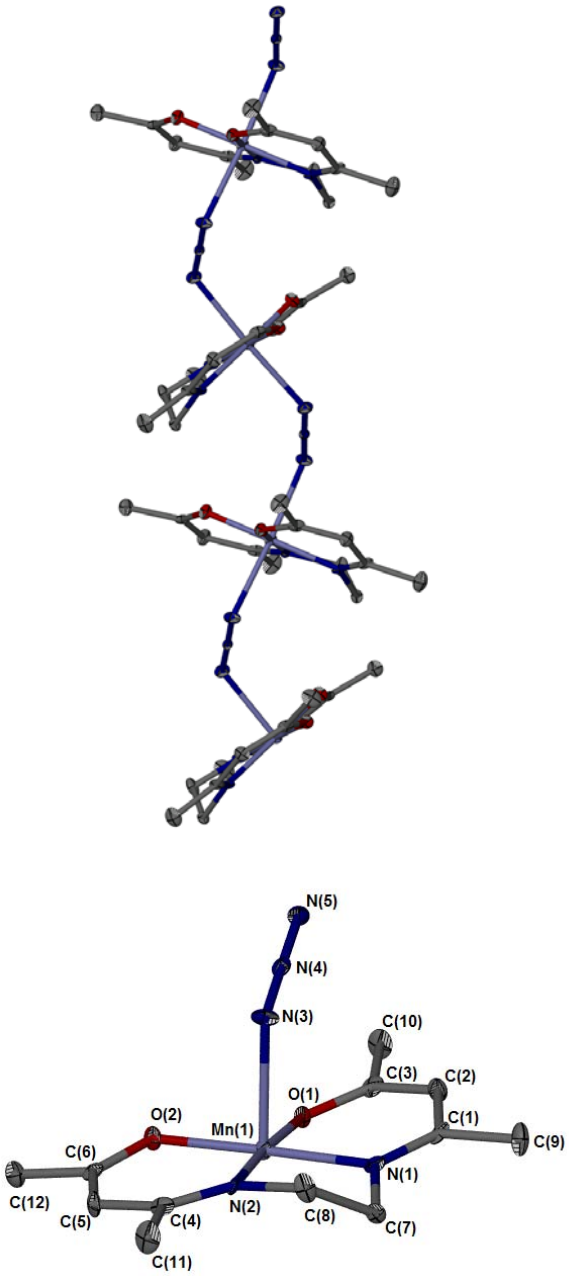

Figure 3-2. Thermal ellipsoid plot of **3-3** at 50% probability. The polymer chain viewed along the *c* axis.

can be used to analyze ligand distortion by defining the three planes that compose the acacen complex, namely, the N_2O_2 plane and the two planes composed of O(1)–N(1)–C(1)–C(3) [**ring 1**] and O(2)–N(2)–C(4)–C(6) [**ring 2**]. The dihedral angles between **ring 1** and **ring 2** and the N_2O_2 plane of **3-1•2H$_2$O** are 7.4º and 1.4º, respectively (Table 3-3). This is in contrast to the same dihedral angles measured in **3-3** found to be 17.2º and 12.9º. In this instance, the bridging azides give a helical shape to the metal-ligand chain resulting from the metal-azide bond angles of 120.1º and 123.9º for Mn(1)–N(3)–N(4) and Mn(1)–N(4)–N(5), respectively. The helical shape assures a steric influence on adjacent complexes by pushing the rings of the ligand further out of plane from one another. Additional indication of this can be seen from the buckling of the ethylene backbone as evidenced by an increase in distance of over 0.12 Å from the N_2O_2 plane for C(8) compared to that in **3-1•2H$_2$O** (Table 3-3).

Table 3-3. Selected Displacements and Dihedral Angles from N_2O_2 Plane.[a]

Structure	Mn-N_2O_2 planar displac. (Å)	C(7)-N_2O_2 planar displac. (Å)	C(8)-N_2O_2 planar displac. (Å)	dihedral ring 1[b] to ring 2[b], (deg)	dihedral ring 1[b] to N_2O_2 plane (deg)	dihedral ring 2[b] to N_2O_2 plane (deg)
3-1•2H$_2$O	0.0139	-0.3893	0.1269	8.3	7.4	1.4
3-3	0.0000	-0.3888	0.2522	4.6	17.2	-12.9
3-3' Mn(1)	0.0624	-0.0416	0.5021	22.4	-8.4	-30.8
3-3' Mn(2)	0.068	-0.3900	0.284	22.2	16.1	7.1
3-3•DMAP	0.0785	0.5119	0.0270	27.0	-22.5	-4.5
3-3''	0.2755	-0.2247	0.2649	8.5	3.2	-11.3
3-4•EtOH	0.0138	-0.2420	0.3022	5.4	9.7	-15.1
3-3•Pyr	0.0925	-0.0771	0.4457	29.8	-8.5	-21.3

[a] for least-square plane analysis see Appendix B

[b] ring 1 = N(1)-O(1)-C(1)-C(3), ring 2 = N(2)-O(2)-C(4)-C(6)

Manganese displacement from the N_2O_2 plane can be a function of coordinating ligands apical to the acacen moiety. In the case of **3-1·2H$_2$O**, the manganese oxygen bond to the acetate ligands differs by 0.0474 Å leading to a displacement of 0.0139 Å of the manganese atom out of the N_2O_2 plane. The addition of benzyl rings in $[(bzacen)MnOAc]_n$ derivative lowers this difference to 0.025 Å with no measurable displacement of the manganese from the coordination plane observed.

In **3-3** the manganese exhibits no measurable planar displacement and the metal azide bond lengths differ by only 0.015 Å. A greater metal displacement of 0.0695Å is obtained with the addition of benzyl rings in $[(bzacen)MnN_3]_n$[56], a complex which also forms a metal azide chain in a helical arrangement. In the structure of $[(salpn)MnN_3]_n$ the metal azide bond lengths differ by only 0.017 Å, however, the phenolate moieties of the salpn lie at 44º angle towards each other consequently forcing the manganese 0.0540 Å out of the N_2O_2 plane[58,59].

In an attempt to isolate and characterize a six-coordinate derivative of $(acacen)MnN_3$ containing a phosphine ligand, crystals of complex **3-3'** were obtained from a CH_2Cl_2 solution of **3-3** in the presence of 20 equivalents of triphenylphosphine. Complex **3-3'** was shown by X-ray crystallography to be a polymorph of **3-3** with a mixed coordination mode of $\mu_{1,1}/\mu_{1,3}$ bridging azides to form a polymer chain of $[((acacen)MnN_3)_2]_n$ (Figure 3-3). Such extended structures containing an end-on (EO) or end-to-end (EE) bridging azide have gained popularity recently because of their ferromagnetic properties, especially in the case of manganese(II) 1D and 3D chains.[62,63,64,65]

It can be seen from Figure 3-3 that the two acacen ligands of the asymmetric unit of **3-3'** are directed towards each other at an angle of 41.2º (from the Mn(1)–N(5)–Mn(2) angle of 138.8º) by the sp^2 hybridized nitrogen atom of the EO bridging azide. This leads to a 30.8º distortion of ring 2 from the Mn(1) N_2O_2 plane, the largest of any such distortion observed in this study. In the extended polymer structure the repeating unit $((acacen)MnN_3)_2$ forms a helical pattern with its neighbor by being rotated approximately 180º and returning to its original orientation every third metal complex along the polymer chain. The EO azide-bridged Mn(1)···Mn(2) separation is 4.356 Å and represents the closest metal–metal distance in any of the polymeric structures reported herein (Table 3-2).

As will be illustrated later in this chapter, it will be demonstrated, *via* IR solution binding studies, that **3-3** will bind DMAP ((4-dimethylamino)pyridine) reversibly to the manganese center (Equiation 3-2) when an excess of the amine is employed. Efforts were made to obtain suitable crystals of the six-coordinate $(acacen)Mn(N_3)(DMAP)$ complex for X-ray crystallographic characterization by layering pentane over a saturated chloroform solution of **3-3** and 10 equivalents of DMAP. The resulting crystals were analyzed and shown to contain an asymmetric unit which included both five- and six-coordinate complexes, **3-3•DMAP** and **3-3''**, respectively (Figure 3-4). This finding is rather remarkable in that the two coexisting complexes found in the solid-state represent both derivatives involved in the equilibrium in equation 3-2 (*vide infra*).

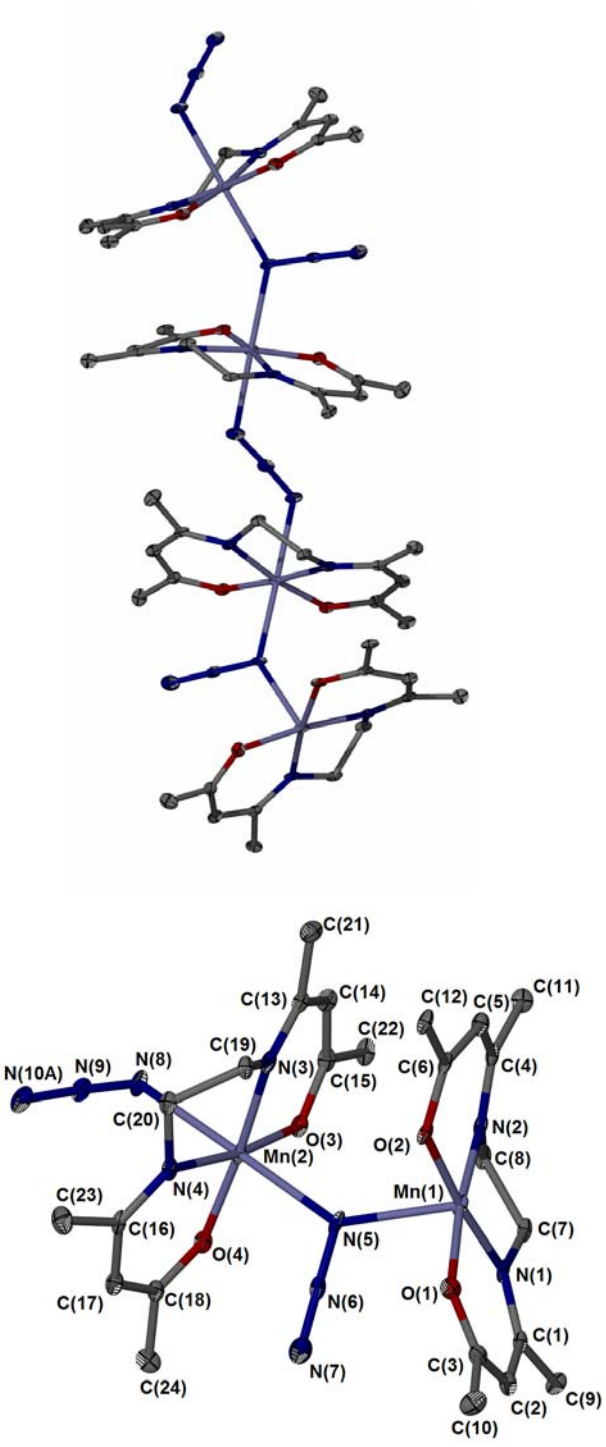

Figure 3-3. Thermal ellipsoid plot of **3-3'** at 50% probability. The polymer chain viewed along the *c* axis.

$$(acacen)MnN_3 + DMAP \rightleftharpoons (acacen)Mn(N_3)(DMAP) \qquad (3\text{-}2)$$

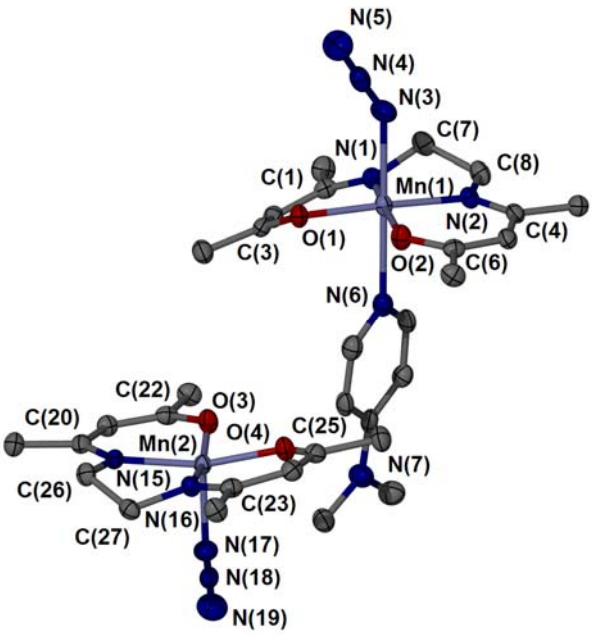

Figure 3-4. Thermal ellipsoid plot of **3-3•DMAP** and **3-3''** at 50% probability.

Six-coordinate manganese derivatives containing heterocyclic amines as apical ligands have previously been structurally characterized, including (bzacen)Mn(NCS)(pyrimidine)[52] and (bzacen)Mn(NCS)(4,4'-bypiridine).[66,67] In the former complex the manganese-pyrimidine bond distance of 2.504 Å is 0.307 Å longer than the Mn–NCS bond distance. This elongation is likely due to the steric influence of the benzyl rings on the heterocyclic amine. Without the influence of the benzyl rings the difference in the two Mn–apical nitrogen bonds is 0.174 Å with the manganese-DAMP

bond distance shortened to 2.388(2). The orientation of the ring system of DMAP and the three atom chain of the azide ligand runs along the bisection of the O(1)–Mn(1)–O(2) angle which may account for the saddle type distortion of the acacen rings.

The structure of **3-3''** is of interest due to the lack of a sixth ligand *trans* to the anion and consequently is more akin to the species in solution. To date the only other instances of coordinatively unsaturated manganese acacen complexes in the solid-state are those previously mentioned, (acacen)MnCl and (bzacen)MnCl. The lack of any steric demand from a sixth ligand is evident by the considerable out-of-plane displacement of the manganese atom from the N_2O_2 plane (Table 4-3). Of the three examples, (acacen)MnCl possesses the largest distance of 0.344 Å, followed by 0.304 Å for (bzacen)MnCl and 0.275Å for **3-3''**. In the former two cases the acacen ligand holds a saddle shape where both of the acetyl imine rings are angled below the Mn-Cl bond (14.9º/18.6º for acacen and 10.6º/14.0º for bzacen). The azide complex, conversely, has a step type arrangement where one ring (**ring 1**) is angled 3.2º toward the Mn–N_3 and the other (**ring 2**) 11.3º below. This is likely due to the close proximity of **3-3•DMAP**. The absence of a sixth ligand also removes any *trans* effect on the metal-azide bond and subsequently leads to a shortened manganese-nitrogen bond distance of 2.084 Å.

Infrared spectroscopic monitoring of the binding studies of complex **3-3** in chloroform with pyridine also reveals the formation of a six-coordinate manganese azide complex. X-ray quality crystals of (acacen)Mn(N_3)(pyridine) (**3-3•pyr**) were obtained and its structure determined to be that depicted in Figure 3-5. As anticipated the structure of **3-3•pyr** bares numerous similarities to **3-3•DMAP** with the manganese

displaced from the N_2O_2 plane by 0.0925Å and a saddle shaped acacen configuration with the ring dihedral angles of 8.5º and 21.3º below the coordination plane. Interestingly, both the azide and pyridine are closely oriented along the line N(2)–Mn(1)–O(1) which represents a nitrogen rich plane of five nitrogen atoms. This coplanar relationship is also seen in **3-3•DMAP** were the azide and DMAP are oriented in much the same way.

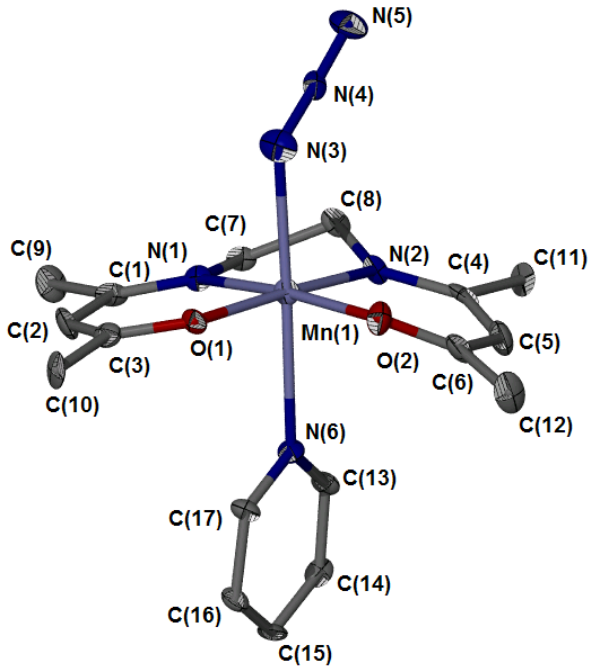

Figure 3-5. Thermal ellipsoid plot of **3-3•pyr** at 50% probability.

Crystals of the synthetically useful intermediate (acacen)$MnNO_3$ were grown by layering ether over a saturated solution of the complex in ethanol. A thermal ellipsoid representation of the ethanol adduct of (acacen)$MnNO_3$, complex **3-4•EtOH**, is provided in Figure 3-6. The structure of **3-4•EtOH** bares some resemblance to **3-1•H_2O** in that manganese forms an octahedral complex consisting of a N_2O_2 coordination plane and two axial ligands bound through oxygen atoms. This results in a nearly identical metal displacement from the N_2O_2 plane of 0.0138Å which can be attributed to a similar difference of 0.054Å in the axial manganese-oxygen bond distances. Originally it was assumed that the nitrate anion would be non-coordinating as seen in the perchlorate derivative, [(bzacen)$Mn(MeOH)_2$]ClO_4.[51] However, coordinated perchlorate and nitrite anions have been observed in the case of manganese bzacen complexes in the presence of methanol, ethanol, and acetonitrile.[68,69] Strong hydrogen bonding between the ethanol proton H(6A) and O(4) of the nitrate ligand leads to a chain-like solid-state structure with a hydrogen-acceptor distance of 1.84Å.

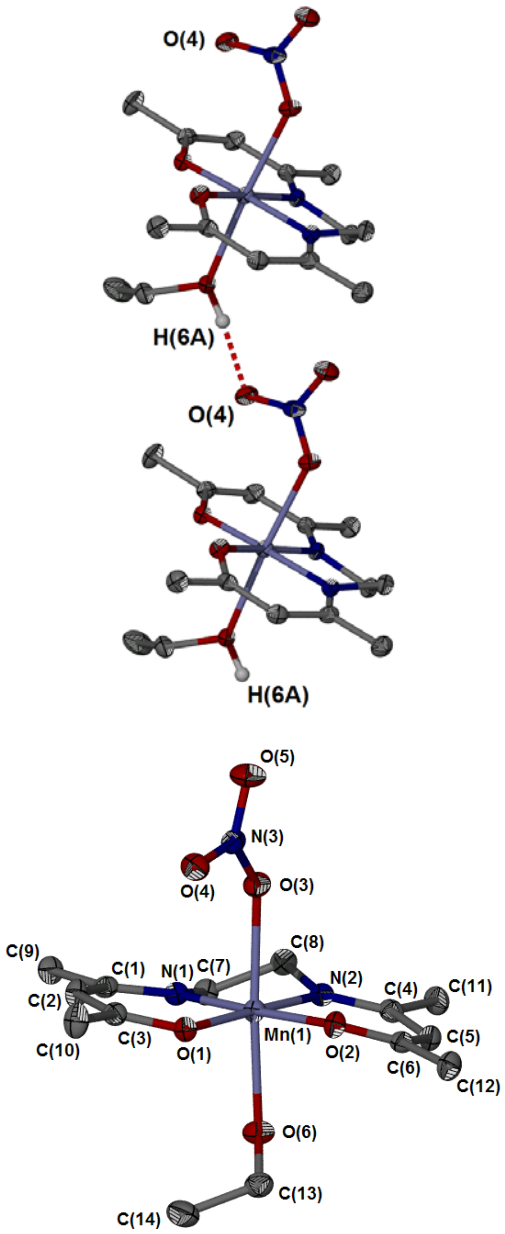

Figure 3-6. Thermal ellipsoid plot of **3-4•EtOH** at 50% probability. The hydrogen bond is viewed along the *a* axis.

Chemistry Pertinent to the Copolymerization of CO_2 and Epoxides in the Presence of Metal Schiff Base Catalysts. Complexes **3-1**, **3-2**, and **3-3** in the presence of 1 equivalent of *n*-Bu_4NN_3 as a cocatalyst, and following the common catalysis protocol (35 bar CO_2 and 80 ºC), were ineffective at copolymerizing CO_2 and cyclohexene oxide.[70] These observations are in stark contrast to the highly active chromium and cobalt Schiff base catalyst systems.[20,23,71] In an effort to understand the reasons for this difference between the closely related d^3 and d^4 transition metal systems, a binding study has been performed on a variety of ligands at the five-coordinate manganese center. To accomplish this the (acacen)MnN_3 derivative has been employed since the ν_{N_3} stretching vibration is quite sensitive to coordination of a sixth ligand at the metal center.[17a,b] An inability of epoxides to bind to the metal center would greatly inhibit or prevent polymerization from occurring. *It should be noted here that a wide range of ligands, including weakly binding epoxides, readily coordinate to the metal center at equimolar concentrations in (salen)CrX derivatives.*

Figure 3-7 illustrates the infrared spectrum of **3-3** in the non-coordinating solvent toluene where the asymmetric stretching mode of azide occurs at 2043 cm^{-1}. Surprisingly, an identical ν_{N_3} vibration is observed at 2043 cm^{-1} when complex **3-3** is dissolved in cyclohexene oxide. That is, even at this very high concentration of cyclohexene oxide, the manganese center remains coordinatively unsaturated. On the other hand, a six-coordinate manganese complex is observed with a ν_{N_3} vibrational mode at 2031 cm^{-1} in the presence of the strongly coordinating pyridine ligand. The solid-state

structure of this six-coordinate manganese derivative, **3-3•pyr**, was described earlier in this report.

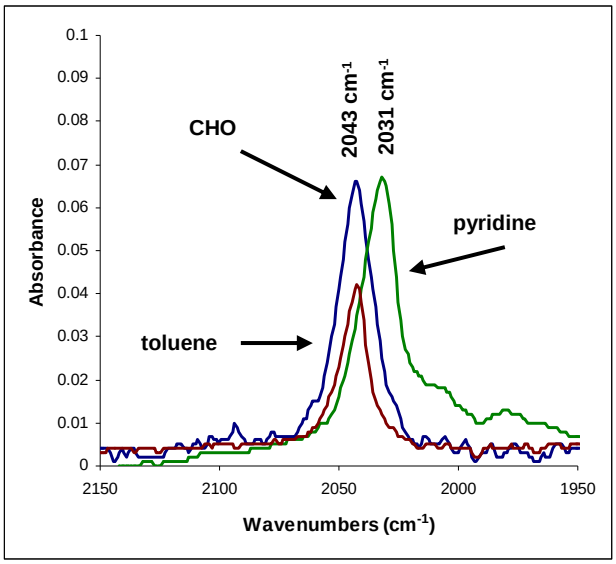

Figure 3-7. Spectra of **3-3** in toluene, cyclohexene oxide and pyridine.

Due to the limited solubility of complex **3-3** in toluene, it was advantageous to change to chloroform as an alternative, slightly more interacting solvent, in order to acquire quantitative spectral data. In chloroform, the five-coordinate manganese azide ν_{N_3} band in complex **3-3** occurs at 2050 cm^{-1}. The addition of one equivalent of $(^{n}Bu_4)NN_3$ to **3-3** failed to result in the formation of a manganese diazide species as is seen with (salen)CrN_3.[27] However, two azide stretching modes are seen in the infrared spectrum of complex **3-3** in the presence of $(^{n}Bu_4)NN_3$, one resulting from **3-3** and the other the result of the "free" azide anion at 2014 cm^{-1} (Figure 3-8). Phosphines display a

similar disinclination to bind to the manganese center in **3-3**, though in this instance no spectroscopic evidence exists for the formation of a (salen)Cr(N_3)(PR_3) complex. The absence of the bulky substituted phenolate rings of salen in acacen could conceivably favor the binding of a bulky ligand such as tricyclohexylphosphine to **3-3**. However, as is readily seen in Figure 3-8, neither 20 equivalents of Cy_3P nor 100 equivalents of (^{n}Bu)$_3$P show any tendency to bind to complex to the metal enter.

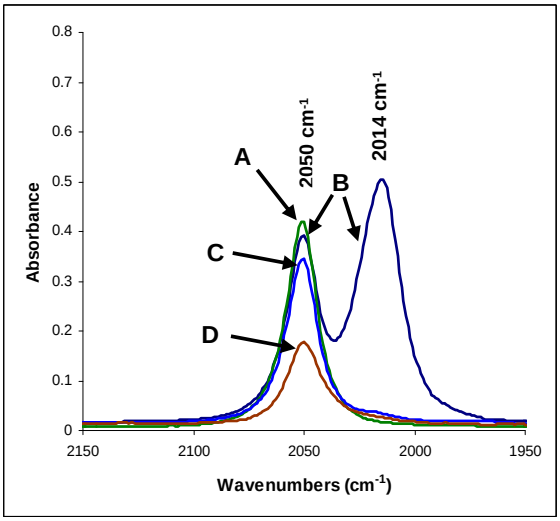

Figure 3-8. Spectra of chloroform solutions of **3-3** with (**A**) representing the five coordinate manganese azide complex, (**B**) the five coordinate complex with 1 eq. "free" azide (from (^{n}Bu$_4$)N$_3$) and (**C**) and (**D**) with 20 eq. of (Cy)$_3$P and 100 eq. (^{n}Bu)$_3$P, respectively.

On the other hand, as previously demonstrated both in the solid-state and in solution, pyridine readily binds to complex **3-3** (Figure 3-9). Other heterocyclic amines such as DMAP and DBU were also found to coordinate to the manganese center in **3-3**. The binding of DMAP to complex **3-3** in chloroform solution proved to be an

equilibrium process as depicted in equation 4, with equal quantities of the five-coordinate **3-3** (ν_{N_3} = 2050 cm^{-1}) and six-coordinate **3-3•DMAP** (ν_{N_3} = 2036 cm^{-1}) occurring at approximately 13.5 equivalents of DMAP (Figure 3-9). *Recall crystallization of this reaction mixture led to isolation of crystals containing **3-3•DMAP** and **3-3** in the unit cell (vide supra).* The K_{eq} at ambient temperature was determined to be 3.07 ± 0.02 M^{-1} over the range of ~12.5 equivalents of DMAP. Beyond this concentration of DMAP, a second reaction occurs where the azide ligand is displaced from **3-3•DMAP** resulting in formation of $[(acacen)Mn(DMAP)_2]N_3$. A similar phenomena was observed for the bicyclic amine DBU (Figure 3-9). However, the sterically more demanding DBU ligand requires a significantly more concentrated solution of amine to affect a similar extend of metal binding as seen in the DMAP case.

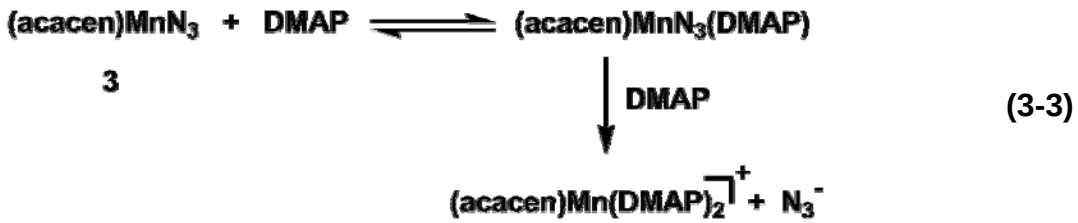

(3-3)

There exists in the literature a substantial amount of mechanistic studies of the copolymerization of propylene oxide and cyclohexene oxide with carbon dioxide in the presence of chromium(III) and cobalt(III) salen catalysts.[9,18,19,22,24,25,27,28b,28h,71,72] The initiation of this process involves either a first- or second-order dependence on catalyst concentration. In either case, metal-binding of the epoxide activates the cyclic ether for ring-opening by an external nucleophile (as seen in Scheme 3-2) or a nucleophile on the

(salen)MX catalyst. Propagation of the polymer chain involves the repeated formation of a carbonate anion by CO_2 insertion followed by the ring-opening of an epoxide by the

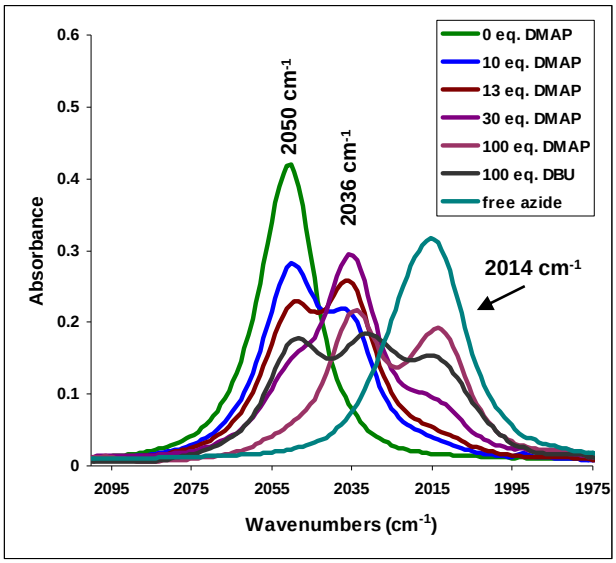

Figure 3-9. Spectra of chloroform solutions of **3-3** with varying concentration of DMAP and DBU. The stretches at 2050 cm-1, 2036 cm-1 and 2014 cm-1 represent five-coordinate, six-coordinate and free azide species, respectively.

same anion. This process is facilitated by the presence of a ligand (cocatalyst) *trans* to the growing polymer chain. That is, it is abundantly clear that a six-coordinate metal complex with a distorted octahedral geometry is necessary for copolymerization to proceed efficiently.

In light of the structural parameters presented herein and elsewhere, it is apparent that these (acacen)MnX complexes are directly related to their (salen)CrX analogs in

Scheme 3-2.

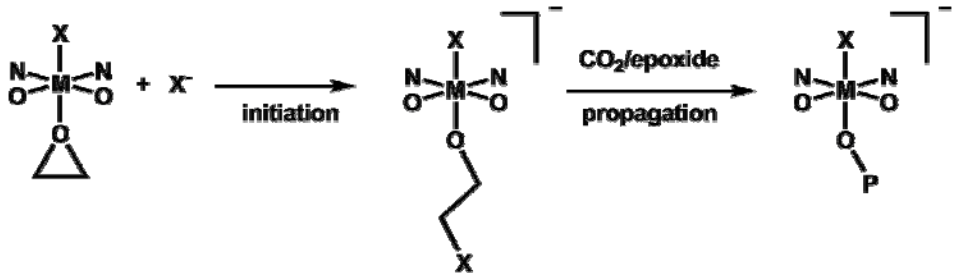

that the acacen ligand bears a saddle or step shape with an axial ligand perpendicular to the N_2O_2 core. The open axial position is critical to the catalytic function of these structurally comparable metal derivatives as it represents an open site for substrate binding. For d^3 chromium(III) octahedral salen complexes the t_{2g} orbitals are half-filled with the e_g antibonding orbitals unoccupied. Similarly, low spin d^6 cobalt(III) octahedral salen complexes possess filled t_{2g} orbitals with unoccupied e_g antibonding orbitals. Conversely, octahedral manganese(III) salen or acacen derivatives are d^4 and are known to be substantially labile due to Jahn-Teller distortion along the z-axis.[73,74] In the case of a high spin S = 2 configuration in the distorted octahedral geometry, the degeneracy of the dz^2 and dx^2-y^2 orbitals is broken with one unpaired electron occupying the dz^2 orbital. In square pyramidal geometry, the dz^2 and dx^2-y^2 (orbitals) also lose degeneracy with the former dramatically lowering in energy (see Figure 3-10). This leads to less distortion along the *z*-direction, making the five-coordinate complex more favorable.

As a consequence of the ineffectiveness of five-coordinate Schiff base derivatives of Mn(III) to bind (activate) weakly coordinating epoxide ligands, thus forming distorted six-coordinate derivatives, these metal complexes are essentially incapable of ring-opening epoxides *via* either first- or second-order initiation processes

effectively. In other words, an octahedral geometry is crucial to an efficient polymerization process.

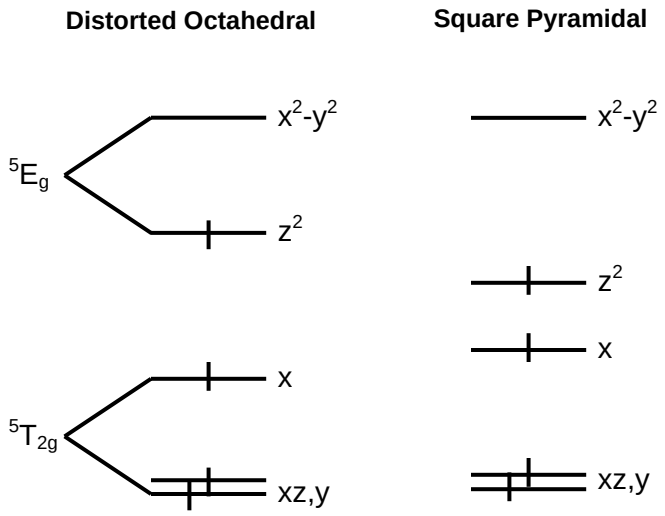

Figure 3-10. Theoretical Ligand Field splittings of *d*-orbitals for six- and five-coordinate Mn(III) complexes.

Indeed, thus far Mn(III) complexes have displayed limited reactivity towards the copolymerization of epoxides and CO_2 with the most active example being Inoue's (tpp)MnOAc catalyst in the presence of cyclohexene oxide.[44] This system afforded low molecular weight copolymer with a TOF of only 16.3 h^{-1} at 80º C, compared to ~1200 h^{-1} under similar reaction conditions for (salen)CrX derivatives. The addition of strongly binding Lewis bases to the (tpp)MnOAc system was shown to inhibit catalytic activity, supportive of a second-order epoxide ring-opening mechanism where the epoxide binding site is blocked in this instance. In that same study, (salphen)MnOAc was ineffective towards formation of copolymer, producing instead only small quantities of poly(cyclohexene oxide).

Conclusions

Several (acacen)MnX complexes have been characterized crystallographically and their reactivity towards serving as catalysts for the copolymerization of cyclohexene oxide and carbon dioxide was evaluated. Although, in the solid-state the azide derivative, (acacen)MnN_3, exists as an extended polymer chain with the azide ligand spanning two manganese centers, in solutions of weakly interacting solvents (acacen)MnN_3 is five-coordinate. The ν_{N_3} stretching vibrational mode in this complex was employed to probe the ability of the manganese to bind a sixth ligand in solution, including anions, epoxides, and heterocyclic amines. This is made possible because the ν_{N_3} stretch in (acacen)MnN_3 shifts to significantly lower frequency upon coordination of an additional axial ligand. The heterocyclic amine donors displayed greatly reduced binding ability in this instance compared to that seen in (salen)CrN_3, however, anions and epoxides displayed *no* inclination to bind as revealed by infrared spectroscopy. Concomitantly, these (acacen)MnX complexes exhibited very limited tendency to couple epoxides and CO_2 to afford copolymer or cyclic carbonate products.

CHAPTER IV

STUDIES OF THE CARBON DIOXIDE AND EPOXIDE COUPLING REACTION IN THE PRESENCE OF FLUORINATED MANGANESE(III) ACACEN COMPLEXES: KINETICS OF EPOXIDE RING-OPENING*

Introduction

As a consequence of the findings obtained with (acacen)MnX derivatives, it is surmised that an increase in the electrophilicity of the metal center of manganese(III) should facilitate the binding of important ligands to the open coordination site. This, in turn, would aid in the formation of the octahedral geometry about the metal center that is critical to the copolymerization process. To examine this hypothesis, a series of previously unreported manganese(III) acacen derivatives have been prepared which possess electron withdrawing trifluoromethyl groups attached to the carbons α to the

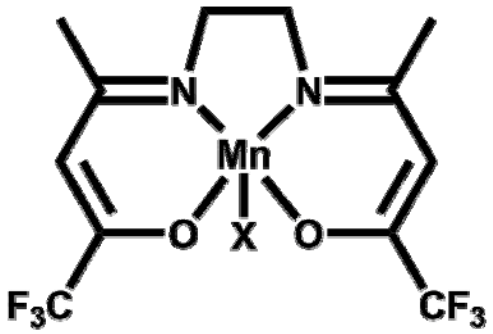

Figure 4-1. Structures of (tfacacen)MnX complexes. **4-1**: X=N_3 , **4-2**: X=Cl , **4-3**: X=NCO , **4-4**: X=NCS.

coordinated oxygen atoms of the ligand (Figure 4-1). The complexes of the form (tfacacen)MnX (tfacacen = *N,N'-bis*(trifluoroacetylacetone)-1,2-ethylenediimine) have been subjected to an extensive spectroscopic examination of the binding of various Lewis bases, such as cyclohexene oxide or DMAP, and anions, such as azide, to the metal center. Also, a kinetic study of epoxide ring-opening in the presence of these metal complexes has been undertaken in an effort to examine mechanistic aspects of the initial step of the polymerization process. In addition, the structural characterization of two complexes possessing the pseudohalides cyanate and thiocyanate are reported along with epoxide ring-opening experiments with these new azide-type initiators.

Experimental

Methods and Materials. Unless otherwise stated, all syntheses and manipulations were carried out on a double-manifold Schlenk vacuum line under an argon atmosphere or in an argon filled glovebox. Methanol, diethyl ether, dichloromethane, and pentane were freshly purified by an MBraun Manual Solvent

Purification System packed with Alcoa F200 activated alumina desiccant. Ethanol was freshly distilled from Mg/I_2. Cyclohexene oxide was purchased from TCI America and freshly distilled from CaH_2. Ethylenediamine (Aldrich), sodium azide (Aldrich), sodium cyanate (Alfa Aesar), potassium thiocycante (MCB), *tetra-n*-butylammoniumazide (TCI America), and $Mn(OAc)_3 \bullet 2H_2O$ (Strem Chemicals Inc.) were all used as received without further purification. 4-(*N,N'*-dimethylamino)pyridine (DMAP, Aldrich) was recrystallized from ethanol/diethyl ether. 1,1,1-Trifluoro-2,4-pentanedione (Aldrich Organics) was dried over molecular sieves before use. Bone dry carbon dioxide equipped with a liquid dip-tube was purchased from Scott Specialty Gases.

The synthesis of *N,N'-bis*(trifluoroacetylacetone)-1,2-ethylenediimine [(tfacacen)H_2] was adapted from a literature procedure.[33] Elemental analysis was provided by Canadian Microanalytical Service LTD, Delta, British Columbia. All infrared spectra were recorded using a Mattson 6021 FTIR spectrometer with DTGS and MCT detectors. All ^{1}H NMR were acquired using Unity+ 300 MHz and VXR 300 MHz superconducting NMR spectrometers.

Synthesis of *N,N'-bis*(trifluoroacetylacetone)-1,2-ethylenediimine [(tfacacen)H_2]. An ethanol solution was prepared by the addition of 5.00 g (32.4 mmol) 1,1,1-trifluoro-2,4-pentanedione to 40 mL of freshly distilled EtOH in a 100-mL round-bottom flask equipped with a stir bar. This flask was placed in an ice bath (0ºC) and ethylenediamine was added dropwise 0.975 g (16.2 mmol). The resulting mixture was stirred for 4 hrs while being warmed to room temperature. The flask was then placed in a freezer for 18 hrs. The final product was collected by filtration, rinsed with cold

ethanol and air dried. Yield 1.62g (30.2%) of colorless crystals. ^{1}H NMR ($CDCl_3$, 300 MHz): δ 11.20 (s, 2H) , 5.39 (s, 2H), 3.63 (t, 4H), 2.07 (s, 6H). Anal. Calcd. for $C_{12}H_{14}F_6N_2O_2$: C, 43.38; H, 4.25; N, 8.43. Found C, 43.60; H, 4.26; N, 8.64.

Synthesis of [*N,N'-bis*(trifluoroacetylacetone)-1,2-ethylenediimine] manganese(III) azide [(tfacacen)MnN$_3$] (4-1). To a 250-mL round-bottom flask 1.00 g of (tfacacen)H_2 (3.00 mmol) and 0.949 g $Mn(OAc)_3$•$2H_2O$ (3.54 mmol) were added along with 40 mL MeOH and a Teflon stir bar. After 18 hrs reaction time, the solvent was removed by rotary evaporation and the resulting solid was dissolved in 100 mL water. Unreacted starting material was removed by filtration and the aqueous solution was added to a 1000-mL separatory funnel. Any residual ligand was extracted with 50 mL CH_2Cl_2 and discarded. To this solution 30 g NaN_3 was added and dissolved by vigorous shaking resulting in the formation of a brown precipitant. The product was extracted by 2 × 200 mL portions of CH_2Cl_2 and collected in a 500-mL round-bottom flask equipped with a stir bar. After reducing the solution volume to approximately 300 mL, 10 g Na_2SO_4 was added and the mixture stirred for 1 hour. The solution was filtered and reduced to a minimal volume. The final product was recrystallized by the slow addition of 200 mL diethyl ether followed by filtration to give 1.28 g (61.6 % yield) of a dark brown solid. The magnetic moment of complex **4-1** was determined by the Evans' method to be 4.79 BM.[75] Anal. Calcd. for $C_{12}H_{12}F_6N_5O_2Mn$: C, 33.74; H, 2.83; N, 16.39. Found C, 33.61; H, 2.61; N, 15.77.

Synthesis of [*N,N'-bis*(trifluoroacetylacetone)-1,2-ethylenediimine] manganese(III) chloride [(tfacacen)MnCl] (4-2). The same procedure employed for

preparing **4-1** was used, replacing NaN_3 with NaCl. A dark green microcrystalline product was collected (76.8% yield). Crystals suitable for X-ray analysis were obtained by slow diffusion of diethyl ether into a CH_2Cl_2 solution of the complex. Anal. Calcd. for $C_{12}H_{12}F_6ClN_2O_2Mn$: C, 34.27; H, 2.88; N, 6.66. Found C, 34.15; H, 2.74; N, 6.68.

Synthesis of [*N,N'-bis*(trifluoroacetylacetone)-1,2-ethylenediimine] manganese(III) isocyanate [(tfacacen)MnNCO] (4-3). The same procedure employed with **4-1** was used replacing NaN_3 with NaOCN. A dark brown microcrystalline product was collected (42.7% yield). Crystals suitable for X-ray analysis were obtained by slow diffusion of diethyl ether into a CH_2Cl_2 solution of the complex. Anal. Calcd. for $C_{13}H_{12}F_6N_3O_3Mn$: C, 36.55; H, 2.83; N, 9.84. Found C, 36.37; H, 2.73; N, 9.71.

Synthesis of [*N,N'*-bis(trifluoroacetylacetone)-1,2-ethylenediimine] manganese(III) isothiocyanate [(tfacacen)MnNCS] (4-4). The same procedure employed for preparing **4-1** was used, replacing NaN_3 with KSCN. A green microcrystalline product was collected (78.7% yield). Crystals suitable for X-ray analysis were obtained by slow diffusion of diethyl ether into a CH_2Cl_2 solution of the complex. Anal. Calcd. for $C_{13}H_{12}F_6SN_3O_2Mn$: C, 35.23; H, 2.73; N, 9.48. Found C, 34.33; H, 2.57; N, 9.71.

Statistical Deconvolution of FTIR Spectra. Where noted FTIR spectra were deconvoluted using Peakfit Version 4.12.[76] Statistical treatment was a residuals method utilizing a combination Gaussian-Lorentzian summation of amplitudes with a linear baseline and Savitsky-Golay smoothing.

Rate Studies. Studies involving the ring-opening of cyclohexene oxide by **4-1**, **4-3**, and **4-4** were monitored via FTIR by the removal and analysis of solution aliquots at intervals of five to ten minutes. The reaction mixtures were heated in an oil bath and stirred under argon. Solution aliquots were collected by syringe and injected into an IR solution cell. For reaction order studies, four CH_2Cl_2 solutions of 67:1, 100:1, 150:1, 225:1 CHO:catalyst ratios were analyzed at 25ºC. For activation energy determination, four CH_2Cl_2 solutions of CHO:catalyst = 67 were monitored at 10, 20, 25, and 30ºC.

Copolymerization Reactions. Polymerization experiments were performed using a 300-mL Parr autoclave heated to 80ºC overnight under vacuum. Reaction mixtures were prepared by dissolving 50 mg of catalyst and an appropriate amount of cocatalyst in neat cyclohexene oxide and then added to the reactor by injection port. Typical reactions were run at 60-80ºC under 35-55 bar CO_2 pressure for 6 hours. Following each reaction, the contents of the reactor were dissolved in CH_2Cl_2 and analyzed by FTIR to ascertain the presence of cyclic carbonate and polycarbonate. Percent CO_2 linkages was determined by ^{1}H NMR.

X-Ray Structural Studies. Single crystals of **4-2**, **4-3**, and **4-4** suitable for X-ray diffraction were obtained by slow diffusion of diethyl ether into concentrated CH_2Cl_2 solutions of the respective compound. Single crystals of **[(tfacacenMnO)]$_2$** were obtain by slow evaporation of a reaction mixture containing **4-1** dissolved in neat cyclohexene oxide. For all reported structures a Leica IC A, MZ 75 microscope was used to identify suitable crystals of the same habit. Each crystal was coated in paratone oil, affixed to a Nylon loop and placed under streaming nitrogen (110K) in a Bruker SMART 1000 CCD

or Bruker-D8 Adv GADDS diffractometer. Table 4-1 contains crystallographic data for the four structures reported herein. Space group determination was made on the basis of systematic absences and intensity statistics. Crystal structures were solved by direct methods and refined by full-matrix least squares on F^2. All H atoms were placed in idealized positions with fixed isotropic displacement parameters equal to 1.5 times (1.2 for methyl protons) the equivalent isotropic displacement parameters of the atom to which they are attached. All non-hydrogen atoms were refined using anisotropic displacement parameters.

Programs used: data collection and cell refinement, SMART WNT/2000 Version 5.632[45] or FRAMBO Version 4.1.05 (GADDS);[46] data reductions, SAINTPLUS Version 6.63[36] absorption correction, SADABS,[47] structural solutions, SHELXS-97,[37] structural refinement, SHELXL-97,[38] graphics and publication materials, SHEXTL Version 6.14[39] and X-Seed Version 1.5.[40]

Results and Discussion

Synthesis and X-ray Structures. Straightforward methods for the synthesis of manganese(III) complexes of the general formula (acacen)MnX have been described by Boucher and Day.[30] Their methodology involves the reaction of $Mn(OAc)_3 \cdot 2H_2O$ and H_2acacen to provide (acacen)MnOAc with subsequent metathesis of the acetate derivative with NaX to yield the desired (acacen)MnX complex. The (tfacacen)MnX

Table 4-1. Crystallographic Data for (tfacacen)MnX Derivatives.

	4-2	**4-3**	**4-4**	**[(tfacacen)MnOH]$_2$**
empirical formula	$C_{12}H_{12}ClF_6MnN_2O_2$	$C_{13}H_{12}F_6MnN_3O_3$	$C_{27}H_{26}Cl_2F_{12}Mn_2N_6O_4S_2$	$C_{30}H_{34}F_{12}Mn_2N_4O_7$
Fw	420.63	427.20	971.44	900.49
temp(K)	110(2)	110(2)	110(2)	110(2)
cryst. system	Monoclinic	Monoclinic	Monoclinic	Monoclinic
space group	$P2_1/n$	$P2_1/c$	Cc	$P2_1/n$
a (Å)	11.314(3)	7.8313(13)	21.596(8)	9.8052(12)
b (Å)	12.587(3)	18.525(3)	11.332(4)	15.8879(19)
c (Å)	11.775(3)	12.565(2)	15.887(6)	12.0655(15)
β (deg)	110.135(5)	118.476(11)	101.996(6)	107.354(2)
V (Å^3)	1574.4(7)	1602.3(5)	3803(2)	1794.1(4)
D(calcd)(g/cm^3)	1.775	1.771	1.697	1.667
Z	4	4	4	2
abs. coeff. (mm^{-1})	1.081	7.538	1.015	0.817
obs. relfcns	3564	2350	8477	3023
unique relfcns [$I > 2\sigma$(I)]	2099	1740	7549	2556
restraints/params	0/219	0/237	2/500	0/255
goodness-of-fit on F^2	1.004	0.997	1.005	1.001
R, [a] [$I > 2\sigma$(I)]	0.0547	0.0649	0.0578	0.0535
R_w, [b] [$I > 2\sigma$(I)]	0.1178	0.1631	0.1507	0.1292

[a] $R = \Sigma||F_o| - |F_c||/\Sigma|F_o|$ [b] $R_w = \{[\Sigma w(F_o^2 - F_c^2)^2]/[\Sigma w(F_o^2)^2]\}^{1/2}$, $w = 1/[\sigma^2(F_o^2) + (aP)^2 + bP$, where $P = [\max(F_o^2),0) + 2(F_c^2)]/3$.

complexes (**4-1, 4-2**) were prepared in a similar manner *via* the intermediate (tfacacen)MnOAc and NaX. The presence of the -CF_3 substituents on the acacen ligand greatly reduces the solubility of the resulting (tfacacen)MnX complexes. This hampered the use of a more convenient route which was previously employed for the synthesis of acacen derivatives which relies on the formation of a reactive nitrate intermediate in aqueous solution.[77] Crystallographic data for the X-ray structures of complexes **4-2**, **4-3**, **4-4**, and **[(tfacacen)MnOH]$_2$** are presented in Table 4-1, with pertinent bond angles and distances presented in Table 4-2.

Unfortunately, attempts to characterize complex **4-1** crystallography have thus far failed. However, numerous examples of azide bridged solid state extended 1-D polymeric structures exist for similar complexes containing manganese(III) with both acacen and salen derivatives.[56,74,78,] The structure of complex **4-2** is shown in Figure 4-2 and, like the nonfluorinated version, is a five-coordinate, near square-pyramidal complex.[30] In this instance, the structure, however, takes on a step-type ring system where the two plains composed of O(1)–N(1)–C(1)–C(3) [**ring 1**] and O(2)–N(2)–C(4)–C(6) [**ring 2**] are 5.9º above and 9.1º below the N_2O_2 plane, respectively (Table 4-3). Such deviation is likely due to the added steric bulk of the two -CF_3 groups. In other respects the bond angles and distances of the coordination sphere are comparable; including a large metal displacement of 0.311 Å from the N_2O_2 plane (compared to 0.344 Å for the non-flourinated structure).

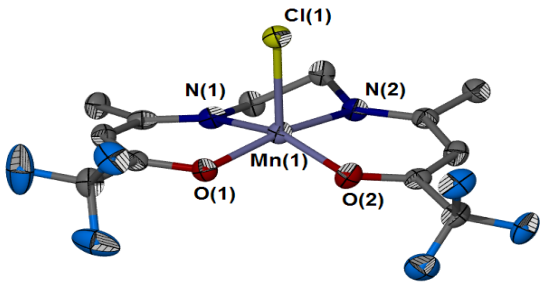

Figure 4-2. Thermal ellipsoid plot of complex **4-2** at 50% probability. Hydrogen atoms omitted for clarity.

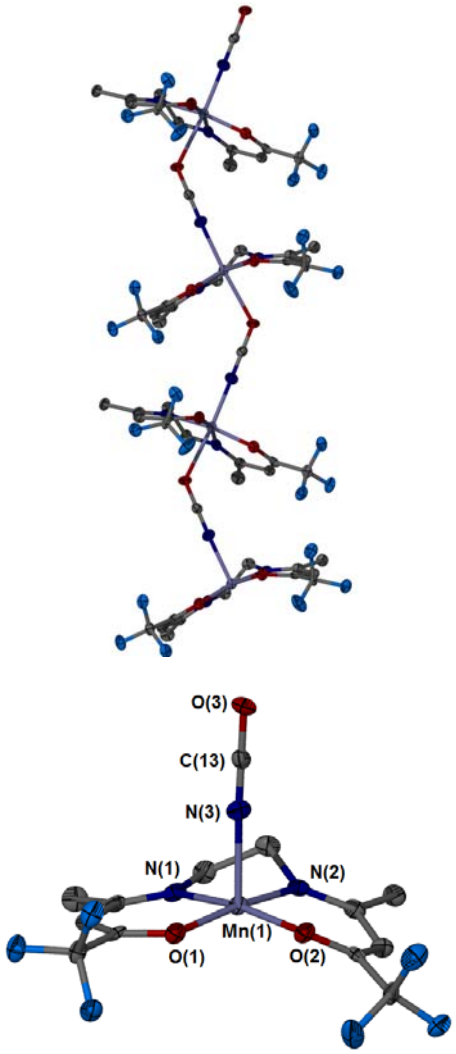

Figure 4-3. Thermal ellipsoid plot of complex **4-3** at 50% probability. The polymer chain viewed along the *c* axis. Hydrogen atoms omitted for clarity.

The polymeric solid state structure of complex **4-3** is presented in Figure 4-3. As with azide, a helical shape is obtained through bridging cyanates where Mn(1)-O(3) and Mn(1)-N(3) bonds are elongated over the longest ligand nitrogen and oxygen bonds by 0.505 Å and 0.115 Å, respectively. Though the nature of the $\mu_{1,3}$ bridge complicates determining if the anion is O(3) bound (cyanate) or N(3) bound (isocyanate), the greater

Table 4-2. Selected Bond Distances and Angles for Complexes **4-2, 4-3, 4-4,** and **[(tfacacen)MnO]$_2$**.

		4-2	
N_2O_2 plane			
Mn(1)-O(1)	1.886(3)	Mn(1)-N(1)	1.991(3)
Mn(1)-O(2)	1.901(3)	Mn(1)-N(2)	1.972(3)
Mn(1)-Cl(1)	2.3807(12)		
O(2)-Mn(1)-O(1)	88.92(12)	O(1)-Mn(1)-N(1)	91.10(13)
O(2)-Mn(1)-N(2)	91.12(13)	N(1)-Mn(1)-N(2)	83.74(14)
		4-3	
N_2O_2 plane			
Mn(1)-O(1)	1.911(4)	Mn(1)-N(1)	2.022(5)
Mn(1)-O(2)	1.919(4)	Mn(1)-N(2)	1.981(4)
O(2)-Mn(1)-O(1)	92.40(15)	O(1)-Mn(1)-N(1)	92.06(17)
O(2)-Mn(1)-N(2)	90.80(17)	N(1)-Mn(1)-N(2)	83.07(18)
isocyanate bridge, $\mu_{1,3}$			
Mn(1)-O(3)	2.424(4)	Mn(1)-N(3)	2.137(5)
N(3)-C(13)	1.163(7)	C(13)-O(3)	1.211(7)
O(1)-Mn(1)-N(3)	96.23(17)	Mn(1)-N(3)-C(13)	176.8(5)
O(1)-Mn(1)-O(3)	87.69(15)	Mn(1)-O(3)-C(13)	129.2(4)
metal-to-metal			
Mn-Mn (polymeric)	6.31(6)		
		4-4	
N_2O_2 plane			
Mn(1)-O(1)	1.907(3)	Mn(2)-O(3)	1.907(3)
Mn(1)-O(2)	1.916(3)	Mn(2)-O(4)	1.916(3)
Mn(1)-N(1)	1.999(3)	Mn(2)-N(4)	1.984(4)
Mn(1)-N(2)	1.995(4)	Mn(2)-N(5)	1.963(4)
O(2)-Mn(1)-O(1)	93.09(13)	O(4)-Mn(2)-O(3)	93.44(13)
O(2)-Mn(1)-N(2)	91.11(15)	O(4)-Mn(2)-N(5)	91.30(15)
O(1)-Mn(1)-N(1)	92.38(14)	O(3)-Mn(2)-N(4)	91.65(15)
N(1)-Mn(1)-N(2)	83.08(14)	N(4)-Mn(2)-N(5)	83.04(16)
isothiocyanate bridge, $\mu_{1,3}$			
Mn(1)-N(3)	2.202(4)	Mn(2)-N(6)	2.168(4)
Mn(2)-S(1)	2.9036(15)	Mn(1)-S(2)	2.8367(15)
N(3)-C(13)	1.150(6)	C(13)-S(1)	1.640(5)
N(6)-C(26)	1.166(6)	C(26)-S(2)	1.638(4)
Mn(1)-N(3)-C(13)	173.4(4)	Mn(2)-N(6)-C(26)	162.8(4)
Mn(2)-S(1)-C(13)	96.74(14)	Mn(1)-S(2)-C(26)	107.12(15)
metal-to-metal			
Mn(1)-Mn(1) (poly.)	12.19(4)	Mn(1)-Mn(2)	6.28(2)
		[(tfacacen)MnO]$_2$	
Mn(1)-O(1)	1.9301(19)	Mn(1)-N(1)	2.038(2)
Mn(1)-O(2)	1.970(2)	Mn(1)-N(2)	1.982(2)
Mn(1)-O(3)	1.8103(19)	Mn(1)-Mn(1)#	2.7326(8)
Mn(1)-O(3)#	1.821(2)		
Mn(1)-O(3)-Mn(1)	97.63(9)	O(3)-Mn(1)-O(3)#	82.38(9)
O(1)-Mn(1)-N(2)	168.82(9)		

Table 4-3. Selected Displacements and Dihedral Angles from the N_2O_2 Plane for Complexes **4-2**, **4-3** and **4-4**. [a]

structure	Mn-N_2O_2 planar displac. (Å)	dihedral ring 1[b] to ring 2[b], (deg)	dihedral ring 1[b] to N_2O_2 plane (deg)	dihedral ring 2[b] to N_2O_2 plane (deg)
4-2	0.3011	10.2	5.9	-9.1
4-3	0.1696	31.8	-6.2	-25.9
4-4 [Mn(1)]	0.0890	28.6	-7.8	-20.9
4-4 [Mn(2)]	0.1278	34.5	-15.3	-19.2

[a] for least-square plane analysis see supporting information

[b] ring 1 = N(1)-O(1)-C(1)-C(3), ring 2 = N(2)-O(2)-C(4)-C(6)

degree of elongation of the metal-oxygen bond along with evidence to be presented later (vide infra) reliably indicates that the latter case is the one most probable. The helical shape can be attributed to the Mn(1)-O(3)-C(13) bond angle of 129.2(4)º which, combined with a C(13)-O(3) bond length of 1.211(7) Å, indicates sp^2 hybridization at O(3). Steric interactions between adjacent complexes along the coordination chain leads to prominent deformation of the tfacacen ring system where **ring 2** lies 25.9º below the N_2O_2 plane and at a dihedral angle of 31.8º to **ring 1**.

The structure of complex **4-4** also reveals a helical 1-D coordination polymer comprised of a dimetallic asymmetric unit (Figure 4-4). Many examples of nitrogen bound thiocyanate complexes of manganese have been characterized with instances of $\mu_{1,3}$ bridging and bridged polymer chains.[52,53,78,79] Day et al. solved the polymeric structure of $(acac)_2MnSCN$ with nitrogen and sulfur metal bond distances of 2.189(5) and 2.880(2) Å, respectively.[80] Complex **4-4** exhibits similar distances with Mn(1)-N(3) and Mn(2)-N(6) equal to 2.202(4) and 2.168(4) Å along with Mn(1)-S(2) and Mn(2)-

S(1) equal to 2.8367(15) and 2.9036(15) Å, respectively. It appears that a *trans* influence of the sulfur donor ligand exists as evidenced by a shorter Mn(1)-S(2) bond

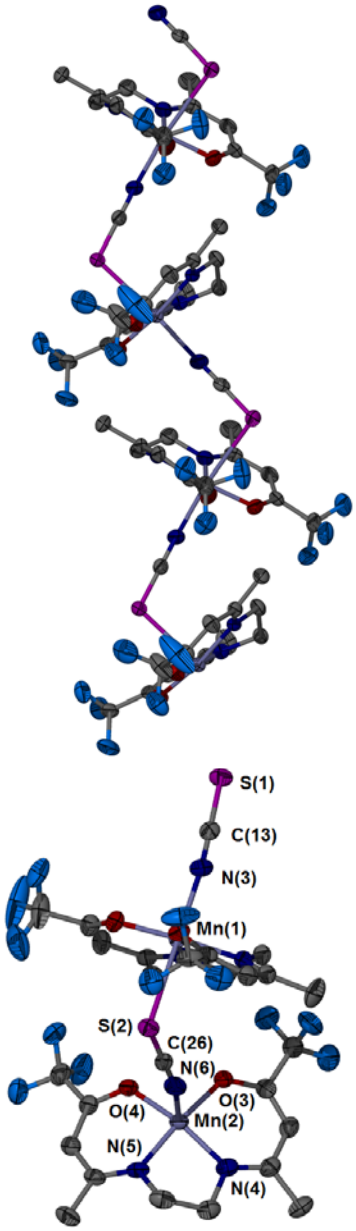

Figure 4-4. Thermal ellipsoid plot of complex **4-4** at 50% probability. The polymer chain viewed along the *a* axis. Hydrogen atoms and CH_2Cl_2 were omitted for clarity.

distance and an elongated Mn(1)-N(3) distance. The most striking feature of the structure is the pronounced zigzag shape of the thiocyanate-manganese chain, consisting of carbon-sulfur-manganese bond angles of 107.12(15)º and 96.74(14)º. In the latter case the angle approaches 90º, indicating a nearly unhybridized sulfur anion.

In an attempt to isolate and crystallize a bound, ring-opened epoxide to a manganese(III) center (*vita infra*) complex, **4-1** was dissolved in neat CHO and the solution left to slowly evaporate. Crystals were obtained and analyzed crystallographically with the structure acquired presented in Figure 4-5 along with pertinent bond angles and distances given on Table 4-2. It consists of two bridged manganese complexes where the flexible tfacacen ligand has folded back to allow for the two available coordination sites to be *cis* to each other. Although every attempt was made to exclude H_2O and oxygen, spurious amounts of both have led to the oxidation of Mn(III) to Mn(IV) as no evidence of μ-hydroxo bridges were found.

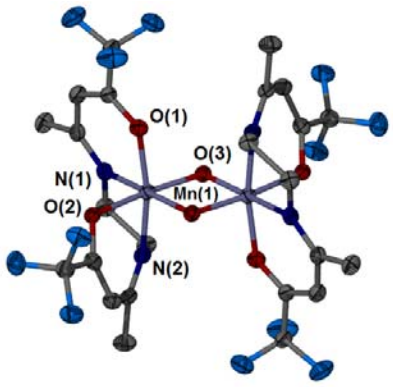

Figure 4-5. Thermal ellipsoid plot of **[(tfacacen)MnO]$_2$** at 50% probability.Hydrogen atoms and the disordered cyclohexene oxide molecule were omitted for clarity.

Boucher and Coe have synthesized two manganese(IV) salen complexes and have outlined a reaction pathway where H_2O coordinates to a manganese(III) center followed by deprotonation with a base to form a monomeric hydroxide intermediate.[81] Dimerization occurs followed by abstraction of the two hydroxo-bridging protons by base. Oxidation and subsequent formation of the di μ-oxo takes place in the presence of oxygen and water. A similar pathway can be envisaged starting from a metal bound ring-opened alkoxide protonated by water to give the azido-alcohol and the complex (tfacacen)MnOH. Dimerization of (tfacacen)MnOH follows accompanied by the necessary deformation of the $N_2O_2^{-2}$ ligand. Proton extraction and oxidation results in the di μ-oxo bridged species, which is seen as the thermodynamically stable product. Other di μ-oxo manganese(IV) salen complexes have been synthesized, and all bond angles and distances for **[(tfacacen)MnO]$_2$** agree well with published data.[82,83]

Mechanistic Aspects of the Epoxide Ring-Opening Process. The reluctance of (acacen)MnX complexes to form octahedral intermediates consisting of a coordinated epoxide as an initial step in the copolymerization mechanism has been identified as a major reason manganese(III) catalytic systems have shown only modest activity for epoxide ring-opening.[77] In addition, the inability to form stable octahedral anionic intermediates with two *trans* coordinated apical anions should greatly inhibit copolymer propagation. Scheme 4-1 illustrates the various intermediates involved in the copolymerization mechanism. Initial ring-opening takes place by either a reaction first order in catalyst (route **A**) with an external initiator X^-, such as when anionic cocatalysts

are employed, or by a reaction second order in catalyst with the initiator provided by another epoxide bound metal species (route **B**).[28e] In either case, an anionic octahedral complex is formed consisting of a metal alkoxide bound *trans* to X. A reluctance to form an octahedral complex is indicative of manganese (III) d^4 high spin systems, where the complex is destabilized by the presence of a singly occupied e_g antibonding orbital resulting in Jahn-Teller distortion along the z axis. For this reason manganese(III) acacen complexes are inhibited from binding these important ligands and thus have a limited propensity towards polymer initiation and propagation.

Scheme 4-1

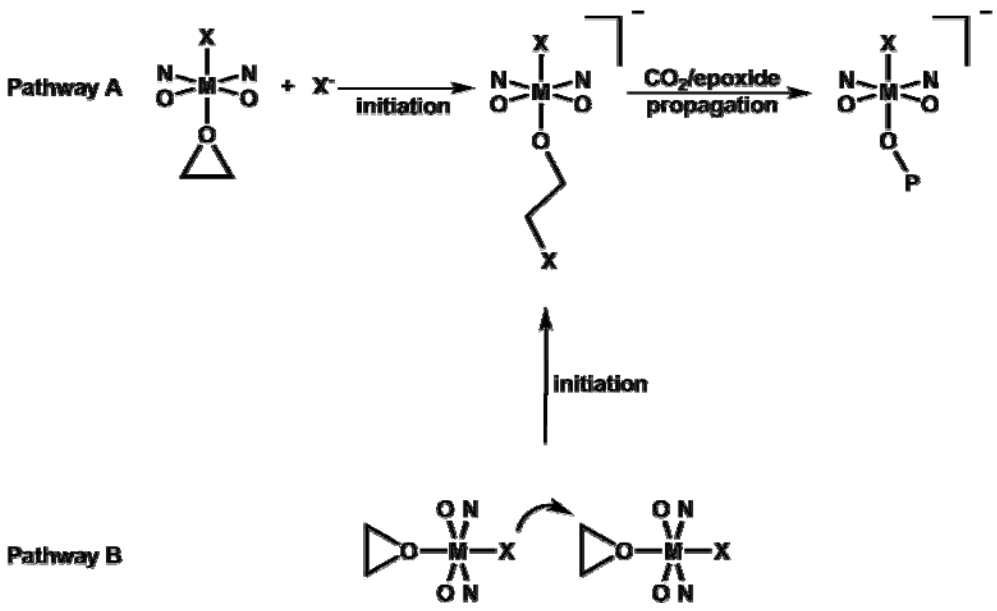

The addition of fluorinated methyl groups to the acacen ligand was undertaken in an effort to increase the electrophilicity of the coordinatively unsaturated manganese(III)

center. This in turn should increase the ability of the metal center to bind substrates such as epoxides. To understand the effect of the more withdrawing ligand, binding studies of complex **4-1** were undertaken in both coordinating and noncoordinating solvents (Figure 4-6). Essential to definitive monitoring of this process is the distinct difference seen in the asymmetric stretching frequencies of five and six coordinate metal azides. A five coordinate azide species is identified at 2050 cm^{-1} in CH_2Cl_2, while in coordinating CHO a stretch representing a six coordinate azide is apparent at 2038 cm^{-1}. A similar shift to lower frequency of the ν_{N_3} vibration occurs with the addition of 5 equivalents of strongly coordinating DMAP. With the addition of 1 equivalent $(^{n}Bu)_4NN_3$ in CH_2Cl_2, the formation of an anionic diazide pecies is apparent. The binding of CHO implies that the initial ring opening of a metal bound, activated epoxide should be possible in the absence of an added cocatalyst (Scheme 4-1, Route B). In addition, the ability of complex **4-1** to form a diazide species with only one equivalent of azide indicates that anions in a catalys/cocatalyst binary system may facilitate initiation and propagation of the growing polymer chain.

Complex **4-1** was evaluated as a catalyst for the copolymerization of CO_2 and cyclohexene oxide under typical reaction conditions (40-80ºC, 35-55 bar CO_2 pressure, 6 hour reaction time). In cases where no cocatalyst was employed, a small amount of polymeric material was produced with TOF's not exceeding 11 h^{-1} at 80ºC. This material proved to be predominately polyether with only 4-7% polycarbonate linkages.

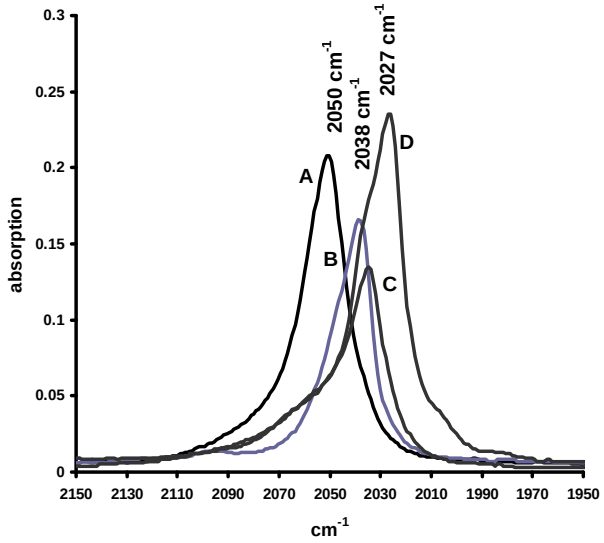

Figure 4-6. FTIR spectra of complex **4-1** in solutions of CH_2Cl_2 (**A**) and CHO (**B**). Spectra (**C**) and (**D**) are CH_2Cl_2 solutions with **5** equiv. DMAP and **1** equiv. $(^nBu)_4NN_3$, respectively.

When a cocatalyst was employed, results varied widely depending on the nature of the cocatalyst. For example, with 1 or 3 equivalents of DMAP no appreciable amount of polymeric material was formed, giving only small amounts of cyclic carbonate. However, when 1 equivalent of $(^nBu)_4NN_3$ was utilized, a copolymer possessing 87% polycarbonate linkages was produced with a TOF of 2.3 h^{-1} at 80ºC. This efficiency in producing polycarbonate has parallels to chromium(III) and cobalt(III) salen systems where anionic cocatalyst not only offer high activity but are selective towards the production of polycarbonates to the exclusion of polyether and decreased amounts of cyclic carbonate formation.[9,24,84]

As is illustrated in Scheme 4-1, ionic cocatalysts allow for an anion to be coordinated *trans* to the growing polymer chain. This activates the metal alkoxide bond

(or alternately, metal carbonate) towards nucleophilic attack of the electropositive carbon of CO_2 (or epoxide) and thus, insertion (Scheme 4-2). Without the use of a cocatalyst, epoxide occupies the *trans* coordination site and the metal alkoxide moiety is not sufficiently nucleophilic to facilitate CO_2 insertion. Conversely, in the presence of a strong nitrogen donor, epoxide is unable to coordinate to the metal, effectively eliminating all polymer formation. Inoue reported similar phenomena when using (tpp)MnOAc for the copolymerization of CO_2 and cyclohexene oxide.[44] In that study, the addition of one equivalent of Ph_3P, pyridine or *N*-methylimidazole was detrimental to catalyst activity, percent carbonate linkages, and polymer molecular weight.

Scheme 4-2

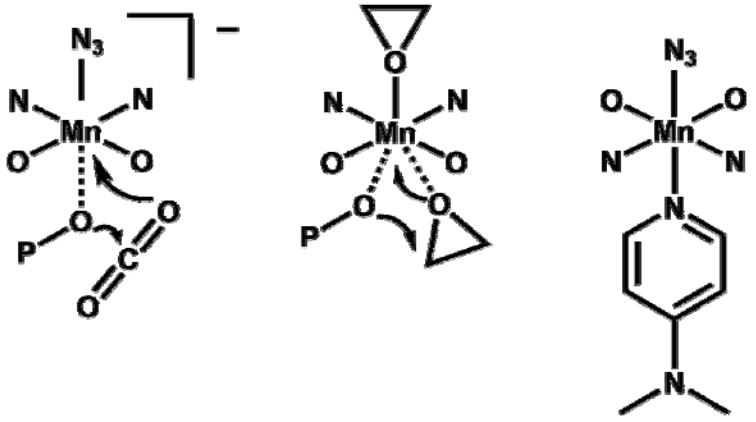

We can take advantage of the ability of complex **4-1** to bind and ring-open cyclohexene oxide to assess the mechanistic aspects of the initial ring-opening step in the copolymerization process. Referring to Scheme 4-1, the second-order process represented by Pathway B is identical to that described by Jacobsen for the asymmetric ring-opening of cyclopentene oxide *via* a bimetallic reaction involving a chiral

chromium(III) salen complex.[17a,b] These researchers elucidated this bimetallic ring-opening pathway by monitoring the formation of the resulting azido alcohol by GC analysis. It would be of value to confirm the generality of this reaction course by the direct observation of the consumption of the metal azide species. Figure 4-7 depicts a plot of the initial rate of ring-opening *vs* [**4-1**]^2 employing complex **4-1** at various ratios of cyclohexene oxide (CHO) in dichloromethane at 25ºC. The linear relationship observed confirms that, in this instance, in the absence of a cocatalyst, epoxide ring-opening is second-order in catalyst concentration. The greatly reduced activity of

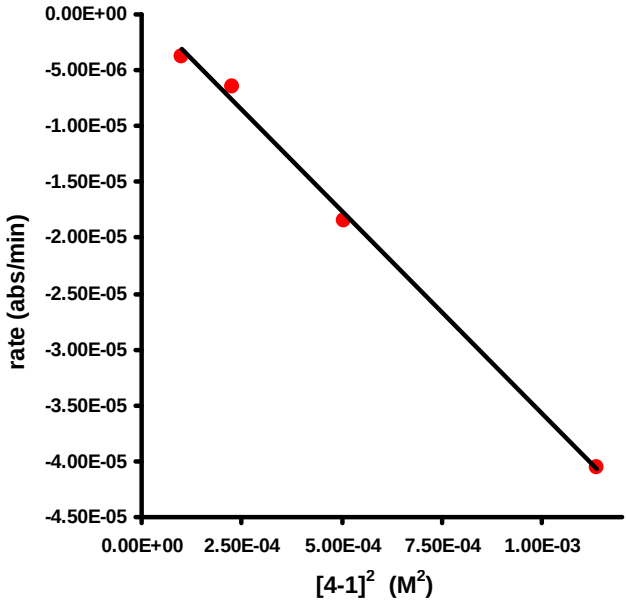

Figure 4-7. Linear relationship between initial rate and [**4-1**]^2. Rates determined by monitoring the disappearance of complex **4-1** at 2050 cm^{-1} by FTIR. A 2.25 M CHO solution in CH_2Cl_2 was employed with CHO:**4-1** ratios of 67, 100, 150 and 225.

complex **4-1** as compared to its (salen)CrX analogs ideally facilitates this study.[18,19] The activation energy for this second-order process was determined from an Arrhenius plot

of the ln(initial rate) *vs* temperature and found to be 71.0 ± 6.0 kJ/mol (Figure 4-8).

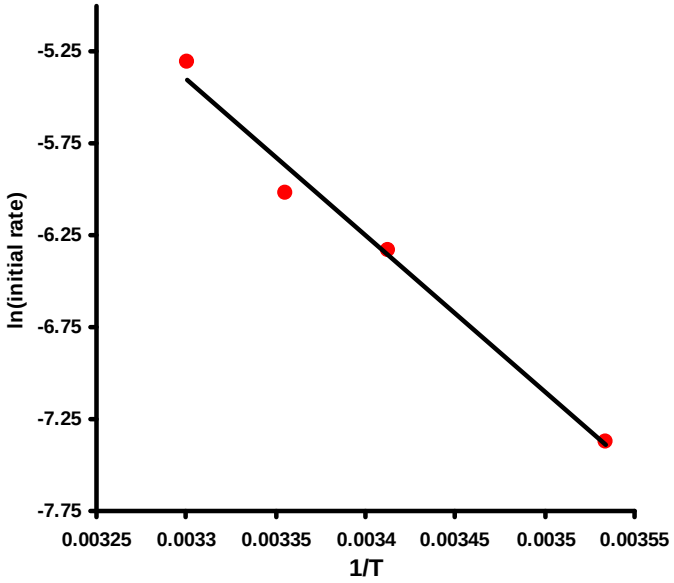

Figure 4-8. Arrhenius plot for the ring-opening of CHO derived fromCH_2Cl_2 solutions of CHO: **4-1** = 67 at 10ºC, 20ºC, 25ºC, and 30ºC.

With the bimetallic process confirmed, a study of the monometallic ring-opening of an epoxide assisted by a cocatalyst (Pathway A) was undertaken. The reaction of complex **4-1** with 150 equiv. CHO and 1 equiv DMAP in CH_2Cl_2 at 40ºC was monitored by FTIR. In stark contrast to the cleanly defined absorptions in the ν_{N_3} region observed in the bimetallic process, a number of overlapping azide stretching frequencies ranging from 2040 cm^{-1} to 2095 cm^{-1} rapidly developed, thus prohibiting detailed rate analysis (Figure 4-9). In addition, the formation of organic azide was retarded as evidenced by the more than 4 hrs required to completely consume the metal azide stretch at 2040 cm^{-1} (when compared to 1.5 hrs in the absence of DMAP). Statistical deconvolution revealed four bands midway through the reaction located at 2042, 2062, 2073, and 2093 cm^{-1}.

The bands at 2042 cm^{-1} and 2093 cm^{-1} can be assigned to the six coordinated manganese azide and organic azide, respectively. The remaining two bands at 2062 and 2073 cm^{-1} are ostensibly attributed to metal azides of alternate coordination number or bonding mode. A large amount of literature exists concerning metal-azide binding and coordination with salen-type Schiff base ligands and di, tri, and tetradentate nitrogen containing ligands of manganese (III),[56] manganese(II),[63,64,85] and cobalt(III).[86] Definitive descriptions regarding the nature of these species are not possible based on infrared data alone. However, considering the flexibility of the tfacacen ligand, numerous

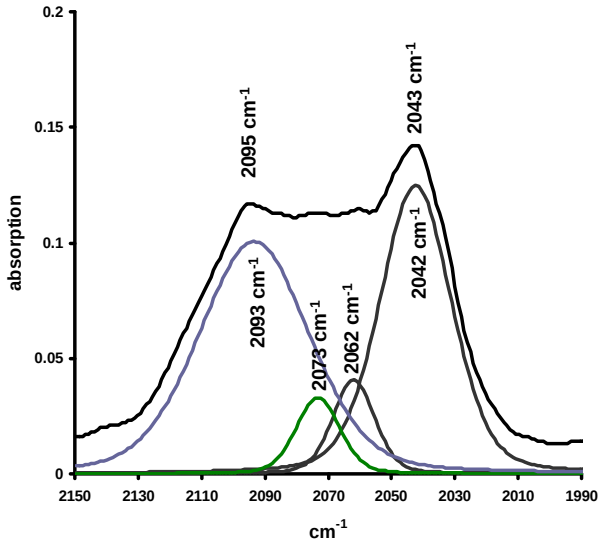

Figure 4-9. FTIR spectrum of a reaction at 40º C of a CHO:**4-1** = 150 in CH_2Cl_2 with 1 equiv DMAP at 73 minutes. The underlying curves represent statistical deconvolution of asymmetric azide stretches.

possibilities exist including *cis* bound terminal azide/azide or azide/donor ligands, bridged $\mu_{1,1}/\mu_{1,3}$ (EO or EE) bimetallic azides complexes, or 1-D azide coordination polymers.

Similar behavior was observed upon the addition of 1 equiv $(^n\text{Bu})_4\text{NN}_3$ to a CH_2Cl_2 solution of complex **1** with a CHO:**1** ratio of 100 at 40º C (Figure 4-10). The anticipated diazide species is observed at 2026 cm^{-1}, however, there is rapid formation of an intense peak at 2062 cm^{-1}. Within 4 hrs the diazide species is consumed leaving the absorbance at 2062 cm^{-1} and organic azide at 2098 cm^{-1}. Full conversion to organic azide is not achieved until more than 20 hrs into the reaction. This is approximately nine times slower than the bimetallic reaction involving complex **1** at the same CHO:**1** ratio.

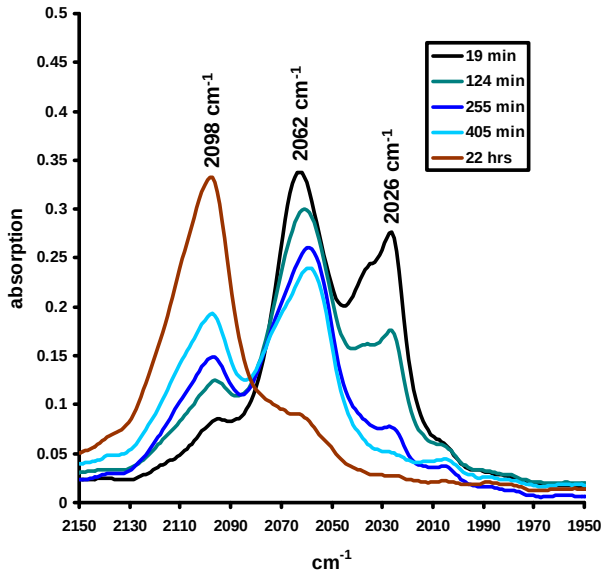

Figure 4-10. FTIR spectra of a reaction of CHO:**4-1** = 100 in CH_2Cl_2 with 1 equiv $(^n\text{Bu})_4\text{NN}_3$ at 40º C.

Without structural information as to the identity of the new metal azide species in the presence of Lewis bases, the underlying reason for the decreased reaction rate is unclear. The formation of the species at 2062 cm^{-1} is reproducible in the absence of epoxide and its formation is enhanced by heat. Thus, the more thermodynamically stable species may be unable to readily bind epoxide *via* displacement of the anions of a diazide species. If the tfacacen ligand were to adopt a nonplanar bonding mode, the two available coordination sites would be either *cis* in a monometallic diazide complex, or occupied by bridging azides (Scheme 4-3). In the former case, the requisite activation of a bound epoxide or anion as facilitated by a *trans* donor ligand would be very low. The latter case seems less likely as it would require the loss of an azide resulting in the formation of "free azide" anion, a species which formed in only small quantities throughout the reaction. In any case, this catalytic behavior is not a likely model for the chromium and cobalt salen catalytic systems due to its slow rate of ring-opening and susceptibility to alternate bonding modes.

Scheme 4-3

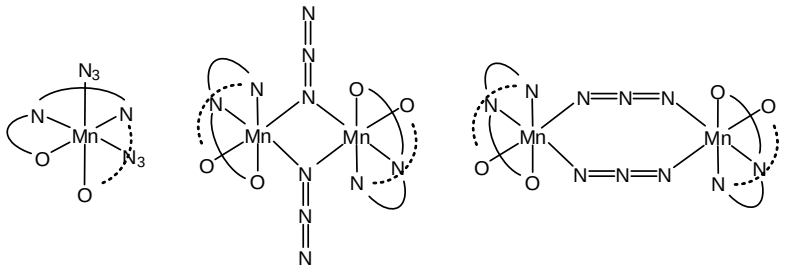

Considering the critical features the azide moiety provides to the mechanistic study of the copolymerization of CO_2 and epoxides it would be advantageous if other highly active anions possessing such convenient infrared stretching frequencies could be utilized. Azide falls into the larger category termed the pseudohalogens of which the most important are cyanide (CN^-), cyanate (OCN^-), thiocyanate (SCN^-).[87] Boucher and Day have prepared several manganese(III) acacen complexes with these anions and reported stretching frequencies indicative of a *N*-bound anions.[30] For first row transition metals, *N*-bonded isothiocyanates predominate and display an asymmetric stretch from 2050 to 2080 cm^{-1} if terminally bound, and in the vicinity of 2100 cm^{-1} or higher for bridged end-on (through nitrogen) or end-to-end.[52,88,89] Cyanates also show a strong preference for binding through nitrogen, thus giving isocyanate complexes with stretching frequencies ranging from 2100 to 2300 cm^{-1} for typical binding modes.[87,90]

Complexes **4-3** and **4-4** were prepared and evaluated for their ability to ring-open cyclohexene oxide in the same manner as described with complex **4-1**. Figure 4-11 displays the infrared stretching frequencies of five coordinate manganese(III) isocyanate and isothiocyanate in CH_2Cl_2. For complex **4-3**, a stretching band containing a slight shoulder is evident at 2196 cm^{-1} and is typical of isocyanate complexes. For complex **4-4** a stretch similar in appearance to **4-3** is seen at 2051 cm^{-1} and is typical for a nitrogen bound isothiocyanate complex. Presumably, the ring-opening of cyclohexene oxide by a thiocyanate anion proceeds along a bimetallic pathway where a metal-bound isothiocyanate nucleophilicity attacks the α carbon of a coordinated epoxide though the carbon-sulfide moiety. This in turn would lead to a ring-opened metal bound alkyl

thiocyanate alkoxide. A reaction carried out with a CHO:**4-4** ratio of 67 at 40ºC in CH_2Cl_2 for 2 hrs was monitored by FTIR and resulted in complete consumption of metal-bound isothiocyanate and the formation of a broad stretch at 2191 cm^{-1} (Figure 4-11). This latter species is in good agreement with alkyl-thiocyanates synthesized by other methods.[91] Interestingly, organic thiocyanates have been produced through the ring-opening of epoxides with ammonium thiocyanate in the presence of TPP transition metal complexes, tetraarylporphrin derivatives, and aza-crown ethers.[92] This, combined with the fact the ring-opening of CHO with **4-4** proceeds at rates comparable to **4-1** under similar reaction conditions, indicates that the thiocyanate anion may be well suited as an initiator for copolymerization of CO_2 and epoxides.

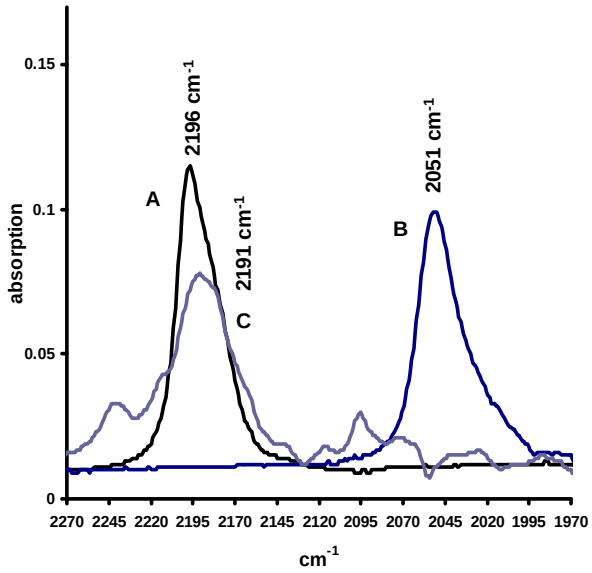

Figure 4-11. FTIR spectra of CH_2Cl_2 solutions of (**A**) complex **4-3** and (**B**) complex **4-4** and (**C**) a reaction mixture following the ring-opening of CHO by complex **4-4**.

The effectiveness of cyanate is less clear, though preliminary results show that **4-3** catalyzes the ring-opening of CHO at a considerably lower rate. In a reaction with a CHO:**4-3** ratio of 100:1 at 40 ºC in CH_2Cl_2, no appreciable amount of organic product was observed by FTIR until more than 20 hrs reaction time. Eventually, a product does appear at 2261 cm^{-1} and is ostensibly assigned to that of organic cyanate in analogy to the production of organic thiocyanate from an isothiocyanate initiator. However, alkyl cyanates are rare whereas alkyl isocyanates are well known organic compounds.[93] Indeed, organic isocyanates show absorbances in the range of 2200 to 2300 cm^{-1}, though the formation of such a product seems contrary to the nuclophillic attack of the carbonyl moiety of a nitrogen bound isocyanate.

Conclusions

The synthesis and structural characterization of Schiff base complexes of the formula (tfacacen)MnX (X = Cl, N_3, NCO, NCS) have been described. The presence of the highly electron withdrawing $–CF_3$ substituents in these derivatives, as compared to their acacen analogs, has enabled these d^4 high-spin complexes to readily bind to a sixth ligand, e.g., epoxide. This property has made it possible to monitor the epoxide ring-opening pathway utilizing the ν_{N_3} vibrational mode in (tfacacen)MnN_3. In this instance, the ring-opening reaction was demonstrated to be second-order in metal complex, analogous to the well-studied (salen)CrX system. Relative to the chromium(III) salen derivatives, the (tfacacen)MnX derivatives are considerably slower at facilitating the epoxide ring-opening process. Concomitantly, because of the electrophilicity of the

manganese(III) complexes, their effectiveness at promoting the CO_2 insertion process is greatly reduced compared to the (salen)CrX and (salen)CoX derivatives. Hence, the manganese(III) complexes are not efficient catalysts for the copolymerization of epoxides and CO_2 to afford polycarbonates. Unlike the greatly enhanced reactivity of the (salen)CrX and (salen)CoX complexes towards CO_2/epoxide coupling in the presence of Lewis base cocatalysts (e.g., anions and *N*-heterocyclic amines), (tfacacen)MnX complexes were shown to be greatly inhibited towards this process upon addition of such cocatalysts.

CHAPTER V

X-RAY CRYSTAL STRUCTURES OF FIVE-COORDINATE MANGANESE(III) SALEN AZIDE DERIVATIVES AND THEIR BINDING ABILITIES TOWARDS EPOXIDES

Introduction

The comprehensive examination of manganese(III) acacen derivatives has elucidated their ability to catalyze the copolymerization of CO_2 and epoxide, bind ligands relevant to the copolymerization process, and ring-open cyclohexene oxide. These complexes have proven well suited for a comparative study due to close structural similarities to chromium(III) and cobalt(III) salen complexes. However, an excellent compliment to these studies would be a direct examination of the salen ligand itself. In particular, a binding study of manganese(III) complexes containing the highly substituted salen derivatives typically employed in this field would allow for comparison to and confirmation of the findings with acacen.

Scheme 5-1 depicts the series of manganese(III) salen complexes that have been synthesized for this study. The salen complexes presented are typical of those found in highly successful chromium and cobalt salen catalysts (see Chapter I). The *t*-butyl groups at the 3 and 5 positions of the phenolate rings provide solubility in organic solvents as well as electron donation to a metal center. In addition, the chiral cyclohexylene backbone can facilitate the formation of regioregular and sterioregular

polycarbonate, as is the case with cobalt(III). The choice of azide as an apical ligand is critical for monitoring the formation of five and six coordinate metal complexes using IR spectroscopy. In this way, the propensities to bind epoxide and other ligands can easily be measured. The synthesis of these complexes is also described, along with X-ray crystal structures of **5-1** and **5-3**. Magnetic moments have been measured in order to relate electronic configuration of the manganese(III) to binding ability.

Scheme 5-1

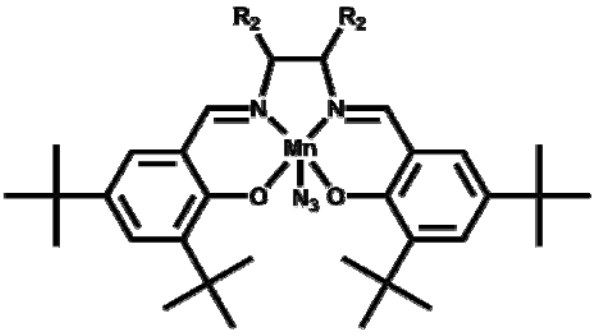

5-1: R_2 = H, H
5-2: R_2 = -C_4H_4-
5-3: R_2 = (1*R*, 2*R*) -C_4H_8-

Experimental

Reagents and General Procedures. Unless otherwise stated, all syntheses and manipulations were carried out on a double-manifold Schlenk vacuum line under an argon atmosphere or in an argon filled glovebox. Methanol, pentane, and dichloromethane were freshly purified by an MBraun Manual Solvent Purification System packed with Alcoa F200 activated alumina desiccant. Cyclohexene oxide was

purchased from TCI America and freshly distilled from CaH_2. Ethylenediamine (Aldrich), 1,2-phenylenediamine (Aldrich), sodium azide (Aldrich), and $Mn(OAc)_3 \cdot 2H_2O$ (Strem Chemicals Inc.) were all used as received without further purification. The synthesis of (salen)H_2(*N,N′-bis*(3,5-di-*tert*-butylsalicylidene)-1,2-ethlyenediimine), (salphen)H_2(*N,N′-bis*(3,5-di-*tert*-butylsalicyl-idene)-1,2-phenylene-diimine), and (1*R*,2*R*)-(salcy)H_2((1*R*,2*R*)-*N,N′-bis*(3,5-di-*tert*-butylsalicylidene)-1,2-cyclohexanediimine)) were accomplished according to published procedures.[20,94]

Elemental analysis was provided by Canadian Microanalytical Service LTD, Delta, British Columbia. Infrared spectra were recorded using a Mattson 6021 FTIR spectrometer with DTGS and MCT detectors. All ^1H NMR were acquired using Unity+ 300 MHz and VXR 300 MHz superconducting NMR spectrometers. Magnetic susceptibility measurements were carried out according to the Evans' method.[75]

Synthesis of [*N,N′-bis*(3,5-di-*tert*-butylsalicylidene)-1,2-ethlyenediimine] manganese(III) azide (5-1). To a 125-mL round-bottom flask was added 0.50 g of (salen)H_2 (1.02 mmol), 0.245 g $Mn(OAc)_3 \cdot 2H_2O$ (0.91 mmol), a stir bar, and 30 mL MeOH. The resulting suspension was stirred in air for 18 hrs followed by filtration to remove unreacted ligand. Subsequently, the solution was added to a 1-L separatory funnel containing a concentrated aqueous solution of sodium azide (30g in 100 mL distilled H_2O). The mixture was shaken vigorously for 10 minutes with frequent venting. The product was then extracted with two 100 mL portions of CH_2Cl_2 and collected in a 500 mL round-bottom-flask. This flask was equipped with a large stir bar and the stirred solution was dried in the presence of 10 g Na_2SO_4. After filtration the

solvent volume was reduced *via* rotary-evaporation. The final product was crystallized by the slow addition of 200 mL of pentane to the concentrated solution followed by filtration and drying of the dark brown product in air (0.537 g, 70% yield). Crystals suitable for X-ray analysis were obtained by slow diffusion of hexane into a concentrated CH_2Cl_2 solution of the complex. μ_{eff} = 4.89 μ_B. Anal. Calcd for $C_{32}H_{46}N_5O_2Mn$: C, 65.40; H, 7.89; N, 11.92. Found C, 65.12; H, 7.98; N, 11.53.

Synthesis of [*N,N'-bis*(3,5-di-*tert*-butylsalicylidene)-1,2-phenylenediimine] manganese(III) azide (5-2). The procedure employed in the synthesis of **5-1** was used replacing (salen)H_2 with (salphen)H_2. A brown-red solid was collected (88.8% yield). μ_{eff} = 4.95 μ_B. Anal. Calcd for $C_{36}H_{46}N_5O_2Mn$: C, 68.01; H, 7.29; N, 11.02. Found C, 66.92; H, 7.38; N, 10.42.

Synthesis of [((1*R*,2*R*)-*N,N'-bis*(3,5-di-*tert*-butylsalicylidene)-1,2-cyclohexenediimine] manganese(III) azide (5-3). The procedure employed in the synthesis of **5-1** was used replacing (salen)H_2 with (1*R*,2*R*)-(salcy)H_2. A brown-red microcrystalline product was collected (68.2% yield). Crystals suitable for X-ray analysis were obtained by slow diffusion of hexane into a concentrated CH_2Cl_2 solution of the complex. μ_{eff} = 4.88 μ_B. Anal. Calcd for $C_{36}H_{52}N_5O_2Mn$: C, 67.37; H, 8.17; N, 10.91. Found C, 66.11; H, 7.95; N, 10.52.

X-ray Structural Studies. Single crystals of **5-1** and **5-3** suitable for X-ray diffraction were obtained as described. For each structure a Leica IC A, MZ 75 microscope was used to identify suitable crystals of the same habit. Each crystal was coated in paratone oil, affixed to a Nylon loop and placed under streaming nitrogen

(110K) in a Bruker SMART 1000 CCD or Bruker APEX II CCD. Table 5-1 contains crystallographic data for the two structures reported herein. Space group determinations were made on the basis of systematic absences and intensity statistics. Crystal structures were solved by direct methods and refined by full-matrix least squares on F^2. All H atoms were placed in idealized positions with fixed isotropic displacement parameters equal to 1.5 times (1.2 for methyl protons) the equivalent isotropic displacement parameters of the atom to which they are attached. All non-hydrogen atoms were refined using anisotropic displacement parameters.

Programs used: data collection and cell refinement, SMART WNT/2000 Version 5.632[45] or BCP Version 2.0.1.9,[95] data reductions, SAINTPLUS Version 6.63[36] absorption correction, SADABS,[47] structural solutions, SHELXS-97,[37] structural refinement, SHELXL-97,[38] graphics and publication materials, SHEXTL Version 6.14[39] and X-Seed Version 1.5.[40]

Table 5-1. Crystallographic Data for Complexes **5-1** and **5-3**.

	5-1	**5-3**
empirical formula	$C_{32}H_{46}MnN_5O_2$	$C_{36}H_{52}MnN_5O_2$
Fw	587.68	641.77
temp(K)	110(2)	110(2)
cryst. system	Triclinic	Monoclinic
space group	P-1	P2(1)
a (Å)	6.366(6)	17.772(3)
b (Å)	14.059(6)	11.5307(19)
c (Å)	18.474(7)	18.530(3)
α (deg)	89.741(17)	90.00
β (deg)	89.633(12)	112.178(3)
γ (deg)	78.682(12)	90.00
V (Å^3)	1621.3(19)	3516.1(10)
D(calcd)(g/cm^3)	1.204	1.771
Z	2	4
abs. coeff. (mm^{-1})	0.442	0.413
obs. relfcns	5320	16068
unique relfcns [$I > 2\sigma$(I)]	3619	11457
restraints/params	0/375	1/817
goodness-of-fit on F^2	1.000	0.990
R, [a] [$I > 2\sigma$(I)]	0.0695	0.0484
R_w, [b] [$I > 2\sigma$(I)]	0.1385	0.0954

[a] $R = \Sigma||F_o| - |F_c||/\Sigma|F_o|$ [b] $R_w = \{[\Sigma w(F_o^2 - F_c^2)^2]/[\Sigma w(F_o^2)^2]\}^{1/2}$, $w = 1/[\sigma^2(F_o^2) + (aP)^2 + bP$, where $P = [\max(F_o^2),0) + 2(F_c^2)]/3$.

Results and Discussion

Synthesis of (salen)MnN$_3$ Complexes. The synthesis of (salen)manganese(III) azide complexes was achieved *via* the route outlined in Scheme 5-2. This procedure is carried out at ambient temperature and differs from those utilizing manganese(III) salts as previously reported by Jacobsen and others.[94,96] It is adapted from Boucher and Day's preparation of manganese(III) acacen derivatives.[30] The (salen)MnN$_3$ complexes were isolated as brown or red-brown crystalline samples in good yield (70-90%) from a concentrated CH_2Cl_2 solution upon addition of pentane. Satisfactory elemental analyses were obtained on the five-coordinate complexes, and μ_{eff} values of 4.88-4.95 μ_B were

determined by the Evans' method.[75] Hence, the complexes are d^4 high spin manganese(III) derivatives.

Scheme 5-2

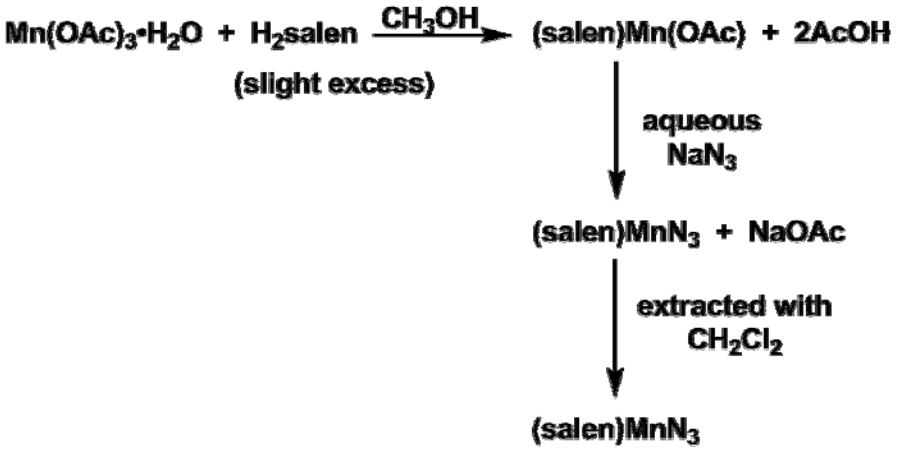

X-ray Crystal Structures. It was important to characterize these manganese(III) azide complexes *via* X-ray crystallography since many manganese complexes of this type exhibit a strong preference towards aggregation in the solid state. That is, typically these derivatives adopt one of two coordination modes. One bonding motif involves the dimerization of two manganese salen complexes through the oxygen atoms of the salen ligand. The other oxygen atom from each salen ligand occupies the sixth coordination site of the adjacent metal center, forming an elongated Mn–O bond ranging from 2.8-3.2 Å depending on the nature of the ligand.[78b,78d] The *trans* bound azides display typical Mn–N bond distances ranging from 2.103-2.130 Å. The other predominating bonding mode involves an extended structure consisting of manganese(III) salen complexes bridged by azide in a $\mu_{1,3}$ fashion, forming a 1-D

coordination polymer.[58,59,78a,78e] In these instances the metal–nitrogen bond distances span 2.280 to 2.349 Å. This elongation along the z-axis is due to a classical Jahn-Teller distortion generally found in manganese(III) high-spin complexes.

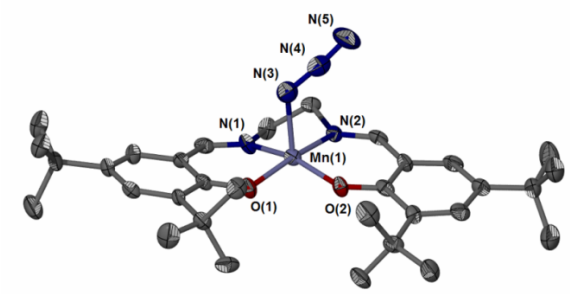

Figure 5-1. Thermal ellipsoid plot of **5-1** at 50% probability. Hydrogen atoms omitted for clarity.

The structures of complexes **5-1** and **5-3** are shown in Figures 5-1 and 5-2, and selected metrical parameters are compiled in Table 5-2. Both structures are monomeric and display no form of aggregation as discussed above. This is likely due to the bulky *t*-butyl groups located at the 3 and 5 positions of the salen phenolate moieties. Without aggregation, these complexes form five coordinate, near square pyramidal geometries with metal-azide bond distances of 2.118(6) to 2.083(3) Å for **5-1** and **5-3**, respectively. Without a *trans* influence from a sixth ligand, as is the case with bridged polymeric structures, these manganese azide bond distances more closely resemble those of the aforementioned dimerized structures with only weakly coordinated oxygens. In each case the azide is rotated away from the *t*-butyl groups located at the 3 position. The

most dramatic example of this is seen in complex **5-3**, where the azide is projected back toward the diimine moiety of the ligand.

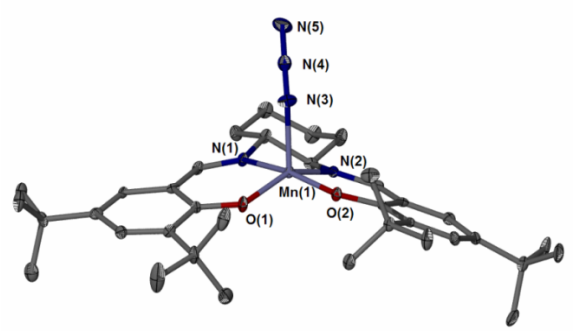

Figure 5-2. Thermal ellipsoid plot of **5-3** at 50% probability. Hydrogen atoms omitted for clarity. One of two complexes in the asymmetric unit.

The two structures bear similar metal displacements, with the manganese residing 0.3396 Å above the N_2O_2 plane for **5-1** and 0.3487 Å for **5-3**.[97] When considering the configuration of the salen ring system it can be seen that complex **5-1** has a stepped shape with phenolate moieties positioned above and below the N_2O_2 plane. This differs from complex **5-3**, which exhibits a saddle shape with both phenolate moieties positioned below the N_2O_2 plane. Several unsuccessful attempts were made to determine the crystal structure of complex **5-2**. However, the crystal structure of (salphen)CrCl(THF) indicates that a phenylene backbone instills near total planarity to the entire ligand.[19] This would act in a way to minimize steric repulsion between two complex molecules and possibly adopt one of the two aggregated bonding modes previously mentioned, despite the presence of the *t*-butyl groups.

Table 5-2. Selected Bond Distances and Angles for Complexes **5-1** and **5-3**.[a]

5-1			
Mn(1)-O(1)	1.854(4)	N(3)-N(4)	1.215(8)
Mn(1)-O(2)	1.858(4)	N(4)-N(5)	1.151(8)
Mn(1)-N(3)	2.118(6)	Mn(1)-N(1)	1.968(5)
		Mn(1)-N(2)	1.935(5)
O(2)-Mn(1)-O(1)	93.11(17)	O(1)-Mn(1)-N(1)	89.75(18)
O(2)-Mn(1)-N(2)	90.49(18)	N(1)-Mn(1)-N(2)	82.5(2)
O(1)-Mn(1)-N(3)	99.1(2)	N(1)-Mn(1)-N(3)	94.6(2)
O(2)-Mn(1)-N(3)	106.0(2)	N(2)-Mn(1)-N(3)	91.7(2)
Mn(1)-N(3)-N(4)	117.8(5)	N(3)-N(4)-N(5)	174.7(7)
5-3			
Mn(1)-O(1)	1.877(2)	N(3)-N(4)	1.179(4)
Mn(1)-O(2)	1.868(2)	N(4)-N(5)	1.170(4)
Mn(1)-N(3)	2.083(3)	Mn(1)-N(1)	1.971(3)
		Mn(1)-N(2)	1.981(3)
O(2)-Mn(1)-O(1)	90.91(10)	O(1)-Mn(1)-N(1)	90.30(11)
O(2)-Mn(1)-N(2)	91.02(11)	N(1)-Mn(1)-N(2)	81.96(11)
O(1)-Mn(1)-N(3)	106.21(13)	N(1)-Mn(1)-N(3)	92.24(13)
O(2)-Mn(1)-N(3)	106.0(2)	N(2)-Mn(1)-N(3)	104.48(13)
Mn(1)-N(3)-N(4)	135.7(3)	N(3)-N(4)-N(5)	178.2(4)

[a] Units for bond distances and bond angles are (Å) and (º), respectively.

Binding Studies of (salen)MnN_3 Complexes to a Sixth Ligand. As mentioned in the introduction (salen)CrX complexes are extremely effective as catalysts for the copolymerization of epoxides and carbon dioxide in the presence of anionic cocatalysts. A survey of the reported crystal structures of these metal complexes reveals that only one five-coordinate, square-pyramidal complex has been crystallographically characterized, i.e., (salcy)CrCl, where salen = *N,N′-bis*(3,5-di-*tert*-butylsalicylidene)-1,2-cyclohexenediimine.[18] All chromium(III) azide analogs characterized in the solid-state by X-ray analysis have a sixth ligand occupying the other axial site, e.g., THF, epoxide,

or DMAP.,[17b,20,27] This is due to the propensity of chromium(III) d^3 complexes to form stable octahedral derivatives. Hence, the Mn(III) complexes reported herein, complexes **5-1** and **5-3**, should serve as good structural models of these active chromium catalysts but contain an added *d*-electron occupying an e_g antibonding orbital. The presence of an added *d*-electron in (salen)MnX complexes should greatly alter their catalytic activity by limiting their ability to bind a sixth ligand. This is readily elucidated in Scheme 5-2 where the epoxide ring-opening process requires substrate binding to the metal center prior to metal alkoxide formation. Subsequent addition of carbon dioxide results in CO_2 insertion into the metal-alkoxide bond with concomitant formation of a metallocarbonate species and copolymer chain propagation.

Scheme 5-2

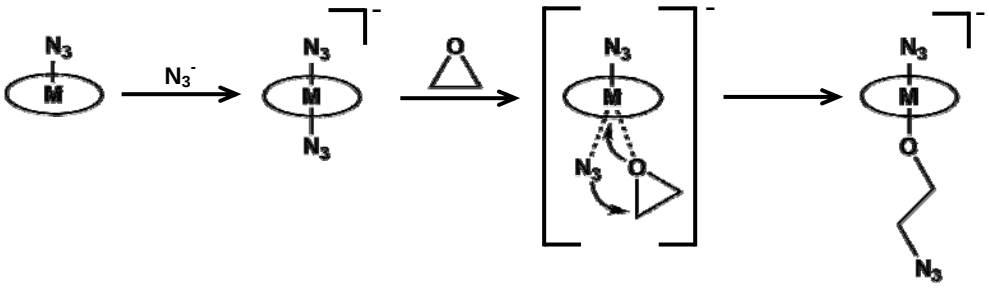

In Chapter III, it was shown that d^4 high-spin, five-coordinate (acacen)MnX complexes strongly resist binding to epoxide or azide ligands, and consequently are ineffective as catalysts for the CO_2/epoxide coupling reaction.[77] By way of contrast,

the addition of electron-withdrawing -CF_3 substituents to the acacen ligand greatly enhances the ability of (tfacacen)MnX complexes to bind a sixth ligand (Chapter IV).[98] This is the result of an increase in the electrophilicity of the manganese center. Indeed, these latter manganese(III) derivatives were demonstrated to easily ring-open cyclohexene oxide *via* a bimetallic pathway. Since (salen)MnX complexes have been examined as catalysts for carbon dioxide/epoxide coupling reactions by several research groups, it was of interest to compare (salen)MnN_3 derivatives to these acacen Mn(III) derivatives for their propensity to bind epoxides or other Lewis bases.[44,99]

Ligand binding studies were conducted on these five-coordinate, d^4 high-spin (salen)MnN_3 complexes utilizing the asymmetric stretching frequency of the azide ligand by infrared spectroscopy. As mentioned earlier these intense and energy isolated vibrational modes in (salen)MnN_3 derivatives in non-coordinating solvents are sensitive to the addition of a sixth ligand *trans* to the azide group. Thereby, this spectroscopic method provides easy monitoring of the metal's coordination sphere. Figure 5-3 displays the azide stretching band for each of the complexes dissolved in dichloromethane. These ν_{N_3} modes at 2046-2048 cm^{-1} are typical for five-coordinate manganese(III) complexes where an azide group occupies the apical position of a near square pyramidal geometry.

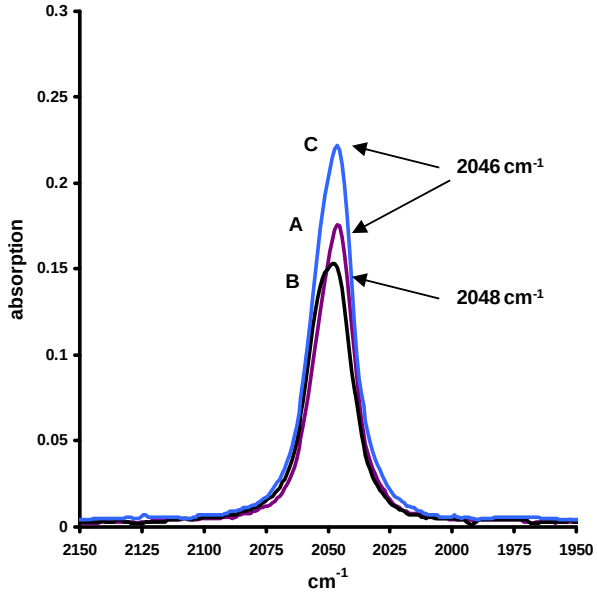

Figure 5-3. FTIR spectra of 0.012 M dichloromethane solutions of (**A**) complex **5-1**, (**B**) complex **5-2** and (**C**) complex **5-3**. The ν_{N3} stretches at 2048 and 2046 cm^{-1} represent five-coordinate manganese azide species.

As illustrated in Figure 5-4 the addition of one equivalent of azide anion to these (salen)MnN_3 derivatives results in new azide stretching frequencies at 2020 and 2006 cm^{-1}. These ν_{N3} vibrational modes correspond to *trans*-(salen)$Mn(N_3)_2^-$ and free azide, respectively (Chapter IV). It is evident that azide binding is not quantitative. That is, under these conditions an equilibrium is established in solution (eq. 5-1), where the equilibrium position is favored to the left. This differs significantly from the ability of (salen)CrN_3 and (tfacacen)MnN_3 which have been shown to bind anions quantitatively, and is indicative of these metal centers being much more electrophilic.

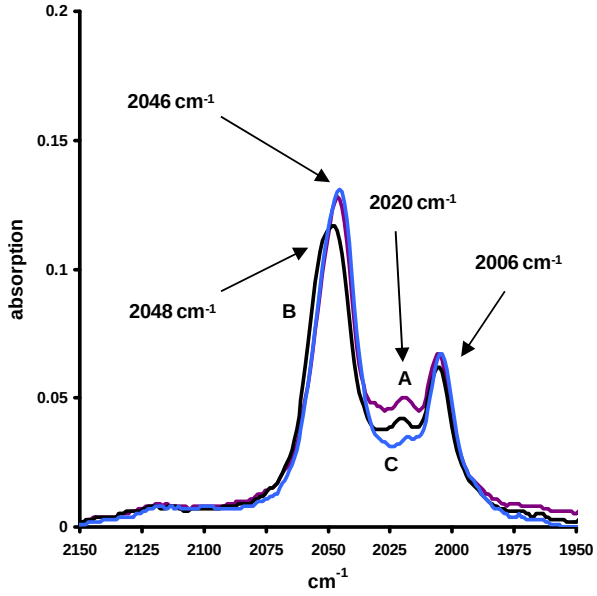

Figure 5-4. FTIR spectra of 0.012 M dichloromethane solutions of (**A**) complex **5-1**, (**B**) complex **5-2** and (**C**) complex **5-3** with the addition of 1 equiv $[PPN]N_3$. The bands at 2020 cm^{-1} and 2006 cm^{-1} represent diazide manganese complexes and free azide, respectively.

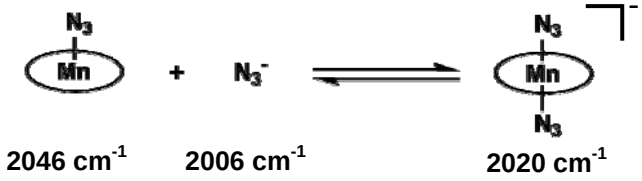

(5-1)

Of more significance to the copolymerization reaction of epoxides and CO_2 is the activation of epoxides for ring-opening and polymer chain propagation by coordination to the metal center (Scheme 5-2). In this regard the infrared spectra in the ν_{N_3} region of complexes **5-1** to **5-3** dissolved in neat cyclohexene oxide are provided in Figure 5-5. As noted the ν_{N_3} vibrational modes undergo the expected wavenumber shift to lower

frequencies indicative of epoxide binding. This epoxide binding is further supported by the formation of small quantities of organic azide resulting from epoxide ring-opening by the azide nucleophile as evident by the band at 2096 cm^{-1}.

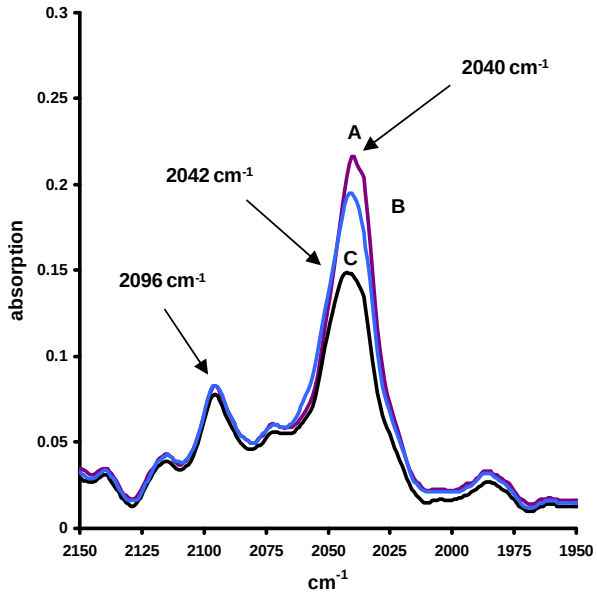

Figure 5-5. FTIR spectra of 0.012 M cyclohexene oxide solutions of (**A**) complex **5-1**, (**B**) complex **5-2** and (**C**) complex **5-3**. The bands at 2042 cm^{-1} and 2040 cm^{-1} represent (salen)MnN_3 epoxide adducts, while 2096 cm^{-1} is organic azide.

With this binding data in hand for (acacen)MnN_3, (tfacacen)MnN_3, and (salen)MnN_3 derivatives it is possible to assess their relative effectiveness as catalysts for the copolymerization of epoxides and carbon dioxide. As previously mentioned, (acacen)MnX complexes are unable to bind anions or epoxides and hence are completely ineffective as catalysts. On the other hand, (tfacacen)MnX complexes readily bind and ring-open epoxides *via* a bimetallic pathway, but because of their electrophilic character

do not insert carbon dioxide in a facile manner. From the studies presented herein, (salen)MnX derivatives containing electron-donating *t*-butyl substituents which are required for solubility are intermediate in binding character and hence would be expected to exhibit some low level catalytic activity as compared to their chromium(III) analogs.[44,99]

Conclusions

An efficient protocol has been developed for the synthesis of several high-spin, d^4 (salen)manganese(III) azide derivatives in good yield and purity. These complexes have been crystallized as five-coordinate monomeric complexes as revealed by X-ray crystallography. As such they should be excellent structural models of their (salen)CrN_3 analogs which have eluded crystallization in the absence of a sixth ligand. By way of contrast, there is a dramatic difference in the catalytic reactivity of these manganese(III) complexes with respect to the highly active d^3 chromium and low-spin d^6 cobalt counterparts for the copolymerization of epoxides and CO_2. That is, it is apparent from these studies that in order for (salen)MX complexes to serve as effective catalysts for this copolymerization process the metal center should be substitutionally inert, electrophilic enough to bind an activate epoxides for ring-opening, and at the same time, be sufficiently nucleophilic to promote carbon dioxide insertion into the resulting metal-alkoxide bond. Furthermore, the presence of an electron in the e^*_g d-orbital of manganese(III) which causes its derivatives to be substitutionally labile, should lead to the dissociation of the growing polymer chain and facile cyclic carbonate formation.

Indeed, these manganese(III) complexes have been shown to be effective catalysts for the production of cyclic carbonates from propylene oxide or styrene oxide and CO_2.[99]

CHAPTER VI

CONCLUSIONS

Summary of Work

This work has been concerned with studies related to the copolymerization of CO_2 and epoxide by transition metal Schiff base complexes. Specifically, the investigations are centered around chromium(III) or manganese(III) acacen catalyst development as an alternative to chromium(III) or cobalt(III) salen catalysts. The hope was to develop catalytic systems with improved properties. In each instance, these systems did not surpass or approach the exceptional characteristics of chromium(III) salen. In the case of (*t*-butylacacen)CrCl(**2-1**), with 1 equivalent [PPN]Cl, a TOF of $150h^{-1}$ was achieved for the production of PCHC. This is some 8 times less active than the most active salen complexes.[20] Manganese(III) acacen complexes proved virtually inert to the copolymerization process while substituted tfacacen complexes, though far more active, only achieved TOF for polycarbonate of less than 3 h^{-1} in the presence of one equivalent $(^{n}Bu)_4NN_3$.

Although manganese(III) acacen complexes may not rival current catalysts, they have proven useful in kinetic and mechanistic studies of the copolymerization process. For instance, the fact that complex **2-1** is active towards copolymerization indicates that ligand systems besides salen, still possessing an N_2O_2 plane, are effective. In other words, the same or similar pathways for initiation and propagation that exist for salen

also apply to similar ligands. Chapters III and IV relate the use of manganese(III) acacen complexes in binding, kinetic and mechanistic studies. Their limited ability to bind relevant substrates in an octahedral fashion has led to a greater understanding of the coordination chemistry involved at the active metal site. Some key observations that can be drawn from this work are summarized as follows.

Firstly, complexes unable to bind epoxides such as CHO or PO to the metal center will be unable to facilitate copolymerization *via* a bimetallic or monometallic (cocatalyst) mechanism. This is observed by the fact that complex **3-3** was unable to facilitate the formation of polycarbonate or bind CHO. On the other hand complex **4-1**, possessing a more electrophilic metal center, was able to bind epoxide and, consequently, catalyzed the formation of polycarbonate. This idea is further supported by the fact that chromium(III) salen complexes quantitatively bind CHO and are exceptionally active towards the formation of polycarbonate.[19] The rate of initial ring-opening also appears to be proportional to the rate of polycarbonate formation. Complex **4-1** will readily ring-open 60 to 200 equivalents CHO in 40 to 240 minutes at temperatures ranging from 10 to 40 ºC. Chromium(III) salen complexes, however, will perform the same reaction with one equivalent CHO at room temperature.

Secondly, manganese(III) complexes have proven to be of value due to their structural similarities to chromium(III) and cobalt(III) salen complexes. This is evident from the structural information presented in this and other works. In most cases this allows for comparative studies to be made that these analogs will accurately mimic their salen counterparts. This assertion was further supported by the binding studies

conducted on manganese(III) salen complexes in Chapter V. From this several useful comparisons may be drawn between the two ligands. Firstly, the lower steric bulk of acacen complexes containing suitable bridging apical ligands can lead to aggregation in the solid state. This has also been seen with manganese(III) salen complexes that do not contain bulky substituents on the phenolates.[78] For complexes that do contain these groups aggregation is not seen in the solid state (Chapter V). This is an important characteristic for chromium(III) salen azide complexes as they are known to aggregate in solution without the presence of a coordinating ligand such as THF or epoxide.[XX] In other words, under certain conditions azide complexes can aggregate resulting in inhibited catalysis. Thus, the *t*-butyl substituents typically found with salens in this chemistry may not only provide electron density to the metal center but also discourage aggregation in solution.

It has also been informative to compare the binding of manganese(III) acacen, tfacacen and salen complexes. Since ligand binding to a metal center is proportional to the electrophilicity of the metal it can be concluded that the salens typically employed in this catalysis have an intermediate withdrawing ability in between acacen and tfacacen. The former will only bind strongly coordinating ligands such as cyclic amines (i.e. pyridine and DMAP) at high equivalents (10 to 100). The fluorinated version of the ligand will bind DMAP, azide and at 5 to 1 equivalents, respectively. The salen ligands studies in this work will bind azide and DMAP more readily than acacen but less so than tfacacen. From this it can be inferred that salen ligands without electron donating *t*-butyl groups are quite withdrawing in nature. It can further be imagined, though less directly,

that the manganese(III) tetraphenyl porphyrin complexes of Inoue, which represent the most active manganese based catalytic systems yet developed, contain amongst the most electrophilic metal centers of their kind.[44]

Remarks on the Field of Polycarbonates

The health concerns and costly, potentially harmful manufacture of polycarbonates such as BPA-PC indicates that there is a need for new polymeric materials that circumvent these disadvantages and provide useful and inexpensive products to the marketplace. In addition, the overall drive in our society to produce materials from renewable resources is growing. The only commercially produced polycarbonate from the copolymerization of CO_2 and epoxide is PPC. It has found use in the ceramics industry as a binder on account of the polymer's clean decomposition temperature at around 250 ºC.[100] However, the production of PPC and control of its properties presents many challenges.[101] Issues arise from high polyether insertion, poor regio- and sterio selectivity, inefficiencies in monomer conversion and the simultaneous production of cyclic carbonate. This leads to a broad range of glass transition and decomposition temperatures when proceeding from one reaction condition or catalyst to the next. Also, the polymer's propensity to convert to cyclic carbonate during processing (extrusion) can be an issue, especially when trace amounts of metal catalyst are present.[101]

The application of chromium(III) and cobalt(III) salen catalysts could potentially circumvent many of these issues. However, due to the high costs of these catalysts the

most widely used catalyst for a typical batch process is based on zinc glutarate and not salen complexes.[101] In order to offset costs, the ideal homogeneous system would have activities similar to those in polyolefin production. In that way, extraction of the metal and extended work-up of the polymer is rendered unnecessary. This means that catalyst activities would have to be more than 10 times greater than the most active zinc based system.[12e] Obviously, a significant breakthrough in activity must take place with the salen catalysts in question for their widespread application to become a reality.

Despite this decade's major discoveries into the copolymerization of CO_2 and epoxide the actual industrial contributions to this class of polycarbonates is small. Baring major developments, it appears as though this promising area may decline in interest and be henceforth known as an excellent proof-of-principle in green chemistry and little else. Only a few companies currently specialize in the production of PPC. One company, Novomer, is a start-up co-founded by Professor Geoffrey Coates of Cornell. Its goals are to offer green, high performance biodegradable polymers to industrial and consumer markets.[102] A more established company is Empower Materials out of Newark, Delaware. This company offers a small line of polyalkylene carbonates such as PPC and poly(ethylene carbonate) that are used in the binding and other sacrificial structure applications. Hopefully, through incremental improvements or major breakthroughs, these companies and others can continue to drive this field towards profitability and greater research investment. Certainly, society's need for renewable and greener materials is constant and massive.

Future Directions in the Field of Polycarbonates

One way to circumvent the expense of transition metal salen catalysts would be a homogeneous system capable of being prepared in epoxide monomer immediately preceding the polymerization reaction. In order words, the catalyst would be prepared *in situ*. This would remove the need of isolating a catalyst at the end of a costly synthesis and work-up. Preliminary results on the part of this author have shown this to be possible. The catalyst synthesis involves dissolving equal molar amounts of acacen (see Chapter II) and $CrCl_3(THF)_3$ in neat CHO at room temperature. After the initial formation of a green colored solution, a dark brown color forms within 30 minutes mixing. Although no crystallographic or elemental analysis has been performed on this catalyst, mass spectrometry analysis gives a peak at 274.0707 m/z in the positive mode. This corresponds to the cation $[(acacen)Cr]^+$ and demonstrates that a chromium acacen complex of some kind is present in the CHO catalyst mixture.

It is intriguing to note that attempts at synthesizing (acacen)CrCl through a variety of methods and with numerous solvents have in all cases resulted in an insoluble green powder that has proven difficult to characterize. The synthesis of a catalyst in the presence of a reactive monomer like CHO suggests that whatever complex being formed may require a ring-opening step in order to either synthesize or stabilize the species. Polymerization reactions in the presence of the *in situ* catalyst and 0.5 and 1.0 equivalents of $(^nBu)_4NN_3$ have been performed for the synthesis of PCHC.[103] At 80 ºC, 34.5 bar CO_2 pressure and one equivalent cocatalyst PCHC was produced with TON = 863 and TOF = 690 h^{-1}. At 0.5 equivalents cocatalyst a TON = 452 and TOF = 387 h^{-1}

was achieved. Molecular weights of the polymers as determined by GPC were 7,592 Da and 8188 Da for 1.0 and 0.5 equivalents cocatalyst, respectively. A polymerization reaction ran with no cocatalyst failed to form any polycarbonate products. The lower molecular weights of these polymers are likely the result of spurious amounts of HCl left over from the synthesis of the catalysts. If these issues can be resolved (perhaps through the addition of base) along with the successful application of other epoxides (i.e. PO) the lower cost of this approach may lead to a greater application of homogeneous transition metal Schiff base catalysts. For tables and figures related to these reactions see Appendix B.

Apart from catalyst design, an expansion in the current array of monomers that are capable of activation would be highly advantageous. The formation of PCHC from CHO is well known and is the focus of a large amount of academic research. Unfortunately, the properties of this material, even at very high molecular weights, are markedly inferior to BPA-PC, its most likely replacement.[104] Lu has reported the copolymerization of some terminal epoxides other then PO with CO_2, though without analysis of polymer properties.[105] Coates has reported the copolymerization of CO_2 and limonene oxide, a natural product. Although a remarkable experiment in green chemistry, activities were prohibitively low.[8]

Similarly, little work has taken place with new *meso* epoxides, i.e. CHO derivatives. This approach could offer advantages over terminal epoxides such as lower levels of cyclic production, higher activities and a greater choice of catalysts. One monomer that has received some attention may offer a great deal of flexibility in

polymer properties. Coates and Tan have both synthesized terpolymers with CHO and vinylcyclohexene oxide (VCHO, 4-vinyl-1-cyclohexene-1, 2-epoxide).[106],[107] Crosslinked polycarbonate particles on the nanoscale were achieved by reacting a 38% vinyl-containing polymer with Grubb's catalyst. This cross-metathesis increased the glass transition temperature from 114 ºC for PHCH to 194 ºC for the treated polymer. Conceivably, other alterations in the polymer could take place across the reactive double bond and result in an array of improved properties.

Other catalysts can be utilized as well. The previously mentioned two researchers employed either yttrium or zinc based catalyst systems. This author has found that chromium(III) salen complexes are also applicable. One experiment yielded poly(vinyl cyclohexene carbonate) (PVCHC) with a TOF of 548 h^{-1}, a M_n of 22244 Da and a PDI of 1.261.[108] This activity is comparable to that of PCHC and purification of the polymer is carried out in an identical way.[109] Preliminary differential scanning calorimetry tests have placed the T_g of PVCHC between 50 and 55 ºC, somewhat less than PCHC.[104] Steps have not been taken to describe the regio- or stereoselectivity of the polymer; however, it is likely atactic in nature considering that the monomer feed was racemic and the catalyst employed lacked a chiral backbone. Nevertheless, control of polymer tacticity might be available from either a chiral chromium catalyst or from a cobalt(III) salen based chiral system such as the many currently used to synthesize regio- or stereoregular PPC.

Ironically, the highest impact in the area of CO_2 utilization for polycarbonate production is found in the formation of BPA-PC. Asahi Kasei Corporation of Japan has

developed a large scale production plant capable of producing 150,000 tons/year of BPA-PC using CO_2 as a feedstock.[110] The process avoids the large amounts of water and chlorinated solvent produced in the well known interfacial, biphasic reaction (Chapter I). Also, new solid state and melt polymerization techniques have led polymers of high clarity and molecular weight at temperatures lower than those traditionally used with melt polymerizations.

Scheme 6-1.

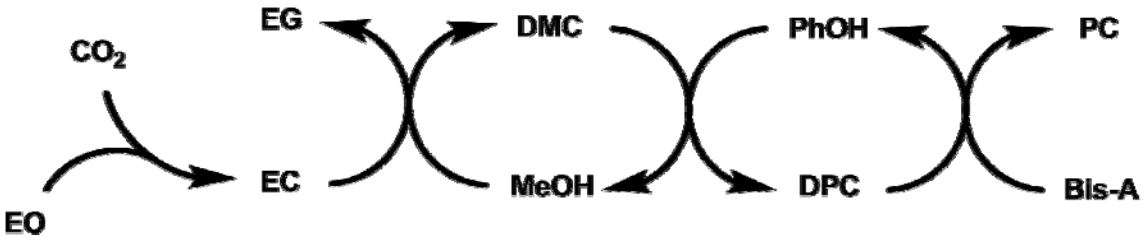

The reaction involves the formation of ethylene carbonate (EC) from the reaction of ethylene oxide (EO) and CO_2 in the presence of a catalyst such as alkaline earth meal halides, amines, ammonium or phsophonium salts or anion-exchange resins (Scheme 6-1).[110] The ethylene carbonate then reacts with methanol (an intermediate) to produce dimethyl carbonate (DMC) and the only side product of the process, ethylene glycol (EG). Dimethyl carbonate is then converted to diphenyl carbonate (DPC) by a reaction with phenol. This phenol is an intermediate produced by the polymerization of diphenyl carbonate with bisphenol A to form BPA-PC. Each intermediate is generated and used in the process so that the net reaction can be stated as EO, CO_2 and BPA combining to

produce BPA-PC. In this way, the use of phosgene is completely circumvented by combining an epoxide with CO_2, an entirely benign and plentiful feedstock. The only issue that is not addressed by the approach is the health concerns currently revolving around BPA itself (Chapter I).

REFERENCES

1. Arakawa, H.; Aresta, M.; Armor, J. N.; Barteau, M. A.; Beckman, E. J.; Bell, A. T.; Bercaw, J. E.; Creutz, C.; Dinjus, E.; Dixon, D. A.; Domen, K.; DuBois, D. L.; Eckert, J.; Fujita, E.; Gibson, D. H.; Goddard, W. A.; Goodman, D. W.; Keller, J.; Kubas, G. J.; Kung, H. H.; Lyons, J. E.; Manzer, L. E.; Marks, T. J.; Morokuma, K.; Nicholas, K. N.; Periana, R.; Que, L.; Rostrup-Nielson, J.; Sachtler, W. M. H.; Schmidt, L. D.; Sen, A.; Somorjai, G. A.; Stair, P. C.; Stults, B. R.; Tumas, W. *Chem. Rev.* **2001**, *101*, 953-996.
2. Aresta, M.; Dibenedetto, A. *J. Chem. Soc., Dalton Trans.* **2007**, *28*, 2975-2992.
3. Song, C. *Catal. Today* **2006**, *115*, 2-32.
4. *Handbook of Polycarbonate Science and Technology*; Legrand, D. G.; Bendler, J. T., Eds.; Marcel Dekker, Inc.: New York, 2000.
5. *Engineering Plastics Handbook*; Margolis, J. M., Ed.; McGraw-Hill, New York, 2006.
6. Brunelle, D. J.; Smigelski Jr., P. M.; Boden, E. P. Chapters 1 and 2, *Advances in Polycarbonates*, Brunelle, D. J.; Korn, M. R., ACS Symposium Series 898, American Chemical Society: Washington, DC, 2005.
7. (a) Hileman, B. *Chem. Eng. News* **2007**, *85*(11), 13. (b) Hileman, B. *Chem. Eng. News* **2007**, *85(32)*, 8-9. (c) Hileman, B. *Chem. Eng. News* **2007**, *85*(36), 31-33.
8. Byrne, C. M.; Allen, S. D.; Lobkovsky, E. B.; Coates, G. W. *J. Chem. Chem. Soc.* **2004**, *126*, 11404-11405.

9. Lu, X. B.; Shi, L.; Wang, Y. M.; Zhang, R.; Zhang, Y. J.; Peng, X. J.; Zhang, Z. C.; Li, B. *J. Am. Chem. Soc.* **2006**, *128*, 1664-1674.

10. Inoue, S.; Kionuma, H.; Tsuruta, T. *Polym. Sci. Part B: Polym. Lett.* **1969**, *7*, 287-292.

11. (a) Kuran, W.; Pasykiewicz, S.; Skupinska, J.; Rokicki, A. *Makromol. Chem.* **1976**, *177*, 11-20. (b) Kobayashi, M.; Inoue, S.; Tsuruta, T. *J. Polym. Sci. Polym. Chem. Ed.* **1973**, *11*, 2383-2385. (c) Soga, K.; Imai, E.; Hattori, I. *Polym. J.* **1981**, *13*, 407-410. (d) Motika, S. (Air Products and Chemicals, Inc., Acro Chemical Co., and Mitsui Petrochemical Industries Ltd.). U.S. Patent 5,026,676, 1991. (e) Gorecki, P.; Kuran, W.; *J. Polym. Sci. Part C* **1985**, *23*, 299-304. (f) Ree, M.; Bae, J.Y.; Jung, J.H.; Shin, T.J. *J. Polym. Sci. Part A* **1999**, *37*, 1863-1876.

12. (a) Darensbourg, D. J.; Holtcamp, M. W.; Khandelwal, B.; Klausmeyer, K. K.; Reibenspies, J. H. *J. Am. Chem. Soc.* **1995**, *117*, 538-539. (b) Cheng, M.; Lobkovsky, E. B.; Coates, G. W. *J. Am. Chem. Soc.* **1998**, *120*, 11018-11019. (c) Darensbourg, D. J.; Holtcamp, M. W.; Struck, G. E.; Zimmer, M. S.; Niezgoda, S. A.; Rainey, P.; Robertson, J. B.; Draper, J. D.; Reibenspies. J. H. *J. Am. Chem. Soc.* **1999**, *121*, 107-116. (d) Darensbourg, D. J.; Wildeson, J. R.; Yarbrough, J. C.; Reibenspies, J. H. *J. Am. Chem. Soc.* **2000**, *122*, 12487-12496. (e) Moore, D. R.; Cheng, M.; Lobkovsky, E. B.; Coates, G. W. *Angew. Chem. Int. Ed.* **2002**, *41*, 2599-2602.

13. (a) Aida, T.; Ishikawa, M.; Inoue, S. *Macromolecules* **1986**, *19*, 8-13. (b) Mang,

S.; Cooper, A. I.; Colclough, M. E.; Chauhan, N.; Holmes, A. B. *Macromolecules* **2000**, *33*, 303-308.

14. Larrow, J. F.; Jacobsen, E. N. *Top. Organomet. Chem.* **2004**, *6*, 123-152.

15. (a) Jacobsen, E. N.; Zhang, W.; Muci, A. R.; Ecker, J R.; Deng, L. *J. Am Chem Soc.* **1991**, *113*, 7063-7064. (b) Bandes, B. D.; Jacobsen, E. N. *J. Org. Chem.* **1994**, *59*, 4378-4380. (c) Palucki, M.; Finney, N. S.; Pospisil, P. J.; Güler, M. L.; Ishida, T.; Jacobsen, E. N. *J. Am. Chem. Soc.* **1998**, *120*, 948-954.

16. (a) Tokunaga, M.; Larrow, J. F.; Kakiuchi, F.; Jacobsen, E. N. *Science* **1997**, *277*, 936-938. (b) Nielsen, L. P. C.; Stevenson, C. P.; Blackmond, D. G.; Jacobsen, E. N. *J. Am. Chem.. Soc.* **2004**, *126*, 1360-1362.

17. (a) Martinez, L. E.; Leighton, J. L.; Carste, D.H.; Jacobsen, E. N. *J. Am. Chem. Soc.* **1995**, *117*, 5897-5898. (b) Hansen, K. B.; Leighton, J. L.; Jacobsen, E. N. *J. Am. Chem. Soc.* **1996**, *118*, 10924-10925. (c) Leighton, J. L.; Jacobsen, E. N. *J. Org. Chem.* **1996**, *61*, 389-390. (d) Brandes, B. D.; Jacobsen, E. N. *Synlett*, **2001**, *SI*, 1013-1015.

18. Darensbourg, D. J.; Yarbrough, J. C. *J. Am. Chem. Soc.* **2002**, *124*, 6335-6342.

19. Darensbourg, D. J.; Mackiewicz, R. M.; Rodgers, J. L.; Fang, C. C.; Billodeaux, D. R.; Reibenspies, J. H. *Inorg. Chem.* **2004**, *43*, 6024-6034.

20. Darensbourg, D. J.; Mackiewicz, R. M.; Billodeaux, D. R. *Organometallics* **2005**, *24*, 144-148.

21. Darensbourg, D. J.; Yarbrough, J. C.; Ortiz, C.; Fang, C. C. *J. Am. Chem. Soc.* **2003**, *125*, 7586-7591.

22. Darensbourg, D. J.; Phelps, A. L. *Inorg. Chem.* **2005**, *44*, 4622-4629.

23. (a) Qin, Z.; Thomas, C.M.; Lee, S.; Coates, G.W. *Angew. Chem. Int. Ed.* **2003**, *42*, 5484-5487. (b) Lu, X.,-B.; Wang, Y. *Angew. Chem. Int. Ed.* **2004**, *43*, 3574-3577.

24. Cohen, C. T.; Chu, T.; Coates, G. W. *J. Am. Chem. Soc.* **2005**, *127*, 10869-10878.

25. (a) Chisholm, M. H.; Zhou, Z. *J. Am. Chem. Soc.* **2004**, *126*, 11030-11039. (b) Luinstra, G. A.; Haas, G. R.; Molnar, F.; Barnhart, V.; Eberhardt, R.; Rieger, B. *Chem. Eur. J.* **2005**, *11*, 6298-6314.

26. (c) Darensbourg, D. J. *Chem. Rev.* **2007**, *107*, 2388-2410.

27. (a) Darensbourg, D. J.; Mackiewicz, R. M.; Rodgers, J. L. *J. Am. Chem. Soc.* **2005**, *127*, 14026-14038. (b) Darensbourg, D. J.; Mackiewicz, R. M. Rodgers, J. L. *J. Am. Chem. Soc.* **2005**, *127*, 17565-17565.

28. For reviews and recent contributions to this area see: (a) Super, M. S.; Beckman, E. J. *Trends. Polym. Sci.* **1997**, *5*, 236-240. (b) Kuran, W.; *Prog. Polym. Sci.* **1998**, *23*, 919-992. (c) Lu, X. B.; Wang, Y. *Angew. Chem., Int. Ed.* **2004**, *43*, 3574-3577. (d) Sugimoto, H.; Inoue, S.; *J. Polym Sci., Part A: Polym. Chem.* **2004**, *42*, 5561-5573. (e) Darensbourg, D. J.; Mackiewicz, R. M.; Phelps, A. L.; Billodeaux, D. R. *Acc. Chem. Res.* **2004**, *37*, 836-844. (f) Chisholm, M. H.; Zhou, Z. *J. Mater. Chem.* **2004**, *14*, 3081-3092. (g) Moore, D. R.; Coates, G. W. *Angew. Chem., Int. Ed.* **2004**, *43*, 6618-6639. (h) Paddock, R. L.; Nguyen, S. T.

Macromolecules **2005**, *38*, 6251-6253. (i) Cohen, C. T.; Thomas, C. M.; Peretti, K. L.; Lobkovsky, E. B.; Coates, G. W. *Dalton Trans.* **2006**, *1*, 237-249.

29. (a) Gerlach, D. H.; Holm, R. H. *Inorg. Chem.* **1970**, *9*, 588-594. (b) Lindoy, L. F.; Moody, W. E.; Taylor, D. *Inorg. Chem.* **1977**, *16*, 1962-1968. (c) Larkworthy, L. F.; Povey, D. C.; Sandell, B. *Inorg. Chim. Acta* **1984**, *83*, L29-L30. (d) Böttcher, A.; Takeuchi, T.; Hardcastle, K. I.; Meade, T. J.; Gray, H. B.; Cwikel, D.; Kapon, M.; Dori, Zvi *Inorg. Chem.* **1997**, *36*, 2498-2504. (e) Vohs, J. K.; Miller, D. O.; Denomme, D. R.; Ziller, J. W.; Fahlman, B. D. *Acta Crystallogr., Sect. C* **2005**, *C61*, m287-m288.

30. (c) Boucher, L. J.; Day, V. W. *Inorg. Chem.* **1977**, *16*, 1360-1367.

31. Casiraghi, G.; Casnati, G.; Puglia, G.; Satori, G.; Terenghi, J. *Chem. Soc., Perkin Trans 1.* **1980**, *9*, 1862-1865.

32. Adams, J. T.; Hauser, C. R. *J. Am. Chem. Soc.* **1944**, *66*, 1220-1222.

33. McCarthy P. J.; Hovey, R. J.; Ueno, K.; Martell, A. E.; *J. Am. Chem. Soc.* **1955**, *77*, 5820-5824.

34. Darensbourg, D. J.; Frantz, E. B.; Andreatta, J. R. *Inorg. Chim. Acta* **2007**, *360*, 523-528.

35. SMART 1000 CCD: Bruker Analytical X-ray Systems: Madison, WI, 1999.

36. SAINT V6.63 “Program for Reduction of Area Detector Data” BRUKER AXS Inc., 5465 East Cheryl Parkway, Madison, WI 53711-5373 USA.

37. Sheldrick, G. (1997) SHELXS-97 “Program for Crystal Structure Solution”; Institüt für Anorganische Chemie der Universität, Temmanstrassa 4, D-3400 Gottingen, Germany.

38. Sheldrick, G. (1997) SHELXL-97 “Profram for Crystal Structure Refinement”, Institüt für Anorganische Chemie der Universität, Temmanstrassa 4, D-3400 Gottingen, Germany.

39. Sheldrick, G. M. (2000) SHELXTL Version 6.14, Bruker-Nonius Inc., Madison, Wisconsin, USA.

40. Barbour, L. J., (1999) “X-Seed –A Software Tool for Supramolecular Crystallography”, *J. Supramol. Chem.* **2001**, *1*, 189-191.

41. Sanzenbacher, R.; Bottcher, A.; Elias, H.; Huber, M.; Haase, W.; Glerup, J.; Jensen, T. B.; Neuburger, M.; Zehnder, M.; Olsen, C. E.; Springborg, J. *Inorg. Chem.* **1996**, *35*, 7493-7499.

42. Darensbourg, D.J.; Ortiz, C.G.; Billodeaux, D.R. *Inorg. Chim. Acta*. **2003**, *357*, 2143-2149.

43. Srivastava, R.; Bennur, T.H.; Srinivas, D. *J. Mol. Catal.* **2005**, *226*, 199-205.

44. Sugimoto, H.; Ohshima, H.; Inoue, S. *J. Polym. Sci. Part A* **2003**, *41*, 3549-3555.

45. SMART V5.632 “Program for Data Collection on Area Detectors” BRUKER AXS Inc., 5465 East Cheryl Parkway, Madison, WI 53711-5373 USA.

46. FRAMBO:FRAME Buffer Operation Version 41.05 “Program for Data Collection on Area Detectors” BRUKER AXS Inc., 5465 East Cheryl Parkway, Madison, WI 53711-5373 USA.

47. SADABS, Sheldrick, G.M. "Program for Absorption Correction of Area Detector Frames", Bruker AXS., 5465 East Cheryl Parkway, Madison, WI 53711-5373 USA.

48. Beurskens, P., Admiraal, G., Beurskens, G., Bosman, S., Garicia-Granda, R., Gould, J., Smykalla, A. and Smykalla, C. (1999). DIRDIF-99 program system, Technical Report for the Crystallography Laboratory, University of Nijimegen, The Netherlands.

49. Farrugia, L.J. *J. Appl. Cryst.* **1999**, *32*, 837-838.

50. Feng, Y; Liu, S. *Acta Cryst.* **1996**, *52*, 2768-2770.

51. Liu, S.; Feng, Y. *Polyhedron* **1996**, *15*, 4195-4201.

52. Feng, Y. L.; Liu, S. X. *J. Coord. Chem.* **1998**, *44*, 81-90.

53. Zhou, Y.-Z.; Zheng, X.-F.; Han, D.; Zhang, H.-Y.; Shen, X.-Q.; Niu, C.-Y.; Chen, P.-K.; Hou, H.-W.; Zhu, Y. *Synth. React. Inorg. Metal-Org. Nano-Metal Chem.* **2006**, *36*, 693-699.

54. Wang, S.-W.; Zhou, J. –H.; Li, B.-L.; Zhang, Y. *Chin. J. Inorg. Chem* **2004**, *20*, 1433-1466.

55. Haider, S. Z.; Hashem, A.; Khan, M. S.; Malik, K. M. A.; Hursthouse, M. B. *J. Bangladesh Acad. Sci.* **1985**, *9*, 105-112.

56. Feng, Y. *Chinese J. Struct. Chem.* **2002**, *21*, 352-354.

57. Davies, J.E.; Gatehouse, B.M.; Murray, K.S. *J.C.S. Dalton* **1973**, *22*, 2523-2527.

58. Li, H.; Zhong, Z.J.; Duan, C.-Y.; You, X.-Z.; Mak, T. C.W.; Wu, B. *Inorg. Chim Acta* **1998**, *271*, 99-104.

59. Reddy, K. R.; Rajasekharan, M.V.; Tuchagues, J.-P. *Inorg. Chem.* **1998**, *37*, 5978-5982.

60. Bonadies, J.A.; Kirk, M.L.; Lah, M.S.; Kessissoglou, D.P.; Hatfield, W.E.; Pecoraro, V.L. *Inorg. Chem.* **1989**, *28*, 2037-2044.

61. Stults, B.R.; Marianelli, R.S.; Day, V.W. *Inorg. Chem.* **1975**, *14*, 722-730.

62. Ray, U.; Jasimunddin, S.; Ghosh, B. K.; Monfort, M.; Ribas, J.; Mostafa, G.; Lu, T. –H.; Sinha, C. *Eur. J. Inorg, Chem.* **2004**, 250-259.

63. Ghosh, A. K.; Ghoshal, D.; Zangrando, E.; Ribas, J.; Chaudhuri, N. R. *Inorg. Chem.* **2005**, *44*, 1786-1793.

64. Bai, S.-Q.; Gao, E.-Q.; He, Z.; Fang, C.-F.; Yue, Y.-F.; Yan, C.-H. *Eur. J. Inorg. Chem.* **2006**, 407-415.

65. Das, A.; Rosair, G. M.; El Fallah, M. S.; Ribas J.; Mitra, S. *Inorg. Chem.* **2006**, *45*, 3301-3306.

66. Liu, S.X.; Feng, Y.L. *Chem. J. Chin. Univ.* **1996**, *17*, 509-514.

67. Feng, Y.; Liu, S. *Chinese J. Struct. Chem.* **1998**, *17*, 125-128.

68. Xu, D.; Chen, B.; Chen, K.; Chen, C.; Miki, K.; Kasai, N. *Bull. Chem. Soc. Jpn.* **1989**, *62*, 2384.

69. Feng, Y; Liu, S. *Chem. J. Chin. Univ.* **2001**, *22*, 887-891.

70. Trace quantities of the cyclic carbonate were afforded which are attributed to the cocatalysts, (n-Bu_4)NN_3.

71. (a) Xiao, Y.; Wang, Z.; Ding, K. *Macromolecules* **2006**, *39*, 128-137. (b) Xiao, Y.; Wang, Z.; Ding, K. *Chem. Eur. J.* **2005**, *11*, 3668-3678.

72. Cohen, C.T.; Coates, G.W. *J. Polym. Sci. Part A: Polym. Chem.* **2006**, *44*, 5182-5191.

73. Boucher and Day have measured the magnetic moments for a variety of Mn(III) acacen complexes and found them to be high spin with values ranging from 4.30 to 5.09μ_B in both the solid state and in solution.

74. Miyasaka, H.; Saitoh, A.; Abe, S. *Coord. Chem. Rev.* **2007**, *251*, 2622-2664.

75. (a) Evans, D. F. *J. Chem. Soc.* **1959**, 2003. (b) Grant, D. H. *J. Chem. Educ.* **1995**, *72*, 39. (c) Girolami, G. A.; Rauchfuss, T. B.; Angelici, R. J. *Synthesis and Technique in Inorganic Chemistry: A Laboratory Manual*; University Science Books: Sausalito, CA, 1999; 3rd Ed., 125-126.

76. *Peakfit* for Windows v4.12; © Copyright 2003; SYSTAT Software Inc: San Jose, CA 2003.

77. Darensbourg, D. J.; Frantz, E. B. *Inorg. Chem.* **2007**, *46*, 5967-5978.

78. (a) Panja, A.; Shaikh, N.; Vojtisek, P.; Gao, S.; Banerjee, P. *New J. Chem.* **2002**, *26*, 1025-1028. (b) Saha, S.; Mal, D.; Koner, S.; Bhattacherjee, A.; Gütlich, P.; Mondal, S.; Mukherjee, M.; Okamoto, K. -I. *Polyhedron* **2004**, *23*, 1811-1817. (c) Deoghoria, S.; Bera, S. K.; Moulton, B.; Zaworotko, M. J.; Tuchagues, J. -P.; Mostafa, G.; Lu, T., -H.; Chandra, S. K. *Polyhedron*, **2005**, *24* 343-350. (d) Lu, Z.; Yuan, M.; Pan, F.; Gao, S.; Zhang, D.; Zhu, D. *Inorg. Chem.* **2006**, *45*, 3538-3548. (e) Ko, H. H.; Lim, J. H.; Kim, H. C.; Hong, C. S. *Inorg. Chem.* **2006**, *45*,

8847-8849. (f) Yuan, M.; Zhao, F.; Zhang, W.; Wang, Z.-M.; Gao, S. *Inorg. Chem* **2007**, *46*, 11235-11242.

79. (a) Sakata, K.; Nakamura, H.; Hashimoto, M. *Inorg. Chim. Acta* **1984**, *83*, L67-L70. (b) Massoud, S. S.; Mautner, F. A. *Inorg. Chim. Acta* **2005**, *358*, 3334-3340. (c) Sen, S.; Mitra, S.; Luneau, D.; Fallah, M. S. E.; Ribas, J. *Polyhedron* **2006**, *25*, 2737-2744. (d) Bréfuel, N.; Shova, S.; Tuchagues, J. -P. *Eur. J. Chem.* **2007**, 4326-4334.

80. Stults, B. R.; Day, R. O.; Marianelli, R. S.; Day, V. W. *Inorg. Chem.* **1979**, *18*, 1847-1852.

81. Boucher, L. J.; Coe, C. G. *Inorg. Chem.* **1975**, *14*, 1289-1294.

82. Torayama, H.; Nishide, T.; Asada, H.; Fujiwara, M.; Matsushita, T.; *Polyhedron* **1998**, *17*, 105-118.

83. (a) Bhaduri, S.; Tasiopoulos, A. J.; Bolcar, M. A.; Abboud, K. A.; Streib, W. E.; Christou, G. *Inorg. Chem.* **2003**, *42*, 1483-1492. (b) Ruiz-García, R.; Pardo, E.; Munoz, M. C.; Cano, J. *Inorg. Chim. Acta* **2007**, *360*, 221-232.

84. (a) Darensbourg, D. J.; Mackiewicz, R. M.; Rodgers, J. L.; Phelps, A. L. *Inorg. Chem.* **2004, *43***,1831-1833. (b) Darensbourg, D. J.; Bottarelli, P.; Andreatta, J. R. *Macromolecules* **2007**, *40*, 7727-7729.

85. (a) Liu, C. -M.; Gao, S.; Zhang, D. -Q.; Liu, Z. -L.; Zhu, D. -B. *Inorg. Chim. Acta* **2005**, *358*, 834-838. (b) Ni, Z. -L.; Kou, H. -Z.; Zheng, L.; Zhao, Y. -H.; Zhang, L. -F.; Wang, R. -W.; Cui, A. -L.; Sato, O. *Inorg. Chem.* **2005**, *44*, 4728-

4736. (c) Yu, M.-M.; Ni, Z.-H.; Zhao, C.-C.; Cui, A.-L.; Kou, H.-Z. *Eur. J. Inorg. Chem.* **2007**, 5670-5676.

86. (a) Massoud, S. S. *Polyhedron* **1994**, *13*, 3127-3134. (b) Goher, M. A. S.; Al-Salem, N. A.; Mautner, F. A.; *Polyhedron* **1997**, *21* 3747-3755. (c) Massoud, S. S.; Mautner, F. A.; Abu-Youssef, M.; Shuaib, N. M. *Polyhedron* **1999**, *18*, 2287-2291. (d) Sharma, R. P.; Sharma, R.; Bala, R.; Quiros, M.; Salas, J. M. *J. Coord. Chem.* **2003**, *56*, 1581-1586. (e) Sharma, R.P.; Sharma, R.; Bala, R.; Singh, K.N.; Pretto, L.; Ferretti, V. *J. Mol. Struct.* **2006**, *784*, 109-116. (f) Sharma, R. P.; Sharma, R.; Bala, R.; Venugopalan, P. *J. Mol. Struct.* **2006**, *787*, 69-75. (g) Sharma, R. P.; Sharma, R.; Bala, R.; Burrows, A. D.; Mahon, M. F.; Cassar, K. *J. Mol. Struct.* **2006**, *794*, 173-180.

87. Nakamoto, K. Section III-16. *Infrared and Raman Spectra of Inorganic and Coordination Compounds*, 5th ed.; Wiley & Sons, Inc.: New York, 1997, Part B, 116-126.

88. Boudalis, A. K.; Clemente-Juan, J.-M.; Dahan, F.; Tuchagues, J.-P *Inorg. Chem.* **2004**, *43*, 1574-1586.

89. Mauro, A.E.; Haddad, P. S.; Zorel Jr., H. E.; Santos, R. H. A.; Ananias, S. R.; Martins, F. R.; Tarrasqui, L. H. R. *Transition Met. Chem.* **2004**, *29*, 893-899.

90. Youngme, S.; Phatchimkun, J.; Suksangpanya, U.; Pakawatchai, C.; van Albada, G. A.; Reedijk, J. *Inorg. Chem. Comm.* **2005**, *8*, 882-885.

91. (a) Fujiki, K.; Yoshida, E. *Synth. Commun.* **1999**, *29*, 3289-3294. (b) Renard, P. -Y.; Schwebel, H.; Vayron, P.; Leclerc, E.; Dias, S.; Mioskowski, C.

Tetrahedron Lett. **2001**, *42*, 8479-8481. (c) Iranpoor, N.; Firouzabadi, H.; Nowrouzi, N. *Tetrahedron* **2006**, *62*, 5498-5501.

92. (a) Sharghi, H.; Nasseri, M. A.; Nejad, A. H. *J. Mol. Catal.* **2003**, *206*, 53-57. (b) Sharghi, H.; Nejad, A. H.; Nasseri, M. A. *New J. Chem.* **2004**, *28*, 946-951. (c) Sharghi, H.; Beni, A. S.; Khalifeh, R. *Helv. Chi. Acta* **2007**, *90*, 1373-1385.

93. March, J.; Smith, M. S.; *March's Advanced Organic Chemistry: Reactions, Mechanisms, and Structure*, 5th ed.; Wiley & Sons, Inc.: New York, 2001.

94. Larrow, J. F.; Jacobsen, E. N. *J. Org. Chem.* **1994**, *59*, 1939-1942.

95. Bruker Configuration Program V 2.0.1.9 "Program for Data Collection on Area Detectors" BRUKER AXS Inc., 5465 East Cheryl Parkway, Madison, WI 53711-5373 USA.

96. (a) Boucher, L. J.; Farrell, M. O. *J. Inorg. Nucl. Chem.* **1973**, *35*, 3731-3738. (b) Zhang, W.; Jacobsen, E. N. *J. Org. Chem.* **1991**, *56*, 2296-2298.

97. Least-squares plane analysis calculated with XP available from the SHELXTL suite of programs.[39]

98. Darensbourg, D. J.; Frantz, E. B. *Inorg. Chem.* **2008**, in press.

99. Jutz, F.; Grunwaldt, J. -D.; Baiker, A.; *J. Mol. Catal. A: Chemical* **2008**, *279*, 94-103.

100. Yan, H.; Cannon, W. R.; Shanefield, D. J. *Ceram. Int.* **1998**, *24*, 433-439.

101. Luinstra, G. A. *Polym. Rev.* **2008**, *48*, 192-219.

102. Novomer company website. http://www.novomer.com (accessed 04.06.08).

103. In a 50-mL round bottom flask equipped with a Teflon stir bar 36.0 mg of acacen (0.165 mmol) and 61.0 mg of $CrCl_3(THF)_3$ (0.163 mmol) were added and dissolved in 10 mL freshly distilled CHO. Over the next 30 minutes the green solution turned dark brown as the $CrCl_3(THF)_3$ slowly dissolved. After 17 hrs reaction time the CHO was removed by vacuum in an effort to eliminate HCl that might have formed in the reaction. A fresh 10 mL of CHO was added and the tacky brown solid redissolved. To another 50-mL round bottom flask equipped with a Teflon stir bar, 46.0 mg of $(^nBu)_4NN_3$ (0.161 mmol, for 1 equivalent) was added and dissolved in 10 mL freshly distilled CHO. The two monomer solutions were loaded stepwise into a Parr reactor at reaction temperature followed by the addition of CO_2.

104. Koning, C.; Wildeson, J.; Parton, R.; Plum, B.; Steeman, P.; Darensbourg, D. J. *Polymer* **2001**, *42*, 3995-4004.

105. Lu, X. B.; Shi, L.; Wang, Y. M.; Zhang, R.; Zhang, Y. J.; Peng, X. J.; Zhang, Z. C.; Li, B. *J. Am. Chem. Soc.* **2006**, *128*, 1664-1674.

106. Hsu, T. -J.; Tan, C, -S. *Polymer* **2002**, *43*, 4535-4543.

107. Cherian, A. E.; Sun, F. C.; Sheiko, S. S.; Coates, G. W. *J. Am. Chem. Soc.* **2007**, *129*, 11350-11351.

108. Reaction conditions: To a 50-mL round-bottom-flask 50 mg of (salen)CrCl (0.0865 mmol) and 50 mg of PPNCl (0.0865 mmol) were added along with a stir bar. To the flask 15 mL of CH_2Cl_2 were added and the mixture stirred overnight. The solvent was removed by vacuum and the residue redissolved in 10 mL

VCHO. The resulting solution was hazy in appearance as it appears [(salen)$CrCl_2$][PPN] was not soluble. An *in situ* React IR apparatus was prepared beforehand by heating under vacuum at 80 ºC overnight (see Experimental Section of Chapter II). The catalyst solution was loaded into the reactor by injection port followed by an additional 10 mL of VHCO. The reaction was monitored by ATR FTIR until the just after the maximum initial rate of polymer formation was reached. Molecular weights were determined by GPC analysis.

109. Polymer samples were purified by first dissolving a moderate amount of polymer (2 to 5 g) in a minimum amount of CH_2Cl_2 (10 to 15 mL). To a 500-mL beaker equipped with a large stir bar 475.0 of MeOH were added followed by 25.0 mL concentrated HCl. The solution was then covered by a watch glass and heated to ~50 ºC. With vigorous stirring the polymer solution is slowly added to the vortex of the stirring solution. Over time the polymer collects at the bottom and is removed after the acidified methanol is discarded. The polymer is then dried in a vacuum oven. This procedure can be repeated until the color of the methanol solution is colorless after the purification step.

110. Fukuoka, S.; Tojo, M.; Hachiya, H.; Aminaka, M.; Hasegawa, K. *Polym. J.* **2007**, *39*, 91-114.

APPENDIX A

TABLES OF STRUCTURAL DATA

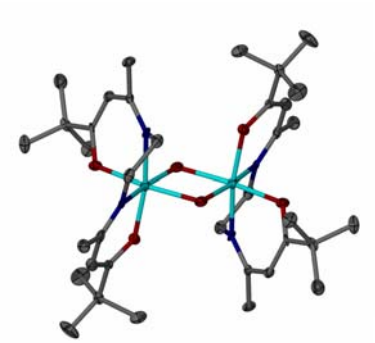

2-2

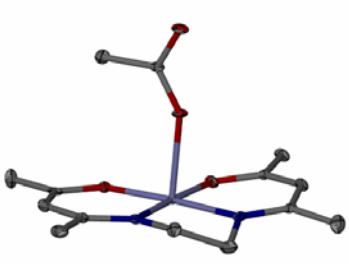

3-1•2H_2O

3-3

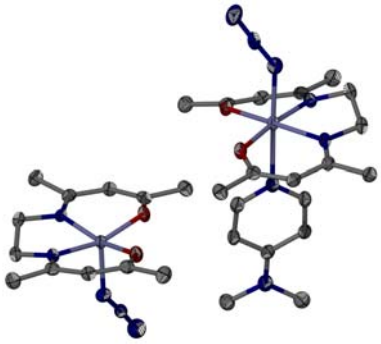

3-3''•(3-3•DMAP)

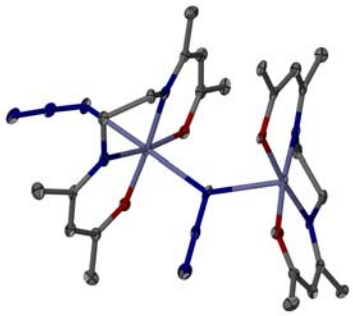

3-3'

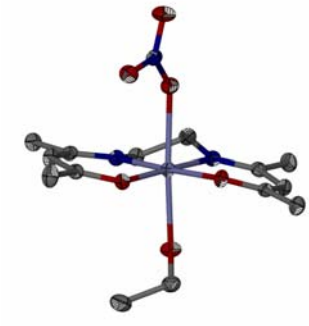

3-4•EtOH

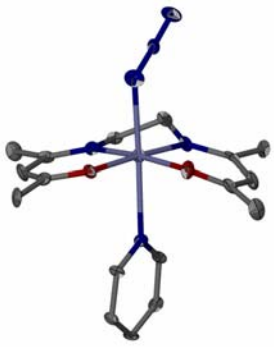

3-3•pyr

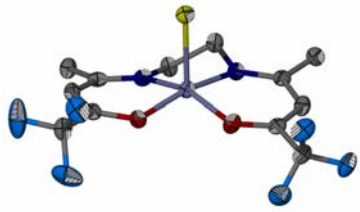

4-1

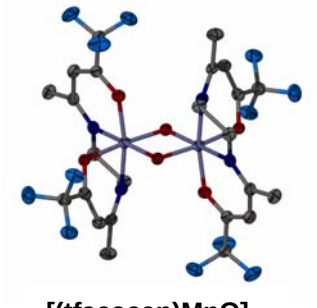

[(tfacacen)MnO]$_2$

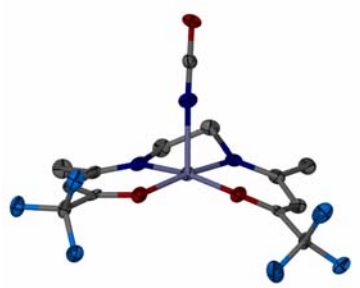

4-3

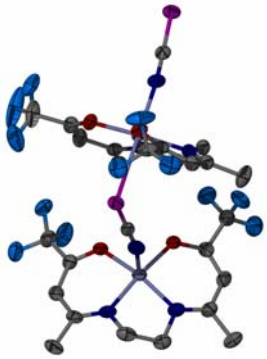

4-4

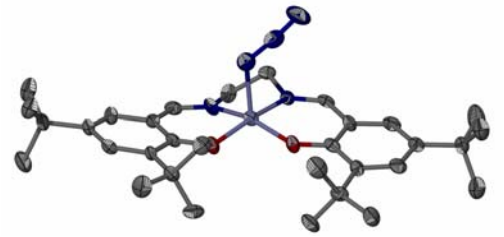

5-1

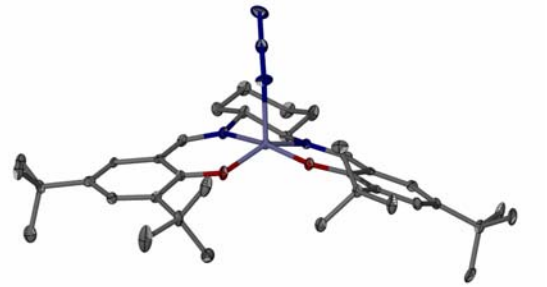

5-3

Table A-1. Crystal data and structure refinement for **2-2**.

Identification code	ddef1	
Empirical formula	C18.50 H32 Cl Cr N2 O3	
Formula weight	417.91	
Temperature	293(2) K	
Wavelength	1.54178 Å	
Crystal system	Triclinic	
Space group	P-1	
Unit cell dimensions	a = 9.730(4) Å	α= 72.606(13)°.
	b = 10.607(4) Å	β= 76.207(15)°.
	c = 11.275(4) Å	γ = 87.307(14)°.
Volume	1078.1(6) $Å^3$	
Z	2	
Density (calculated)	1.287 Mg/m^3	
Absorption coefficient	5.655 mm^{-1}	
F(000)	444	
Crystal size	0.10 x 0.01 x 0.01 mm^3	
Theta range for data collection	6.33 to 58.85°.	
Index ranges	-10<=h<=10, -11<=k<=11, -12<=l<=11	
Reflections collected	8492	
Independent reflections	2961 [R(int) = 0.1699]	
Completeness to theta = 58.85°	95.5 %	
Absorption correction	Semi-empirical from equivalents	
Max. and min. transmission	0.9456 and 0.6017	
Refinement method	Full-matrix least-squares on F^2	
Data / restraints / parameters	2961 / 6 / 243	
Goodness-of-fit on F^2	1.083	
Final R indices [I>2sigma(I)]	R1 = 0.0674, wR2 = 0.1311	
R indices (all data)	R1 = 0.1447, wR2 = 0.1544	
Largest diff. peak and hole	0.545 and -0.616 e.$Å^{-3}$	

Table A-2. Atomic coordinates (x 10^4) and equivalent isotropic displacement parameters ($Å^2$x 10^3) for **2-2**. U(eq) is defined as one third of the trace of the orthogonalized U^{ij} tensor.

	x	y	z	U(eq)
Cr(1)	9732(1)	1470(1)	4805(1)	17(1)
O(1)	8736(5)	2693(4)	3642(4)	18(1)
O(2)	7976(5)	1161(4)	6124(4)	18(1)
O(3)	9315(5)	10(4)	4160(4)	21(1)
N(1)	11530(6)	2167(4)	3478(5)	13(1)
N(2)	10393(6)	2759(5)	5547(5)	16(1)
C(1)	9074(7)	2847(5)	2417(6)	13(2)
C(2)	10437(7)	2808(6)	1736(6)	16(2)
C(3)	11657(8)	2696(5)	2250(6)	16(2)
C(4)	12585(7)	2361(6)	4132(7)	21(2)
C(5)	11886(7)	3166(6)	5034(7)	22(2)
C(6)	9631(8)	3278(6)	6397(6)	20(2)
C(7)	8168(8)	2933(6)	6933(6)	25(2)
C(8)	7450(7)	1943(6)	6789(6)	17(2)
C(9)	7800(7)	3113(6)	1809(6)	19(2)
C(10)	7006(8)	4290(6)	2115(7)	30(2)
C(11)	6823(8)	1857(6)	2458(7)	27(2)
C(12)	8197(8)	3340(7)	381(7)	29(2)
C(13)	13034(7)	3310(6)	1365(6)	25(2)
C(14)	10253(8)	4254(6)	6859(6)	25(2)
C(15)	5870(8)	1606(6)	7462(6)	23(2)
C(16)	5769(8)	176(6)	8269(7)	30(2)
C(17)	5221(9)	2469(7)	8290(8)	51(3)

C(18)	5071(8)	1758(8)	6405(8)	47(2)
C(1S)	9530(30)	141(15)	9143(19)	77(8)
Cl(1S)	11147(3)	838(2)	9082(3)	87(1)

Table A-3. Bond lengths [Å] and angles [°] for 2-2.

Cr(1)-O(2)	1.947(5)
Cr(1)-O(1)	1.953(5)
Cr(1)-O(3)	1.992(4)
Cr(1)-O(3)#1	1.993(5)
Cr(1)-N(2)	2.001(6)
Cr(1)-N(1)	2.014(5)
O(1)-C(1)	1.302(7)
O(2)-C(8)	1.289(7)
O(3)-Cr(1)#1	1.993(5)
N(1)-C(3)	1.307(8)
N(1)-C(4)	1.453(9)
N(2)-C(6)	1.308(8)
N(2)-C(5)	1.463(8)
C(1)-C(2)	1.370(9)
C(1)-C(9)	1.530(10)
C(2)-C(3)	1.426(10)
C(3)-C(13)	1.507(9)
C(4)-C(5)	1.537(9)
C(6)-C(7)	1.426(10)
C(6)-C(14)	1.497(9)
C(7)-C(8)	1.358(10)
C(8)-C(15)	1.549(10)
C(9)-C(12)	1.511(10)
C(9)-C(10)	1.522(8)
C(9)-C(11)	1.555(9)
C(15)-C(17)	1.511(9)
C(15)-C(16)	1.512(9)
C(15)-C(18)	1.539(11)
C(1S)-Cl(1S)	1.74(2)
C(1S)-Cl(1S)#2	1.93(2)
Cl(1S)-C(1S)#2	1.93(2)
O(2)-Cr(1)-O(1)	88.68(19)
O(2)-Cr(1)-O(3)	93.15(18)
O(1)-Cr(1)-O(3)	89.94(19)
O(2)-Cr(1)-O(3)#1	92.68(19)
O(1)-Cr(1)-O(3)#1	169.83(19)
O(3)-Cr(1)-O(3)#1	79.9(2)
O(2)-Cr(1)-N(2)	90.1(2)
O(1)-Cr(1)-N(2)	98.5(2)
O(3)-Cr(1)-N(2)	171.0(2)
O(3)#1-Cr(1)-N(2)	91.6(2)
O(2)-Cr(1)-N(1)	168.21(19)
O(1)-Cr(1)-N(1)	86.7(2)
O(3)-Cr(1)-N(1)	97.7(2)
O(3)#1-Cr(1)-N(1)	93.8(2)
N(2)-Cr(1)-N(1)	79.8(2)
C(1)-O(1)-Cr(1)	121.6(4)
C(8)-O(2)-Cr(1)	125.8(4)
Cr(1)-O(3)-Cr(1)#1	100.1(2)
C(3)-N(1)-C(4)	122.8(6)
C(3)-N(1)-Cr(1)	126.7(5)
C(4)-N(1)-Cr(1)	108.1(4)
C(6)-N(2)-C(5)	118.3(6)
C(6)-N(2)-Cr(1)	127.0(5)
C(5)-N(2)-Cr(1)	114.6(4)
O(1)-C(1)-C(2)	123.4(6)
O(1)-C(1)-C(9)	113.1(6)
C(2)-C(1)-C(9)	123.4(6)

C(1)-C(2)-C(3)	124.6(6)
N(1)-C(3)-C(2)	119.6(6)
N(1)-C(3)-C(13)	122.0(7)
C(2)-C(3)-C(13)	118.2(6)
N(1)-C(4)-C(5)	106.7(6)
N(2)-C(5)-C(4)	109.0(6)
N(2)-C(6)-C(7)	121.4(6)
N(2)-C(6)-C(14)	121.7(7)
C(7)-C(6)-C(14)	116.9(6)
C(8)-C(7)-C(6)	126.3(6)
O(2)-C(8)-C(7)	125.6(6)
O(2)-C(8)-C(15)	112.0(6)
C(7)-C(8)-C(15)	122.4(6)
C(12)-C(9)-C(10)	110.0(6)
C(12)-C(9)-C(1)	113.3(6)
C(10)-C(9)-C(1)	109.8(6)
C(12)-C(9)-C(11)	109.3(6)
C(10)-C(9)-C(11)	108.7(6)
C(1)-C(9)-C(11)	105.6(5)
C(17)-C(15)-C(16)	109.7(6)
C(17)-C(15)-C(18)	109.8(7)
C(16)-C(15)-C(18)	108.9(6)
C(17)-C(15)-C(8)	113.9(6)
C(16)-C(15)-C(8)	107.4(6)
C(18)-C(15)-C(8)	106.9(5)
Cl(1S)-C(1S)-Cl(1S)#2	104.2(10)
C(1S)-Cl(1S)-C(1S)#2	75.8(10)

Symmetry transformations used to generate equivalent atoms:
#1 -x+2,-y,-z+1 #2 -x+2,-y,-z+2

Table A-4. Anisotropic displacement parameters ($Å^2 x\ 10^3$) for **2-2**. The anisotropic displacement factor exponent takes the form: $-2\pi^2[\ h^2\ a^{*2}U^{11} + ... + 2\ h\ k\ a^*\ b^*\ U^{12}\ ]$

	U^{11}	U^{22}	U^{33}	U^{23}	U^{13}	U^{12}
Cr(1)	22(1)	12(1)	15(1)	-4(1)	-4(1)	0(1)
O(1)	23(3)	18(2)	14(3)	-8(2)	-2(2)	-6(2)
O(2)	22(3)	18(2)	17(3)	-9(2)	-7(2)	1(2)
O(3)	25(3)	20(2)	15(3)	-3(2)	-1(2)	-2(2)
N(1)	15(3)	10(3)	10(3)	3(2)	-6(3)	1(2)
N(2)	15(3)	18(2)	11(3)	2(2)	-5(2)	12(2)
C(1)	18(4)	7(3)	18(4)	-8(3)	-8(3)	7(3)
C(2)	16(4)	13(3)	17(4)	-1(3)	-2(3)	-2(3)
C(3)	25(4)	8(3)	15(4)	-3(3)	-3(3)	3(3)
C(4)	10(4)	25(4)	26(4)	-2(3)	-8(3)	0(3)
C(5)	23(5)	19(3)	24(4)	-3(3)	-12(3)	2(3)
C(6)	33(5)	9(3)	19(4)	-2(3)	-11(4)	2(3)
C(7)	38(5)	18(4)	21(4)	-11(3)	-8(4)	5(3)
C(8)	22(4)	15(3)	11(3)	-3(3)	-3(3)	5(3)
C(9)	10(4)	17(3)	31(4)	-12(3)	-4(3)	0(3)
C(10)	34(5)	20(4)	43(5)	-12(4)	-20(4)	9(4)
C(11)	28(5)	29(4)	30(4)	-8(3)	-17(4)	-3(4)
C(12)	27(5)	30(4)	33(5)	-11(4)	-11(4)	7(4)
C(13)	16(4)	28(4)	18(4)	5(3)	4(3)	0(3)
C(14)	33(5)	14(3)	28(4)	-10(3)	-3(4)	-3(3)
C(15)	22(5)	22(4)	24(4)	-6(3)	-5(3)	8(3)
C(16)	30(5)	31(4)	22(4)	-1(3)	-1(4)	-9(4)
C(17)	31(6)	38(5)	72(7)	-28(5)	28(5)	-6(4)
C(18)	10(5)	69(6)	48(6)	5(5)	-8(4)	6(4)
C(1S)	140(20)	21(8)	94(16)	-35(10)	-64(16)	28(12)
Cl(1S)	61(2)	48(1)	136(3)	-34(2)	14(2)	1(1)

Table A-5. Hydrogen coordinates ($x\ 10^4$) and isotropic displacement parameters ($Å^2 x\ 10^3$)

for **2-2**.

	x	y	z	U(eq)
H(3)	9682	71	3192	26
H(2)	10576	2858	878	19
H(4A)	13410	2835	3520	25
H(4B)	12880	1516	4615	25
H(5A)	12359	3017	5728	26
H(5B)	11966	4101	4571	26
H(7)	7656	3435	7429	29
H(10A)	7565	5084	1655	45
H(10B)	6829	4173	3016	45
H(10C)	6122	4357	1865	45
H(11A)	6538	1731	3363	41
H(11B)	7328	1101	2302	41
H(11C)	6001	1965	2111	41
H(12A)	7360	3514	53	44
H(12B)	8636	2568	200	44
H(12C)	8845	4083	-18	44
H(13A)	13203	4139	1492	37
H(13B)	12982	3454	495	37
H(13C)	13793	2728	1544	37
H(14A)	10939	3828	7324	37
H(14B)	9515	4589	7408	37
H(14C)	10704	4971	6140	37
H(16A)	6293	66	8914	45
H(16B)	6156	-372	7735	45
H(16C)	4795	-76	8670	45
H(17A)	4252	2194	8691	77
H(17B)	5260	3373	7770	77
H(17C)	5737	2387	8935	77
H(18A)	4106	1458	6786	71
H(18B)	5514	1240	5858	71
H(18C)	5094	2670	5911	71
H(1SA)	9660	-428	8607	93
H(1SB)	8891	821	8874	93

Table A-6. Crystal data and structure refinement for **3-1·2H$_2$O**.

Identification code	ddef	
Empirical formula	C14 H24 Mn N2 O5.50	
Formula weight	363.29	
Temperature	110(2) K	
Wavelength	0.71073 Å	
Crystal system	Monoclinic	
Space group	P2/c	
Unit cell dimensions	a = 17.165(2) Å	α= 90°.
	b = 6.7320(9) Å	β= 109.339(2)°.
	c = 14.886(2) Å	γ = 90°.
Volume	1623.1(4) Å^3	
Z	4	
Density (calculated)	1.487 Mg/m^3	
Absorption coefficient	0.841 mm^{-1}	
F(000)	764	
Crystal size	0.20 x 0.10 x 0.10 mm^3	
Theta range for data collection	1.26 to 25.00°.	
Index ranges	-20<=h<=19, -8<=k<=8, -17<=l<=17	
Reflections collected	10674	
Independent reflections	2790 [R(int) = 0.0729]	
Completeness to theta = 25.00°	98.1 %	

Absorption correction	Semi-empirical from equivalents
Max. and min. transmission	0.9206 and 0.8498
Refinement method	Full-matrix least-squares on F^2
Data / restraints / parameters	2790 / 12 / 209
Goodness-of-fit on F^2	1.057
Final R indices [I>2sigma(I)]	R1 = 0.0557, wR2 = 0.1361
R indices (all data)	R1 = 0.0728, wR2 = 0.1511
Largest diff. peak and hole	0.952 and -1.162 e.$Å^{-3}$

Table A-7. Atomic coordinates (x 10^4) and equivalent isotropic displacement parameters ($Å^2$x 10^3) for **3-1·2H$_2$O**. U(eq) is defined as one third of the trace of the orthogonalized U^{ij} tensor.

	x	y	z	U(eq)
Mn(1)	2237(1)	2712(1)	2624(1)	10(1)
C(1)	3954(2)	2667(4)	3964(2)	13(1)
C(2)	3641(2)	2467(4)	4737(3)	17(1)
C(3)	2831(2)	2597(3)	4675(2)	11(1)
C(4)	1739(2)	2465(3)	526(2)	12(1)
C(5)	906(2)	2530(4)	473(3)	18(1)
C(6)	603(2)	2658(4)	1220(2)	14(1)
C(7)	3783(2)	3262(4)	2301(2)	19(1)
C(8)	3214(2)	2416(4)	1373(2)	15(1)
C(9)	4869(2)	2783(4)	4197(3)	22(1)
C(10)	2589(2)	2557(4)	5558(2)	16(1)
C(11)	1900(2)	2295(4)	-397(3)	19(1)
C(12)	-297(2)	2700(4)	1063(3)	22(1)
C(13)	1960(2)	-2270(4)	2482(2)	12(1)
C(14)	1049(2)	-2307(4)	2021(3)	23(1)
N(1)	3457(2)	2788(3)	3074(2)	13(1)
N(2)	2354(2)	2583(3)	1343(2)	12(1)
O(1)	2213(2)	2821(3)	3893(2)	14(1)
O(2)	1067(1)	2729(2)	2113(2)	13(1)
O(3)	2330(1)	-609(3)	2704(1)	16(1)
O(4)	2357(1)	-3901(3)	2641(1)	17(1)
O(1W)	5000	9168(5)	2500	70(2)
O(2W)	3950(2)	7706(3)	3436(2)	26(1)

Table A-8. Bond lengths [Å] and angles [°] for **3-1·2H$_2$O**.

Mn(1)-O(2)	1.898(2)
Mn(1)-O(1)	1.904(2)
Mn(1)-N(1)	1.977(3)
Mn(1)-N(2)	1.985(3)
Mn(1)-O(3)	2.2414(18)
Mn(1)-O(4)#1	2.2887(19)
C(1)-N(1)	1.319(4)
C(1)-C(2)	1.429(5)
C(1)-C(9)	1.494(5)
C(2)-C(3)	1.366(5)
C(3)-O(1)	1.298(4)
C(3)-C(10)	1.504(5)
C(4)-N(2)	1.323(4)
C(4)-C(5)	1.406(5)
C(4)-C(11)	1.493(5)
C(5)-C(6)	1.379(5)
C(6)-O(2)	1.304(4)
C(6)-C(12)	1.484(5)
C(7)-N(1)	1.472(4)
C(7)-C(8)	1.514(5)
C(8)-N(2)	1.465(4)
C(13)-O(4)	1.273(3)
C(13)-O(3)	1.275(3)
C(13)-C(14)	1.486(5)

O(4)-Mn(1)#2	2.2887(19)
O(2)-Mn(1)-O(1)	91.71(10)
O(2)-Mn(1)-N(1)	176.00(10)
O(1)-Mn(1)-N(1)	91.77(11)
O(2)-Mn(1)-N(2)	92.62(11)
O(1)-Mn(1)-N(2)	175.67(10)
N(1)-Mn(1)-N(2)	83.92(12)
O(2)-Mn(1)-O(3)	94.28(7)
O(1)-Mn(1)-O(3)	90.56(7)
N(1)-Mn(1)-O(3)	87.67(8)
N(2)-Mn(1)-O(3)	88.85(8)
O(2)-Mn(1)-O(4)#1	94.47(7)
O(1)-Mn(1)-O(4)#1	88.96(7)
N(1)-Mn(1)-O(4)#1	83.61(8)
N(2)-Mn(1)-O(4)#1	90.97(8)
O(3)-Mn(1)-O(4)#1	171.25(9)
N(1)-C(1)-C(2)	121.6(3)
N(1)-C(1)-C(9)	120.7(3)
C(2)-C(1)-C(9)	117.7(3)
C(3)-C(2)-C(1)	125.9(3)
O(1)-C(3)-C(2)	125.3(3)
O(1)-C(3)-C(10)	114.0(3)
C(2)-C(3)-C(10)	120.6(3)
N(2)-C(4)-C(5)	122.6(3)
N(2)-C(4)-C(11)	121.0(3)
C(5)-C(4)-C(11)	116.5(3)
C(6)-C(5)-C(4)	127.2(3)
O(2)-C(6)-C(5)	123.9(3)
O(2)-C(6)-C(12)	114.4(3)
C(5)-C(6)-C(12)	121.7(3)
N(1)-C(7)-C(8)	109.5(3)
N(2)-C(8)-C(7)	109.8(3)
O(4)-C(13)-O(3)	121.3(3)
O(4)-C(13)-C(14)	119.3(2)
O(3)-C(13)-C(14)	119.5(2)
C(1)-N(1)-C(7)	120.8(3)
C(1)-N(1)-Mn(1)	126.8(2)
C(7)-N(1)-Mn(1)	112.0(2)
C(4)-N(2)-C(8)	120.9(3)
C(4)-N(2)-Mn(1)	125.5(2)
C(8)-N(2)-Mn(1)	113.3(2)
C(3)-O(1)-Mn(1)	127.3(2)
C(6)-O(2)-Mn(1)	128.1(2)
C(13)-O(3)-Mn(1)	147.2(2)
C(13)-O(4)-Mn(1)#2	144.8(2)

Symmetry transformations used to generate equivalent atoms:
#1 x,y+1,z #2 x,y-1,z

Table A-9. Anisotropic displacement parameters ($Å^2 x\ 10^3$) for **3-1·2H$_2$O**. The anisotropic displacement factor exponent takes the form: $-2\pi^2[\ h^2\ a^{*2}U^{11} + ...\ + 2\ h\ k\ a^*\ b^*\ U^{12}\ ]$

	U^{11}	U^{22}	U^{33}	U^{23}	U^{13}	U^{12}
Mn(1)	15(1)	5(1)	9(1)	0(1)	3(1)	0(1)
C(1)	15(2)	4(1)	19(2)	-3(1)	3(2)	0(1)
C(2)	26(2)	11(1)	9(2)	-1(1)	-2(2)	1(1)
C(3)	12(1)	7(1)	12(1)	0(1)	2(1)	-1(1)
C(4)	15(1)	8(1)	12(1)	1(1)	4(1)	-1(1)
C(5)	23(2)	13(1)	12(2)	1(1)	-2(2)	-2(1)
C(6)	21(2)	5(1)	17(2)	2(1)	6(2)	0(1)
C(7)	25(2)	12(1)	21(2)	0(1)	8(2)	-3(1)
C(8)	17(2)	15(1)	13(2)	-2(1)	5(2)	-1(1)
C(9)	20(2)	24(2)	18(2)	-3(1)	3(2)	2(1)

C(10)	23(2)	10(1)	12(2)	0(1)	4(2)	3(1)
C(11)	28(2)	15(2)	14(2)	1(1)	9(2)	-3(1)
C(12)	17(2)	28(2)	16(2)	0(1)	-1(2)	0(1)
C(13)	20(2)	8(1)	10(2)	-1(1)	7(1)	-1(1)
C(14)	19(2)	12(2)	30(2)	1(1)	-1(2)	1(1)
N(1)	16(2)	7(1)	16(2)	-1(1)	4(1)	-2(1)
N(2)	15(2)	6(1)	14(2)	0(1)	5(1)	1(1)
O(1)	21(2)	9(1)	11(1)	0(1)	2(1)	1(1)
O(2)	14(1)	9(1)	13(1)	0(1)	2(1)	0(1)
O(3)	22(2)	6(1)	20(1)	1(1)	5(1)	-2(1)
O(4)	24(2)	4(1)	22(1)	-1(1)	7(1)	3(1)
O(1W)	115(4)	19(2)	113(4)	0	86(4)	0
O(2W)	21(2)	17(1)	37(2)	-4(1)	3(1)	0(1)

Table A-10. Hydrogen coordinates (x 10^4) and isotropic displacement parameters ($Å^2$x 10^3) for **3-1·2H_2O**.

	x	y	z	U(eq)
H(2)	4031	2222	5349	21
H(5)	508	2479	-148	22
H(7A)	4342	2689	2445	23
H(7B)	3824	4720	2244	23
H(8A)	3288	3150	831	18
H(8B)	3351	1004	1318	18
H(9A)	5055	1688	3884	32
H(9B)	5138	2685	4887	32
H(9C)	5015	4052	3971	32
H(10A)	2299	3788	5599	23
H(10B)	3086	2437	6119	23
H(10C)	2226	1419	5530	23
H(11A)	2009	3617	-604	28
H(11B)	1417	1717	-879	28
H(11C)	2381	1440	-313	28
H(12A)	-445	1564	1385	33
H(12B)	-602	2628	379	33
H(12C)	-438	3936	1321	33
H(14A)	913	-2380	1328	34
H(14B)	810	-1096	2186	34
H(14C)	821	-3470	2243	34
H(1W1)	4712	8227	2752	105
H(1W2)	3611	8555	3472	39
H(2W2)	3542	6933	3266	39

Table A-11. Crystal data and structure refinement for **3-3**.

Identification code	data0m	
Empirical formula	C12 H18 Mn N5 O2	
Formula weight	319.25	
Temperature	110(2) K	
Wavelength	1.54178 Å	
Crystal system	Monoclinic	
Space group	P2(1)/c	
Unit cell dimensions	a = 10.2639(11) Å	α= 90°.
	b = 13.5749(15) Å	β= 112.173(6)°.
	c = 11.3173(11) Å	γ = 90°.
Volume	1460.2(3) $Å^3$	
Z	4	
Density (calculated)	1.452 Mg/m^3	
Absorption coefficient	7.441 mm^{-1}	

F(000)	664
Crystal size	0.15 x 0.06 x 0.01 mm^3
Theta range for data collection	4.65 to 61.06°.
Index ranges	-11<=h<=11, -15<=k<=15, -12<=l<=12
Reflections collected	10112
Independent reflections	2238 [R(int) = 0.1593]
Completeness to theta = 61.06°	100.0 %
Absorption correction	Semi-empirical from equivalents
Max. and min. transmission	0.9293 and 0.4015
Refinement method	Full-matrix least-squares on F^2
Data / restraints / parameters	2238 / 0 / 185
Goodness-of-fit on F^2	1.004
Final R indices [I>2sigma(I)]	R1 = 0.0488, wR2 = 0.1013
R indices (all data)	R1 = 0.0721, wR2 = 0.1057
Largest diff. peak and hole	0.724 and -0.672 e.$Å^{-3}$

Table A-12. Atomic coordinates (x 10^4) and equivalent isotropic displacement parameters ($Å^2$x 10^3) for **3-3**. U(eq) is defined as one third of the trace of the orthogonalized U^{ij} tensor.

	x	y	z	U(eq)
C(1)	2605(4)	869(3)	10325(4)	13(1)
C(2)	3353(5)	1321(3)	11532(4)	17(1)
C(3)	3093(4)	2251(3)	11873(4)	16(1)
C(4)	-2289(4)	2337(3)	7616(4)	16(1)
C(9)	3185(5)	-100(3)	10070(5)	23(1)
C(10)	4017(4)	2677(4)	13139(4)	23(1)
C(11)	-3382(5)	1879(4)	6443(4)	25(1)
Mn(1)	446(1)	2412(1)	9759(1)	12(1)
N(1)	1467(4)	1249(3)	9486(3)	14(1)
N(2)	-1123(3)	1878(3)	8269(3)	13(1)
N(3)	-235(4)	1540(3)	11154(3)	18(1)
N(4)	416(4)	1596(2)	12263(4)	13(1)
N(5)	1068(4)	3366(3)	8378(3)	18(1)
O(1)	2070(3)	2817(2)	11181(3)	15(1)
O(2)	-657(3)	3506(2)	9920(3)	14(1)
C(5)	-2583(4)	3305(3)	7937(4)	16(1)
C(6)	-1791(4)	3816(3)	9023(4)	13(1)
C(7)	727(4)	827(3)	8206(4)	13(1)
C(8)	-815(4)	873(3)	7932(4)	18(1)
C(12)	-2238(5)	4849(3)	9226(4)	19(1)

Table A-13. Bond lengths [Å] and angles [°] for **3-3**.

C(1)-N(1)	1.302(5)
C(1)-C(2)	1.428(6)
C(1)-C(9)	1.516(6)
C(2)-C(3)	1.376(6)
C(2)-H(2)	0.9500
C(3)-O(1)	1.298(5)
C(3)-C(10)	1.504(6)
C(4)-N(2)	1.303(5)
C(4)-C(5)	1.426(6)
C(4)-C(11)	1.511(6)
C(9)-H(9A)	0.9800
C(9)-H(9B)	0.9800
C(9)-H(9C)	0.9800
C(10)-H(10A)	0.9800
C(10)-H(10B)	0.9800
C(10)-H(10C)	0.9800
C(11)-H(11A)	0.9800
C(11)-H(11B)	0.9800
C(11)-H(11C)	0.9800

Mn(1)-O(1)	1.909(3)
Mn(1)-O(2)	1.917(3)
Mn(1)-N(2)	1.978(3)
Mn(1)-N(1)	1.982(4)
Mn(1)-N(3)	2.284(4)
Mn(1)-N(5)	2.299(4)
N(1)-C(7)	1.475(5)
N(2)-C(8)	1.483(5)
N(3)-N(4)	1.180(5)
N(4)-N(5)#1	1.185(5)
N(5)-N(4)#2	1.185(5)
O(2)-C(6)	1.293(5)
C(5)-C(6)	1.378(6)
C(5)-H(5)	0.9500
C(6)-C(12)	1.520(6)
C(7)-C(8)	1.495(6)
C(7)-H(7A)	0.9900
C(7)-H(7B)	0.9900
C(8)-H(8A)	0.9900
C(8)-H(8B)	0.9900
C(12)-H(12A)	0.9800
C(12)-H(12B)	0.9800
C(12)-H(12C)	0.9800

N(1)-C(1)-C(2)	122.5(4)
N(1)-C(1)-C(9)	120.9(4)
C(2)-C(1)-C(9)	116.6(4)
C(3)-C(2)-C(1)	124.8(4)
C(3)-C(2)-H(2)	117.6
C(1)-C(2)-H(2)	117.6
O(1)-C(3)-C(2)	124.9(4)
O(1)-C(3)-C(10)	115.0(4)
C(2)-C(3)-C(10)	120.0(4)
N(2)-C(4)-C(5)	122.2(4)
N(2)-C(4)-C(11)	121.3(4)
C(5)-C(4)-C(11)	116.5(4)
C(1)-C(9)-H(9A)	109.5
C(1)-C(9)-H(9B)	109.5
H(9A)-C(9)-H(9B)	109.5
C(1)-C(9)-H(9C)	109.5
H(9A)-C(9)-H(9C)	109.5
H(9B)-C(9)-H(9C)	109.5
C(3)-C(10)-H(10A)	109.5
C(3)-C(10)-H(10B)	109.5
H(10A)-C(10)-H(10B)	109.5
C(3)-C(10)-H(10C)	109.5
H(10A)-C(10)-H(10C)	109.5
H(10B)-C(10)-H(10C)	109.5
C(4)-C(11)-H(11A)	109.5
C(4)-C(11)-H(11B)	109.5
H(11A)-C(11)-H(11B)	109.5
C(4)-C(11)-H(11C)	109.5
H(11A)-C(11)-H(11C)	109.5
H(11B)-C(11)-H(11C)	109.5
O(1)-Mn(1)-O(2)	93.22(12)
O(1)-Mn(1)-N(2)	174.23(13)
O(2)-Mn(1)-N(2)	92.55(13)
O(1)-Mn(1)-N(1)	90.92(13)
O(2)-Mn(1)-N(1)	175.87(13)
N(2)-Mn(1)-N(1)	83.31(14)
O(1)-Mn(1)-N(3)	87.95(13)
O(2)-Mn(1)-N(3)	89.42(13)
N(2)-Mn(1)-N(3)	92.10(14)
N(1)-Mn(1)-N(3)	90.74(14)
O(1)-Mn(1)-N(5)	91.88(13)
O(2)-Mn(1)-N(5)	87.34(13)

N(2)-Mn(1)-N(5)	88.40(14)
N(1)-Mn(1)-N(5)	92.52(14)
N(3)-Mn(1)-N(5)	176.74(14)
C(1)-N(1)-C(7)	123.4(4)
C(1)-N(1)-Mn(1)	125.7(3)
C(7)-N(1)-Mn(1)	110.9(2)
C(4)-N(2)-C(8)	122.2(4)
C(4)-N(2)-Mn(1)	125.9(3)
C(8)-N(2)-Mn(1)	111.9(2)
N(4)-N(3)-Mn(1)	120.2(3)
N(3)-N(4)-N(5)#1	178.8(4)
N(4)#2-N(5)-Mn(1)	123.9(3)
C(3)-O(1)-Mn(1)	126.0(3)
C(6)-O(2)-Mn(1)	124.6(3)
C(6)-C(5)-C(4)	125.5(4)
C(6)-C(5)-H(5)	117.2
C(4)-C(5)-H(5)	117.2
O(2)-C(6)-C(5)	126.1(4)
O(2)-C(6)-C(12)	114.6(4)
C(5)-C(6)-C(12)	119.3(4)
N(1)-C(7)-C(8)	107.4(4)
N(1)-C(7)-H(7A)	110.2
C(8)-C(7)-H(7A)	110.2
N(1)-C(7)-H(7B)	110.2
C(8)-C(7)-H(7B)	110.2
H(7A)-C(7)-H(7B)	108.5
N(2)-C(8)-C(7)	107.3(3)
N(2)-C(8)-H(8A)	110.3
C(7)-C(8)-H(8A)	110.3
N(2)-C(8)-H(8B)	110.3
C(7)-C(8)-H(8B)	110.3
H(8A)-C(8)-H(8B)	108.5
C(6)-C(12)-H(12A)	109.5
C(6)-C(12)-H(12B)	109.5
H(12A)-C(12)-H(12B)	109.5
C(6)-C(12)-H(12C)	109.5
H(12A)-C(12)-H(12C)	109.5
H(12B)-C(12)-H(12C)	109.5

Symmetry transformations used to generate equivalent atoms:
#1 x,-y+1/2,z+1/2 #2 x,-y+1/2,z-1/2

Table A-14. Anisotropic displacement parameters ($Å^2 x\ 10^3$) for **3-3**. The anisotropic displacement factor exponent takes the form: $-2\pi^2[\ h^2\ a^{*2}U^{11} + ...\ + 2\ h\ k\ a^*\ b^*\ U^{12}\ ]$

	U^{11}	U^{22}	U^{33}	U^{23}	U^{13}	U^{12}
C(1)	5(2)	19(2)	17(2)	-6(2)	6(2)	-5(2)
C(2)	14(2)	19(2)	14(2)	1(2)	2(2)	4(2)
C(3)	7(2)	25(3)	17(2)	0(2)	5(2)	-2(2)
C(4)	8(2)	27(3)	11(2)	1(2)	2(2)	-3(2)
C(9)	11(2)	21(3)	32(3)	-4(2)	3(2)	5(2)
C(10)	13(2)	32(3)	13(2)	-5(2)	-6(2)	2(2)
C(11)	11(2)	35(3)	19(2)	-8(2)	-6(2)	2(2)
Mn(1)	7(1)	15(1)	11(1)	0(1)	1(1)	1(1)
N(1)	12(2)	20(2)	10(2)	-2(2)	6(2)	-1(2)
N(2)	9(2)	17(2)	15(2)	1(2)	8(2)	5(2)
N(3)	22(2)	22(2)	7(2)	1(2)	4(2)	-4(2)
N(4)	14(2)	9(2)	19(2)	-1(2)	11(2)	-1(2)
N(5)	20(2)	23(2)	10(2)	-1(2)	5(2)	-5(2)
O(1)	12(2)	15(2)	17(2)	2(1)	6(1)	4(1)
O(2)	10(2)	17(2)	13(2)	-2(1)	0(1)	2(1)
C(5)	8(2)	20(2)	17(2)	1(2)	0(2)	7(2)
C(6)	9(2)	19(2)	14(2)	-1(2)	7(2)	-3(2)
C(7)	14(2)	12(2)	10(2)	-2(2)	2(2)	0(2)

C(8)	17(3)	14(2)	15(2)	-7(2)	-3(2)	0(2)
C(12)	15(2)	19(2)	20(3)	2(2)	3(2)	4(2)

Table A-15. Hydrogen coordinates (x 10^4) and isotropic displacement parameters ($Å^2$x 10^3) for **3-3**.

	x	y	z	U(eq)
H(2)	4084	952	12145	20
H(9A)	2482	-620	9942	34
H(9B)	4042	-268	10800	34
H(9C)	3405	-39	9302	34
H(10A)	4221	3368	13027	34
H(10B)	4899	2305	13480	34
H(10C)	3532	2636	13736	34
H(11A)	-3024	1860	5753	38
H(11B)	-4246	2272	6173	38
H(11C)	-3584	1207	6640	38
H(5)	-3393	3625	7353	20
H(7A)	1023	136	8182	15
H(7B)	949	1209	7560	15
H(8A)	-1361	739	7018	22
H(8B)	-1072	376	8446	22
H(12A)	-2398	4871	10026	29
H(12B)	-3109	5024	8514	29
H(12C)	-1496	5318	9268	29

Table A-16. Crystal data and structure refinement for **3-3"·(3-3·DMAP)**.

Identification code	ddef38g	
Empirical formula	C31 H48 Mn2 N12 O4	
Formula weight	762.69	
Temperature	110(2) K	
Wavelength	0.71073 Å	
Crystal system	Monoclinic	
Space group	P2(1)/c	
Unit cell dimensions	a = 8.7824(9) Å	α= 90°.
	b = 13.9008(14) Å	β= 90.793(2)°.
	c = 28.352(3) Å	γ = 90°.
Volume	3461.0(6) $Å^3$	
Z	4	
Density (calculated)	1.464 Mg/m^3	
Absorption coefficient	0.785 mm^{-1}	
F(000)	1600	
Crystal size	0.20 x 0.10 x 0.10 mm^3	
Theta range for data collection	2.61 to 25.00°.	
Index ranges	-9<=h<=10, -15<=k<=16, -33<=l<=33	
Reflections collected	19090	
Independent reflections	6101 [R(int) = 0.0289]	
Completeness to theta = 25.00°	99.9 %	
Absorption correction	Semi-empirical from equivalents	
Max. and min. transmission	0.9256 and 0.8588	
Refinement method	Full-matrix least-squares on F^2	
Data / restraints / parameters	6101 / 0 / 452	
Goodness-of-fit on F^2	1.000	
Final R indices [I>2sigma(I)]	R1 = 0.0497, wR2 = 0.1231	
R indices (all data)	R1 = 0.0673, wR2 = 0.1405	
Largest diff. peak and hole	1.704 and -0.311 e.$Å^{-3}$	

Table A-17. Atomic coordinates (x 10^4) and equivalent isotropic displacement parameters ($Å^2$x 10^3) for **3-3”·(3-3·DMAP)**. U(eq) is defined as one third of the trace of the orthogonalized U^{ij} tensor.

	x	y	z	U(eq)
Mn(1)	2701(1)	6844(1)	3793(1)	24(1)
Mn(2)	2415(1)	6814(1)	1184(1)	22(1)
O(1)	3440(2)	5946(1)	3334(1)	26(1)
O(2)	3663(2)	7908(1)	3488(1)	31(1)
O(3)	1506(2)	6017(1)	1644(1)	29(1)
O(4)	2244(2)	7866(1)	1606(1)	30(1)
N(1)	1505(3)	5840(2)	4106(1)	26(1)
N(2)	1694(3)	7686(2)	4262(1)	26(1)
N(3)	4607(3)	6604(2)	4298(1)	39(1)
N(4)	5903(3)	6428(2)	4315(1)	31(1)
N(5)	7205(3)	6255(2)	4348(1)	51(1)
N(6)	597(3)	7057(2)	3260(1)	30(1)
N(7)	-3029(3)	7102(2)	2272(1)	39(1)
N(15)	3168(2)	5684(2)	838(1)	23(1)
N(16)	3900(3)	7519(2)	803(1)	24(1)
N(17)	515(3)	7020(2)	748(1)	32(1)
N(18)	-778(3)	6821(2)	699(1)	27(1)
N(19)	-2059(3)	6648(2)	630(1)	45(1)
C(1)	1082(3)	5026(2)	3915(1)	28(1)
C(2)	1581(3)	4736(2)	3459(1)	30(1)
C(3)	2719(3)	5171(2)	3204(1)	27(1)
C(4)	1788(3)	8629(2)	4283(1)	26(1)
C(5)	2667(3)	9176(2)	3956(1)	28(1)
C(6)	3525(3)	8813(2)	3595(1)	26(1)
C(7)	1143(4)	6104(2)	4590(1)	33(1)
C(8)	734(3)	7162(2)	4602(1)	30(1)
C(9)	80(4)	4338(2)	4176(1)	37(1)
C(10)	3243(3)	4739(2)	2750(1)	34(1)
C(11)	948(3)	9180(2)	4655(1)	30(1)
C(12)	4401(3)	9480(2)	3281(1)	33(1)
C(13)	813(3)	7164(2)	2789(1)	32(1)
C(14)	-315(3)	7199(2)	2459(1)	31(1)
C(15)	-1858(3)	7113(2)	2592(1)	30(1)
C(16)	-2096(3)	7025(2)	3083(1)	29(1)
C(17)	-882(3)	6987(2)	3384(1)	30(1)
C(18)	-2772(4)	7123(2)	1767(1)	35(1)
C(19)	-4606(4)	7102(2)	2426(1)	40(1)
C(20)	2712(3)	4783(2)	897(1)	26(1)
C(21)	1645(3)	4527(2)	1250(1)	26(1)
C(22)	1110(3)	5120(2)	1597(1)	27(1)
C(23)	4412(3)	8403(2)	870(1)	27(1)
C(24)	3970(3)	8969(2)	1264(1)	28(1)
C(25)	2935(3)	8696(2)	1596(1)	28(1)
C(26)	4344(3)	5916(2)	488(1)	28(1)
C(27)	4286(3)	6979(2)	372(1)	27(1)
C(28)	3320(3)	3986(2)	593(1)	31(1)
C(29)	22(3)	4767(2)	1962(1)	32(1)
C(30)	5468(3)	8866(2)	523(1)	32(1)
C(31)	2470(4)	9369(2)	1985(1)	35(1)

Table A-18. Bond lengths [Å] and angles [°] for **3-3”·(3-3·DMAP)**.

Mn(1)-O(2)	1.9161(19)
Mn(1)-O(1)	1.9226(18)
Mn(1)-N(1)	1.966(2)
Mn(1)-N(2)	1.989(2)
Mn(1)-N(3)	2.214(3)
Mn(1)-N(6)	2.388(2)

Mn(2)-O(4)	1.8952(19)
Mn(2)-O(3)	1.8951(18)
Mn(2)-N(16)	1.967(2)
Mn(2)-N(15)	1.972(2)
Mn(2)-N(17)	2.084(2)
O(1)-C(3)	1.301(3)
O(2)-C(6)	1.300(3)
O(3)-C(22)	1.301(3)
O(4)-C(25)	1.305(3)
N(1)-C(1)	1.305(4)
N(1)-C(7)	1.462(3)
N(2)-C(4)	1.315(4)
N(2)-C(8)	1.480(4)
N(3)-N(4)	1.164(4)
N(4)-N(5)	1.171(4)
N(6)-C(17)	1.353(4)
N(6)-C(13)	1.360(4)
N(7)-C(15)	1.362(4)
N(7)-C(18)	1.454(4)
N(7)-C(19)	1.458(4)
N(15)-C(20)	1.325(3)
N(15)-C(26)	1.477(3)
N(16)-C(23)	1.322(4)
N(16)-C(27)	1.476(3)
N(17)-N(18)	1.175(3)
N(18)-N(19)	1.164(4)
C(1)-C(2)	1.429(4)
C(1)-C(9)	1.503(4)
C(2)-C(3)	1.380(4)
C(3)-C(10)	1.499(4)
C(4)-C(5)	1.433(4)
C(4)-C(11)	1.506(4)
C(5)-C(6)	1.377(4)
C(6)-C(12)	1.504(4)
C(7)-C(8)	1.514(4)
C(13)-C(14)	1.355(4)
C(14)-C(15)	1.417(4)
C(15)-C(16)	1.416(4)
C(16)-C(17)	1.358(4)
C(20)-C(21)	1.427(4)
C(20)-C(28)	1.505(4)
C(21)-C(22)	1.371(4)
C(22)-C(29)	1.501(4)
C(23)-C(24)	1.424(4)
C(23)-C(30)	1.506(4)
C(24)-C(25)	1.371(4)
C(25)-C(31)	1.508(4)
C(26)-C(27)	1.514(4)

O(2)-Mn(1)-O(1)	92.27(8)
O(2)-Mn(1)-N(1)	173.60(9)
O(1)-Mn(1)-N(1)	91.83(9)
O(2)-Mn(1)-N(2)	92.93(9)
O(1)-Mn(1)-N(2)	172.96(9)
N(1)-Mn(1)-N(2)	82.58(9)
O(2)-Mn(1)-N(3)	94.25(10)
O(1)-Mn(1)-N(3)	94.61(9)
N(1)-Mn(1)-N(3)	90.30(10)
N(2)-Mn(1)-N(3)	89.73(10)
O(2)-Mn(1)-N(6)	87.75(8)
O(1)-Mn(1)-N(6)	85.30(8)
N(1)-Mn(1)-N(6)	87.70(9)
N(2)-Mn(1)-N(6)	90.17(9)
N(3)-Mn(1)-N(6)	178.00(9)
O(4)-Mn(2)-O(3)	88.83(8)
O(4)-Mn(2)-N(16)	91.22(9)

O(3)-Mn(2)-N(16)	163.33(9)
O(4)-Mn(2)-N(15)	163.46(9)
O(3)-Mn(2)-N(15)	91.42(8)
N(16)-Mn(2)-N(15)	83.86(9)
O(4)-Mn(2)-N(17)	101.45(9)
O(3)-Mn(2)-N(17)	98.50(9)
N(16)-Mn(2)-N(17)	97.82(10)
N(15)-Mn(2)-N(17)	94.87(9)
C(3)-O(1)-Mn(1)	124.14(18)
C(6)-O(2)-Mn(1)	126.74(17)
C(22)-O(3)-Mn(2)	127.15(17)
C(25)-O(4)-Mn(2)	128.89(18)
C(1)-N(1)-C(7)	122.9(2)
C(1)-N(1)-Mn(1)	125.37(19)
C(7)-N(1)-Mn(1)	111.70(17)
C(4)-N(2)-C(8)	119.8(2)
C(4)-N(2)-Mn(1)	126.06(19)
C(8)-N(2)-Mn(1)	114.09(17)
N(4)-N(3)-Mn(1)	142.1(2)
N(3)-N(4)-N(5)	177.7(3)
C(17)-N(6)-C(13)	114.2(3)
C(17)-N(6)-Mn(1)	124.30(18)
C(13)-N(6)-Mn(1)	121.18(19)
C(15)-N(7)-C(18)	122.0(3)
C(15)-N(7)-C(19)	120.8(3)
C(18)-N(7)-C(19)	117.2(3)
C(20)-N(15)-C(26)	120.4(2)
C(20)-N(15)-Mn(2)	125.83(19)
C(26)-N(15)-Mn(2)	113.74(17)
C(23)-N(16)-C(27)	120.6(2)
C(23)-N(16)-Mn(2)	127.65(19)
C(27)-N(16)-Mn(2)	111.32(17)
N(18)-N(17)-Mn(2)	143.3(2)
N(19)-N(18)-N(17)	176.6(3)
N(1)-C(1)-C(2)	122.1(3)
N(1)-C(1)-C(9)	120.8(3)
C(2)-C(1)-C(9)	117.1(3)
C(3)-C(2)-C(1)	125.7(3)
O(1)-C(3)-C(2)	124.6(2)
O(1)-C(3)-C(10)	114.8(3)
C(2)-C(3)-C(10)	120.5(3)
N(2)-C(4)-C(5)	122.3(2)
N(2)-C(4)-C(11)	120.5(2)
C(5)-C(4)-C(11)	117.2(2)
C(6)-C(5)-C(4)	126.3(3)
O(2)-C(6)-C(5)	125.6(3)
O(2)-C(6)-C(12)	114.1(2)
C(5)-C(6)-C(12)	120.3(3)
N(1)-C(7)-C(8)	108.6(2)
N(2)-C(8)-C(7)	109.1(2)
C(14)-C(13)-N(6)	124.9(3)
C(13)-C(14)-C(15)	120.4(3)
N(7)-C(15)-C(16)	122.2(3)
N(7)-C(15)-C(14)	122.7(3)
C(16)-C(15)-C(14)	115.1(3)
C(17)-C(16)-C(15)	119.8(3)
N(6)-C(17)-C(16)	125.6(3)
N(15)-C(20)-C(21)	121.8(2)
N(15)-C(20)-C(28)	120.9(2)
C(21)-C(20)-C(28)	117.4(2)
C(22)-C(21)-C(20)	126.1(3)
O(3)-C(22)-C(21)	123.8(3)
O(3)-C(22)-C(29)	114.5(2)
C(21)-C(22)-C(29)	121.7(3)
N(16)-C(23)-C(24)	122.1(3)
N(16)-C(23)-C(30)	121.0(2)

C(24)-C(23)-C(30)	116.9(2)
C(25)-C(24)-C(23)	125.1(3)
O(4)-C(25)-C(24)	125.0(3)
O(4)-C(25)-C(31)	113.7(2)
C(24)-C(25)-C(31)	121.3(3)
N(15)-C(26)-C(27)	109.7(2)
N(16)-C(27)-C(26)	108.9(2)

Symmetry transformations used to generate equivalent atoms:

Table A-19. Anisotropic displacement parameters ($Å^2 x\ 10^3$) for **3-3”·(3-3·DMAP)**. The anisotropic displacement factor exponent takes the form: $-2\pi^2[\ h^2\ a^{*2}U^{11} + ...\ + 2\ h\ k\ a^*\ b^*\ U^{12}\ ]$

	U^{11}	U^{22}	U^{33}	U^{23}	U^{13}	U^{12}
Mn(1)	26(1)	23(1)	23(1)	-3(1)	6(1)	-2(1)
Mn(2)	24(1)	21(1)	21(1)	-1(1)	3(1)	0(1)
O(1)	27(1)	25(1)	28(1)	-4(1)	6(1)	0(1)
O(2)	35(1)	28(1)	30(1)	-1(1)	11(1)	-3(1)
O(3)	36(1)	25(1)	26(1)	0(1)	10(1)	-3(1)
O(4)	36(1)	27(1)	28(1)	-4(1)	6(1)	-2(1)
N(1)	28(1)	24(1)	25(1)	1(1)	4(1)	-4(1)
N(2)	27(1)	29(1)	22(1)	-3(1)	4(1)	-1(1)
N(3)	31(2)	56(2)	30(1)	-4(1)	-3(1)	2(1)
N(4)	35(2)	32(1)	27(1)	-4(1)	8(1)	-7(1)
N(5)	29(2)	70(2)	55(2)	-3(2)	9(1)	0(1)
N(6)	34(1)	28(1)	29(1)	-1(1)	7(1)	1(1)
N(7)	36(2)	52(2)	31(1)	-2(1)	1(1)	6(1)
N(15)	22(1)	24(1)	23(1)	-1(1)	2(1)	3(1)
N(16)	26(1)	24(1)	22(1)	-1(1)	3(1)	-1(1)
N(17)	25(1)	38(2)	32(1)	1(1)	-3(1)	2(1)
N(18)	33(2)	24(1)	25(1)	1(1)	5(1)	4(1)
N(19)	30(2)	57(2)	50(2)	1(1)	-2(1)	-9(1)
C(1)	26(2)	27(2)	31(2)	4(1)	-1(1)	0(1)
C(2)	27(2)	27(2)	36(2)	-6(1)	-4(1)	1(1)
C(3)	29(2)	23(2)	29(2)	-4(1)	-5(1)	7(1)
C(4)	25(2)	31(2)	22(1)	-6(1)	-1(1)	1(1)
C(5)	28(2)	28(2)	27(1)	-6(1)	-3(1)	2(1)
C(6)	22(1)	28(2)	28(1)	0(1)	-4(1)	-3(1)
C(7)	38(2)	36(2)	25(1)	1(1)	8(1)	-6(1)
C(8)	29(2)	37(2)	26(1)	-5(1)	7(1)	-4(1)
C(9)	38(2)	31(2)	42(2)	0(1)	3(1)	-4(1)
C(10)	35(2)	37(2)	32(2)	-8(1)	0(1)	1(1)
C(11)	30(2)	32(2)	28(2)	-2(1)	1(1)	4(1)
C(12)	34(2)	35(2)	31(2)	3(1)	2(1)	-6(1)
C(13)	33(2)	29(2)	35(2)	0(1)	8(1)	1(1)
C(14)	40(2)	28(2)	26(1)	-3(1)	11(1)	5(1)
C(15)	35(2)	23(2)	31(2)	-4(1)	5(1)	6(1)
C(16)	27(2)	29(2)	32(2)	2(1)	7(1)	2(1)
C(17)	37(2)	29(2)	25(1)	-4(1)	9(1)	2(1)
C(18)	44(2)	33(2)	29(2)	-2(1)	2(1)	1(1)
C(19)	35(2)	46(2)	39(2)	3(2)	1(1)	1(2)
C(20)	23(1)	27(2)	27(1)	-2(1)	-3(1)	2(1)
C(21)	27(2)	23(1)	29(2)	0(1)	1(1)	-4(1)
C(22)	27(2)	27(2)	26(1)	4(1)	-3(1)	-4(1)
C(23)	25(2)	28(2)	29(2)	3(1)	-3(1)	-2(1)
C(24)	26(2)	27(2)	30(2)	-1(1)	-1(1)	-3(1)
C(25)	29(2)	29(2)	26(1)	0(1)	-4(1)	0(1)
C(26)	24(2)	30(2)	29(2)	-4(1)	7(1)	1(1)
C(27)	24(2)	34(2)	22(1)	-1(1)	3(1)	-3(1)
C(28)	30(2)	28(2)	35(2)	-4(1)	4(1)	2(1)
C(29)	34(2)	33(2)	30(2)	5(1)	3(1)	-6(1)
C(30)	35(2)	29(2)	32(2)	1(1)	4(1)	-7(1)
C(31)	35(2)	34(2)	36(2)	-10(1)	2(1)	-1(1)

Table A-20. Hydrogen coordinates (x 10^4) and isotropic displacement parameters ($Å^2$x 10^3) for **3-3”·(3-3·DMAP)**.

	x	y	z	U(eq)
H(2)	1087	4197	3319	36
H(5)	2657	9856	3992	33
H(7A)	2031	5980	4800	39
H(7B)	276	5714	4702	39
H(8A)	-355	7247	4517	36
H(8B)	905	7421	4923	36
H(9A)	613	4115	4462	56
H(9B)	-163	3786	3974	56
H(9C)	-864	4665	4264	56
H(10A)	3130	5213	2496	52
H(10B)	2627	4170	2675	52
H(10C)	4316	4553	2782	52
H(11A)	-136	9011	4640	45
H(11B)	1067	9872	4600	45
H(11C)	1365	9015	4967	45
H(12A)	5455	9255	3258	50
H(12B)	4391	10130	3414	50
H(12C)	3927	9489	2966	50
H(13)	1831	7218	2684	39
H(14)	-70	7282	2136	37
H(16)	-3102	6993	3201	35
H(17)	-1088	6905	3710	36
H(18A)	-2540	7782	1669	53
H(18B)	-3688	6898	1599	53
H(18C)	-1914	6702	1691	53
H(19A)	-4786	6537	2624	60
H(19B)	-5289	7082	2150	60
H(19C)	-4804	7688	2608	60
H(21)	1270	3886	1245	32
H(24)	4427	9585	1299	33
H(26A)	4166	5535	198	33
H(26B)	5363	5749	617	33
H(27A)	5285	7194	254	32
H(27B)	3508	7099	123	32
H(28A)	2991	4089	265	47
H(28B)	2929	3368	704	47
H(28C)	4435	3984	612	47
H(29A)	368	4980	2275	48
H(29B)	-17	4062	1954	48
H(29C)	-995	5027	1895	48
H(30A)	6412	8493	507	48
H(30B)	5701	9523	625	48
H(30C)	4976	8883	211	48
H(31A)	1410	9567	1935	53
H(31B)	3129	9938	1985	53
H(31C)	2570	9039	2290	53

Table A-21. Crystal data and structure refinement for **3-3'**.

Identification code	ddef	
Empirical formula	C24 H36 Mn2 N10 O4	
Formula weight	638.51	
Temperature	110(2) K	
Wavelength	0.71073 Å	
Crystal system	Orthorhombic	
Space group	Pcan	
Unit cell dimensions	a = 13.778(10) Å	α= 90°.
	b = 19.679(15) Å	β= 90°.
	c = 20.056(15) Å	γ = 90°.
Volume	5438(7) $Å^3$	
Z	8	
Density (calculated)	1.560 Mg/m^3	
Absorption coefficient	0.980 mm^{-1}	
F(000)	2656	
Crystal size	0.24 x 0.14 x 0.13 mm^3	
Theta range for data collection	1.80 to 25.00°.	
Index ranges	-16<=h<=16, -23<=k<=23, -23<=l<=23	
Reflections collected	36076	
Independent reflections	4657 [R(int) = 0.1950]	
Completeness to theta = 25.00°	97.0 %	
Absorption correction	Semi-empirical from equivalents	
Max. and min. transmission	0.8831 and 0.7987	
Refinement method	Full-matrix least-squares on F^2	
Data / restraints / parameters	4657 / 204 / 361	
Goodness-of-fit on F^2	1.022	
Final R indices [I>2sigma(I)]	R1 = 0.0793, wR2 = 0.1902	
R indices (all data)	R1 = 0.1151, wR2 = 0.2286	
Largest diff. peak and hole	0.889 and -0.971 e.$Å^{-3}$	

Table A-22. Atomic coordinates (x 10^4) and equivalent isotropic displacement parameters ($Å^2$x 10^3) for **3-3'**. U(eq) is defined as one third of the trace of the orthogonalized U^{ij} tensor.

	x	y	z	U(eq)
Mn(1)	7536(1)	2419(1)	-962(1)	11(1)
Mn(2)	6542(1)	2305(1)	1097(1)	11(1)
O(1)	8292(3)	1625(2)	-1165(2)	16(1)
O(2)	8580(3)	2864(2)	-523(2)	14(1)
O(3)	5472(3)	2788(2)	733(2)	14(1)
O(4)	5803(3)	1488(2)	1189(2)	14(1)
N(1)	6397(3)	2058(3)	-1447(3)	13(1)
N(2)	6711(4)	3220(3)	-859(3)	13(1)
N(3)	7370(4)	3113(3)	1064(3)	14(1)
N(4)	7664(4)	1892(3)	1567(3)	14(1)
N(5)	7057(3)	1946(3)	49(2)	14(1)
N(6)	7072(3)	1335(3)	19(3)	14(1)
N(7)	7089(4)	743(3)	-17(3)	25(1)
N(8)	6020(4)	2656(3)	2171(3)	17(1)
N(9)	6433(3)	2406(3)	2613(3)	14(1)
N(10A)	6856(4)	2124(3)	3057(3)	19(1)
C(1)	6373(4)	1491(3)	-1794(3)	14(1)
C(2)	7174(5)	1046(3)	-1854(3)	17(1)
C(3)	8062(4)	1143(3)	-1572(3)	15(1)
C(4)	7026(4)	3838(3)	-773(3)	13(1)
C(5)	8004(4)	3998(4)	-640(3)	16(1)
C(6)	8698(4)	3513(3)	-498(3)	13(1)
C(7)	5578(4)	2522(3)	-1466(3)	13(1)
C(8)	5687(4)	3028(3)	-911(3)	15(1)
C(9)	5465(4)	1300(3)	-2164(3)	16(1)
C(10)	8884(5)	666(4)	-1714(4)	22(2)

C(11)	6342(4)	4441(3)	-827(3)	17(1)
C(12)	9684(4)	3742(3)	-268(3)	16(1)
C(13)	7068(4)	3742(3)	986(3)	14(1)
C(14)	6091(4)	3905(3)	826(3)	16(1)
C(15)	5373(4)	3440(3)	700(3)	15(1)
C(16)	7685(4)	1289(3)	1835(3)	15(1)
C(17)	6959(4)	802(3)	1744(3)	16(1)
C(18)	6110(4)	912(3)	1427(3)	14(1)
C(19)	8379(4)	2931(3)	1179(3)	13(1)
C(20)	8403(4)	2405(3)	1726(3)	14(1)
C(21)	7761(5)	4329(3)	1057(3)	20(2)
C(22)	4421(4)	3687(4)	450(3)	19(1)
C(23)	8547(5)	1085(4)	2266(4)	23(2)
C(24)	5403(4)	332(3)	1328(4)	19(1)

Table A-23. Bond lengths [Å] and angles [°] for **3-3'**.

Mn(1)-O(2)	1.901(4)
Mn(1)-O(1)	1.921(5)
Mn(1)-N(2)	1.955(5)
Mn(1)-N(1)	1.978(5)
Mn(1)-N(10A)#1	2.320(6)
Mn(1)-N(5)	2.326(5)
Mn(2)-O(3)	1.900(4)
Mn(2)-O(4)	1.911(4)
Mn(2)-N(3)	1.959(5)
Mn(2)-N(4)	1.984(5)
Mn(2)-N(5)	2.328(5)
Mn(2)-N(8)	2.375(6)
O(1)-C(3)	1.291(8)
O(2)-C(6)	1.289(8)
O(3)-C(15)	1.293(8)
O(4)-C(18)	1.301(8)
N(1)-C(1)	1.316(9)
N(1)-C(7)	1.452(8)
N(2)-C(4)	1.303(8)
N(2)-C(8)	1.464(8)
N(3)-C(13)	1.315(8)
N(3)-C(19)	1.454(8)
N(4)-C(16)	1.305(8)
N(4)-C(20)	1.469(8)
N(5)-N(6)	1.205(8)
N(6)-N(7)	1.166(8)
N(8)-N(9)	1.162(7)
N(9)-N(10A)	1.200(8)
N(10A)-Mn(1)#2	2.320(6)
C(1)-C(2)	1.414(9)
C(1)-C(9)	1.502(8)
C(2)-C(3)	1.361(9)
C(2)-H(2A)	0.9500
C(3)-C(10)	1.499(9)
C(4)-C(5)	1.408(9)
C(4)-C(11)	1.520(9)
C(5)-C(6)	1.380(9)
C(5)-H(5A)	0.9500
C(6)-C(12)	1.504(8)
C(7)-C(8)	1.501(9)
C(7)-H(7A)	0.9900
C(7)-H(7B)	0.9900
C(8)-H(8A)	0.9900
C(8)-H(8B)	0.9900
C(9)-H(9A)	0.9800
C(9)-H(9B)	0.9800
C(9)-H(9C)	0.9800
C(10)-H(10A)	0.9800

C(10)-H(10B)	0.9800
C(10)-H(10C)	0.9800
C(11)-H(11A)	0.9800
C(11)-H(11B)	0.9800
C(11)-H(11C)	0.9800
C(12)-H(12A)	0.9800
C(12)-H(12B)	0.9800
C(12)-H(12C)	0.9800
C(13)-C(14)	1.420(9)
C(13)-C(21)	1.506(9)
C(14)-C(15)	1.370(9)
C(14)-H(14A)	0.9500
C(15)-C(22)	1.485(9)
C(16)-C(17)	1.397(9)
C(16)-C(23)	1.523(9)
C(17)-C(18)	1.349(9)
C(17)-H(17A)	0.9500
C(18)-C(24)	1.513(9)
C(19)-C(20)	1.508(9)
C(19)-H(19A)	0.9900
C(19)-H(19B)	0.9900
C(20)-H(20A)	0.9900
C(20)-H(20B)	0.9900
C(21)-H(21A)	0.9800
C(21)-H(21B)	0.9800
C(21)-H(21C)	0.9800
C(22)-H(22A)	0.9800
C(22)-H(22B)	0.9800
C(22)-H(22C)	0.9800
C(23)-H(23A)	0.9800
C(23)-H(23B)	0.9800
C(23)-H(23C)	0.9800
C(24)-H(24A)	0.9800
C(24)-H(24B)	0.9800
C(24)-H(24C)	0.9800

O(2)-Mn(1)-O(1)	93.6(2)
O(2)-Mn(1)-N(2)	91.1(2)
O(1)-Mn(1)-N(2)	173.5(2)
O(2)-Mn(1)-N(1)	173.6(2)
O(1)-Mn(1)-N(1)	92.0(2)
N(2)-Mn(1)-N(1)	83.1(2)
O(2)-Mn(1)-N(10A)#1	86.62(19)
O(1)-Mn(1)-N(10A)#1	86.6(2)
N(2)-Mn(1)-N(10A)#1	89.3(2)
N(1)-Mn(1)-N(10A)#1	90.5(2)
O(2)-Mn(1)-N(5)	89.71(19)
O(1)-Mn(1)-N(5)	90.76(19)
N(2)-Mn(1)-N(5)	93.7(2)
N(1)-Mn(1)-N(5)	93.5(2)
N(10A)#1-Mn(1)-N(5)	175.31(18)
O(3)-Mn(2)-O(4)	92.54(19)
O(3)-Mn(2)-N(3)	91.9(2)
O(4)-Mn(2)-N(3)	175.1(2)
O(3)-Mn(2)-N(4)	172.6(2)
O(4)-Mn(2)-N(4)	91.5(2)
N(3)-Mn(2)-N(4)	83.9(2)
O(3)-Mn(2)-N(5)	92.40(19)
O(4)-Mn(2)-N(5)	89.72(19)
N(3)-Mn(2)-N(5)	92.2(2)
N(4)-Mn(2)-N(5)	93.9(2)
O(3)-Mn(2)-N(8)	88.14(19)
O(4)-Mn(2)-N(8)	89.73(19)
N(3)-Mn(2)-N(8)	88.3(2)
N(4)-Mn(2)-N(8)	85.6(2)
N(5)-Mn(2)-N(8)	179.2(2)

C(3)-O(1)-Mn(1)	126.8(4)
C(6)-O(2)-Mn(1)	124.7(4)
C(15)-O(3)-Mn(2)	126.8(4)
C(18)-O(4)-Mn(2)	126.5(4)
C(1)-N(1)-C(7)	120.0(5)
C(1)-N(1)-Mn(1)	125.8(4)
C(7)-N(1)-Mn(1)	113.8(4)
C(4)-N(2)-C(8)	124.9(5)
C(4)-N(2)-Mn(1)	124.9(4)
C(8)-N(2)-Mn(1)	110.2(4)
C(13)-N(3)-C(19)	123.6(5)
C(13)-N(3)-Mn(2)	125.7(4)
C(19)-N(3)-Mn(2)	110.6(4)
C(16)-N(4)-C(20)	121.4(5)
C(16)-N(4)-Mn(2)	125.8(4)
C(20)-N(4)-Mn(2)	111.2(4)
N(6)-N(5)-Mn(1)	110.6(4)
N(6)-N(5)-Mn(2)	110.6(4)
Mn(1)-N(5)-Mn(2)	138.8(3)
N(7)-N(6)-N(5)	179.2(6)
N(9)-N(8)-Mn(2)	114.9(4)
N(8)-N(9)-N(10A)	177.3(7)
N(9)-N(10A)-Mn(1)#2	128.6(5)
N(1)-C(1)-C(2)	123.4(6)
N(1)-C(1)-C(9)	119.6(5)
C(2)-C(1)-C(9)	117.0(6)
C(3)-C(2)-C(1)	125.4(6)
C(3)-C(2)-H(2A)	117.3
C(1)-C(2)-H(2A)	117.3
O(1)-C(3)-C(2)	125.9(6)
O(1)-C(3)-C(10)	113.3(6)
C(2)-C(3)-C(10)	120.8(6)
N(2)-C(4)-C(5)	123.6(6)
N(2)-C(4)-C(11)	120.8(5)
C(5)-C(4)-C(11)	115.6(6)
C(6)-C(5)-C(4)	123.1(6)
C(6)-C(5)-H(5A)	118.4
C(4)-C(5)-H(5A)	118.4
O(2)-C(6)-C(5)	126.2(6)
O(2)-C(6)-C(12)	115.0(5)
C(5)-C(6)-C(12)	118.8(6)
N(1)-C(7)-C(8)	108.7(5)
N(1)-C(7)-H(7A)	110.0
C(8)-C(7)-H(7A)	110.0
N(1)-C(7)-H(7B)	110.0
C(8)-C(7)-H(7B)	110.0
H(7A)-C(7)-H(7B)	108.3
N(2)-C(8)-C(7)	108.7(5)
N(2)-C(8)-H(8A)	109.9
C(7)-C(8)-H(8A)	109.9
N(2)-C(8)-H(8B)	109.9
C(7)-C(8)-H(8B)	109.9
H(8A)-C(8)-H(8B)	108.3
C(1)-C(9)-H(9A)	109.5
C(1)-C(9)-H(9B)	109.5
H(9A)-C(9)-H(9B)	109.5
C(1)-C(9)-H(9C)	109.5
H(9A)-C(9)-H(9C)	109.5
H(9B)-C(9)-H(9C)	109.5
C(3)-C(10)-H(10A)	109.5
C(3)-C(10)-H(10B)	109.5
H(10A)-C(10)-H(10B)	109.5
C(3)-C(10)-H(10C)	109.5
H(10A)-C(10)-H(10C)	109.5
H(10B)-C(10)-H(10C)	109.5
C(4)-C(11)-H(11A)	109.5

C(4)-C(11)-H(11B)	109.5
H(11A)-C(11)-H(11B)	109.5
C(4)-C(11)-H(11C)	109.5
H(11A)-C(11)-H(11C)	109.5
H(11B)-C(11)-H(11C)	109.5
C(6)-C(12)-H(12A)	109.5
C(6)-C(12)-H(12B)	109.5
H(12A)-C(12)-H(12B)	109.5
C(6)-C(12)-H(12C)	109.5
H(12A)-C(12)-H(12C)	109.5
H(12B)-C(12)-H(12C)	109.5
N(3)-C(13)-C(14)	122.6(6)
N(3)-C(13)-C(21)	120.7(6)
C(14)-C(13)-C(21)	116.7(6)
C(15)-C(14)-C(13)	125.2(6)
C(15)-C(14)-H(14A)	117.4
C(13)-C(14)-H(14A)	117.4
O(3)-C(15)-C(14)	125.2(6)
O(3)-C(15)-C(22)	115.9(6)
C(14)-C(15)-C(22)	118.8(6)
N(4)-C(16)-C(17)	123.6(6)
N(4)-C(16)-C(23)	119.4(6)
C(17)-C(16)-C(23)	117.0(6)
C(18)-C(17)-C(16)	125.0(6)
C(18)-C(17)-H(17A)	117.5
C(16)-C(17)-H(17A)	117.5
O(4)-C(18)-C(17)	126.4(6)
O(4)-C(18)-C(24)	113.6(5)
C(17)-C(18)-C(24)	119.9(6)
N(3)-C(19)-C(20)	107.7(5)
N(3)-C(19)-H(19A)	110.2
C(20)-C(19)-H(19A)	110.2
N(3)-C(19)-H(19B)	110.2
C(20)-C(19)-H(19B)	110.2
H(19A)-C(19)-H(19B)	108.5
N(4)-C(20)-C(19)	107.4(5)
N(4)-C(20)-H(20A)	110.2
C(19)-C(20)-H(20A)	110.2
N(4)-C(20)-H(20B)	110.2
C(19)-C(20)-H(20B)	110.2
H(20A)-C(20)-H(20B)	108.5
C(13)-C(21)-H(21A)	109.5
C(13)-C(21)-H(21B)	109.5
H(21A)-C(21)-H(21B)	109.5
C(13)-C(21)-H(21C)	109.5
H(21A)-C(21)-H(21C)	109.5
H(21B)-C(21)-H(21C)	109.5
C(15)-C(22)-H(22A)	109.5
C(15)-C(22)-H(22B)	109.5
H(22A)-C(22)-H(22B)	109.5
C(15)-C(22)-H(22C)	109.5
H(22A)-C(22)-H(22C)	109.5
H(22B)-C(22)-H(22C)	109.5
C(16)-C(23)-H(23A)	109.5
C(16)-C(23)-H(23B)	109.5
H(23A)-C(23)-H(23B)	109.5
C(16)-C(23)-H(23C)	109.5
H(23A)-C(23)-H(23C)	109.5
H(23B)-C(23)-H(23C)	109.5
C(18)-C(24)-H(24A)	109.5
C(18)-C(24)-H(24B)	109.5
H(24A)-C(24)-H(24B)	109.5
C(18)-C(24)-H(24C)	109.5
H(24A)-C(24)-H(24C)	109.5
H(24B)-C(24)-H(24C)	109.5

Symmetry transformations used to generate equivalent atoms:
#1 -x+3/2,-y+1/2,z-1/2 #2 -x+3/2,-y+1/2,z+1/2

Table A-24. Anisotropic displacement parameters ($Å^2 x\ 10^3$) for **3-3'**. The anisotropic displacement factor exponent takes the form: $-2\pi^2[\ h^2\ a^{*2}U^{11} + ... + 2\ h\ k\ a^*\ b^*\ U^{12}\ ]$

	U^{11}	U^{22}	U^{33}	U^{23}	U^{13}	U^{12}
Mn(1)	6(1)	19(1)	9(1)	-1(1)	-1(1)	1(1)
Mn(2)	7(1)	20(1)	7(1)	1(1)	-1(1)	0(1)
O(1)	12(2)	18(2)	17(2)	1(2)	4(2)	2(2)
O(2)	12(2)	23(2)	8(2)	-2(2)	-2(2)	-2(2)
O(3)	9(2)	22(2)	11(2)	0(2)	-2(2)	1(2)
O(4)	10(2)	21(2)	13(2)	1(2)	2(2)	-4(2)
N(1)	10(2)	23(2)	6(2)	1(2)	1(2)	-3(2)
N(2)	11(2)	22(2)	7(2)	1(2)	3(2)	2(2)
N(3)	10(2)	23(2)	8(2)	-1(2)	2(2)	-3(2)
N(4)	11(2)	21(2)	10(2)	2(2)	-1(2)	2(2)
N(5)	10(2)	26(3)	7(2)	-3(2)	-3(2)	2(2)
N(6)	8(2)	25(3)	10(2)	2(2)	1(2)	-1(2)
N(7)	28(3)	29(4)	18(3)	-1(3)	8(3)	1(3)
N(8)	11(2)	29(3)	9(3)	-1(2)	0(2)	4(2)
N(9)	4(2)	25(3)	14(2)	-3(2)	2(2)	-2(2)
N(10A)	11(2)	31(3)	15(3)	-4(2)	-2(2)	0(2)
C(1)	12(2)	21(3)	9(2)	4(2)	1(2)	-2(2)
C(2)	17(3)	20(3)	13(3)	3(2)	1(2)	-1(2)
C(3)	16(2)	16(3)	14(2)	1(2)	5(2)	2(2)
C(4)	10(2)	22(3)	7(2)	2(2)	2(2)	2(2)
C(5)	14(3)	23(3)	12(3)	1(2)	2(2)	-2(2)
C(6)	10(2)	23(3)	6(2)	-1(2)	3(2)	-4(2)
C(7)	8(2)	24(3)	8(2)	2(2)	3(2)	-3(2)
C(8)	11(2)	25(3)	10(3)	2(2)	5(2)	-1(2)
C(9)	12(3)	21(4)	14(3)	-3(3)	1(2)	-4(3)
C(10)	17(3)	27(4)	23(4)	-6(3)	2(3)	3(3)
C(11)	9(3)	24(3)	19(3)	1(3)	2(2)	1(2)
C(12)	11(3)	28(4)	8(3)	-1(3)	-3(2)	0(3)
C(13)	12(2)	20(3)	10(2)	-1(2)	0(2)	-1(2)
C(14)	10(2)	21(3)	15(3)	-2(2)	3(2)	3(2)
C(15)	10(2)	24(3)	12(2)	2(2)	4(2)	2(2)
C(16)	13(2)	24(3)	8(2)	1(2)	0(2)	3(2)
C(17)	14(3)	23(3)	12(3)	1(2)	1(2)	0(2)
C(18)	12(2)	18(3)	11(2)	2(2)	2(2)	-2(2)
C(19)	8(2)	21(3)	10(3)	4(2)	1(2)	-1(2)
C(20)	10(2)	21(3)	12(3)	1(2)	-2(2)	-1(2)
C(21)	19(3)	21(4)	18(3)	-3(3)	0(3)	-3(3)
C(22)	11(3)	30(4)	14(3)	3(3)	0(2)	3(3)
C(23)	18(3)	28(4)	22(4)	7(3)	-6(3)	-1(3)
C(24)	9(3)	21(4)	26(4)	3(3)	4(3)	1(3)

Table A-25. Hydrogen coordinates ($x\ 10^4$) and isotropic displacement parameters ($Å^2 x\ 10^3$) for **3-3'**.

	x	y	z	U(eq)
H(2A)	7085	647	-2113	20
H(5A)	8194	4462	-648	20
H(7A)	4965	2266	-1411	16
H(7B)	5559	2760	-1901	16
H(8A)	5288	3435	-1005	18
H(8B)	5464	2827	-486	18
H(9A)	4964	1644	-2084	24

H(9B)	5234	857	-2006	24
H(9C)	5604	1275	-2642	24
H(10A)	9460	810	-1465	34
H(10B)	9029	671	-2193	34
H(10C)	8702	205	-1579	34
H(11A)	5684	4279	-923	26
H(11B)	6559	4741	-1188	26
H(11C)	6342	4693	-405	26
H(12A)	10097	3345	-192	23
H(12B)	9619	4000	147	23
H(12C)	9978	4032	-611	23
H(14A)	5922	4372	805	19
H(17A)	7071	361	1918	20
H(19A)	8755	3337	1314	16
H(19B)	8669	2744	766	16
H(20A)	9053	2192	1750	17
H(20B)	8260	2619	2162	17
H(21A)	8411	4157	1162	29
H(21B)	7540	4629	1416	29
H(21C)	7784	4585	637	29
H(22A)	3987	3300	378	28
H(22B)	4516	3930	29	28
H(22C)	4133	3995	779	28
H(23A)	9003	1467	2296	34
H(23B)	8875	693	2065	34
H(23C)	8320	965	2713	34
H(24A)	4828	498	1092	28
H(24B)	5210	151	1764	28
H(24C)	5714	-27	1066	28

Table A-26. Crystal data and structure refinement for **3-4·EtOH**.

Identification code	ddef43m	
Empirical formula	C14 H24 Mn N3 O6	
Formula weight	385.30	
Temperature	110(2) K	
Wavelength	0.71073 Å	
Crystal system	Monoclinic	
Space group	P2(1)/n	
Unit cell dimensions	a = 8.1727(5) Å	α= 90°.
	b = 17.1898(11) Å	β= 94.7680(10)°.
	c = 12.3854(8) Å	γ = 90°.
Volume	1733.97(19) $Å^3$	
Z	4	
Density (calculated)	1.476 Mg/m^3	
Absorption coefficient	0.796 mm^{-1}	
F(000)	808	
Crystal size	0.23 x 0.18 x 0.13 mm^3	
Theta range for data collection	2.03 to 27.55°.	
Index ranges	-10<=h<=10, -21<=k<=21, -16<=l<=16	
Reflections collected	16375	
Independent reflections	3952 [R(int) = 0.0418]	
Completeness to theta = 27.55°	98.8 %	
Absorption correction	Semi-empirical from equivalents	
Max. and min. transmission	0.9036 and 0.8381	
Refinement method	Full-matrix least-squares on F^2	
Data / restraints / parameters	3952 / 0 / 222	
Goodness-of-fit on F^2	0.989	
Final R indices [I>2sigma(I)]	R1 = 0.0689, wR2 = 0.1622	
R indices (all data)	R1 = 0.0880, wR2 = 0.1786	
Largest diff. peak and hole	3.378 and -0.381 e.$Å^{-3}$	

Table A-27. Atomic coordinates (x 10^4) and equivalent isotropic displacement parameters ($Å^2$x 10^3) for **3-4·EtOH**. U(eq) is defined as one third of the trace of the orthogonalized U^{ij} tensor.

	x	y	z	U(eq)
Mn(1)	34(1)	2296(1)	4806(1)	20(1)
O(1)	-942(2)	3238(1)	4286(2)	22(1)
O(2)	-449(2)	1805(1)	3436(2)	24(1)
O(3)	-2314(2)	1802(1)	5462(2)	28(1)
O(4)	-4247(3)	2601(1)	4851(2)	31(1)
O(5)	-4838(3)	1574(1)	5746(2)	39(1)
O(6)	2432(3)	2687(1)	4207(2)	29(1)
N(1)	585(3)	2729(1)	6268(2)	21(1)
N(2)	1151(3)	1357(1)	5398(2)	22(1)
N(3)	-3814(3)	1992(2)	5354(2)	25(1)
C(1)	73(3)	3395(2)	6627(2)	22(1)
C(2)	-945(3)	3908(2)	5962(2)	26(1)
C(3)	-1376(3)	3816(2)	4875(2)	23(1)
C(4)	1654(3)	772(2)	4849(2)	24(1)
C(5)	1313(3)	715(2)	3698(2)	25(1)
C(6)	293(3)	1203(2)	3077(2)	24(1)
C(7)	1740(4)	2221(2)	6940(2)	24(1)
C(8)	1414(4)	1387(2)	6591(2)	26(1)
C(9)	496(4)	3659(2)	7783(2)	27(1)
C(10)	-2422(4)	4418(2)	4265(3)	33(1)
C(11)	2612(4)	105(2)	5392(3)	30(1)
C(12)	-87(4)	1051(2)	1882(2)	30(1)
C(13)	2460(4)	3077(2)	3180(2)	30(1)
C(14)	2523(5)	3938(2)	3330(3)	49(1)

Table A-28. Bond lengths [Å] and angles [°] for **3-4·EtOH**.

Mn(1)-O(1)	1.894(2)
Mn(1)-O(2)	1.9063(19)
Mn(1)-N(2)	1.966(2)
Mn(1)-N(1)	1.975(2)
Mn(1)-O(6)	2.255(2)
Mn(1)-O(3)	2.307(2)
O(1)-C(3)	1.299(3)
O(2)-C(6)	1.297(3)
O(3)-N(3)	1.265(3)
O(4)-N(3)	1.253(3)
O(5)-N(3)	1.233(3)
O(6)-C(13)	1.439(4)
N(1)-C(1)	1.310(4)
N(1)-C(7)	1.488(4)
N(2)-C(4)	1.299(4)
N(2)-C(8)	1.476(4)
C(1)-C(2)	1.426(4)
C(1)-C(9)	1.514(4)
C(2)-C(3)	1.372(4)
C(3)-C(10)	1.505(4)
C(4)-C(5)	1.433(4)
C(4)-C(11)	1.514(4)
C(5)-C(6)	1.372(4)
C(6)-C(12)	1.509(4)
C(7)-C(8)	1.515(4)
C(13)-C(14)	1.493(5)

O(1)-Mn(1)-O(2)	91.49(8)
O(1)-Mn(1)-N(2)	176.42(9)
O(2)-Mn(1)-N(2)	91.35(9)
O(1)-Mn(1)-N(1)	92.70(9)
O(2)-Mn(1)-N(1)	175.76(9)
N(2)-Mn(1)-N(1)	84.48(10)
O(1)-Mn(1)-O(6)	89.18(8)
O(2)-Mn(1)-O(6)	87.76(8)
N(2)-Mn(1)-O(6)	88.75(9)
N(1)-Mn(1)-O(6)	92.89(9)
O(1)-Mn(1)-O(3)	95.49(8)
O(2)-Mn(1)-O(3)	91.92(8)
N(2)-Mn(1)-O(3)	86.59(8)
N(1)-Mn(1)-O(3)	87.09(9)
O(6)-Mn(1)-O(3)	175.33(8)
C(3)-O(1)-Mn(1)	126.09(18)
C(6)-O(2)-Mn(1)	126.23(18)
N(3)-O(3)-Mn(1)	134.01(19)
C(13)-O(6)-Mn(1)	120.49(17)
C(1)-N(1)-C(7)	121.9(2)
C(1)-N(1)-Mn(1)	125.88(19)
C(7)-N(1)-Mn(1)	112.17(18)
C(4)-N(2)-C(8)	121.7(2)
C(4)-N(2)-Mn(1)	126.6(2)
C(8)-N(2)-Mn(1)	111.67(18)
O(5)-N(3)-O(4)	120.6(2)
O(5)-N(3)-O(3)	119.5(3)
O(4)-N(3)-O(3)	120.0(2)
N(1)-C(1)-C(2)	122.1(3)
N(1)-C(1)-C(9)	122.0(3)
C(2)-C(1)-C(9)	115.9(3)
C(3)-C(2)-C(1)	125.8(3)
O(1)-C(3)-C(2)	125.5(3)
O(1)-C(3)-C(10)	114.5(2)
C(2)-C(3)-C(10)	120.1(3)
N(2)-C(4)-C(5)	122.0(3)
N(2)-C(4)-C(11)	121.8(3)
C(5)-C(4)-C(11)	116.1(3)
C(6)-C(5)-C(4)	125.1(3)

O(2)-C(6)-C(5)	125.0(3)
O(2)-C(6)-C(12)	114.3(3)
C(5)-C(6)-C(12)	120.7(3)
N(1)-C(7)-C(8)	107.9(2)
N(2)-C(8)-C(7)	109.0(2)
O(6)-C(13)-C(14)	110.8(3)

Symmetry transformations used to generate equivalent atoms:

Table A-29. Anisotropic displacement parameters ($Å^2 x\ 10^3$) for **3-4·EtOH**. The anisotropic displacement factor exponent takes the form: $-2\pi^2[\ h^2\ a^{*2}U^{11} + ...\ + 2\ h\ k\ a^*\ b^*\ U^{12}\ ]$

	U^{11}	U^{22}	U^{33}	U^{23}	U^{13}	U^{12}
Mn(1)	20(1)	20(1)	20(1)	-1(1)	0(1)	2(1)
O(1)	24(1)	21(1)	21(1)	1(1)	-1(1)	2(1)
O(2)	25(1)	24(1)	22(1)	-4(1)	0(1)	3(1)
O(3)	19(1)	32(1)	33(1)	-1(1)	2(1)	1(1)
O(4)	23(1)	30(1)	40(1)	3(1)	1(1)	3(1)
O(5)	25(1)	47(2)	45(1)	6(1)	7(1)	-8(1)
O(6)	23(1)	36(1)	27(1)	11(1)	1(1)	1(1)
N(1)	20(1)	24(1)	18(1)	2(1)	-1(1)	1(1)
N(2)	20(1)	24(1)	22(1)	1(1)	1(1)	1(1)
N(3)	19(1)	32(1)	25(1)	-9(1)	2(1)	-4(1)
C(1)	19(1)	27(2)	20(1)	-1(1)	2(1)	-2(1)
C(2)	25(1)	24(2)	28(2)	-5(1)	-1(1)	5(1)
C(3)	20(1)	23(2)	26(2)	1(1)	1(1)	0(1)
C(4)	19(1)	22(2)	30(2)	0(1)	0(1)	-1(1)
C(5)	26(1)	22(2)	28(2)	-4(1)	4(1)	1(1)
C(6)	21(1)	25(2)	25(2)	-3(1)	4(1)	-5(1)
C(7)	24(1)	27(2)	20(1)	1(1)	-3(1)	1(1)
C(8)	28(1)	27(2)	24(1)	5(1)	1(1)	4(1)
C(9)	27(2)	30(2)	24(1)	-3(1)	-4(1)	-1(1)
C(10)	37(2)	30(2)	30(2)	-1(1)	-7(1)	13(1)
C(11)	29(2)	22(2)	37(2)	3(1)	2(1)	6(1)
C(12)	33(2)	32(2)	24(2)	-7(1)	2(1)	1(1)
C(13)	32(2)	31(2)	27(2)	6(1)	6(1)	1(1)
C(14)	46(2)	31(2)	71(3)	6(2)	24(2)	-3(2)

Table A-30. Hydrogen coordinates ($x\ 10^4$) and isotropic displacement parameters ($Å^2 x\ 10^3$) for **3-4·EtOH**.

	x	y	z	U(eq)
H(6A)	3539	2635	4454	43
H(2)	-1362	4353	6302	31
H(5A)	1834	308	3337	30
H(7A)	1565	2283	7716	29
H(7B)	2889	2364	6834	29
H(8A)	2362	1056	6842	32
H(8B)	430	1188	6916	32
H(9A)	-263	3418	8257	41
H(9B)	400	4227	7823	41
H(9C)	1623	3504	8017	41
H(10A)	-1821	4635	3682	49
H(10B)	-2684	4835	4762	49
H(10C)	-3440	4176	3955	49
H(11A)	3629	304	5768	44
H(11B)	2878	-275	4843	44
H(11C)	1948	-146	5916	44
H(12A)	-1278	1057	1709	45
H(12B)	350	541	1699	45

H(12C)	422	1455	1464	45
H(13A)	1465	2936	2710	36
H(13B)	3431	2904	2817	36
H(14A)	1591	4106	3722	73
H(14B)	2468	4193	2620	73
H(14C)	3551	4081	3746	73

Table A-31. Crystal data and structure refinement for **3-3·pyr**.

Identification code	ddef470m	
Empirical formula	C17 H23 Mn N6 O2	
Formula weight	398.35	
Temperature	273(2) K	
Wavelength	1.54178 Å	
Crystal system	Monoclinic	
Space group	P2(1)	
Unit cell dimensions	a = 6.5564(5) Å	α= 90°.
	b = 14.1006(11) Å	β= 93.029(4)°.
	c = 10.0027(8) Å	γ = 90°.
Volume	923.45(12) $Å^3$	
Z	2	
Density (calculated)	1.433 Mg/m^3	
Absorption coefficient	6.019 mm^{-1}	
F(000)	416	
Crystal size	0.08 x 0.04 x 0.03 mm^3	
Theta range for data collection	4.43 to 62.81°.	
Index ranges	-7<=h<=7, -15<=k<=16, -11<=l<=11	
Reflections collected	7612	
Independent reflections	2707 [R(int) = 0.0959]	
Completeness to theta = 62.81°	98.8 %	
Absorption correction	Semi-empirical from equivalents	
Max. and min. transmission	0.8401 and 0.6446	
Refinement method	Full-matrix least-squares on F^2	
Data / restraints / parameters	2707 / 1 / 239	
Goodness-of-fit on F^2	1.005	
Final R indices [I>2sigma(I)]	R1 = 0.0471, wR2 = 0.0950	
R indices (all data)	R1 = 0.0612, wR2 = 0.1045	
Absolute structure parameter	0.055(8)	
Largest diff. peak and hole	0.484 and -0.472 e.$Å^{-3}$	

Table A-32. Atomic coordinates (x 10^4) and equivalent isotropic displacement parameters ($Å^2$x 10^3) for **3-3·pyr**. U(eq) is defined as one third of the trace of the orthogonalized U^{ij} tensor.

	x	y	z	U(eq)
Mn(1)	10838(1)	2331(1)	8083(1)	15(1)
O(1)	12582(5)	1738(2)	6880(3)	17(1)
O(2)	12143(5)	3531(2)	7832(4)	23(1)
N(1)	9114(6)	1181(3)	8221(4)	16(1)
N(2)	8813(6)	2897(3)	9218(4)	16(1)
N(3)	12830(6)	1908(4)	9845(5)	26(1)
N(4)	12467(6)	1977(3)	10997(5)	19(1)
N(5)	12131(7)	2024(3)	12131(5)	30(1)
N(6)	8599(6)	2741(3)	6153(4)	17(1)
C(1)	9321(8)	393(4)	7557(5)	20(1)
C(2)	10877(8)	262(4)	6615(5)	20(1)
C(3)	12339(8)	895(4)	6321(5)	21(1)
C(4)	8428(8)	3815(4)	9318(5)	19(1)
C(5)	9504(9)	4508(4)	8625(5)	25(1)
C(6)	11246(8)	4341(4)	7938(5)	21(1)
C(7)	7362(8)	1325(4)	9073(5)	19(1)

C(8)	7778(7)	2161(4)	9970(5)	18(1)
C(9)	7872(9)	-429(4)	7742(6)	30(2)
C(10)	13824(9)	698(4)	5262(6)	27(1)
C(11)	6731(8)	4158(4)	10169(5)	24(1)
C(12)	12301(10)	5158(4)	7272(6)	35(2)
C(13)	9283(8)	2608(3)	4920(5)	19(1)
C(14)	8071(7)	2712(4)	3769(5)	20(1)
C(15)	6043(8)	2970(4)	3856(5)	22(1)
C(16)	5323(8)	3111(3)	5118(5)	19(1)
C(17)	6625(8)	2987(3)	6214(5)	16(1)

Table A-33. Bond lengths [Å] and angles [°] for **3-3·pyr**.

Mn(1)-O(1)	1.898(3)
Mn(1)-O(2)	1.918(4)
Mn(1)-N(2)	1.962(4)
Mn(1)-N(1)	1.986(4)
Mn(1)-N(3)	2.220(5)
Mn(1)-N(6)	2.432(4)
O(1)-C(3)	1.320(6)
O(2)-C(6)	1.292(6)
N(1)-C(1)	1.305(7)
N(1)-C(7)	1.481(6)
N(2)-C(4)	1.323(7)
N(2)-C(8)	1.469(6)
N(3)-N(4)	1.193(6)
N(4)-N(5)	1.168(6)
N(6)-C(17)	1.344(6)
N(6)-C(13)	1.347(6)
C(1)-C(2)	1.437(7)
C(1)-C(9)	1.516(7)
C(2)-C(3)	1.353(7)
C(3)-C(10)	1.503(7)
C(4)-C(5)	1.409(8)
C(4)-C(11)	1.515(7)
C(5)-C(6)	1.384(7)
C(6)-C(12)	1.516(7)
C(7)-C(8)	1.496(7)
C(13)-C(14)	1.372(7)
C(14)-C(15)	1.386(7)
C(15)-C(16)	1.385(7)
C(16)-C(17)	1.365(7)
O(1)-Mn(1)-O(2)	91.03(15)
O(1)-Mn(1)-N(2)	174.49(18)
O(2)-Mn(1)-N(2)	92.14(16)
O(1)-Mn(1)-N(1)	92.75(16)
O(2)-Mn(1)-N(1)	171.45(17)
N(2)-Mn(1)-N(1)	83.52(18)
O(1)-Mn(1)-N(3)	92.05(16)
O(2)-Mn(1)-N(3)	95.35(16)
N(2)-Mn(1)-N(3)	92.14(17)
N(1)-Mn(1)-N(3)	92.18(18)
O(1)-Mn(1)-N(6)	87.72(15)
O(2)-Mn(1)-N(6)	86.64(15)
N(2)-Mn(1)-N(6)	87.96(16)
N(1)-Mn(1)-N(6)	85.84(16)
N(3)-Mn(1)-N(6)	178.00(18)
C(3)-O(1)-Mn(1)	127.0(3)
C(6)-O(2)-Mn(1)	124.1(3)
C(1)-N(1)-C(7)	121.0(4)
C(1)-N(1)-Mn(1)	125.8(4)
C(7)-N(1)-Mn(1)	112.9(3)
C(4)-N(2)-C(8)	123.9(4)
C(4)-N(2)-Mn(1)	125.4(4)

C(8)-N(2)-Mn(1)	110.7(3)
N(4)-N(3)-Mn(1)	127.3(4)
N(5)-N(4)-N(3)	178.4(6)
C(17)-N(6)-C(13)	116.4(5)
C(17)-N(6)-Mn(1)	124.6(3)
C(13)-N(6)-Mn(1)	118.5(3)
N(1)-C(1)-C(2)	122.6(5)
N(1)-C(1)-C(9)	120.4(5)
C(2)-C(1)-C(9)	116.9(5)
C(3)-C(2)-C(1)	126.4(5)
O(1)-C(3)-C(2)	125.0(5)
O(1)-C(3)-C(10)	113.4(5)
C(2)-C(3)-C(10)	121.6(5)
N(2)-C(4)-C(5)	122.6(5)
N(2)-C(4)-C(11)	120.2(5)
C(5)-C(4)-C(11)	117.2(5)
C(6)-C(5)-C(4)	125.1(5)
O(2)-C(6)-C(5)	125.6(5)
O(2)-C(6)-C(12)	114.5(5)
C(5)-C(6)-C(12)	119.8(5)
N(1)-C(7)-C(8)	109.3(4)
N(2)-C(8)-C(7)	108.9(4)
N(6)-C(13)-C(14)	123.2(5)
C(13)-C(14)-C(15)	119.4(5)
C(16)-C(15)-C(14)	118.0(5)
C(17)-C(16)-C(15)	119.0(5)
N(6)-C(17)-C(16)	124.0(5)

Symmetry transformations used to generate equivalent atoms:

Table A-34. Anisotropic displacement parameters ($Å^2 x\ 10^3$) for **3-3·pyr**. The anisotropic displacement factor exponent takes the form: $-2\pi^2[\ h^2\ a^{*2}U^{11} + ... + 2\ h\ k\ a^*\ b^*\ U^{12}\ ]$

	U^{11}	U^{22}	U^{33}	U^{23}	U^{13}	U^{12}
Mn(1)	13(1)	19(1)	15(1)	-1(1)	5(1)	-1(1)
O(1)	17(2)	19(2)	16(2)	1(2)	7(2)	-2(2)
O(2)	21(2)	20(2)	27(2)	-1(2)	7(2)	0(2)
N(1)	15(2)	19(3)	15(3)	-2(2)	6(2)	0(2)
N(2)	12(2)	16(3)	19(3)	-3(2)	3(2)	-2(2)
N(3)	10(2)	44(3)	24(3)	2(2)	2(2)	4(2)
N(4)	13(2)	15(3)	27(3)	-4(2)	-5(2)	-2(2)
N(5)	25(3)	44(4)	20(3)	-6(2)	-2(2)	-2(2)
N(6)	18(2)	18(2)	15(2)	3(2)	0(2)	4(2)
C(1)	20(3)	21(3)	19(3)	9(3)	-1(2)	-6(3)
C(2)	29(3)	9(3)	25(3)	-4(2)	7(3)	-9(3)
C(3)	25(3)	24(3)	14(3)	2(3)	0(3)	9(3)
C(4)	13(3)	30(4)	11(3)	-3(3)	-2(2)	0(3)
C(5)	29(3)	19(3)	27(3)	-6(3)	10(3)	7(3)
C(6)	27(3)	14(3)	23(3)	-4(3)	4(3)	-4(3)
C(7)	12(3)	25(3)	22(3)	-6(3)	3(2)	-4(3)
C(8)	14(2)	23(4)	17(3)	-2(3)	6(2)	2(3)
C(9)	31(3)	24(3)	35(4)	-5(3)	3(3)	-7(3)
C(10)	37(4)	19(3)	27(3)	-2(3)	17(3)	8(3)
C(11)	25(3)	24(3)	25(3)	-7(3)	11(3)	8(3)
C(12)	52(4)	19(3)	36(4)	0(3)	23(3)	-10(3)
C(13)	15(3)	21(4)	20(3)	1(2)	3(2)	1(2)
C(14)	21(3)	19(3)	18(3)	-5(2)	1(2)	3(3)
C(15)	28(3)	22(3)	15(3)	4(2)	-9(3)	-5(3)
C(16)	13(3)	17(3)	29(3)	2(3)	1(2)	1(3)
C(17)	19(3)	16(3)	15(3)	0(2)	3(2)	-2(2)

Table A-35. Hydrogen coordinates ($x\ 10^4$) and isotropic displacement parameters ($Å^2 x\ 10^3$) for **3-3·pyr**.

	x	y	z	U(eq)
H(2)	10880	-314	6163	25
H(5)	9005	5125	8629	30
H(7A)	7159	763	9609	23
H(7B)	6129	1435	8516	23
H(8A)	6505	2406	10281	22
H(8B)	8634	1971	10744	22
H(9A)	8028	-656	8646	45
H(9B)	8179	-931	7136	45
H(9C)	6492	-220	7560	45
H(10A)	13433	1050	4468	41
H(10B)	13817	32	5060	41
H(10C)	15171	885	5581	41
H(11A)	5465	3870	9862	36
H(11B)	6615	4835	10098	36
H(11C)	7038	3987	11086	36
H(12A)	13635	5249	7695	53
H(12B)	11510	5726	7358	53
H(12C)	12425	5017	6341	53
H(13)	10642	2437	4846	22
H(14)	8605	2610	2938	23
H(15)	5191	3046	3090	27
H(16)	3973	3288	5217	23
H(17)	6116	3078	7055	20

Table A-36. Crystal data and structure refinement for **4-1**.

Identification code	ddef51m	
Empirical formula	C12 H12 Cl F6 Mn N2 O2	
Formula weight	420.63	
Temperature	110(2) K	
Wavelength	0.71073 Å	
Crystal system	Monoclinic	
Space group	P2(1)/n	
Unit cell dimensions	a = 11.314(3) Å	α= 90°.
	b = 12.587(3) Å	β= 110.135(5)°.
	c = 11.775(3) Å	γ = 90°.
Volume	1574.4(7) $Å^3$	
Z	4	
Density (calculated)	1.775 Mg/m^3	
Absorption coefficient	1.081 mm^{-1}	
F(000)	840	
Crystal size	0.18 x 0.04 x 0.02 mm^3	
Theta range for data collection	2.15 to 27.62°.	
Index ranges	-14<=h<=14, -16<=k<=15, -13<=l<=15	
Reflections collected	10734	
Independent reflections	3564 [R(int) = 0.0548]	
Completeness to theta = 27.62°	97.3 %	
Absorption correction	Semi-empirical from equivalents	
Max. and min. transmission	0.9787 and 0.8291	
Refinement method	Full-matrix least-squares on F^2	
Data / restraints / parameters	3564 / 0 / 219	
Goodness-of-fit on F^2	0.972	
Final R indices [I>2sigma(I)]	R1 = 0.0549, wR2 = 0.1192	
R indices (all data)	R1 = 0.1010, wR2 = 0.1463	
Largest diff. peak and hole	1.304 and -0.443 e.$Å^{-3}$	

Table A-37. Atomic coordinates (x 10^4) and equivalent isotropic displacement parameters ($Å^2$x 10^3) for **4-1**. U(eq) is defined as one third of the trace of the orthogonalized U^{ij} tensor.

	x	y	z	U(eq)
Mn(1)	4489(1)	2331(1)	6109(1)	23(1)
Cl(1)	2809(1)	3571(1)	5748(1)	27(1)
F(1)	3650(2)	3201(2)	2287(2)	43(1)
F(2)	5270(3)	2279(3)	2475(2)	56(1)
F(3)	5373(3)	3985(3)	2458(2)	69(1)
F(4)	1370(2)	-232(2)	4948(2)	42(1)
F(5)	2357(2)	-1320(2)	6351(2)	39(1)
F(6)	3068(2)	-983(2)	4925(2)	42(1)
O(1)	4642(2)	2397(2)	4565(2)	25(1)
O(2)	3602(3)	1028(2)	5654(2)	29(1)
N(1)	5976(3)	3275(3)	6795(3)	24(1)
N(2)	4698(3)	2087(3)	7822(3)	24(1)
C(1)	6490(4)	3867(3)	6206(4)	25(1)
C(2)	6040(4)	3881(3)	4909(4)	29(1)
C(3)	5221(4)	3167(3)	4213(4)	25(1)
C(4)	4191(4)	1330(3)	8272(4)	24(1)
C(5)	3504(4)	477(3)	7547(4)	28(1)
C(6)	3274(4)	384(3)	6352(4)	25(1)
C(7)	6489(4)	3218(3)	8136(4)	27(1)
C(8)	5407(4)	2980(3)	8567(4)	27(1)
C(9)	7606(4)	4573(3)	6848(4)	30(1)
C(10)	4892(4)	3169(4)	2861(4)	34(1)
C(11)	4309(4)	1340(3)	9586(4)	28(1)
C(12)	2516(4)	-548(3)	5644(4)	30(1)

Table A-38. Bond lengths [Å] and angles [°] for **4-1**.

Mn(1)-O(1)	1.886(3)
Mn(1)-O(2)	1.901(3)
Mn(1)-N(2)	1.972(3)
Mn(1)-N(1)	1.991(3)
Mn(1)-Cl(1)	2.3808(12)
F(1)-C(10)	1.335(5)
F(2)-C(10)	1.333(5)
F(3)-C(10)	1.324(5)
F(4)-C(12)	1.335(5)
F(5)-C(12)	1.333(5)
F(6)-C(12)	1.331(5)
O(1)-C(3)	1.314(5)
O(2)-C(6)	1.296(5)
N(1)-C(1)	1.285(5)
N(1)-C(7)	1.485(5)
N(2)-C(4)	1.314(5)
N(2)-C(8)	1.481(5)
C(1)-C(2)	1.433(6)
C(1)-C(9)	1.516(5)
C(2)-C(3)	1.348(6)
C(2)-H(2)	0.9500
C(3)-C(10)	1.505(6)
C(4)-C(5)	1.424(6)
C(4)-C(11)	1.507(6)
C(5)-C(6)	1.346(6)
C(5)-H(5)	0.9500
C(6)-C(12)	1.521(6)
C(7)-C(8)	1.508(6)
C(7)-H(7A)	0.9900
C(7)-H(7B)	0.9900
C(8)-H(8A)	0.9900

C(8)-H(8B)	0.9900
C(9)-H(9A)	0.9800
C(9)-H(9B)	0.9800
C(9)-H(9C)	0.9800
C(11)-H(11A)	0.9800
C(11)-H(11B)	0.9800
C(11)-H(11C)	0.9800

O(1)-Mn(1)-O(2)	88.92(12)
O(1)-Mn(1)-N(2)	166.85(13)
O(2)-Mn(1)-N(2)	91.13(13)
O(1)-Mn(1)-N(1)	91.09(13)
O(2)-Mn(1)-N(1)	156.93(13)
N(2)-Mn(1)-N(1)	83.74(14)
O(1)-Mn(1)-Cl(1)	97.54(9)
O(2)-Mn(1)-Cl(1)	101.78(9)
N(2)-Mn(1)-Cl(1)	95.32(10)
N(1)-Mn(1)-Cl(1)	101.09(10)
C(3)-O(1)-Mn(1)	123.9(3)
C(6)-O(2)-Mn(1)	126.8(3)
C(1)-N(1)-C(7)	121.2(3)
C(1)-N(1)-Mn(1)	127.1(3)
C(7)-N(1)-Mn(1)	111.6(3)
C(4)-N(2)-C(8)	122.3(3)
C(4)-N(2)-Mn(1)	127.6(3)
C(8)-N(2)-Mn(1)	109.7(3)
N(1)-C(1)-C(2)	121.4(4)
N(1)-C(1)-C(9)	121.6(4)
C(2)-C(1)-C(9)	117.0(4)
C(3)-C(2)-C(1)	123.9(4)
C(3)-C(2)-H(2)	118.0
C(1)-C(2)-H(2)	118.0
O(1)-C(3)-C(2)	127.8(4)
O(1)-C(3)-C(10)	111.5(3)
C(2)-C(3)-C(10)	120.7(4)
N(2)-C(4)-C(5)	121.9(4)
N(2)-C(4)-C(11)	120.8(4)
C(5)-C(4)-C(11)	117.3(4)
C(6)-C(5)-C(4)	124.2(4)
C(6)-C(5)-H(5)	117.9
C(4)-C(5)-H(5)	117.9
O(2)-C(6)-C(5)	127.9(4)
O(2)-C(6)-C(12)	111.4(4)
C(5)-C(6)-C(12)	120.7(4)
N(1)-C(7)-C(8)	107.6(3)
N(1)-C(7)-H(7A)	110.2
C(8)-C(7)-H(7A)	110.2
N(1)-C(7)-H(7B)	110.2
C(8)-C(7)-H(7B)	110.2
H(7A)-C(7)-H(7B)	108.5
N(2)-C(8)-C(7)	106.7(3)
N(2)-C(8)-H(8A)	110.4
C(7)-C(8)-H(8A)	110.4
N(2)-C(8)-H(8B)	110.4
C(7)-C(8)-H(8B)	110.4
H(8A)-C(8)-H(8B)	108.6
C(1)-C(9)-H(9A)	109.5
C(1)-C(9)-H(9B)	109.5
H(9A)-C(9)-H(9B)	109.5
C(1)-C(9)-H(9C)	109.5
H(9A)-C(9)-H(9C)	109.5
H(9B)-C(9)-H(9C)	109.5
F(3)-C(10)-F(2)	108.1(4)
F(3)-C(10)-F(1)	106.6(4)
F(2)-C(10)-F(1)	105.0(4)
F(3)-C(10)-C(3)	113.4(4)

F(2)-C(10)-C(3)	111.5(4)
F(1)-C(10)-C(3)	111.6(4)
C(4)-C(11)-H(11A)	109.5
C(4)-C(11)-H(11B)	109.5
H(11A)-C(11)-H(11B)	109.5
C(4)-C(11)-H(11C)	109.5
H(11A)-C(11)-H(11C)	109.5
H(11B)-C(11)-H(11C)	109.5
F(6)-C(12)-F(5)	106.9(3)
F(6)-C(12)-F(4)	107.6(4)
F(5)-C(12)-F(4)	106.8(3)
F(6)-C(12)-C(6)	111.5(3)
F(5)-C(12)-C(6)	113.1(3)
F(4)-C(12)-C(6)	110.6(3)

Symmetry transformations used to generate equivalent atoms:

Table A-39. Anisotropic displacement parameters ($Å^2 x\ 10^3$) for **4-1**. The anisotropic displacement factor exponent takes the form: $-2\pi^2[\ h^2\ a^{*2}U^{11} + ... + 2\ h\ k\ a^*\ b^*\ U^{12}\ ]$

	U^{11}	U^{22}	U^{33}	U^{23}	U^{13}	U^{12}
Mn(1)	23(1)	24(1)	18(1)	1(1)	3(1)	-2(1)
Cl(1)	26(1)	28(1)	25(1)	1(1)	5(1)	2(1)
F(1)	34(2)	65(2)	24(2)	8(1)	0(1)	5(1)
F(2)	61(2)	80(2)	26(2)	-8(2)	12(1)	25(2)
F(3)	84(2)	90(2)	27(2)	9(2)	12(2)	-46(2)
F(4)	32(2)	38(2)	42(2)	0(1)	-6(1)	-2(1)
F(5)	44(2)	28(1)	37(2)	4(1)	3(1)	-13(1)
F(6)	45(2)	37(2)	44(2)	-14(1)	13(1)	-7(1)
O(1)	25(2)	28(2)	18(2)	-1(1)	5(1)	-2(1)
O(2)	36(2)	26(2)	19(2)	-1(1)	3(1)	-6(1)
N(1)	22(2)	26(2)	21(2)	-3(1)	1(2)	1(2)
N(2)	24(2)	28(2)	17(2)	-2(1)	3(1)	-2(2)
C(1)	23(2)	25(2)	24(2)	-3(2)	4(2)	5(2)
C(2)	30(2)	29(2)	29(2)	6(2)	11(2)	1(2)
C(3)	22(2)	28(2)	23(2)	3(2)	7(2)	6(2)
C(4)	20(2)	27(2)	25(2)	3(2)	6(2)	5(2)
C(5)	28(2)	28(2)	27(2)	7(2)	7(2)	1(2)
C(6)	21(2)	24(2)	27(2)	2(2)	4(2)	3(2)
C(7)	26(2)	33(2)	19(2)	-3(2)	3(2)	-6(2)
C(8)	29(2)	28(2)	20(2)	-2(2)	5(2)	-6(2)
C(9)	24(2)	31(2)	31(3)	1(2)	7(2)	-7(2)
C(10)	30(3)	41(3)	28(3)	5(2)	5(2)	-5(2)
C(11)	28(2)	33(2)	21(2)	3(2)	6(2)	3(2)
C(12)	26(2)	27(2)	30(3)	2(2)	2(2)	-3(2)

Table A-40. Hydrogen coordinates ($x\ 10^4$) and isotropic displacement parameters ($Å^2 x\ 10^3$) for **4-1**.

	x	y	z	U(eq)
H(2)	6336	4426	4518	35
H(5)	3187	-60	7932	34
H(7A)	6888	3901	8476	32
H(7B)	7132	2650	8400	32
H(8A)	5724	2781	9433	32
H(8B)	4858	3612	8464	32
H(9A)	7392	5041	7414	44
H(9B)	7816	5004	6251	44
H(9C)	8330	4131	7294	44

H(11A)	5201	1316	10093	43
H(11B)	3875	721	9759	43
H(11C)	3928	1991	9761	43

Table A- 41. Crystal data and structure refinement for **4-3**.

Identification code	newbhuv	
Empirical formula	C13 H12 F6 Mn N3 O3	
Formula weight	427.20	
Temperature	110(2) K	
Wavelength	1.54178 Å	
Crystal system	Monoclinic	
Space group	P21/c	
Unit cell dimensions	a = 7.8313(13) Å	α= 90°.
	b = 18.525(3) Å	β= 118.476(11)°.
	c = 12.565(2) Å	γ = 90°.
Volume	1602.3(5) $Å^3$	
Z	4	
Density (calculated)	1.771 Mg/m^3	
Absorption coefficient	7.538 mm^{-1}	
F(000)	856	
Crystal size	0.50 x 0.30 x 0.02 mm^3	
Theta range for data collection	4.66 to 61.11°.	
Index ranges	-7<=h<=8, -20<=k<=20, -14<=l<=13	
Reflections collected	8904	
Independent reflections	2350 [R(int) = 0.1163]	
Completeness to theta = 61.11°	95.5 %	
Absorption correction	Semi-empirical from equivalents	
Max. and min. transmission	0.8639 and 0.1166	
Refinement method	Full-matrix least-squares on F^2	
Data / restraints / parameters	2350 / 0 / 237	
Goodness-of-fit on F^2	0.997	
Final R indices [I>2sigma(I)]	R1 = 0.0649, wR2 = 0.1631	
R indices (all data)	R1 = 0.0868, wR2 = 0.1811	
Largest diff. peak and hole	0.692 and -0.601 e.$Å^{-3}$	

Table A-42. Atomic coordinates (x 10^4) and equivalent isotropic displacement parameters ($Å^2$x 10^3) for **4-3**. U(eq) is defined as one third of the trace of the orthogonalized U^{ij} tensor.

	x	y	z	U(eq)
Mn(1)	4781(1)	2325(1)	692(1)	19(1)
F(1)	2119(4)	4497(2)	-798(3)	30(1)
F(2)	4193(4)	4833(2)	-1375(3)	31(1)
F(3)	2056(4)	4024(2)	-2389(3)	30(1)
F(4)	-688(5)	1322(2)	-1856(3)	47(1)
F(5)	-165(4)	245(2)	-1134(3)	32(1)
F(6)	-1124(5)	1070(2)	-340(3)	36(1)
O(1)	3630(5)	3137(2)	-346(3)	22(1)
O(2)	2318(5)	1854(2)	128(3)	22(1)
O(3)	4741(6)	3288(2)	3977(3)	28(1)
N(1)	7488(6)	2643(2)	1085(4)	21(1)
N(2)	6155(6)	1448(2)	1597(4)	20(1)
N(3)	4855(7)	2794(3)	2268(5)	28(1)
C(1)	7964(7)	3194(3)	663(5)	21(1)
C(2)	6537(8)	3717(3)	-84(5)	22(1)
C(3)	4604(8)	3659(3)	-487(5)	20(1)
C(4)	5499(8)	795(3)	1429(5)	24(1)
C(5)	3492(8)	642(3)	553(5)	25(1)

C(6)	2130(7)	1164(3)	25(5)	18(1)
C(7)	8985(8)	2119(3)	1884(5)	26(1)
C(8)	8131(8)	1662(3)	2502(5)	27(1)
C(9)	10042(8)	3319(4)	924(6)	32(2)
C(10)	3266(8)	4260(3)	-1267(5)	24(1)
C(11)	6745(9)	163(3)	2124(5)	29(1)
C(12)	44(8)	942(3)	-833(5)	23(1)
C(13)	4811(7)	3036(3)	3109(5)	22(1)

Table A-43. Bond lengths [Å] and angles [°] for **4-3**.

Mn(1)-O(1)	1.911(4)
Mn(1)-O(2)	1.919(4)
Mn(1)-N(2)	1.981(4)
Mn(1)-N(1)	2.022(5)
Mn(1)-N(3)	2.137(5)
Mn(1)-O(3)#1	2.424(4)
F(1)-C(10)	1.360(6)
F(2)-C(10)	1.328(6)
F(3)-C(10)	1.343(6)
F(4)-C(12)	1.332(6)
F(5)-C(12)	1.333(6)
F(6)-C(12)	1.348(7)
O(1)-C(3)	1.296(6)
O(2)-C(6)	1.286(6)
O(3)-C(13)	1.211(7)
O(3)-Mn(1)#2	2.424(4)
N(1)-C(1)	1.284(7)
N(1)-C(7)	1.485(7)
N(2)-C(4)	1.291(7)
N(2)-C(8)	1.472(7)
N(3)-C(13)	1.163(7)
C(1)-C(2)	1.439(8)
C(1)-C(9)	1.517(7)
C(2)-C(3)	1.352(7)
C(2)-H(2)	0.9500
C(3)-C(10)	1.523(8)
C(4)-C(5)	1.453(8)
C(4)-C(11)	1.509(7)
C(5)-C(6)	1.355(7)
C(5)-H(5)	0.9500
C(6)-C(12)	1.524(7)
C(7)-C(8)	1.503(8)
C(7)-H(7A)	0.9900
C(7)-H(7B)	0.9900
C(8)-H(8A)	0.9900
C(8)-H(8B)	0.9900
C(9)-H(9A)	0.9800
C(9)-H(9B)	0.9800
C(9)-H(9C)	0.9800
C(11)-H(11A)	0.9800
C(11)-H(11B)	0.9800
C(11)-H(11C)	0.9800
O(1)-Mn(1)-O(2)	92.40(15)
O(1)-Mn(1)-N(2)	170.81(17)
O(2)-Mn(1)-N(2)	90.80(17)
O(1)-Mn(1)-N(1)	92.07(17)
O(2)-Mn(1)-N(1)	167.19(17)
N(2)-Mn(1)-N(1)	83.07(18)
O(1)-Mn(1)-N(3)	96.23(17)
O(2)-Mn(1)-N(3)	96.09(18)
N(2)-Mn(1)-N(3)	91.99(18)
N(1)-Mn(1)-N(3)	95.36(19)
O(1)-Mn(1)-O(3)#1	87.69(15)

O(2)-Mn(1)-O(3)#1	82.72(15)
N(2)-Mn(1)-O(3)#1	84.17(16)
N(1)-Mn(1)-O(3)#1	85.46(16)
N(3)-Mn(1)-O(3)#1	175.95(16)
C(3)-O(1)-Mn(1)	124.3(3)
C(6)-O(2)-Mn(1)	122.4(3)
C(13)-O(3)-Mn(1)#2	129.2(4)
C(1)-N(1)-C(7)	120.6(5)
C(1)-N(1)-Mn(1)	127.4(4)
C(7)-N(1)-Mn(1)	111.9(4)
C(4)-N(2)-C(8)	124.6(5)
C(4)-N(2)-Mn(1)	127.6(4)
C(8)-N(2)-Mn(1)	107.8(3)
C(13)-N(3)-Mn(1)	176.8(5)
N(1)-C(1)-C(2)	121.1(5)
N(1)-C(1)-C(9)	121.6(5)
C(2)-C(1)-C(9)	117.3(5)
C(3)-C(2)-C(1)	124.9(5)
C(3)-C(2)-H(2)	117.5
C(1)-C(2)-H(2)	117.5
O(1)-C(3)-C(2)	129.5(5)
O(1)-C(3)-C(10)	111.4(4)
C(2)-C(3)-C(10)	119.1(5)
N(2)-C(4)-C(5)	120.6(5)
N(2)-C(4)-C(11)	122.4(5)
C(5)-C(4)-C(11)	117.0(5)
C(6)-C(5)-C(4)	123.1(5)
C(6)-C(5)-H(5)	118.4
C(4)-C(5)-H(5)	118.4
O(2)-C(6)-C(5)	129.3(5)
O(2)-C(6)-C(12)	111.9(4)
C(5)-C(6)-C(12)	118.8(5)
N(1)-C(7)-C(8)	108.4(5)
N(1)-C(7)-H(7A)	110.0
C(8)-C(7)-H(7A)	110.0
N(1)-C(7)-H(7B)	110.0
C(8)-C(7)-H(7B)	110.0
H(7A)-C(7)-H(7B)	108.4
N(2)-C(8)-C(7)	108.4(4)
N(2)-C(8)-H(8A)	110.0
C(7)-C(8)-H(8A)	110.0
N(2)-C(8)-H(8B)	110.0
C(7)-C(8)-H(8B)	110.0
H(8A)-C(8)-H(8B)	108.4
C(1)-C(9)-H(9A)	109.5
C(1)-C(9)-H(9B)	109.5
H(9A)-C(9)-H(9B)	109.5
C(1)-C(9)-H(9C)	109.5
H(9A)-C(9)-H(9C)	109.5
H(9B)-C(9)-H(9C)	109.5
F(2)-C(10)-F(3)	107.4(5)
F(2)-C(10)-F(1)	107.1(4)
F(3)-C(10)-F(1)	106.2(4)
F(2)-C(10)-C(3)	114.1(4)
F(3)-C(10)-C(3)	111.2(4)
F(1)-C(10)-C(3)	110.6(5)
C(4)-C(11)-H(11A)	109.5
C(4)-C(11)-H(11B)	109.5
H(11A)-C(11)-H(11B)	109.5
C(4)-C(11)-H(11C)	109.5
H(11A)-C(11)-H(11C)	109.5
H(11B)-C(11)-H(11C)	109.5
F(4)-C(12)-F(5)	107.5(5)
F(4)-C(12)-F(6)	106.0(5)
F(5)-C(12)-F(6)	106.4(4)
F(4)-C(12)-C(6)	111.3(4)

F(5)-C(12)-C(6)	114.0(4)
F(6)-C(12)-C(6)	111.1(5)
N(3)-C(13)-O(3)	179.2(6)

Symmetry transformations used to generate equivalent atoms:
#1 x,-y+1/2,z-1/2 #2 x,-y+1/2,z+1/2

Table A-44. Anisotropic displacement parameters ($Å^2 x\ 10^3$) for **4-3**. The anisotropic displacement factor exponent takes the form: $-2\pi^2[\ h^2\ a^{*2}U^{11} + ... + 2\ h\ k\ a^*\ b^*\ U^{12}\ ]$

	U^{11}	U^{22}	U^{33}	U^{23}	U^{13}	U^{12}
Mn(1)	14(1)	21(1)	19(1)	1(1)	4(1)	1(1)
F(1)	22(2)	24(2)	40(2)	1(2)	12(2)	4(1)
F(2)	22(2)	23(2)	35(2)	7(2)	5(2)	-1(1)
F(3)	25(2)	30(2)	22(2)	4(1)	0(2)	-2(1)
F(4)	39(2)	51(2)	26(2)	17(2)	-6(2)	-15(2)
F(5)	29(2)	29(2)	31(2)	-9(2)	10(2)	-8(1)
F(6)	24(2)	38(2)	46(2)	-10(2)	15(2)	-3(2)
O(1)	12(2)	25(2)	23(2)	-1(2)	4(2)	-1(2)
O(2)	12(2)	23(2)	21(2)	-1(2)	0(2)	0(2)
O(3)	33(2)	35(2)	19(2)	0(2)	14(2)	2(2)
N(1)	12(2)	24(3)	19(2)	-3(2)	0(2)	3(2)
N(2)	15(2)	27(3)	14(2)	1(2)	4(2)	5(2)
N(3)	26(3)	32(3)	25(3)	-5(2)	10(2)	-1(2)
C(1)	17(3)	25(3)	17(3)	-5(2)	4(2)	-5(2)
C(2)	18(3)	24(3)	20(3)	-2(2)	7(3)	-1(2)
C(3)	17(3)	19(3)	19(3)	-11(2)	6(3)	-4(2)
C(4)	22(3)	30(3)	19(3)	4(3)	9(3)	3(2)
C(5)	24(3)	29(3)	21(3)	-1(3)	10(3)	0(2)
C(6)	22(3)	22(3)	13(3)	3(2)	10(2)	1(2)
C(7)	15(3)	28(3)	26(3)	3(3)	2(3)	5(2)
C(8)	20(3)	33(3)	21(3)	3(3)	5(3)	7(2)
C(9)	17(3)	41(4)	36(3)	0(3)	11(3)	3(3)
C(10)	17(3)	19(3)	32(3)	1(2)	9(3)	-2(2)
C(11)	32(3)	25(3)	23(3)	6(3)	8(3)	6(3)
C(12)	23(3)	15(3)	24(3)	5(2)	5(3)	-2(2)
C(13)	20(3)	24(3)	19(3)	2(3)	7(3)	-1(2)

Table A-45. Hydrogen coordinates ($x\ 10^4$) and isotropic displacement parameters ($Å^2 x\ 10^3$) for **4-3**.

	x	y	z	U(eq)
H(2)	6986	4136	-312	26
H(5)	3117	154	341	30
H(7A)	10144	2379	2495	32
H(7B)	9386	1810	1399	32
H(8A)	8943	1228	2858	32
H(8B)	8085	1940	3161	32
H(9A)	10878	3376	1799	48
H(9B)	10106	3757	507	48
H(9C)	10485	2904	637	48
H(11A)	7949	164	2067	43
H(11B)	6038	-288	1782	43
H(11C)	7056	200	2976	43

Table A-46. Crystal data and structure refinement for **4-4**.

Identification code	second	
Empirical formula	C27 H26 Cl2 F12 Mn2 N6 O4 S2	
Formula weight	971.44	
Temperature	110(2) K	
Wavelength	0.71073 Å	
Crystal system	Monoclinic	
Space group	Cc	
Unit cell dimensions	a = 21.596(8) Å	α= 90°.
	b = 11.332(4) Å	β= 101.996(6)°.
	c = 15.887(6) Å	γ = 90°.
Volume	3803(2) $Å^3$	
Z	4	
Density (calculated)	1.697 Mg/m^3	
Absorption coefficient	1.015 mm^{-1}	
F(000)	1944	
Crystal size	0.30 x 0.20 x 0.15 mm^3	
Theta range for data collection	1.93 to 27.56°.	
Index ranges	-27<=h<=27, -14<=k<=14, -20<=l<=20	
Reflections collected	20584	
Independent reflections	8477 [R(int) = 0.0528]	
Completeness to theta = 27.56°	98.4 %	
Absorption correction	Semi-empirical from equivalents	
Max. and min. transmission	0.8626 and 0.7505	
Refinement method	Full-matrix least-squares on F^2	
Data / restraints / parameters	8477 / 2 / 500	
Goodness-of-fit on F^2	1.005	
Final R indices [I>2sigma(I)]	R1 = 0.0578, wR2 = 0.1507	
R indices (all data)	R1 = 0.0635, wR2 = 0.1592	
Absolute structure parameter	-0.025(17)	
Largest diff. peak and hole	1.832 and -0.505 e.$Å^{-3}$	

Table A-47. Atomic coordinates (x 10^4) and equivalent isotropic displacement parameters ($Å^2$x 10^3) for **4-4**. U(eq) is defined as one third of the trace of the orthogonalized U^{ij} tensor.

	x	y	z	U(eq)
Mn(1)	2959(1)	5751(1)	2055(1)	33(1)
Mn(2)	5321(1)	2446(1)	2266(1)	37(1)
S(1)	5988(1)	474(1)	3212(1)	45(1)
S(2)	4087(1)	6062(1)	1430(1)	40(1)
Cl(1)	529(2)	1542(2)	3653(1)	105(1)
Cl(2)	1133(2)	1964(4)	2242(2)	144(1)
F(1)	3181(2)	8453(3)	126(2)	63(1)
F(2)	2523(2)	7790(3)	-953(2)	64(1)
F(3)	2187(2)	8692(3)	45(3)	78(1)
F(4)	3727(2)	417(3)	2955(2)	69(1)
F(5)	3253(2)	677(3)	1653(3)	71(1)
F(6)	3695(2)	-984(3)	2037(3)	71(1)
F(7)	6489(2)	4122(3)	5248(2)	67(1)
F(8)	5484(2)	4371(3)	4896(2)	70(1)
F(9)	5856(2)	2627(3)	5126(2)	81(1)
F(10)	4059(4)	7497(3)	5028(3)	146(3)
F(11)	4290(2)	8310(4)	3911(4)	104(2)
F(12)	3363(2)	8490(3)	4157(2)	69(1)
O(1)	3282(2)	6877(3)	2927(2)	41(1)
O(2)	2670(1)	6945(3)	1209(2)	38(1)
O(3)	4582(1)	1583(3)	2370(2)	43(1)
O(4)	5425(1)	3116(3)	3394(2)	45(1)
N(1)	3342(2)	4401(3)	2792(2)	34(1)
N(2)	2682(2)	4481(3)	1189(2)	35(1)
N(3)	2054(2)	5594(4)	2480(3)	44(1)

N(4)	5400(2)	1548(3)	1221(2)	42(1)
N(5)	6101(2)	3203(3)	2090(3)	41(1)
N(6)	4751(2)	3923(4)	1684(3)	48(1)
C(1)	3722(2)	4459(4)	3543(3)	36(1)
C(2)	3870(3)	5558(4)	3990(3)	47(1)
C(3)	3638(2)	6633(4)	3667(3)	45(1)
C(4)	2549(2)	4601(4)	357(3)	41(1)
C(5)	2561(2)	5732(4)	-57(3)	44(1)
C(6)	2612(2)	6774(4)	384(3)	38(1)
C(7)	3222(2)	3253(4)	2341(3)	43(1)
C(8)	2637(2)	3361(4)	1640(3)	40(1)
C(9)	4035(2)	3375(4)	3991(3)	43(1)
C(10)	3839(4)	7747(5)	4194(4)	73(2)
C(11)	2397(3)	3528(5)	-224(3)	64(2)
C(12)	2620(2)	7937(5)	-111(3)	48(1)
C(13)	1615(2)	5532(4)	2781(3)	39(1)
C(14)	5105(2)	576(4)	927(3)	45(1)
C(15)	4594(2)	127(4)	1293(3)	46(1)
C(16)	4376(2)	653(3)	1932(3)	41(1)
C(17)	6545(2)	3708(3)	2660(3)	41(1)
C(18)	6493(2)	3800(4)	3546(3)	43(1)
C(19)	5956(2)	3520(4)	3838(3)	43(1)
C(20)	5932(2)	1960(5)	836(3)	49(1)
C(21)	6120(2)	3177(5)	1169(3)	50(1)
C(22)	5278(3)	-120(5)	220(4)	60(1)
C(23)	3767(3)	174(4)	2152(4)	53(1)
C(24)	7122(2)	4242(5)	2423(4)	53(1)
C(25)	5947(3)	3667(4)	4781(4)	53(1)
C(26)	4477(2)	4815(4)	1583(3)	37(1)
C(27)	521(4)	2384(6)	2733(5)	75(2)

Table A-48. Bond lengths [Å] and angles [°] for **4-4**.

Mn(1)-O(1)	1.907(3)
Mn(1)-O(2)	1.916(3)
Mn(1)-N(2)	1.995(4)
Mn(1)-N(1)	1.999(3)
Mn(1)-N(3)	2.202(4)
Mn(1)-S(2)	2.8367(15)
Mn(2)-O(3)	1.907(3)
Mn(2)-O(4)	1.916(3)
Mn(2)-N(5)	1.963(4)
Mn(2)-N(4)	1.984(4)
Mn(2)-N(6)	2.168(4)
Mn(2)-S(1)	2.9036(15)
S(1)-C(13)#1	1.640(5)
S(2)-C(26)	1.638(4)
Cl(1)-C(27)	1.743(8)
Cl(2)-C(27)	1.733(9)
F(1)-C(12)	1.327(6)
F(2)-C(12)	1.320(6)
F(3)-C(12)	1.329(5)
F(4)-C(23)	1.326(7)
F(5)-C(23)	1.349(7)
F(6)-C(23)	1.331(6)
F(7)-C(25)	1.352(6)
F(8)-C(25)	1.321(7)
F(9)-C(25)	1.331(6)
F(10)-C(10)	1.342(8)
F(11)-C(10)	1.319(9)
F(12)-C(10)	1.320(8)
O(1)-C(3)	1.294(5)
O(2)-C(6)	1.306(5)
O(3)-C(16)	1.290(5)
O(4)-C(19)	1.299(6)

N(1)-C(1)	1.302(6)
N(1)-C(7)	1.482(6)
N(2)-C(4)	1.301(6)
N(2)-C(8)	1.470(6)
N(3)-C(13)	1.150(6)
N(4)-C(14)	1.310(6)
N(4)-C(20)	1.484(6)
N(5)-C(17)	1.307(6)
N(5)-C(21)	1.473(6)
N(6)-C(26)	1.166(6)
C(1)-C(2)	1.436(6)
C(1)-C(9)	1.507(6)
C(2)-C(3)	1.374(7)
C(2)-H(2)	0.9500
C(3)-C(10)	1.527(7)
C(4)-C(5)	1.444(7)
C(4)-C(11)	1.520(7)
C(5)-C(6)	1.365(7)
C(5)-H(5)	0.9500
C(6)-C(12)	1.537(6)
C(7)-C(8)	1.505(6)
C(7)-H(7A)	0.9900
C(7)-H(7B)	0.9900
C(8)-H(8A)	0.9900
C(8)-H(8B)	0.9900
C(9)-H(9A)	0.9800
C(9)-H(9B)	0.9800
C(9)-H(9C)	0.9800
C(11)-H(11A)	0.9800
C(11)-H(11B)	0.9800
C(11)-H(11C)	0.9800
C(13)-S(1)#2	1.640(5)
C(14)-C(15)	1.442(7)
C(14)-C(22)	1.483(7)
C(15)-C(16)	1.344(7)
C(15)-H(15)	0.9500
C(16)-C(23)	1.529(7)
C(17)-C(18)	1.439(7)
C(17)-C(24)	1.502(6)
C(18)-C(19)	1.372(6)
C(18)-H(18)	0.9500
C(19)-C(25)	1.511(7)
C(20)-C(21)	1.502(8)
C(20)-H(20A)	0.9900
C(20)-H(20B)	0.9900
C(21)-H(21A)	0.9900
C(21)-H(21B)	0.9900
C(22)-H(22A)	0.9800
C(22)-H(22B)	0.9800
C(22)-H(22C)	0.9800
C(24)-H(24A)	0.9800
C(24)-H(24B)	0.9800
C(24)-H(24C)	0.9800
C(27)-H(27A)	0.9900
C(27)-H(27B)	0.9900

O(1)-Mn(1)-O(2)	93.09(13)
O(1)-Mn(1)-N(2)	174.97(14)
O(2)-Mn(1)-N(2)	91.11(15)
O(1)-Mn(1)-N(1)	92.38(14)
O(2)-Mn(1)-N(1)	170.22(14)
N(2)-Mn(1)-N(1)	83.08(14)
O(1)-Mn(1)-N(3)	92.62(15)
O(2)-Mn(1)-N(3)	95.30(14)
N(2)-Mn(1)-N(3)	89.74(15)
N(1)-Mn(1)-N(3)	92.54(14)

O(1)-Mn(1)-S(2)	87.67(11)
O(2)-Mn(1)-S(2)	81.07(9)
N(2)-Mn(1)-S(2)	90.25(11)
N(1)-Mn(1)-S(2)	91.06(10)
N(3)-Mn(1)-S(2)	176.37(11)
O(3)-Mn(2)-O(4)	93.44(13)
O(3)-Mn(2)-N(5)	174.32(15)
O(4)-Mn(2)-N(5)	91.30(15)
O(3)-Mn(2)-N(4)	91.65(15)
O(4)-Mn(2)-N(4)	166.37(15)
N(5)-Mn(2)-N(4)	83.04(16)
O(3)-Mn(2)-N(6)	91.24(15)
O(4)-Mn(2)-N(6)	92.21(16)
N(5)-Mn(2)-N(6)	91.70(15)
N(4)-Mn(2)-N(6)	100.31(17)
O(3)-Mn(2)-S(1)	83.98(11)
O(4)-Mn(2)-S(1)	82.66(11)
N(5)-Mn(2)-S(1)	93.53(11)
N(4)-Mn(2)-S(1)	85.32(11)
N(6)-Mn(2)-S(1)	172.74(12)
C(13)#1-S(1)-Mn(2)	96.74(14)
C(26)-S(2)-Mn(1)	107.12(15)
C(3)-O(1)-Mn(1)	125.2(3)
C(6)-O(2)-Mn(1)	123.3(3)
C(16)-O(3)-Mn(2)	125.0(3)
C(19)-O(4)-Mn(2)	124.5(3)
C(1)-N(1)-C(7)	120.0(3)
C(1)-N(1)-Mn(1)	127.2(3)
C(7)-N(1)-Mn(1)	112.3(3)
C(4)-N(2)-C(8)	124.3(4)
C(4)-N(2)-Mn(1)	126.6(3)
C(8)-N(2)-Mn(1)	109.1(3)
C(13)-N(3)-Mn(1)	173.3(4)
C(14)-N(4)-C(20)	118.6(4)
C(14)-N(4)-Mn(2)	127.5(3)
C(20)-N(4)-Mn(2)	113.1(3)
C(17)-N(5)-C(21)	122.0(4)
C(17)-N(5)-Mn(2)	128.4(3)
C(21)-N(5)-Mn(2)	109.6(3)
C(26)-N(6)-Mn(2)	162.8(4)
N(1)-C(1)-C(2)	122.0(4)
N(1)-C(1)-C(9)	121.8(4)
C(2)-C(1)-C(9)	116.2(4)
C(3)-C(2)-C(1)	123.9(4)
C(3)-C(2)-H(2)	118.0
C(1)-C(2)-H(2)	118.0
O(1)-C(3)-C(2)	129.0(4)
O(1)-C(3)-C(10)	111.6(4)
C(2)-C(3)-C(10)	119.2(4)
N(2)-C(4)-C(5)	122.4(4)
N(2)-C(4)-C(11)	120.5(4)
C(5)-C(4)-C(11)	117.1(4)
C(6)-C(5)-C(4)	122.8(4)
C(6)-C(5)-H(5)	118.6
C(4)-C(5)-H(5)	118.6
O(2)-C(6)-C(5)	128.6(4)
O(2)-C(6)-C(12)	112.2(4)
C(5)-C(6)-C(12)	119.2(4)
N(1)-C(7)-C(8)	108.7(3)
N(1)-C(7)-H(7A)	109.9
C(8)-C(7)-H(7A)	109.9
N(1)-C(7)-H(7B)	109.9
C(8)-C(7)-H(7B)	109.9
H(7A)-C(7)-H(7B)	108.3
N(2)-C(8)-C(7)	107.5(3)
N(2)-C(8)-H(8A)	110.2

C(7)-C(8)-H(8A)	110.2
N(2)-C(8)-H(8B)	110.2
C(7)-C(8)-H(8B)	110.2
H(8A)-C(8)-H(8B)	108.5
C(1)-C(9)-H(9A)	109.5
C(1)-C(9)-H(9B)	109.5
H(9A)-C(9)-H(9B)	109.5
C(1)-C(9)-H(9C)	109.5
H(9A)-C(9)-H(9C)	109.5
H(9B)-C(9)-H(9C)	109.5
F(11)-C(10)-F(12)	107.5(5)
F(11)-C(10)-F(10)	107.7(6)
F(12)-C(10)-F(10)	106.9(7)
F(11)-C(10)-C(3)	111.0(6)
F(12)-C(10)-C(3)	111.9(5)
F(10)-C(10)-C(3)	111.6(5)
C(4)-C(11)-H(11A)	109.5
C(4)-C(11)-H(11B)	109.5
H(11A)-C(11)-H(11B)	109.5
C(4)-C(11)-H(11C)	109.5
H(11A)-C(11)-H(11C)	109.5
H(11B)-C(11)-H(11C)	109.5
F(2)-C(12)-F(1)	106.7(4)
F(2)-C(12)-F(3)	107.5(4)
F(1)-C(12)-F(3)	107.4(5)
F(2)-C(12)-C(6)	113.2(4)
F(1)-C(12)-C(6)	109.8(4)
F(3)-C(12)-C(6)	111.9(4)
N(3)-C(13)-S(1)#2	178.8(4)
N(4)-C(14)-C(15)	120.6(4)
N(4)-C(14)-C(22)	122.5(5)
C(15)-C(14)-C(22)	116.9(5)
C(16)-C(15)-C(14)	124.4(4)
C(16)-C(15)-H(15)	117.8
C(14)-C(15)-H(15)	117.8
O(3)-C(16)-C(15)	129.4(4)
O(3)-C(16)-C(23)	112.5(4)
C(15)-C(16)-C(23)	117.9(4)
N(5)-C(17)-C(18)	120.9(4)
N(5)-C(17)-C(24)	122.0(4)
C(18)-C(17)-C(24)	117.1(4)
C(19)-C(18)-C(17)	123.9(4)
C(19)-C(18)-H(18)	118.0
C(17)-C(18)-H(18)	118.0
O(4)-C(19)-C(18)	127.7(4)
O(4)-C(19)-C(25)	112.6(4)
C(18)-C(19)-C(25)	119.7(4)
N(4)-C(20)-C(21)	108.7(4)
N(4)-C(20)-H(20A)	110.0
C(21)-C(20)-H(20A)	110.0
N(4)-C(20)-H(20B)	110.0
C(21)-C(20)-H(20B)	110.0
H(20A)-C(20)-H(20B)	108.3
N(5)-C(21)-C(20)	107.9(4)
N(5)-C(21)-H(21A)	110.1
C(20)-C(21)-H(21A)	110.1
N(5)-C(21)-H(21B)	110.1
C(20)-C(21)-H(21B)	110.1
H(21A)-C(21)-H(21B)	108.4
C(14)-C(22)-H(22A)	109.5
C(14)-C(22)-H(22B)	109.5
H(22A)-C(22)-H(22B)	109.5
C(14)-C(22)-H(22C)	109.5
H(22A)-C(22)-H(22C)	109.5
H(22B)-C(22)-H(22C)	109.5
F(4)-C(23)-F(6)	107.9(4)

F(4)-C(23)-F(5)	105.5(4)
F(6)-C(23)-F(5)	106.1(5)
F(4)-C(23)-C(16)	112.2(4)
F(6)-C(23)-C(16)	113.6(4)
F(5)-C(23)-C(16)	111.0(4)
C(17)-C(24)-H(24A)	109.5
C(17)-C(24)-H(24B)	109.5
H(24A)-C(24)-H(24B)	109.5
C(17)-C(24)-H(24C)	109.5
H(24A)-C(24)-H(24C)	109.5
H(24B)-C(24)-H(24C)	109.5
F(8)-C(25)-F(9)	107.2(5)
F(8)-C(25)-F(7)	106.8(4)
F(9)-C(25)-F(7)	107.2(5)
F(8)-C(25)-C(19)	111.7(5)
F(9)-C(25)-C(19)	110.2(4)
F(7)-C(25)-C(19)	113.4(4)
N(6)-C(26)-S(2)	179.2(5)
Cl(2)-C(27)-Cl(1)	110.6(4)
Cl(2)-C(27)-H(27A)	109.5
Cl(1)-C(27)-H(27A)	109.5
Cl(2)-C(27)-H(27B)	109.5
Cl(1)-C(27)-H(27B)	109.5
H(27A)-C(27)-H(27B)	108.1

Symmetry transformations used to generate equivalent atoms:
#1 x+1/2,y-1/2,z #2 x-1/2,y+1/2,z

Table A-49. Anisotropic displacement parameters ($Å^2 x\ 10^3$) for **4-4**. The anisotropic displacement factor exponent takes the form: $-2\pi^2[\ h^2\ a^{*2}U^{11} + ... + 2\ h\ k\ a^*\ b^*\ U^{12}\ ]$

	U^{11}	U^{22}	U^{33}	U^{23}	U^{13}	U^{12}
Mn(1)	37(1)	32(1)	31(1)	1(1)	7(1)	4(1)
Mn(2)	35(1)	33(1)	47(1)	-2(1)	18(1)	1(1)
S(1)	45(1)	44(1)	53(1)	7(1)	22(1)	3(1)
S(2)	37(1)	35(1)	50(1)	6(1)	11(1)	5(1)
Cl(1)	159(2)	89(1)	79(1)	7(1)	52(1)	30(1)
Cl(2)	180(3)	154(3)	128(2)	-16(2)	100(2)	-20(2)
F(1)	72(2)	47(2)	70(2)	11(1)	19(2)	-8(1)
F(2)	75(2)	75(2)	44(2)	20(1)	18(1)	4(2)
F(3)	95(3)	73(2)	83(2)	40(2)	55(2)	51(2)
F(4)	87(2)	44(2)	89(2)	-12(2)	48(2)	-19(2)
F(5)	39(2)	60(2)	114(3)	-3(2)	15(2)	-6(1)
F(6)	83(2)	36(2)	98(3)	-10(2)	31(2)	-17(2)
F(7)	72(2)	68(2)	62(2)	-20(2)	14(2)	-19(2)
F(8)	75(2)	75(2)	68(2)	-30(2)	32(2)	-8(2)
F(9)	134(4)	56(2)	59(2)	-8(1)	36(2)	-35(2)
F(10)	264(9)	55(2)	71(3)	-12(2)	-79(4)	9(3)
F(11)	73(3)	55(2)	167(5)	-16(2)	-11(3)	-14(2)
F(12)	108(3)	40(2)	56(2)	-13(1)	12(2)	4(2)
O(1)	50(2)	34(1)	38(2)	-4(1)	6(1)	2(1)
O(2)	44(2)	37(2)	33(1)	6(1)	11(1)	11(1)
O(3)	38(2)	38(2)	57(2)	-10(1)	19(1)	-3(1)
O(4)	40(2)	44(2)	57(2)	-11(1)	23(1)	-6(1)
N(1)	32(2)	33(2)	40(2)	4(1)	10(1)	3(1)
N(2)	32(2)	38(2)	35(2)	-2(1)	7(1)	1(1)
N(3)	43(2)	52(2)	41(2)	4(2)	14(2)	11(2)
N(4)	45(2)	42(2)	40(2)	5(2)	14(2)	9(2)
N(5)	44(2)	33(2)	51(2)	7(1)	25(2)	6(1)
N(6)	40(2)	41(2)	66(2)	0(2)	16(2)	5(2)
C(1)	40(2)	36(2)	35(2)	5(2)	14(2)	4(2)
C(2)	55(3)	39(2)	41(2)	2(2)	-4(2)	-1(2)
C(3)	48(2)	45(2)	39(2)	-1(2)	3(2)	1(2)

C(4)	37(2)	45(2)	38(2)	-1(2)	5(2)	0(2)
C(5)	41(2)	53(3)	36(2)	0(2)	5(2)	1(2)
C(6)	31(2)	45(2)	37(2)	5(2)	7(2)	7(2)
C(7)	52(2)	31(2)	46(2)	5(2)	14(2)	4(2)
C(8)	43(2)	32(2)	43(2)	-1(2)	8(2)	-3(2)
C(9)	42(2)	42(2)	44(2)	10(2)	6(2)	5(2)
C(10)	100(5)	42(3)	58(3)	-3(2)	-27(3)	-5(3)
C(11)	100(4)	57(3)	32(2)	-10(2)	7(2)	-7(3)
C(12)	51(3)	51(3)	46(2)	14(2)	21(2)	19(2)
C(13)	41(2)	33(2)	41(2)	3(2)	7(2)	10(2)
C(14)	50(2)	40(2)	44(2)	-2(2)	9(2)	10(2)
C(15)	51(2)	32(2)	53(2)	-6(2)	9(2)	4(2)
C(16)	41(2)	26(2)	56(3)	5(2)	11(2)	3(2)
C(17)	36(2)	28(2)	64(3)	7(2)	23(2)	1(2)
C(18)	44(2)	30(2)	58(3)	1(2)	17(2)	-4(2)
C(19)	46(2)	31(2)	55(3)	-6(2)	15(2)	-2(2)
C(20)	53(3)	53(3)	45(2)	3(2)	18(2)	6(2)
C(21)	44(2)	56(3)	53(3)	15(2)	19(2)	8(2)
C(22)	73(3)	55(3)	57(3)	-13(2)	24(3)	12(3)
C(23)	57(3)	32(2)	77(3)	-7(2)	29(2)	-12(2)
C(24)	36(2)	50(3)	77(3)	10(2)	21(2)	-3(2)
C(25)	66(3)	39(2)	60(3)	-10(2)	24(2)	-9(2)
C(26)	39(2)	33(2)	41(2)	-4(2)	12(2)	-2(2)
C(27)	80(5)	62(4)	71(4)	0(3)	-16(3)	-16(3)

Table A-50. Hydrogen coordinates (x 10^4) and isotropic displacement parameters ($Å^2$x 10^3) for **4-4**.

	x	y	z	U(eq)
H(2)	4144	5542	4541	57
H(5)	2533	5753	-662	52
H(7A)	3161	2630	2753	51
H(7B)	3589	3033	2090	51
H(8A)	2611	2691	1235	47
H(8B)	2254	3357	1891	47
H(9A)	3709	2820	4091	64
H(9B)	4304	3601	4543	64
H(9C)	4295	2999	3629	64
H(11A)	2683	2880	7	96
H(11B)	2453	3727	-804	96
H(11C)	1958	3286	-248	96
H(15)	4399	-590	1068	55
H(18)	6851	4071	3953	51
H(20A)	5799	1976	201	59
H(20B)	6296	1415	993	59
H(21A)	6553	3363	1089	60
H(21B)	5824	3769	851	60
H(22A)	5295	403	-267	90
H(22B)	4960	-736	36	90
H(22C)	5693	-485	423	90
H(24A)	7377	3617	2234	80
H(24B)	7375	4645	2925	80
H(24C)	6992	4811	1955	80
H(27A)	111	2280	2325	91
H(27B)	567	3230	2890	91

Table A-51. Crystal data and structure refinement for **[(acacen)MnO]$_2$**.

Identification code	joestry	
Empirical formula	C30 H34 Cl0 F12 Mn2 N4 O7	
Formula weight	900.49	
Temperature	110(2) K	
Wavelength	0.71073 Å	
Crystal system	Monoclinic	
Space group	P2(1)/n	
Unit cell dimensions	a = 9.8052(12) Å	α= 90°.
	b = 15.8879(19) Å	β= 107.354(2)°.
	c = 12.0655(15) Å	γ = 90°.
Volume	1794.1(4) Å^3	
Z	2	
Density (calculated)	1.667 Mg/m^3	
Absorption coefficient	0.817 mm^{-1}	
F(000)	912	
Crystal size	0.29 x 0.20 x 0.18 mm^3	
Theta range for data collection	2.18 to 25.00°.	
Index ranges	-11<=h<=11, -18<=k<=18, -14<=l<=14	
Reflections collected	12577	
Independent reflections	3023 [R(int) = 0.0382]	
Completeness to theta = 25.00°	95.5 %	
Absorption correction	Semi-empirical from equivalents	
Max. and min. transmission	0.8669 and 0.7975	
Refinement method	Full-matrix least-squares on F^2	
Data / restraints / parameters	3023 / 0 / 255	
Goodness-of-fit on F^2	1.001	
Final R indices [I>2sigma(I)]	R1 = 0.0535, wR2 = 0.1292	
R indices (all data)	R1 = 0.0615, wR2 = 0.1435	
Largest diff. peak and hole	1.653 and -0.358 e.Å^{-3}	

Table A-52. Atomic coordinates (x 10^4) and equivalent isotropic displacement parameters (Å^{2}x 10^3) for **[(acacen)MnO]$_2$**. U(eq) is defined as one third of the trace of the orthogonalized U^{ij} tensor.

	x	y	z	U(eq)
Mn(1)	8630(1)	264(1)	9845(1)	24(1)
F(1)	7679(2)	-2318(1)	11347(2)	55(1)
F(2)	6431(3)	-2274(1)	9563(2)	53(1)
F(3)	5435(2)	-2070(1)	10896(2)	49(1)
F(4)	6523(2)	922(1)	5508(2)	40(1)
F(5)	4851(2)	774(1)	6306(2)	44(1)
F(6)	6225(2)	-267(1)	6248(2)	41(1)
O(1)	7887(2)	-834(1)	10032(2)	27(1)
O(2)	7008(2)	385(1)	8423(2)	26(1)
O(3)	10262(2)	117(1)	11021(2)	25(1)
O(1H)	-850(7)	854(4)	3844(5)	63(2)
N(1)	7653(3)	787(1)	10952(2)	27(1)
N(2)	9035(3)	1473(1)	9685(2)	27(1)
C(1)	6703(3)	437(2)	11352(2)	29(1)
C(2)	6315(3)	-430(2)	11141(3)	31(1)
C(3)	6956(3)	-974(2)	10567(2)	27(1)
C(4)	8771(3)	1889(2)	8727(2)	29(1)
C(5)	8070(3)	1500(2)	7638(2)	30(1)
C(6)	7198(3)	827(2)	7576(2)	28(1)
C(7)	8094(3)	1668(2)	11276(3)	31(1)
C(8)	9377(3)	1865(2)	10837(2)	29(1)
C(9)	5972(3)	904(2)	12098(3)	35(1)
C(10)	6614(3)	-1907(2)	10594(3)	31(1)
C(11)	9082(4)	2820(2)	8705(3)	38(1)
C(12)	6204(3)	567(2)	6400(3)	31(1)
C(1H)	-114(7)	43(5)	3793(5)	95(2)

C(2H)	438(13)	710(4)	4526(10)	146(4)
C(3H)	790(7)	654(4)	5811(7)	111(3)

Table A-53. Bond lengths [Å] and angles [°] for **[(acacen)MnO]$_2$**.

Mn(1)-O(3)	1.8103(19)
Mn(1)-O(3)#1	1.821(2)
Mn(1)-O(1)	1.9301(19)
Mn(1)-O(2)	1.970(2)
Mn(1)-N(2)	1.982(2)
Mn(1)-N(1)	2.038(2)
Mn(1)-Mn(1)#1	2.7326(8)
F(1)-C(10)	1.332(4)
F(2)-C(10)	1.337(4)
F(3)-C(10)	1.337(4)
F(4)-C(12)	1.332(4)
F(5)-C(12)	1.339(4)
F(6)-C(12)	1.339(4)
O(1)-C(3)	1.285(4)
O(2)-C(6)	1.299(4)
O(3)-Mn(1)#1	1.821(2)
O(1H)-C(2H)	1.305(13)
O(1H)-C(1H)	1.487(10)
O(1H)-H(1H)	1.2497
O(1H)-H(2HA)	0.9011
N(1)-C(1)	1.297(4)
N(1)-C(7)	1.483(4)
N(2)-C(4)	1.289(4)
N(2)-C(8)	1.467(4)
C(1)-C(2)	1.431(4)
C(1)-C(9)	1.504(4)
C(2)-C(3)	1.372(4)
C(2)-H(2)	0.9500
C(3)-C(10)	1.523(4)
C(4)-C(5)	1.429(4)
C(4)-C(11)	1.513(4)
C(5)-C(6)	1.358(4)
C(5)-H(5)	0.9500
C(6)-C(12)	1.519(4)
C(7)-C(8)	1.535(4)
C(7)-H(7A)	0.9900
C(7)-H(7B)	0.9900
C(8)-H(8A)	0.9900
C(8)-H(8B)	0.9900
C(9)-H(9A)	0.9800
C(9)-H(9B)	0.9800
C(9)-H(9C)	0.9800
C(11)-H(11A)	0.9800
C(11)-H(11B)	0.9800
C(11)-H(11C)	0.9800
C(1H)-C(2H)	1.383(12)
C(1H)-C(3H)#2	1.443(10)
C(1H)-H(1)	0.9601
C(1H)-H(1H)	0.9600
C(2H)-C(3H)	1.487(12)
C(2H)-H(2HA)	0.9600
C(2H)-H(2HB)	0.9600
C(3H)-C(1H)#2	1.443(10)
C(3H)-H(3HA)	0.9600
C(3H)-H(3HB)	0.9601
O(3)-Mn(1)-O(3)#1	82.38(9)
O(3)-Mn(1)-O(1)	93.87(8)
O(3)#1-Mn(1)-O(1)	94.40(9)
O(3)-Mn(1)-O(2)	172.21(9)

O(3)#1-Mn(1)-O(2)	89.87(8)
O(1)-Mn(1)-O(2)	87.43(8)
O(3)-Mn(1)-N(2)	92.61(9)
O(3)#1-Mn(1)-N(2)	95.48(10)
O(1)-Mn(1)-N(2)	168.82(9)
O(2)-Mn(1)-N(2)	87.38(9)
O(3)-Mn(1)-N(1)	90.99(9)
O(3)#1-Mn(1)-N(1)	171.46(9)
O(1)-Mn(1)-N(1)	91.40(9)
O(2)-Mn(1)-N(1)	96.66(9)
N(2)-Mn(1)-N(1)	79.39(10)
O(3)-Mn(1)-Mn(1)#1	41.33(6)
O(3)#1-Mn(1)-Mn(1)#1	41.04(6)
O(1)-Mn(1)-Mn(1)#1	95.49(6)
O(2)-Mn(1)-Mn(1)#1	130.91(6)
N(2)-Mn(1)-Mn(1)#1	95.38(7)
N(1)-Mn(1)-Mn(1)#1	132.10(7)
C(3)-O(1)-Mn(1)	124.35(18)
C(6)-O(2)-Mn(1)	118.02(18)
Mn(1)-O(3)-Mn(1)#1	97.63(9)
C(2H)-O(1H)-C(1H)	58.9(5)
C(2H)-O(1H)-H(1H)	94.9
C(1H)-O(1H)-H(1H)	39.9
C(2H)-O(1H)-H(2HA)	47.3
C(1H)-O(1H)-H(2HA)	104.2
H(1H)-O(1H)-H(2HA)	129.9
C(1)-N(1)-C(7)	119.5(3)
C(1)-N(1)-Mn(1)	126.9(2)
C(7)-N(1)-Mn(1)	113.60(19)
C(4)-N(2)-C(8)	124.0(2)
C(4)-N(2)-Mn(1)	126.24(19)
C(8)-N(2)-Mn(1)	108.36(17)
N(1)-C(1)-C(2)	122.0(3)
N(1)-C(1)-C(9)	122.3(3)
C(2)-C(1)-C(9)	115.7(3)
C(3)-C(2)-C(1)	124.0(3)
C(3)-C(2)-H(2)	118.0
C(1)-C(2)-H(2)	118.0
O(1)-C(3)-C(2)	130.3(3)
O(1)-C(3)-C(10)	111.9(2)
C(2)-C(3)-C(10)	117.8(3)
N(2)-C(4)-C(5)	121.1(3)
N(2)-C(4)-C(11)	122.0(3)
C(5)-C(4)-C(11)	116.8(3)
C(6)-C(5)-C(4)	120.9(3)
C(6)-C(5)-H(5)	119.5
C(4)-C(5)-H(5)	119.5
O(2)-C(6)-C(5)	128.2(3)
O(2)-C(6)-C(12)	112.7(2)
C(5)-C(6)-C(12)	118.9(3)
N(1)-C(7)-C(8)	107.8(2)
N(1)-C(7)-H(7A)	110.1
C(8)-C(7)-H(7A)	110.1
N(1)-C(7)-H(7B)	110.1
C(8)-C(7)-H(7B)	110.1
H(7A)-C(7)-H(7B)	108.5
N(2)-C(8)-C(7)	105.1(2)
N(2)-C(8)-H(8A)	110.7
C(7)-C(8)-H(8A)	110.7
N(2)-C(8)-H(8B)	110.7
C(7)-C(8)-H(8B)	110.7
H(8A)-C(8)-H(8B)	108.8
C(1)-C(9)-H(9A)	109.5
C(1)-C(9)-H(9B)	109.5
H(9A)-C(9)-H(9B)	109.5
C(1)-C(9)-H(9C)	109.5

H(9A)-C(9)-H(9C)	109.5
H(9B)-C(9)-H(9C)	109.5
F(1)-C(10)-F(2)	106.4(3)
F(1)-C(10)-F(3)	106.6(3)
F(2)-C(10)-F(3)	106.4(2)
F(1)-C(10)-C(3)	111.0(2)
F(2)-C(10)-C(3)	112.0(2)
F(3)-C(10)-C(3)	114.1(2)
C(4)-C(11)-H(11A)	109.5
C(4)-C(11)-H(11B)	109.5
H(11A)-C(11)-H(11B)	109.5
C(4)-C(11)-H(11C)	109.5
H(11A)-C(11)-H(11C)	109.5
H(11B)-C(11)-H(11C)	109.5
F(4)-C(12)-F(6)	106.9(2)
F(4)-C(12)-F(5)	107.0(2)
F(6)-C(12)-F(5)	106.7(2)
F(4)-C(12)-C(6)	113.6(2)
F(6)-C(12)-C(6)	111.4(2)
F(5)-C(12)-C(6)	110.9(2)
C(2H)-C(1H)-C(3H)#2	120.5(6)
C(2H)-C(1H)-O(1H)	54.0(6)
C(3H)#2-C(1H)-O(1H)	112.0(6)
C(2H)-C(1H)-H(1)	109.5
C(3H)#2-C(1H)-H(1)	107.0
O(1H)-C(1H)-H(1)	140.5
C(2H)-C(1H)-H(1H)	105.5
C(3H)#2-C(1H)-H(1H)	107.1
O(1H)-C(1H)-H(1H)	56.6
H(1)-C(1H)-H(1H)	106.5
O(1H)-C(2H)-C(1H)	67.1(8)
O(1H)-C(2H)-C(3H)	123.2(8)
C(1H)-C(2H)-C(3H)	123.1(6)
O(1H)-C(2H)-H(2HA)	43.7
C(1H)-C(2H)-H(2HA)	108.6
C(3H)-C(2H)-H(2HA)	109.3
O(1H)-C(2H)-H(2HB)	129.5
C(1H)-C(2H)-H(2HB)	104.1
C(3H)-C(2H)-H(2HB)	103.6
H(2HA)-C(2H)-H(2HB)	106.8
C(1H)#2-C(3H)-C(2H)	113.8(6)
C(1H)#2-C(3H)-H(3HA)	107.9
C(2H)-C(3H)-H(3HA)	106.8
C(1H)#2-C(3H)-H(3HB)	108.2
C(2H)-C(3H)-H(3HB)	112.2
H(3HA)-C(3H)-H(3HB)	107.6

Symmetry transformations used to generate equivalent atoms:
#1 -x+2,-y,-z+2 #2 -x,-y,-z+1

Table A-54. Anisotropic displacement parameters ($Å^2 x\ 10^3$) for **[(acacen)MnO]$_2$**. The anisotropic displacement factor exponent takes the form: $-2\pi^2[\ h^2\ a^{*2}U^{11} + ...\ + 2\ h\ k\ a^*\ b^*\ U^{12}\ ]$

	U^{11}	U^{22}	U^{33}	U^{23}	U^{13}	U^{12}
Mn(1)	24(1)	24(1)	23(1)	0(1)	7(1)	-1(1)
F(1)	49(1)	37(1)	73(1)	22(1)	10(1)	2(1)
F(2)	87(2)	31(1)	48(1)	-11(1)	30(1)	-13(1)
F(3)	48(1)	37(1)	73(1)	-4(1)	34(1)	-13(1)
F(4)	49(1)	43(1)	27(1)	5(1)	8(1)	-4(1)
F(5)	31(1)	59(1)	36(1)	0(1)	0(1)	2(1)
F(6)	58(1)	29(1)	31(1)	-3(1)	6(1)	-4(1)
O(1)	31(1)	24(1)	26(1)	-1(1)	9(1)	-1(1)
O(2)	24(1)	28(1)	25(1)	2(1)	7(1)	-1(1)

O(3)	25(1)	28(1)	23(1)	0(1)	8(1)	-1(1)
O(1H)	52(3)	72(4)	60(3)	16(3)	7(3)	18(3)
N(1)	25(1)	28(1)	26(1)	-2(1)	6(1)	3(1)
N(2)	25(1)	25(1)	31(1)	-2(1)	9(1)	-3(1)
C(1)	24(1)	35(2)	26(1)	2(1)	7(1)	3(1)
C(2)	26(2)	39(2)	28(2)	1(1)	9(1)	-2(1)
C(3)	24(1)	30(1)	25(1)	3(1)	6(1)	-1(1)
C(4)	26(1)	28(1)	34(2)	2(1)	11(1)	-4(1)
C(5)	34(2)	30(2)	27(1)	2(1)	11(1)	0(1)
C(6)	31(2)	28(1)	24(1)	-1(1)	7(1)	3(1)
C(7)	34(2)	29(1)	30(2)	-5(1)	9(1)	-2(1)
C(8)	34(2)	27(1)	27(1)	-5(1)	9(1)	-6(1)
C(9)	31(2)	39(2)	39(2)	-4(1)	15(1)	-2(1)
C(10)	29(2)	31(2)	38(2)	2(1)	16(1)	0(1)
C(11)	49(2)	27(1)	42(2)	2(1)	19(2)	-4(1)
C(12)	32(2)	29(2)	32(2)	0(1)	8(1)	-2(1)
C(1H)	82(4)	149(6)	60(3)	12(4)	29(3)	44(4)
C(2H)	214(12)	65(4)	201(11)	25(5)	124(10)	8(5)
C(3H)	92(4)	84(4)	111(5)	-10(4)	-39(4)	24(4)

Table A-55. Hydrogen coordinates (x 10^4) and isotropic displacement parameters ($Å^2$x 10^3) for **[(acacen)MnO]2**.

	x	y	z	U(eq)
H(2)	5567	-641	11414	37
H(5)	8217	1715	6948	36
H(7A)	8364	1736	12129	37
H(7B)	7296	2057	10918	37
H(8A)	9500	2481	10782	35
H(8B)	10266	1625	11364	35
H(9A)	6528	844	12916	53
H(9B)	5013	672	11978	53
H(9C)	5899	1502	11886	53
H(11A)	8384	3138	8975	57
H(11B)	9017	2991	7911	57
H(11C)	10046	2935	9217	57
H(1)	618	-189	3505	114
H(1H)	-815	284	3138	114
H(2HA)	-149	1196	4256	175
H(2HB)	1344	820	4402	175
H(3HA)	456	1165	6066	133
H(3HB)	1801	619	6183	133

Table A-56. Crystal data and structure refinement for **5-1**.

Identification code	ddmn1	
Empirical formula	C32 H46 Mn N5 O2	
Formula weight	587.68	
Temperature	90(2) K	
Wavelength	0.71073 Å	
Crystal system	Triclinic	
Space group	P-1	
Unit cell dimensions	a = 6.366(6) Å	α= 89.741(17)°.
	b = 14.059(6) Å	β= 89.633(12)°.
	c = 18.474(7) Å	γ = 78.682(12)°.
Volume	1621.3(19) $Å^3$	
Z	2	
Density (calculated)	1.204 Mg/m^3	
Absorption coefficient	0.442 mm^{-1}	
F(000)	628	
Crystal size	0.30 x 0.10 x 0.10 mm^3	
Theta range for data collection	1.84 to 25.00°.	
Index ranges	-7<=h<=7, -16<=k<=16, -21<=l<=21	
Reflections collected	13183	
Independent reflections	5320 [R(int) = 0.0969]	
Completeness to theta = 25.00°	92.9 %	
Absorption correction	Semi-empirical from equivalents	
Max. and min. transmission	0.9572 and 0.8789	
Refinement method	Full-matrix least-squares on F^2	
Data / restraints / parameters	5320 / 0 / 375	
Goodness-of-fit on F^2	1.000	
Final R indices [I>2sigma(I)]	R1 = 0.0695, wR2 = 0.1385	
R indices (all data)	R1 = 0.1036, wR2 = 0.1554	
Extinction coefficient	0.015(2)	
Largest diff. peak and hole	0.479 and -0.722 e.$Å^{-3}$	

Table A-57. Atomic coordinates (x 10^4) and equivalent isotropic displacement parameters ($Å^2$x 10^3) for **5-1**. U(eq) is defined as one third of the trace of the orthogonalized U^{ij} tensor.

	x	y	z	U(eq)
Mn(1)	-91(2)	4455(1)	1840(1)	29(1)
O(1)	983(6)	5452(3)	2264(2)	35(1)
O(2)	293(6)	3696(3)	2672(2)	33(1)
N(1)	-1581(8)	5374(3)	1117(3)	35(1)
N(2)	-1824(7)	3612(3)	1423(2)	28(1)
N(3)	2523(9)	3894(4)	1150(3)	48(1)
N(4)	2669(8)	3071(5)	927(3)	47(2)
N(5)	2858(11)	2317(5)	666(4)	74(2)
C(1)	-1136(10)	6201(4)	959(3)	35(2)
C(2)	430(10)	6639(4)	1310(3)	31(1)
C(3)	1413(9)	6258(4)	1967(3)	29(1)
C(4)	2874(9)	6745(4)	2300(3)	27(1)
C(5)	3273(9)	7588(4)	1966(3)	31(1)
C(6)	2355(10)	7975(4)	1307(3)	33(1)
C(7)	899(10)	7494(4)	1006(3)	35(2)
C(8)	-2179(9)	2802(4)	1688(3)	32(2)
C(9)	-1474(10)	2396(4)	2376(3)	33(2)
C(10)	-307(9)	2872(4)	2863(3)	32(1)
C(11)	215(9)	2456(4)	3551(3)	31(1)
C(12)	-331(10)	1567(4)	3696(3)	40(2)
C(13)	-1447(9)	1071(4)	3233(4)	37(1)
C(14)	-2032(11)	1499(5)	2585(3)	41(2)
C(15)	-3247(10)	5014(4)	712(3)	37(2)
C(16)	-2537(9)	3922(4)	688(3)	32(1)
C(17)	3960(9)	6353(4)	3010(3)	35(2)

C(18)	5435(12)	7001(5)	3287(4)	58(2)
C(19)	2268(11)	6310(5)	3606(3)	46(2)
C(20)	5321(10)	5337(4)	2888(3)	42(2)
C(21)	2896(10)	8912(4)	983(3)	35(2)
C(22)	5313(10)	8900(5)	1031(4)	48(2)
C(23)	2313(12)	9025(5)	182(4)	56(2)
C(24)	1615(12)	9779(5)	1405(4)	61(2)
C(25)	1375(10)	2967(4)	4108(3)	37(2)
C(26)	3596(12)	3079(5)	3809(4)	57(2)
C(27)	26(12)	3965(4)	4258(4)	50(2)
C(28)	1727(12)	2409(5)	4815(3)	52(2)
C(29)	-1962(13)	96(5)	3472(4)	50(2)
C(30)	158(16)	-633(6)	3640(4)	73(2)
C(31)	-3339(14)	216(5)	4172(4)	74(3)
C(32)	-3124(19)	-353(6)	2900(5)	95(3)

Table A-58. Bond lengths [Å] and angles [°] for **5-1**.

Mn(1)-O(1)	1.854(4)
Mn(1)-O(2)	1.858(4)
Mn(1)-N(2)	1.935(5)
Mn(1)-N(1)	1.968(5)
Mn(1)-N(3)	2.118(6)
O(1)-C(3)	1.332(7)
O(2)-C(10)	1.335(7)
N(1)-C(1)	1.281(7)
N(1)-C(15)	1.472(7)
N(2)-C(8)	1.297(7)
N(2)-C(16)	1.472(7)
N(3)-N(4)	1.215(8)
N(4)-N(5)	1.151(8)
C(1)-C(2)	1.431(8)
C(1)-H(1)	0.9500
C(2)-C(7)	1.407(8)
C(2)-C(3)	1.423(7)
C(3)-C(4)	1.405(8)
C(4)-C(5)	1.400(8)
C(4)-C(17)	1.534(8)
C(5)-C(6)	1.414(8)
C(5)-H(5)	0.9500
C(6)-C(7)	1.372(8)
C(6)-C(21)	1.543(8)
C(7)-H(7)	0.9500
C(8)-C(9)	1.429(8)
C(8)-H(8)	0.9500
C(9)-C(10)	1.420(8)
C(9)-C(14)	1.427(9)
C(10)-C(11)	1.410(8)
C(11)-C(12)	1.386(8)
C(11)-C(25)	1.531(8)
C(12)-C(13)	1.390(8)
C(12)-H(12)	0.9500
C(13)-C(14)	1.358(9)
C(13)-C(29)	1.533(8)
C(14)-H(14)	0.9500
C(15)-C(16)	1.512(8)
C(15)-H(15A)	0.9900
C(15)-H(15B)	0.9900
C(16)-H(16A)	0.9900
C(16)-H(16B)	0.9900
C(17)-C(18)	1.523(8)
C(17)-C(20)	1.535(8)
C(17)-C(19)	1.546(8)
C(18)-H(18A)	0.9800

C(18)-H(18B)	0.9800
C(18)-H(18C)	0.9800
C(19)-H(19A)	0.9800
C(19)-H(19B)	0.9800
C(19)-H(19C)	0.9800
C(20)-H(20A)	0.9800
C(20)-H(20B)	0.9800
C(20)-H(20C)	0.9800
C(21)-C(23)	1.527(9)
C(21)-C(22)	1.539(9)
C(21)-C(24)	1.540(9)
C(22)-H(22A)	0.9800
C(22)-H(22B)	0.9800
C(22)-H(22C)	0.9800
C(23)-H(23A)	0.9800
C(23)-H(23B)	0.9800
C(23)-H(23C)	0.9800
C(24)-H(24A)	0.9800
C(24)-H(24B)	0.9800
C(24)-H(24C)	0.9800
C(25)-C(28)	1.515(8)
C(25)-C(27)	1.519(8)
C(25)-C(26)	1.551(10)
C(26)-H(26A)	0.9800
C(26)-H(26B)	0.9800
C(26)-H(26C)	0.9800
C(27)-H(27A)	0.9800
C(27)-H(27B)	0.9800
C(27)-H(27C)	0.9800
C(28)-H(28A)	0.9800
C(28)-H(28B)	0.9800
C(28)-H(28C)	0.9800
C(29)-C(32)	1.504(10)
C(29)-C(31)	1.548(10)
C(29)-C(30)	1.558(12)
C(30)-H(30A)	0.9800
C(30)-H(30B)	0.9800
C(30)-H(30C)	0.9800
C(31)-H(31A)	0.9800
C(31)-H(31B)	0.9800
C(31)-H(31C)	0.9800
C(32)-H(32A)	0.9800
C(32)-H(32B)	0.9800
C(32)-H(32C)	0.9800

O(1)-Mn(1)-O(2)	93.11(17)
O(1)-Mn(1)-N(2)	167.11(18)
O(2)-Mn(1)-N(2)	90.49(18)
O(1)-Mn(1)-N(1)	89.75(18)
O(2)-Mn(1)-N(1)	158.43(19)
N(2)-Mn(1)-N(1)	82.5(2)
O(1)-Mn(1)-N(3)	99.1(2)
O(2)-Mn(1)-N(3)	106.0(2)
N(2)-Mn(1)-N(3)	91.7(2)
N(1)-Mn(1)-N(3)	94.6(2)
C(3)-O(1)-Mn(1)	129.6(3)
C(10)-O(2)-Mn(1)	133.2(3)
C(1)-N(1)-C(15)	120.0(5)
C(1)-N(1)-Mn(1)	125.7(4)
C(15)-N(1)-Mn(1)	114.2(4)
C(8)-N(2)-C(16)	120.5(5)
C(8)-N(2)-Mn(1)	127.3(4)
C(16)-N(2)-Mn(1)	111.8(4)
N(4)-N(3)-Mn(1)	117.8(5)
N(5)-N(4)-N(3)	174.7(7)
N(1)-C(1)-C(2)	125.8(5)

N(1)-C(1)-H(1)	117.1
C(2)-C(1)-H(1)	117.1
C(7)-C(2)-C(3)	120.5(5)
C(7)-C(2)-C(1)	118.0(5)
C(3)-C(2)-C(1)	121.5(5)
O(1)-C(3)-C(4)	120.0(5)
O(1)-C(3)-C(2)	121.3(5)
C(4)-C(3)-C(2)	118.7(5)
C(5)-C(4)-C(3)	117.7(5)
C(5)-C(4)-C(17)	122.2(5)
C(3)-C(4)-C(17)	120.0(5)
C(4)-C(5)-C(6)	124.9(5)
C(4)-C(5)-H(5)	117.5
C(6)-C(5)-H(5)	117.5
C(7)-C(6)-C(5)	115.7(5)
C(7)-C(6)-C(21)	123.3(5)
C(5)-C(6)-C(21)	120.9(5)
C(6)-C(7)-C(2)	122.4(6)
C(6)-C(7)-H(7)	118.8
C(2)-C(7)-H(7)	118.8
N(2)-C(8)-C(9)	125.9(5)
N(2)-C(8)-H(8)	117.0
C(9)-C(8)-H(8)	117.0
C(10)-C(9)-C(14)	119.4(6)
C(10)-C(9)-C(8)	122.2(5)
C(14)-C(9)-C(8)	118.4(5)
O(2)-C(10)-C(11)	120.6(5)
O(2)-C(10)-C(9)	120.6(5)
C(11)-C(10)-C(9)	118.9(6)
C(12)-C(11)-C(10)	117.6(6)
C(12)-C(11)-C(25)	121.7(5)
C(10)-C(11)-C(25)	120.8(5)
C(11)-C(12)-C(13)	125.4(6)
C(11)-C(12)-H(12)	117.3
C(13)-C(12)-H(12)	117.3
C(14)-C(13)-C(12)	116.6(6)
C(14)-C(13)-C(29)	123.8(6)
C(12)-C(13)-C(29)	119.6(6)
C(13)-C(14)-C(9)	122.0(6)
C(13)-C(14)-H(14)	119.0
C(9)-C(14)-H(14)	119.0
N(1)-C(15)-C(16)	105.9(5)
N(1)-C(15)-H(15A)	110.6
C(16)-C(15)-H(15A)	110.6
N(1)-C(15)-H(15B)	110.6
C(16)-C(15)-H(15B)	110.6
H(15A)-C(15)-H(15B)	108.7
N(2)-C(16)-C(15)	106.5(4)
N(2)-C(16)-H(16A)	110.4
C(15)-C(16)-H(16A)	110.4
N(2)-C(16)-H(16B)	110.4
C(15)-C(16)-H(16B)	110.4
H(16A)-C(16)-H(16B)	108.6
C(18)-C(17)-C(4)	111.5(5)
C(18)-C(17)-C(20)	107.8(5)
C(4)-C(17)-C(20)	109.9(5)
C(18)-C(17)-C(19)	107.3(5)
C(4)-C(17)-C(19)	110.6(5)
C(20)-C(17)-C(19)	109.7(5)
C(17)-C(18)-H(18A)	109.5
C(17)-C(18)-H(18B)	109.5
H(18A)-C(18)-H(18B)	109.5
C(17)-C(18)-H(18C)	109.5
H(18A)-C(18)-H(18C)	109.5
H(18B)-C(18)-H(18C)	109.5
C(17)-C(19)-H(19A)	109.5

C(17)-C(19)-H(19B)	109.5
H(19A)-C(19)-H(19B)	109.5
C(17)-C(19)-H(19C)	109.5
H(19A)-C(19)-H(19C)	109.5
H(19B)-C(19)-H(19C)	109.5
C(17)-C(20)-H(20A)	109.5
C(17)-C(20)-H(20B)	109.5
H(20A)-C(20)-H(20B)	109.5
C(17)-C(20)-H(20C)	109.5
H(20A)-C(20)-H(20C)	109.5
H(20B)-C(20)-H(20C)	109.5
C(23)-C(21)-C(22)	106.6(5)
C(23)-C(21)-C(24)	109.2(6)
C(22)-C(21)-C(24)	110.4(6)
C(23)-C(21)-C(6)	111.7(5)
C(22)-C(21)-C(6)	110.9(5)
C(24)-C(21)-C(6)	108.0(5)
C(21)-C(22)-H(22A)	109.5
C(21)-C(22)-H(22B)	109.5
H(22A)-C(22)-H(22B)	109.5
C(21)-C(22)-H(22C)	109.5
H(22A)-C(22)-H(22C)	109.5
H(22B)-C(22)-H(22C)	109.5
C(21)-C(23)-H(23A)	109.5
C(21)-C(23)-H(23B)	109.5
H(23A)-C(23)-H(23B)	109.5
C(21)-C(23)-H(23C)	109.5
H(23A)-C(23)-H(23C)	109.5
H(23B)-C(23)-H(23C)	109.5
C(21)-C(24)-H(24A)	109.5
C(21)-C(24)-H(24B)	109.5
H(24A)-C(24)-H(24B)	109.5
C(21)-C(24)-H(24C)	109.5
H(24A)-C(24)-H(24C)	109.5
H(24B)-C(24)-H(24C)	109.5
C(28)-C(25)-C(27)	108.7(5)
C(28)-C(25)-C(11)	112.1(5)
C(27)-C(25)-C(11)	108.6(5)
C(28)-C(25)-C(26)	108.0(5)
C(27)-C(25)-C(26)	109.3(6)
C(11)-C(25)-C(26)	110.1(5)
C(25)-C(26)-H(26A)	109.5
C(25)-C(26)-H(26B)	109.5
H(26A)-C(26)-H(26B)	109.5
C(25)-C(26)-H(26C)	109.5
H(26A)-C(26)-H(26C)	109.5
H(26B)-C(26)-H(26C)	109.5
C(25)-C(27)-H(27A)	109.5
C(25)-C(27)-H(27B)	109.5
H(27A)-C(27)-H(27B)	109.5
C(25)-C(27)-H(27C)	109.5
H(27A)-C(27)-H(27C)	109.5
H(27B)-C(27)-H(27C)	109.5
C(25)-C(28)-H(28A)	109.5
C(25)-C(28)-H(28B)	109.5
H(28A)-C(28)-H(28B)	109.5
C(25)-C(28)-H(28C)	109.5
H(28A)-C(28)-H(28C)	109.5
H(28B)-C(28)-H(28C)	109.5
C(32)-C(29)-C(13)	112.6(6)
C(32)-C(29)-C(31)	108.6(7)
C(13)-C(29)-C(31)	110.7(6)
C(32)-C(29)-C(30)	107.5(7)
C(13)-C(29)-C(30)	109.6(6)
C(31)-C(29)-C(30)	107.6(6)
C(29)-C(30)-H(30A)	109.5

C(29)-C(30)-H(30B)	109.5
H(30A)-C(30)-H(30B)	109.5
C(29)-C(30)-H(30C)	109.5
H(30A)-C(30)-H(30C)	109.5
H(30B)-C(30)-H(30C)	109.5
C(29)-C(31)-H(31A)	109.5
C(29)-C(31)-H(31B)	109.5
H(31A)-C(31)-H(31B)	109.5
C(29)-C(31)-H(31C)	109.5
H(31A)-C(31)-H(31C)	109.5
H(31B)-C(31)-H(31C)	109.5
C(29)-C(32)-H(32A)	109.5
C(29)-C(32)-H(32B)	109.5
H(32A)-C(32)-H(32B)	109.5
C(29)-C(32)-H(32C)	109.5
H(32A)-C(32)-H(32C)	109.5
H(32B)-C(32)-H(32C)	109.5

Symmetry transformations used to generate equivalent atoms:

Table A-59. Anisotropic displacement parameters ($Å^2 x\ 10^3$) for **5-1**. The anisotropic displacement factor exponent takes the form: $-2\pi^2[\ h^2\ a^{*2}U^{11} + ...\ + 2\ h\ k\ a^*\ b^*\ U^{12}\ ]$

	U^{11}	U^{22}	U^{33}	U^{23}	U^{13}	U^{12}
Mn(1)	28(1)	28(1)	28(1)	1(1)	-7(1)	0(1)
O(1)	44(3)	26(2)	37(2)	1(2)	-13(2)	-11(2)
O(2)	36(2)	26(2)	40(2)	-1(2)	-11(2)	-11(2)
N(1)	33(3)	23(3)	47(3)	-4(2)	-10(2)	-2(2)
N(2)	25(3)	24(3)	31(3)	1(2)	-2(2)	2(2)
N(3)	45(4)	46(4)	49(4)	4(3)	1(3)	-2(3)
N(4)	37(3)	59(4)	42(4)	9(3)	-2(3)	0(3)
N(5)	84(5)	53(4)	75(5)	-20(4)	9(4)	12(4)
C(1)	34(4)	34(4)	31(4)	-3(3)	0(3)	7(3)
C(2)	44(4)	25(3)	22(3)	1(2)	-1(3)	-4(3)
C(3)	31(3)	20(3)	30(4)	-2(3)	-6(3)	5(2)
C(4)	30(3)	18(3)	32(3)	1(2)	1(3)	-3(2)
C(5)	29(3)	27(3)	34(4)	-6(3)	-7(3)	0(2)
C(6)	40(4)	21(3)	38(4)	0(3)	1(3)	-7(3)
C(7)	38(4)	26(3)	39(4)	7(3)	-4(3)	-4(3)
C(8)	30(3)	32(4)	33(4)	-14(3)	-2(3)	-4(3)
C(9)	40(4)	24(3)	38(4)	-6(3)	-2(3)	-10(3)
C(10)	23(3)	29(3)	41(4)	-9(3)	0(3)	0(3)
C(11)	27(3)	24(3)	38(4)	3(3)	-5(3)	2(3)
C(12)	47(4)	31(4)	35(4)	1(3)	-2(3)	10(3)
C(13)	44(4)	33(3)	34(4)	-7(3)	0(3)	-10(3)
C(14)	49(4)	40(4)	34(4)	-13(3)	1(3)	-9(3)
C(15)	31(4)	39(4)	41(4)	10(3)	-12(3)	-8(3)
C(16)	33(3)	41(4)	22(3)	-4(3)	-6(3)	-5(3)
C(17)	43(4)	30(3)	28(4)	0(3)	-11(3)	-1(3)
C(18)	72(5)	63(5)	45(5)	3(4)	-23(4)	-29(4)
C(19)	49(4)	56(5)	28(4)	-7(3)	1(3)	0(3)
C(20)	34(4)	42(4)	45(4)	10(3)	-8(3)	4(3)
C(21)	41(4)	23(3)	42(4)	0(3)	0(3)	-9(3)
C(22)	49(4)	50(4)	47(4)	13(3)	-4(3)	-15(3)
C(23)	62(5)	52(5)	56(5)	24(4)	-13(4)	-20(4)
C(24)	68(5)	30(4)	84(6)	-6(4)	12(4)	-6(3)
C(25)	38(4)	39(4)	30(3)	-4(3)	-6(3)	0(3)
C(26)	63(5)	51(5)	56(5)	3(4)	-24(4)	-3(4)
C(27)	71(5)	30(4)	48(4)	-13(3)	-10(4)	-6(3)
C(28)	83(6)	35(4)	35(4)	5(3)	-20(4)	-8(4)
C(29)	77(5)	32(4)	44(4)	-1(3)	8(4)	-16(4)
C(30)	106(7)	36(4)	75(5)	8(4)	19(6)	-9(4)
C(31)	100(7)	41(5)	77(6)	13(4)	20(5)	-7(4)

C(32)	166(10)	58(6)	78(7)	5(5)	-40(6)	-61(6)

Table A-60. Hydrogen coordinates (x 10^4) and isotropic displacement parameters ($Å^2$x 10^3) for **5-1**.

	x	y	z	U(eq)
H(1)	-1915	6554	574	42
H(5)	4234	7924	2199	37
H(7)	181	7746	577	42
H(8)	-2981	2447	1399	39
H(12)	92	1273	4150	48
H(14)	-2837	1191	2261	49
H(15A)	-3376	5288	216	44
H(15B)	-4652	5195	960	44
H(16A)	-3739	3615	542	39
H(16B)	-1348	3737	337	39
H(18A)	6460	7088	2907	87
H(18B)	6213	6698	3712	87
H(18C)	4580	7634	3423	87
H(19A)	2990	6086	4060	69
H(19B)	1355	5858	3461	69
H(19C)	1384	6957	3676	69
H(20A)	6435	5373	2526	63
H(20B)	4404	4902	2715	63
H(20C)	5992	5087	3344	63
H(22A)	6093	8404	705	72
H(22B)	5795	8753	1529	72
H(22C)	5592	9537	890	72
H(23A)	3140	8479	-90	84
H(23B)	2646	9634	-2	84
H(23C)	779	9036	125	84
H(24A)	1936	10384	1208	92
H(24B)	2014	9719	1917	92
H(24C)	79	9787	1358	92
H(26A)	4297	3433	4160	86
H(26B)	3408	3440	3351	86
H(26C)	4485	2436	3727	86
H(27A)	-1380	3895	4445	75
H(27B)	-158	4344	3808	75
H(27C)	746	4298	4616	75
H(28A)	2539	2741	5146	78
H(28B)	2532	1752	4722	78
H(28C)	339	2374	5034	78
H(30A)	-179	-1235	3835	110
H(30B)	985	-348	3996	110
H(30C)	1001	-774	3194	110
H(31A)	-4645	704	4091	110
H(31B)	-2520	426	4567	110
H(31C)	-3725	-405	4299	110
H(32A)	-3257	-1007	3053	143
H(32B)	-2318	-390	2444	143
H(32C)	-4554	46	2831	143

Table A-61. Crystal data and structure refinement for **5-3**.

Identification code	ddef90b	
Empirical formula	C36 H52 Mn N5 O2	
Formula weight	641.77	
Temperature	110(2) K	
Wavelength	0.71073 Å	
Crystal system	Monoclinic	
Space group	P2(1)	
Unit cell dimensions	a = 17.772(3) Å	α= 90°.
	b = 11.5307(19) Å	β= 112.178(3)°.
	c = 18.530(3) Å	γ = 90°.
Volume	3516.1(10) $Å^3$	
Z	4	
Density (calculated)	1.212 Mg/m^3	
Absorption coefficient	0.413 mm^{-1}	
F(000)	1376	
Crystal size	0.40 x 0.30 x 0.08 mm^3	
Theta range for data collection	1.24 to 27.58°.	
Index ranges	-23<=h<=23, -14<=k<=14, -24<=l<=24	
Reflections collected	40279	
Independent reflections	16068 [R(int) = 0.0634]	
Completeness to theta = 27.58°	99.3 %	
Absorption correction	Semi-empirical from equivalents	
Max. and min. transmission	0.9677 and 0.8523	
Refinement method	Full-matrix least-squares on F^2	
Data / restraints / parameters	16068 / 1 / 817	
Goodness-of-fit on F^2	0.990	
Final R indices [I>2sigma(I)]	R1 = 0.0484, wR2 = 0.0954	
R indices (all data)	R1 = 0.0851, wR2 = 0.1098	
Absolute structure parameter	-0.046(15)	
Largest diff. peak and hole	0.374 and -0.336 e.$Å^{-3}$	

Table A-62. Atomic coordinates (x 10^4) and equivalent isotropic displacement parameters ($Å^2$x 10^3) for **5-3**. U(eq) is defined as one third of the trace of the orthogonalized U^{ij} tensor.

	x	y	z	U(eq)
Mn(1)	8335(1)	6176(1)	327(1)	12(1)
Mn(2)	8283(1)	1543(1)	5287(1)	13(1)
O(1)	7449(1)	6460(2)	619(1)	17(1)
O(2)	7638(1)	5664(2)	-654(1)	14(1)
O(3)	7653(1)	2140(2)	4301(1)	16(1)
O(4)	7366(1)	1249(2)	5529(1)	18(1)
N(1)	9059(2)	7021(3)	1254(2)	14(1)
N(2)	9116(2)	6772(3)	-114(2)	12(1)
N(3)	8809(2)	4577(3)	808(2)	24(1)
N(4)	9458(2)	4217(3)	1194(2)	21(1)
N(5)	10094(2)	3831(3)	1570(2)	33(1)
N(6)	9170(2)	1205(3)	4913(2)	15(1)
N(7)	8933(2)	475(3)	6132(2)	16(1)
N(8)	8734(2)	3071(3)	5907(2)	25(1)
N(9)	9379(2)	3501(3)	6194(2)	18(1)
N(10)	10005(2)	3947(3)	6490(2)	33(1)
C(1)	8872(2)	7399(3)	1823(2)	14(1)
C(2)	8101(2)	7290(3)	1889(2)	14(1)
C(3)	7408(2)	6857(3)	1277(2)	13(1)
C(4)	6642(2)	6870(3)	1356(2)	15(1)
C(5)	6631(2)	7265(3)	2052(2)	17(1)
C(6)	7307(2)	7696(3)	2683(2)	16(1)
C(7)	8033(2)	7716(3)	2582(2)	14(1)

C(8)	9010(2)	6747(3)	-853(2)	15(1)
C(9)	8336(2)	6244(3)	-1469(2)	15(1)
C(10)	7680(2)	5704(3)	-1354(2)	13(1)
C(11)	7034(2)	5242(3)	-2013(2)	12(1)
C(12)	7063(2)	5431(3)	-2736(2)	16(1)
C(13)	7690(2)	6021(3)	-2873(2)	15(1)
C(14)	8330(2)	6389(3)	-2231(2)	16(1)
C(15)	9892(2)	7132(3)	1255(2)	16(1)
C(16)	9783(2)	7485(3)	429(2)	16(1)
C(17)	10591(2)	7425(4)	327(2)	22(1)
C(18)	11187(2)	8264(3)	908(2)	25(1)
C(19)	11286(2)	7995(3)	1744(2)	22(1)
C(20)	10476(2)	7961(4)	1852(2)	19(1)
C(21)	5867(2)	6485(4)	681(2)	22(1)
C(22)	5940(2)	5247(4)	430(2)	29(1)
C(23)	5120(2)	6560(6)	907(2)	48(2)
C(24)	5714(2)	7325(4)	-14(2)	32(1)
C(25)	7196(2)	8149(3)	3410(2)	16(1)
C(26)	8011(2)	8439(4)	4070(2)	22(1)
C(27)	6689(2)	9249(4)	3195(2)	26(1)
C(28)	6753(2)	7244(4)	3718(2)	27(1)
C(29)	6319(2)	4598(3)	-1910(2)	15(1)
C(30)	6615(2)	3596(3)	-1327(2)	24(1)
C(31)	5830(2)	5471(4)	-1629(2)	19(1)
C(32)	5736(2)	4077(3)	-2688(2)	26(1)
C(33)	7594(2)	6334(3)	-3715(2)	19(1)
C(34)	7251(2)	5311(4)	-4275(2)	27(1)
C(35)	7009(3)	7366(4)	-3969(2)	28(1)
C(36)	8412(2)	6684(4)	-3751(2)	33(1)
C(37)	9080(2)	1127(3)	4193(2)	16(1)
C(38)	8376(2)	1434(3)	3532(2)	13(1)
C(39)	7691(2)	1972(3)	3611(2)	14(1)
C(40)	7035(2)	2324(3)	2921(2)	18(1)
C(41)	7093(2)	2067(3)	2213(2)	19(1)
C(42)	7749(2)	1501(3)	2114(2)	18(1)
C(43)	8392(2)	1200(4)	2787(2)	17(1)
C(44)	8739(2)	178(3)	6717(2)	20(1)
C(45)	7982(2)	405(3)	6797(2)	15(1)
C(46)	7308(2)	888(3)	6180(2)	14(1)
C(47)	6541(2)	913(3)	6264(2)	15(1)
C(48)	6513(2)	499(3)	6961(2)	17(1)
C(49)	7180(2)	62(3)	7586(2)	15(1)
C(50)	7904(2)	6(3)	7484(2)	16(1)
C(51)	9928(2)	876(3)	5569(2)	16(1)
C(52)	9679(2)	17(3)	6060(2)	17(1)
C(53)	10393(2)	-242(4)	6816(2)	24(1)
C(54)	11098(2)	-728(3)	6619(2)	30(1)
C(55)	11338(2)	84(3)	6095(2)	25(1)
C(56)	10604(2)	375(4)	5347(2)	22(1)
C(57)	6284(2)	2938(3)	2969(2)	18(1)
C(58)	6537(2)	4065(3)	3428(2)	25(1)
C(59)	5666(2)	3242(4)	2159(2)	27(1)
C(60)	5866(2)	2149(4)	3363(2)	21(1)
C(61)	7703(2)	1174(4)	1299(2)	25(1)
C(62)	7441(3)	2227(4)	753(2)	31(1)
C(63)	8522(3)	727(4)	1312(2)	39(1)
C(64)	7065(3)	205(4)	986(2)	33(1)
C(65)	5769(2)	1312(4)	5584(2)	19(1)
C(66)	5872(2)	2568(4)	5360(2)	23(1)
C(67)	5608(2)	480(4)	4898(2)	21(1)
C(68)	5026(2)	1292(4)	5815(2)	30(1)
C(69)	7051(2)	-471(3)	8296(2)	18(1)
C(70)	6500(2)	289(4)	8564(2)	29(1)
C(71)	6649(2)	-1658(3)	8047(2)	22(1)
C(72)	7850(2)	-631(4)	8987(2)	26(1)

Table A-63. Bond lengths [Å] and angles [°] for **5-3**.

Mn(1)-O(2)	1.868(2)
Mn(1)-O(1)	1.877(2)
Mn(1)-N(1)	1.971(3)
Mn(1)-N(2)	1.981(3)
Mn(1)-N(3)	2.083(3)
Mn(2)-O(3)	1.875(2)
Mn(2)-O(4)	1.877(2)
Mn(2)-N(7)	1.985(3)
Mn(2)-N(6)	1.985(3)
Mn(2)-N(8)	2.090(3)
O(1)-C(3)	1.331(4)
O(2)-C(10)	1.327(4)
O(3)-C(39)	1.320(4)
O(4)-C(46)	1.317(4)
N(1)-C(1)	1.295(4)
N(1)-C(15)	1.486(4)
N(2)-C(8)	1.310(4)
N(2)-C(16)	1.480(4)
N(3)-N(4)	1.179(4)
N(4)-N(5)	1.170(4)
N(6)-C(37)	1.286(4)
N(6)-C(51)	1.483(4)
N(7)-C(44)	1.302(5)
N(7)-C(52)	1.480(4)
N(8)-N(9)	1.176(4)
N(9)-N(10)	1.159(4)
C(1)-C(2)	1.427(5)
C(1)-H(1)	0.9500
C(2)-C(3)	1.414(4)
C(2)-C(7)	1.422(5)
C(3)-C(4)	1.423(5)
C(4)-C(5)	1.375(5)
C(4)-C(21)	1.535(5)
C(5)-C(6)	1.413(5)
C(5)-H(5)	0.9500
C(6)-C(7)	1.371(5)
C(6)-C(25)	1.526(5)
C(7)-H(7)	0.9500
C(8)-C(9)	1.429(5)
C(8)-H(8)	0.9500
C(9)-C(10)	1.407(5)
C(9)-C(14)	1.419(5)
C(10)-C(11)	1.427(4)
C(11)-C(12)	1.377(5)
C(11)-C(29)	1.544(5)
C(12)-C(13)	1.408(5)
C(12)-H(12)	0.9500
C(13)-C(14)	1.367(4)
C(13)-C(33)	1.547(5)
C(14)-H(14)	0.9500
C(15)-C(16)	1.524(4)
C(15)-C(20)	1.533(4)
C(15)-H(15)	1.0000
C(16)-C(17)	1.519(5)
C(16)-H(16)	1.0000
C(17)-C(18)	1.535(5)
C(17)-H(17A)	0.9900
C(17)-H(17B)	0.9900
C(18)-C(19)	1.524(5)
C(18)-H(18A)	0.9900
C(18)-H(18B)	0.9900
C(19)-C(20)	1.526(5)
C(19)-H(19A)	0.9900

C(19)-H(19B)	0.9900
C(20)-H(20A)	0.9900
C(20)-H(20B)	0.9900
C(21)-C(22)	1.522(6)
C(21)-C(23)	1.538(5)
C(21)-C(24)	1.551(6)
C(22)-H(22A)	0.9800
C(22)-H(22B)	0.9800
C(22)-H(22C)	0.9800
C(23)-H(23A)	0.9800
C(23)-H(23B)	0.9800
C(23)-H(23C)	0.9800
C(24)-H(24A)	0.9800
C(24)-H(24B)	0.9800
C(24)-H(24C)	0.9800
C(25)-C(27)	1.520(5)
C(25)-C(26)	1.539(5)
C(25)-C(28)	1.540(5)
C(26)-H(26A)	0.9800
C(26)-H(26B)	0.9800
C(26)-H(26C)	0.9800
C(27)-H(27A)	0.9800
C(27)-H(27B)	0.9800
C(27)-H(27C)	0.9800
C(28)-H(28A)	0.9800
C(28)-H(28B)	0.9800
C(28)-H(28C)	0.9800
C(29)-C(30)	1.532(5)
C(29)-C(31)	1.542(5)
C(29)-C(32)	1.544(5)
C(30)-H(30A)	0.9800
C(30)-H(30B)	0.9800
C(30)-H(30C)	0.9800
C(31)-H(31A)	0.9800
C(31)-H(31B)	0.9800
C(31)-H(31C)	0.9800
C(32)-H(32A)	0.9800
C(32)-H(32B)	0.9800
C(32)-H(32C)	0.9800
C(33)-C(35)	1.532(5)
C(33)-C(36)	1.534(5)
C(33)-C(34)	1.537(5)
C(34)-H(34A)	0.9800
C(34)-H(34B)	0.9800
C(34)-H(34C)	0.9800
C(35)-H(35A)	0.9800
C(35)-H(35B)	0.9800
C(35)-H(35C)	0.9800
C(36)-H(36A)	0.9800
C(36)-H(36B)	0.9800
C(36)-H(36C)	0.9800
C(37)-C(38)	1.427(4)
C(37)-H(37)	0.9500
C(38)-C(43)	1.417(5)
C(38)-C(39)	1.421(5)
C(39)-C(40)	1.427(5)
C(40)-C(41)	1.386(5)
C(40)-C(57)	1.543(5)
C(41)-C(42)	1.407(5)
C(41)-H(41)	0.9500
C(42)-C(43)	1.380(4)
C(42)-C(61)	1.530(5)
C(43)-H(43)	0.9500
C(44)-C(45)	1.432(5)
C(44)-H(44)	0.9500
C(45)-C(50)	1.409(5)

C(45)-C(46)	1.421(5)
C(46)-C(47)	1.428(5)
C(47)-C(48)	1.394(5)
C(47)-C(65)	1.542(5)
C(48)-C(49)	1.402(5)
C(48)-H(48)	0.9500
C(49)-C(50)	1.369(5)
C(49)-C(69)	1.545(5)
C(50)-H(50)	0.9500
C(51)-C(52)	1.520(4)
C(51)-C(56)	1.522(5)
C(51)-H(51)	1.0000
C(52)-C(53)	1.524(4)
C(52)-H(52)	1.0000
C(53)-C(54)	1.537(5)
C(53)-H(53A)	0.9900
C(53)-H(53B)	0.9900
C(54)-C(55)	1.522(5)
C(54)-H(54A)	0.9900
C(54)-H(54B)	0.9900
C(55)-C(56)	1.539(4)
C(55)-H(55A)	0.9900
C(55)-H(55B)	0.9900
C(56)-H(56A)	0.9900
C(56)-H(56B)	0.9900
C(57)-C(60)	1.523(5)
C(57)-C(58)	1.525(5)
C(57)-C(59)	1.529(5)
C(58)-H(58A)	0.9800
C(58)-H(58B)	0.9800
C(58)-H(58C)	0.9800
C(59)-H(59A)	0.9800
C(59)-H(59B)	0.9800
C(59)-H(59C)	0.9800
C(60)-H(60A)	0.9800
C(60)-H(60B)	0.9800
C(60)-H(60C)	0.9800
C(61)-C(62)	1.535(5)
C(61)-C(63)	1.536(5)
C(61)-C(64)	1.541(5)
C(62)-H(62A)	0.9800
C(62)-H(62B)	0.9800
C(62)-H(62C)	0.9800
C(63)-H(63A)	0.9800
C(63)-H(63B)	0.9800
C(63)-H(63C)	0.9800
C(64)-H(64A)	0.9800
C(64)-H(64B)	0.9800
C(64)-H(64C)	0.9800
C(65)-C(67)	1.531(5)
C(65)-C(68)	1.534(5)
C(65)-C(66)	1.536(6)
C(66)-H(66A)	0.9800
C(66)-H(66B)	0.9800
C(66)-H(66C)	0.9800
C(67)-H(67A)	0.9800
C(67)-H(67B)	0.9800
C(67)-H(67C)	0.9800
C(68)-H(68A)	0.9800
C(68)-H(68B)	0.9800
C(68)-H(68C)	0.9800
C(69)-C(72)	1.523(5)
C(69)-C(70)	1.531(5)
C(69)-C(71)	1.533(5)
C(70)-H(70A)	0.9800
C(70)-H(70B)	0.9800

C(70)-H(70C)	0.9800
C(71)-H(71A)	0.9800
C(71)-H(71B)	0.9800
C(71)-H(71C)	0.9800
C(72)-H(72A)	0.9800
C(72)-H(72B)	0.9800
C(72)-H(72C)	0.9800

O(2)-Mn(1)-O(1)	90.91(10)
O(2)-Mn(1)-N(1)	168.34(12)
O(1)-Mn(1)-N(1)	90.30(11)
O(2)-Mn(1)-N(2)	91.02(11)
O(1)-Mn(1)-N(2)	148.58(12)
N(1)-Mn(1)-N(2)	81.96(11)
O(2)-Mn(1)-N(3)	98.55(12)
O(1)-Mn(1)-N(3)	106.21(13)
N(1)-Mn(1)-N(3)	92.24(13)
N(2)-Mn(1)-N(3)	104.48(13)
O(3)-Mn(2)-O(4)	92.67(10)
O(3)-Mn(2)-N(7)	162.12(12)
O(4)-Mn(2)-N(7)	89.90(11)
O(3)-Mn(2)-N(6)	89.59(11)
O(4)-Mn(2)-N(6)	157.38(13)
N(7)-Mn(2)-N(6)	81.44(12)
O(3)-Mn(2)-N(8)	100.96(12)
O(4)-Mn(2)-N(8)	102.04(13)
N(7)-Mn(2)-N(8)	95.79(13)
N(6)-Mn(2)-N(8)	99.61(13)
C(3)-O(1)-Mn(1)	131.8(2)
C(10)-O(2)-Mn(1)	132.8(2)
C(39)-O(3)-Mn(2)	131.2(2)
C(46)-O(4)-Mn(2)	130.7(2)
C(1)-N(1)-C(15)	122.2(3)
C(1)-N(1)-Mn(1)	126.3(2)
C(15)-N(1)-Mn(1)	111.4(2)
C(8)-N(2)-C(16)	119.0(3)
C(8)-N(2)-Mn(1)	125.2(2)
C(16)-N(2)-Mn(1)	114.7(2)
N(4)-N(3)-Mn(1)	135.7(3)
N(5)-N(4)-N(3)	178.2(4)
C(37)-N(6)-C(51)	123.4(3)
C(37)-N(6)-Mn(2)	124.9(2)
C(51)-N(6)-Mn(2)	111.09(19)
C(44)-N(7)-C(52)	120.7(3)
C(44)-N(7)-Mn(2)	124.2(3)
C(52)-N(7)-Mn(2)	115.1(2)
N(9)-N(8)-Mn(2)	135.3(3)
N(10)-N(9)-N(8)	177.9(4)
N(1)-C(1)-C(2)	126.2(3)
N(1)-C(1)-H(1)	116.9
C(2)-C(1)-H(1)	116.9
C(3)-C(2)-C(7)	120.0(3)
C(3)-C(2)-C(1)	122.5(3)
C(7)-C(2)-C(1)	117.3(3)
O(1)-C(3)-C(2)	121.6(3)
O(1)-C(3)-C(4)	118.9(3)
C(2)-C(3)-C(4)	119.5(3)
C(5)-C(4)-C(3)	116.9(3)
C(5)-C(4)-C(21)	122.3(3)
C(3)-C(4)-C(21)	120.8(3)
C(4)-C(5)-C(6)	125.7(3)
C(4)-C(5)-H(5)	117.1
C(6)-C(5)-H(5)	117.1
C(7)-C(6)-C(5)	116.3(3)
C(7)-C(6)-C(25)	123.8(3)
C(5)-C(6)-C(25)	119.8(3)

C(6)-C(7)-C(2)	121.5(3)
C(6)-C(7)-H(7)	119.3
C(2)-C(7)-H(7)	119.3
N(2)-C(8)-C(9)	126.2(3)
N(2)-C(8)-H(8)	116.9
C(9)-C(8)-H(8)	116.9
C(10)-C(9)-C(14)	120.6(3)
C(10)-C(9)-C(8)	123.4(3)
C(14)-C(9)-C(8)	115.9(3)
O(2)-C(10)-C(9)	121.2(3)
O(2)-C(10)-C(11)	119.9(3)
C(9)-C(10)-C(11)	118.8(3)
C(12)-C(11)-C(10)	117.3(3)
C(12)-C(11)-C(29)	122.1(3)
C(10)-C(11)-C(29)	120.5(3)
C(11)-C(12)-C(13)	125.1(3)
C(11)-C(12)-H(12)	117.5
C(13)-C(12)-H(12)	117.5
C(14)-C(13)-C(12)	116.7(3)
C(14)-C(13)-C(33)	122.9(3)
C(12)-C(13)-C(33)	120.1(3)
C(13)-C(14)-C(9)	121.3(3)
C(13)-C(14)-H(14)	119.3
C(9)-C(14)-H(14)	119.3
N(1)-C(15)-C(16)	105.8(2)
N(1)-C(15)-C(20)	117.2(3)
C(16)-C(15)-C(20)	110.8(3)
N(1)-C(15)-H(15)	107.5
C(16)-C(15)-H(15)	107.6
C(20)-C(15)-H(15)	107.5
N(2)-C(16)-C(17)	116.3(3)
N(2)-C(16)-C(15)	107.5(2)
C(17)-C(16)-C(15)	110.1(3)
N(2)-C(16)-H(16)	107.6
C(17)-C(16)-H(16)	107.6
C(15)-C(16)-H(16)	107.5
C(16)-C(17)-C(18)	108.6(3)
C(16)-C(17)-H(17A)	110.0
C(18)-C(17)-H(17A)	110.0
C(16)-C(17)-H(17B)	110.0
C(18)-C(17)-H(17B)	110.0
H(17A)-C(17)-H(17B)	108.3
C(19)-C(18)-C(17)	111.6(3)
C(19)-C(18)-H(18A)	109.3
C(17)-C(18)-H(18A)	109.3
C(19)-C(18)-H(18B)	109.3
C(17)-C(18)-H(18B)	109.3
H(18A)-C(18)-H(18B)	108.0
C(18)-C(19)-C(20)	112.7(3)
C(18)-C(19)-H(19A)	109.0
C(20)-C(19)-H(19A)	109.0
C(18)-C(19)-H(19B)	109.0
C(20)-C(19)-H(19B)	109.0
H(19A)-C(19)-H(19B)	107.8
C(19)-C(20)-C(15)	109.6(3)
C(19)-C(20)-H(20A)	109.7
C(15)-C(20)-H(20A)	109.7
C(19)-C(20)-H(20B)	109.7
C(15)-C(20)-H(20B)	109.7
H(20A)-C(20)-H(20B)	108.2
C(22)-C(21)-C(4)	111.5(3)
C(22)-C(21)-C(23)	108.5(4)
C(4)-C(21)-C(23)	111.2(3)
C(22)-C(21)-C(24)	109.9(3)
C(4)-C(21)-C(24)	108.6(3)
C(23)-C(21)-C(24)	107.0(3)

C(21)-C(22)-H(22A)	109.5
C(21)-C(22)-H(22B)	109.5
H(22A)-C(22)-H(22B)	109.5
C(21)-C(22)-H(22C)	109.5
H(22A)-C(22)-H(22C)	109.5
H(22B)-C(22)-H(22C)	109.5
C(21)-C(23)-H(23A)	109.5
C(21)-C(23)-H(23B)	109.5
H(23A)-C(23)-H(23B)	109.5
C(21)-C(23)-H(23C)	109.5
H(23A)-C(23)-H(23C)	109.5
H(23B)-C(23)-H(23C)	109.5
C(21)-C(24)-H(24A)	109.5
C(21)-C(24)-H(24B)	109.5
H(24A)-C(24)-H(24B)	109.5
C(21)-C(24)-H(24C)	109.5
H(24A)-C(24)-H(24C)	109.5
H(24B)-C(24)-H(24C)	109.5
C(27)-C(25)-C(6)	108.3(3)
C(27)-C(25)-C(26)	108.3(3)
C(6)-C(25)-C(26)	112.2(3)
C(27)-C(25)-C(28)	109.2(3)
C(6)-C(25)-C(28)	110.5(3)
C(26)-C(25)-C(28)	108.2(3)
C(25)-C(26)-H(26A)	109.5
C(25)-C(26)-H(26B)	109.5
H(26A)-C(26)-H(26B)	109.5
C(25)-C(26)-H(26C)	109.5
H(26A)-C(26)-H(26C)	109.5
H(26B)-C(26)-H(26C)	109.5
C(25)-C(27)-H(27A)	109.5
C(25)-C(27)-H(27B)	109.5
H(27A)-C(27)-H(27B)	109.5
C(25)-C(27)-H(27C)	109.5
H(27A)-C(27)-H(27C)	109.5
H(27B)-C(27)-H(27C)	109.5
C(25)-C(28)-H(28A)	109.5
C(25)-C(28)-H(28B)	109.5
H(28A)-C(28)-H(28B)	109.5
C(25)-C(28)-H(28C)	109.5
H(28A)-C(28)-H(28C)	109.5
H(28B)-C(28)-H(28C)	109.5
C(30)-C(29)-C(31)	110.0(3)
C(30)-C(29)-C(32)	107.2(3)
C(31)-C(29)-C(32)	107.7(3)
C(30)-C(29)-C(11)	111.7(3)
C(31)-C(29)-C(11)	108.8(3)
C(32)-C(29)-C(11)	111.4(3)
C(29)-C(30)-H(30A)	109.5
C(29)-C(30)-H(30B)	109.5
H(30A)-C(30)-H(30B)	109.5
C(29)-C(30)-H(30C)	109.5
H(30A)-C(30)-H(30C)	109.5
H(30B)-C(30)-H(30C)	109.5
C(29)-C(31)-H(31A)	109.5
C(29)-C(31)-H(31B)	109.5
H(31A)-C(31)-H(31B)	109.5
C(29)-C(31)-H(31C)	109.5
H(31A)-C(31)-H(31C)	109.5
H(31B)-C(31)-H(31C)	109.5
C(29)-C(32)-H(32A)	109.5
C(29)-C(32)-H(32B)	109.5
H(32A)-C(32)-H(32B)	109.5
C(29)-C(32)-H(32C)	109.5
H(32A)-C(32)-H(32C)	109.5
H(32B)-C(32)-H(32C)	109.5

C(35)-C(33)-C(36)	109.1(3)
C(35)-C(33)-C(34)	109.8(3)
C(36)-C(33)-C(34)	108.2(3)
C(35)-C(33)-C(13)	107.1(3)
C(36)-C(33)-C(13)	111.1(3)
C(34)-C(33)-C(13)	111.5(3)
C(33)-C(34)-H(34A)	109.5
C(33)-C(34)-H(34B)	109.5
H(34A)-C(34)-H(34B)	109.5
C(33)-C(34)-H(34C)	109.5
H(34A)-C(34)-H(34C)	109.5
H(34B)-C(34)-H(34C)	109.5
C(33)-C(35)-H(35A)	109.5
C(33)-C(35)-H(35B)	109.5
H(35A)-C(35)-H(35B)	109.5
C(33)-C(35)-H(35C)	109.5
H(35A)-C(35)-H(35C)	109.5
H(35B)-C(35)-H(35C)	109.5
C(33)-C(36)-H(36A)	109.5
C(33)-C(36)-H(36B)	109.5
H(36A)-C(36)-H(36B)	109.5
C(33)-C(36)-H(36C)	109.5
H(36A)-C(36)-H(36C)	109.5
H(36B)-C(36)-H(36C)	109.5
N(6)-C(37)-C(38)	126.8(3)
N(6)-C(37)-H(37)	116.6
C(38)-C(37)-H(37)	116.6
C(43)-C(38)-C(39)	121.1(3)
C(43)-C(38)-C(37)	117.1(3)
C(39)-C(38)-C(37)	121.8(3)
O(3)-C(39)-C(38)	121.5(3)
O(3)-C(39)-C(40)	120.2(3)
C(38)-C(39)-C(40)	118.3(3)
C(41)-C(40)-C(39)	117.4(4)
C(41)-C(40)-C(57)	121.8(3)
C(39)-C(40)-C(57)	120.8(3)
C(40)-C(41)-C(42)	125.7(3)
C(40)-C(41)-H(41)	117.2
C(42)-C(41)-H(41)	117.2
C(43)-C(42)-C(41)	116.3(3)
C(43)-C(42)-C(61)	123.2(3)
C(41)-C(42)-C(61)	120.3(3)
C(42)-C(43)-C(38)	121.2(3)
C(42)-C(43)-H(43)	119.4
C(38)-C(43)-H(43)	119.4
N(7)-C(44)-C(45)	126.4(3)
N(7)-C(44)-H(44)	116.8
C(45)-C(44)-H(44)	116.8
C(50)-C(45)-C(46)	121.0(3)
C(50)-C(45)-C(44)	116.8(3)
C(46)-C(45)-C(44)	121.9(3)
O(4)-C(46)-C(45)	121.8(3)
O(4)-C(46)-C(47)	120.1(3)
C(45)-C(46)-C(47)	118.0(3)
C(48)-C(47)-C(46)	117.5(3)
C(48)-C(47)-C(65)	121.8(3)
C(46)-C(47)-C(65)	120.5(3)
C(47)-C(48)-C(49)	125.0(3)
C(47)-C(48)-H(48)	117.5
C(49)-C(48)-H(48)	117.5
C(50)-C(49)-C(48)	116.6(3)
C(50)-C(49)-C(69)	123.2(3)
C(48)-C(49)-C(69)	119.7(3)
C(49)-C(50)-C(45)	121.8(3)
C(49)-C(50)-H(50)	119.1
C(45)-C(50)-H(50)	119.1

N(6)-C(51)-C(52)	106.1(2)
N(6)-C(51)-C(56)	116.2(3)
C(52)-C(51)-C(56)	110.6(3)
N(6)-C(51)-H(51)	107.9
C(52)-C(51)-H(51)	107.9
C(56)-C(51)-H(51)	107.8
N(7)-C(52)-C(51)	107.1(3)
N(7)-C(52)-C(53)	116.7(3)
C(51)-C(52)-C(53)	110.4(3)
N(7)-C(52)-H(52)	107.4
C(51)-C(52)-H(52)	107.4
C(53)-C(52)-H(52)	107.3
C(52)-C(53)-C(54)	108.8(3)
C(52)-C(53)-H(53A)	109.9
C(54)-C(53)-H(53A)	109.9
C(52)-C(53)-H(53B)	109.9
C(54)-C(53)-H(53B)	109.9
H(53A)-C(53)-H(53B)	108.3
C(55)-C(54)-C(53)	112.2(3)
C(55)-C(54)-H(54A)	109.2
C(53)-C(54)-H(54A)	109.2
C(55)-C(54)-H(54B)	109.2
C(53)-C(54)-H(54B)	109.2
H(54A)-C(54)-H(54B)	107.9
C(54)-C(55)-C(56)	111.2(3)
C(54)-C(55)-H(55A)	109.4
C(56)-C(55)-H(55A)	109.4
C(54)-C(55)-H(55B)	109.4
C(56)-C(55)-H(55B)	109.4
H(55A)-C(55)-H(55B)	108.0
C(51)-C(56)-C(55)	109.2(3)
C(51)-C(56)-H(56A)	109.8
C(55)-C(56)-H(56A)	109.8
C(51)-C(56)-H(56B)	109.8
C(55)-C(56)-H(56B)	109.9
H(56A)-C(56)-H(56B)	108.3
C(60)-C(57)-C(58)	109.6(3)
C(60)-C(57)-C(59)	107.9(3)
C(58)-C(57)-C(59)	107.7(3)
C(60)-C(57)-C(40)	110.0(3)
C(58)-C(57)-C(40)	110.1(3)
C(59)-C(57)-C(40)	111.4(3)
C(57)-C(58)-H(58A)	109.5
C(57)-C(58)-H(58B)	109.5
H(58A)-C(58)-H(58B)	109.5
C(57)-C(58)-H(58C)	109.5
H(58A)-C(58)-H(58C)	109.5
H(58B)-C(58)-H(58C)	109.5
C(57)-C(59)-H(59A)	109.5
C(57)-C(59)-H(59B)	109.5
H(59A)-C(59)-H(59B)	109.5
C(57)-C(59)-H(59C)	109.5
H(59A)-C(59)-H(59C)	109.5
H(59B)-C(59)-H(59C)	109.5
C(57)-C(60)-H(60A)	109.5
C(57)-C(60)-H(60B)	109.5
H(60A)-C(60)-H(60B)	109.5
C(57)-C(60)-H(60C)	109.5
H(60A)-C(60)-H(60C)	109.5
H(60B)-C(60)-H(60C)	109.5
C(42)-C(61)-C(62)	110.3(3)
C(42)-C(61)-C(63)	111.7(3)
C(62)-C(61)-C(63)	109.0(3)
C(42)-C(61)-C(64)	107.8(3)
C(62)-C(61)-C(64)	109.2(3)
C(63)-C(61)-C(64)	108.8(4)

C(61)-C(62)-H(62A)	109.5
C(61)-C(62)-H(62B)	109.5
H(62A)-C(62)-H(62B)	109.5
C(61)-C(62)-H(62C)	109.5
H(62A)-C(62)-H(62C)	109.5
H(62B)-C(62)-H(62C)	109.5
C(61)-C(63)-H(63A)	109.5
C(61)-C(63)-H(63B)	109.5
H(63A)-C(63)-H(63B)	109.5
C(61)-C(63)-H(63C)	109.5
H(63A)-C(63)-H(63C)	109.5
H(63B)-C(63)-H(63C)	109.5
C(61)-C(64)-H(64A)	109.5
C(61)-C(64)-H(64B)	109.5
H(64A)-C(64)-H(64B)	109.5
C(61)-C(64)-H(64C)	109.5
H(64A)-C(64)-H(64C)	109.5
H(64B)-C(64)-H(64C)	109.5
C(67)-C(65)-C(68)	108.2(3)
C(67)-C(65)-C(66)	111.7(3)
C(68)-C(65)-C(66)	107.0(3)
C(67)-C(65)-C(47)	108.8(3)
C(68)-C(65)-C(47)	111.2(3)
C(66)-C(65)-C(47)	110.0(3)
C(65)-C(66)-H(66A)	109.5
C(65)-C(66)-H(66B)	109.5
H(66A)-C(66)-H(66B)	109.5
C(65)-C(66)-H(66C)	109.5
H(66A)-C(66)-H(66C)	109.5
H(66B)-C(66)-H(66C)	109.5
C(65)-C(67)-H(67A)	109.5
C(65)-C(67)-H(67B)	109.5
H(67A)-C(67)-H(67B)	109.5
C(65)-C(67)-H(67C)	109.5
H(67A)-C(67)-H(67C)	109.5
H(67B)-C(67)-H(67C)	109.5
C(65)-C(68)-H(68A)	109.5
C(65)-C(68)-H(68B)	109.5
H(68A)-C(68)-H(68B)	109.5
C(65)-C(68)-H(68C)	109.5
H(68A)-C(68)-H(68C)	109.5
H(68B)-C(68)-H(68C)	109.5
C(72)-C(69)-C(70)	107.7(3)
C(72)-C(69)-C(71)	109.0(3)
C(70)-C(69)-C(71)	109.1(3)
C(72)-C(69)-C(49)	111.9(3)
C(70)-C(69)-C(49)	111.6(3)
C(71)-C(69)-C(49)	107.6(3)
C(69)-C(70)-H(70A)	109.5
C(69)-C(70)-H(70B)	109.5
H(70A)-C(70)-H(70B)	109.5
C(69)-C(70)-H(70C)	109.5
H(70A)-C(70)-H(70C)	109.5
H(70B)-C(70)-H(70C)	109.5
C(69)-C(71)-H(71A)	109.5
C(69)-C(71)-H(71B)	109.5
H(71A)-C(71)-H(71B)	109.5
C(69)-C(71)-H(71C)	109.5
H(71A)-C(71)-H(71C)	109.5
H(71B)-C(71)-H(71C)	109.5
C(69)-C(72)-H(72A)	109.5
C(69)-C(72)-H(72B)	109.5
H(72A)-C(72)-H(72B)	109.5
C(69)-C(72)-H(72C)	109.5
H(72A)-C(72)-H(72C)	109.5
H(72B)-C(72)-H(72C)	109.5

Symmetry transformations used to generate equivalent atoms:

Table A-64. Anisotropic displacement parameters ($Å^2 x\ 10^3$) for **5-3**. The anisotropic displacement factor exponent takes the form: $-2\pi^2[\ h^2\ a^{*2}U^{11} + ... + 2\ h\ k\ a^*\ b^*\ U^{12}\ ]$

	U^{11}	U^{22}	U^{33}	U^{23}	U^{13}	U^{12}
Mn(1)	10(1)	16(1)	10(1)	-1(1)	5(1)	-2(1)
Mn(2)	10(1)	17(1)	13(1)	1(1)	5(1)	1(1)
O(1)	13(1)	28(2)	11(1)	-5(1)	5(1)	-3(1)
O(2)	12(1)	21(1)	12(1)	-1(1)	6(1)	-3(1)
O(3)	14(1)	22(2)	9(1)	0(1)	3(1)	2(1)
O(4)	13(1)	25(2)	18(1)	3(1)	8(1)	-2(1)
N(1)	10(1)	22(2)	12(1)	0(1)	5(1)	-2(1)
N(2)	12(1)	13(2)	11(1)	-2(1)	3(1)	0(1)
N(3)	18(2)	20(2)	28(2)	6(1)	3(1)	1(1)
N(4)	22(2)	23(2)	19(2)	-4(2)	8(1)	-3(2)
N(5)	21(2)	35(2)	34(2)	-8(2)	0(2)	11(2)
N(6)	10(1)	18(2)	15(1)	-1(1)	3(1)	-1(1)
N(7)	10(1)	18(2)	20(2)	-1(1)	5(1)	-1(1)
N(8)	17(2)	22(2)	30(2)	-11(2)	3(1)	0(1)
N(9)	25(2)	16(2)	12(2)	5(1)	4(1)	6(2)
N(10)	22(2)	41(2)	28(2)	10(2)	1(2)	-6(2)
C(1)	11(2)	19(2)	11(2)	-1(1)	2(1)	-4(1)
C(2)	11(2)	14(2)	14(2)	4(2)	2(1)	1(1)
C(3)	15(2)	14(2)	12(2)	0(2)	6(1)	1(1)
C(4)	14(2)	17(2)	14(2)	1(2)	4(1)	-2(1)
C(5)	17(2)	22(2)	16(2)	2(2)	9(2)	3(2)
C(6)	19(2)	12(2)	18(2)	3(2)	7(2)	0(2)
C(7)	16(2)	15(2)	8(2)	-1(1)	3(1)	2(1)
C(8)	15(2)	15(2)	18(2)	5(2)	9(1)	2(1)
C(9)	12(2)	16(2)	17(2)	2(2)	4(1)	6(2)
C(10)	16(2)	12(2)	12(2)	-1(2)	6(2)	4(2)
C(11)	12(2)	10(2)	12(2)	-1(1)	3(1)	2(1)
C(12)	16(2)	17(2)	14(2)	-6(1)	5(1)	-2(1)
C(13)	18(2)	16(2)	14(2)	0(1)	8(1)	2(1)
C(14)	17(2)	14(2)	18(2)	0(2)	8(1)	-1(2)
C(15)	11(2)	26(2)	12(2)	1(1)	4(1)	-3(1)
C(16)	14(2)	13(2)	17(2)	0(1)	3(1)	-1(1)
C(17)	17(2)	33(3)	16(2)	0(2)	7(2)	-7(2)
C(18)	16(2)	33(2)	23(2)	1(2)	5(2)	-9(2)
C(19)	14(2)	28(2)	21(2)	-2(2)	4(2)	-5(2)
C(20)	16(2)	23(2)	17(2)	-7(2)	5(2)	-3(2)
C(21)	13(2)	40(3)	14(2)	-5(2)	7(1)	-2(2)
C(22)	32(2)	39(3)	17(2)	-5(2)	12(2)	-20(2)
C(23)	20(2)	100(4)	26(2)	-20(3)	11(2)	-19(3)
C(24)	26(2)	47(3)	16(2)	-4(2)	0(2)	12(2)
C(25)	21(2)	12(2)	19(2)	-5(2)	12(2)	-4(2)
C(26)	27(2)	26(2)	14(2)	-6(2)	8(2)	-4(2)
C(27)	22(2)	32(2)	24(2)	-7(2)	11(2)	-6(2)
C(28)	38(2)	30(2)	19(2)	-6(2)	17(2)	-10(2)
C(29)	14(2)	19(2)	14(2)	-2(2)	6(1)	-4(2)
C(30)	22(2)	18(2)	32(2)	6(2)	10(2)	-4(2)
C(31)	13(2)	29(2)	17(2)	-2(2)	7(2)	-3(2)
C(32)	24(2)	38(3)	17(2)	-11(2)	10(2)	-13(2)
C(33)	24(2)	21(2)	14(2)	0(2)	9(1)	-1(2)
C(34)	44(2)	26(2)	13(2)	-7(2)	13(2)	-2(2)
C(35)	45(3)	26(2)	10(2)	1(2)	6(2)	2(2)
C(36)	36(2)	55(3)	14(2)	1(2)	15(2)	-11(2)
C(37)	13(2)	16(2)	22(2)	-2(2)	10(1)	2(2)
C(38)	19(2)	10(2)	11(2)	1(2)	7(1)	-1(2)
C(39)	14(2)	12(2)	13(2)	-3(2)	4(2)	-7(2)
C(40)	18(2)	16(2)	21(2)	1(2)	9(2)	-5(2)

C(41)	23(2)	17(2)	15(2)	0(2)	5(2)	-4(2)
C(42)	23(2)	13(2)	19(2)	-3(2)	10(2)	-5(2)
C(43)	21(2)	16(2)	18(2)	-4(2)	12(2)	1(2)
C(44)	20(2)	18(2)	17(2)	0(2)	3(2)	-4(2)
C(45)	12(2)	17(2)	16(2)	1(2)	7(1)	-1(2)
C(46)	15(2)	14(2)	13(2)	-2(2)	6(1)	-3(1)
C(47)	13(2)	16(2)	16(2)	-1(2)	4(1)	-1(1)
C(48)	13(2)	20(2)	21(2)	-3(2)	9(2)	-3(2)
C(49)	20(2)	17(2)	10(2)	2(2)	9(1)	-2(2)
C(50)	14(2)	14(2)	17(2)	3(2)	2(1)	2(2)
C(51)	9(2)	21(2)	16(2)	-3(1)	3(1)	1(1)
C(52)	15(2)	19(2)	16(2)	-2(1)	5(1)	5(1)
C(53)	14(2)	35(3)	24(2)	4(2)	7(2)	6(2)
C(54)	19(2)	34(2)	37(2)	8(2)	9(2)	10(2)
C(55)	16(2)	31(2)	27(2)	-5(2)	8(2)	10(2)
C(56)	15(2)	23(2)	28(2)	-5(2)	9(2)	0(2)
C(57)	14(2)	16(2)	17(2)	2(2)	1(2)	-1(2)
C(58)	15(2)	20(2)	40(2)	-1(2)	12(2)	3(2)
C(59)	19(2)	36(2)	25(2)	14(2)	8(2)	10(2)
C(60)	16(2)	26(2)	20(2)	3(2)	7(2)	-2(2)
C(61)	34(2)	28(2)	13(2)	0(2)	11(2)	-2(2)
C(62)	45(2)	33(2)	17(2)	-1(2)	16(2)	-4(2)
C(63)	47(3)	55(3)	22(2)	-6(2)	20(2)	7(2)
C(64)	50(3)	25(2)	22(2)	-1(2)	12(2)	-3(2)
C(65)	12(2)	31(2)	16(2)	2(2)	7(1)	2(2)
C(66)	25(2)	23(2)	20(2)	1(2)	7(2)	8(2)
C(67)	17(2)	24(2)	21(2)	0(2)	6(2)	-7(2)
C(68)	14(2)	55(3)	21(2)	9(2)	7(2)	3(2)
C(69)	20(2)	17(2)	16(2)	-1(2)	7(2)	0(2)
C(70)	47(2)	23(2)	24(2)	2(2)	24(2)	7(2)
C(71)	32(2)	15(2)	23(2)	1(2)	16(2)	-4(2)
C(72)	30(2)	34(2)	15(2)	4(2)	10(2)	-4(2)

Table A-65. Hydrogen coordinates (x 10^4) and isotropic displacement parameters ($Å^2$x 10^3) for **5-3**.

	x	y	z	U(eq)
H(1)	9288	7786	2236	17
H(5)	6124	7247	2114	21
H(7)	8500	8021	2985	16
H(8)	9420	7096	-992	18
H(12)	6626	5140	-3176	19
H(14)	8781	6749	-2297	19
H(15)	10145	6343	1351	20
H(16)	9599	8312	356	19
H(17A)	10517	7644	-212	26
H(17B)	10808	6625	424	26
H(18A)	11723	8209	862	30
H(18B)	10987	9069	779	30
H(19A)	11638	8592	2095	26
H(19B)	11560	7236	1897	26
H(20A)	10238	8748	1783	23
H(20B)	10564	7695	2386	23
H(22A)	6054	4725	875	43
H(22B)	6384	5202	239	43
H(22C)	5430	5018	13	43
H(23A)	4638	6294	470	72
H(23B)	5041	7366	1033	72
H(23C)	5206	6069	1363	72
H(24A)	6173	7289	-184	48
H(24B)	5657	8118	148	48
H(24C)	5214	7099	-446	48

H(26A)	8298	9025	3888	34
H(26B)	8344	7736	4221	34
H(26C)	7911	8740	4520	34
H(27A)	6971	9831	3004	38
H(27B)	6609	9551	3655	38
H(27C)	6160	9075	2786	38
H(28A)	6661	7563	4168	40
H(28B)	7087	6542	3875	40
H(28C)	6230	7050	3306	40
H(30A)	6149	3234	-1255	36
H(30B)	6993	3894	-826	36
H(30C)	6892	3019	-1527	36
H(31A)	5371	5072	-1566	29
H(31B)	5625	6093	-2015	29
H(31C)	6182	5802	-1129	29
H(32A)	6041	3561	-2900	38
H(32B)	5490	4704	-3059	38
H(32C)	5309	3635	-2598	38
H(34A)	6703	5128	-4302	41
H(34B)	7603	4633	-4085	41
H(34C)	7229	5521	-4795	41
H(35A)	7229	8015	-3608	42
H(35B)	6479	7141	-3964	42
H(35C)	6945	7604	-4497	42
H(36A)	8337	6861	-4291	50
H(36B)	8799	6043	-3559	50
H(36C)	8622	7371	-3425	50
H(37)	9530	835	4090	19
H(41)	6651	2293	1754	23
H(43)	8853	829	2750	20
H(44)	9138	-230	7132	24
H(48)	6003	513	7016	21
H(50)	8365	-311	7888	19
H(51)	10145	1584	5892	19
H(52)	9532	-725	5759	20
H(53A)	10230	-814	7128	29
H(53B)	10567	477	7128	29
H(54A)	11574	-857	7108	36
H(54B)	10936	-1486	6355	36
H(55A)	11767	-286	5954	30
H(55B)	11564	809	6381	30
H(56A)	10765	945	5032	26
H(56B)	10410	-335	5031	26
H(58A)	6060	4432	3475	37
H(58B)	6775	4590	3157	37
H(58C)	6940	3896	3950	37
H(59A)	5199	3635	2208	40
H(59B)	5483	2529	1854	40
H(59C)	5920	3755	1894	40
H(60A)	6234	2003	3902	31
H(60B)	5726	1412	3080	31
H(60C)	5370	2524	3360	31
H(62A)	6900	2482	711	46
H(62B)	7425	2011	235	46
H(62C)	7831	2859	963	46
H(63A)	8943	1313	1549	59
H(63B)	8480	571	778	59
H(63C)	8668	10	1618	59
H(64A)	7227	-466	1336	49
H(64B)	7026	-23	464	49
H(64C)	6536	489	961	49
H(66A)	6344	2617	5209	35
H(66B)	5955	3078	5806	35
H(66C)	5383	2809	4921	35
H(67A)	5537	-308	5059	31
H(67B)	6069	497	4731	31

H(67C)	5114	720	4464	31
H(68A)	4554	1608	5388	46
H(68B)	5137	1765	6284	46
H(68C)	4913	492	5921	46
H(70A)	6409	-92	8997	43
H(70B)	5978	403	8131	43
H(70C)	6760	1043	8738	43
H(71A)	7002	-2153	7880	33
H(71B)	6125	-1560	7613	33
H(71C)	6563	-2022	8487	33
H(72A)	8122	121	9135	38
H(72B)	8200	-1163	8844	38
H(72C)	7742	-953	9428	38

Table A-66. Torsion angles [°] for **5-3**.

O(2)-Mn(1)-O(1)-C(3)	179.5(3)
N(1)-Mn(1)-O(1)-C(3)	-12.1(3)
N(2)-Mn(1)-O(1)-C(3)	-87.0(4)
N(3)-Mn(1)-O(1)-C(3)	80.3(3)
O(1)-Mn(1)-O(2)-C(10)	148.7(3)
N(1)-Mn(1)-O(2)-C(10)	52.7(7)
N(2)-Mn(1)-O(2)-C(10)	0.0(3)
N(3)-Mn(1)-O(2)-C(10)	-104.8(3)
O(4)-Mn(2)-O(3)-C(39)	-136.1(3)
N(7)-Mn(2)-O(3)-C(39)	-38.1(6)
N(6)-Mn(2)-O(3)-C(39)	21.4(3)
N(8)-Mn(2)-O(3)-C(39)	121.1(3)
O(3)-Mn(2)-O(4)-C(46)	-174.0(3)
N(7)-Mn(2)-O(4)-C(46)	23.7(3)
N(6)-Mn(2)-O(4)-C(46)	90.7(4)
N(8)-Mn(2)-O(4)-C(46)	-72.2(3)
O(2)-Mn(1)-N(1)-C(1)	104.1(6)
O(1)-Mn(1)-N(1)-C(1)	8.1(3)
N(2)-Mn(1)-N(1)-C(1)	157.6(3)
N(3)-Mn(1)-N(1)-C(1)	-98.1(3)
O(2)-Mn(1)-N(1)-C(15)	-79.0(6)
O(1)-Mn(1)-N(1)-C(15)	-174.9(2)
N(2)-Mn(1)-N(1)-C(15)	-25.5(2)
N(3)-Mn(1)-N(1)-C(15)	78.8(2)
O(2)-Mn(1)-N(2)-C(8)	2.4(3)
O(1)-Mn(1)-N(2)-C(8)	-91.0(4)
N(1)-Mn(1)-N(2)-C(8)	-168.2(3)
N(3)-Mn(1)-N(2)-C(8)	101.5(3)
O(2)-Mn(1)-N(2)-C(16)	170.5(2)
O(1)-Mn(1)-N(2)-C(16)	77.1(3)
N(1)-Mn(1)-N(2)-C(16)	-0.1(2)
N(3)-Mn(1)-N(2)-C(16)	-90.4(2)
O(2)-Mn(1)-N(3)-N(4)	137.6(4)
O(1)-Mn(1)-N(3)-N(4)	-129.0(4)
N(1)-Mn(1)-N(3)-N(4)	-38.0(4)
N(2)-Mn(1)-N(3)-N(4)	44.3(4)
Mn(1)-N(3)-N(4)-N(5)	-159(14)
O(3)-Mn(2)-N(6)-C(37)	-19.0(3)
O(4)-Mn(2)-N(6)-C(37)	77.0(4)
N(7)-Mn(2)-N(6)-C(37)	145.5(3)
N(8)-Mn(2)-N(6)-C(37)	-120.1(3)
O(3)-Mn(2)-N(6)-C(51)	169.6(2)
O(4)-Mn(2)-N(6)-C(51)	-94.4(3)
N(7)-Mn(2)-N(6)-C(51)	-25.9(2)
N(8)-Mn(2)-N(6)-C(51)	68.5(2)
O(3)-Mn(2)-N(7)-C(44)	-119.3(4)
O(4)-Mn(2)-N(7)-C(44)	-20.8(3)
N(6)-Mn(2)-N(7)-C(44)	-179.9(3)
N(8)-Mn(2)-N(7)-C(44)	81.3(3)

O(3)-Mn(2)-N(7)-C(52)	60.8(5)
O(4)-Mn(2)-N(7)-C(52)	159.2(2)
N(6)-Mn(2)-N(7)-C(52)	0.1(2)
N(8)-Mn(2)-N(7)-C(52)	-98.7(2)
O(3)-Mn(2)-N(8)-N(9)	-113.2(4)
O(4)-Mn(2)-N(8)-N(9)	151.6(4)
N(7)-Mn(2)-N(8)-N(9)	60.5(4)
N(6)-Mn(2)-N(8)-N(9)	-21.8(4)
Mn(2)-N(8)-N(9)-N(10)	-165(11)
C(15)-N(1)-C(1)-C(2)	-177.3(3)
Mn(1)-N(1)-C(1)-C(2)	-0.7(5)
N(1)-C(1)-C(2)-C(3)	-7.6(6)
N(1)-C(1)-C(2)-C(7)	176.9(3)
Mn(1)-O(1)-C(3)-C(2)	8.0(5)
Mn(1)-O(1)-C(3)-C(4)	-173.6(3)
C(7)-C(2)-C(3)-O(1)	179.5(3)
C(1)-C(2)-C(3)-O(1)	4.1(6)
C(7)-C(2)-C(3)-C(4)	1.1(5)
C(1)-C(2)-C(3)-C(4)	-174.3(4)
O(1)-C(3)-C(4)-C(5)	178.7(3)
C(2)-C(3)-C(4)-C(5)	-2.8(5)
O(1)-C(3)-C(4)-C(21)	-2.8(5)
C(2)-C(3)-C(4)-C(21)	175.7(4)
C(3)-C(4)-C(5)-C(6)	2.4(6)
C(21)-C(4)-C(5)-C(6)	-176.1(4)
C(4)-C(5)-C(6)-C(7)	0.0(6)
C(4)-C(5)-C(6)-C(25)	177.7(4)
C(5)-C(6)-C(7)-C(2)	-1.9(5)
C(25)-C(6)-C(7)-C(2)	-179.5(3)
C(3)-C(2)-C(7)-C(6)	1.4(6)
C(1)-C(2)-C(7)-C(6)	177.0(3)
C(16)-N(2)-C(8)-C(9)	-170.6(3)
Mn(1)-N(2)-C(8)-C(9)	-3.0(5)
N(2)-C(8)-C(9)-C(10)	0.5(6)
N(2)-C(8)-C(9)-C(14)	176.1(4)
Mn(1)-O(2)-C(10)-C(9)	-2.1(5)
Mn(1)-O(2)-C(10)-C(11)	-179.2(2)
C(14)-C(9)-C(10)-O(2)	-173.3(3)
C(8)-C(9)-C(10)-O(2)	2.2(6)
C(14)-C(9)-C(10)-C(11)	3.9(5)
C(8)-C(9)-C(10)-C(11)	179.3(3)
O(2)-C(10)-C(11)-C(12)	172.4(3)
C(9)-C(10)-C(11)-C(12)	-4.8(5)
O(2)-C(10)-C(11)-C(29)	-5.3(5)
C(9)-C(10)-C(11)-C(29)	177.5(3)
C(10)-C(11)-C(12)-C(13)	1.5(6)
C(29)-C(11)-C(12)-C(13)	179.2(3)
C(11)-C(12)-C(13)-C(14)	2.8(6)
C(11)-C(12)-C(13)-C(33)	-171.1(4)
C(12)-C(13)-C(14)-C(9)	-3.8(6)
C(33)-C(13)-C(14)-C(9)	169.9(4)
C(10)-C(9)-C(14)-C(13)	0.6(6)
C(8)-C(9)-C(14)-C(13)	-175.2(4)
C(1)-N(1)-C(15)-C(16)	-138.3(3)
Mn(1)-N(1)-C(15)-C(16)	44.6(3)
C(1)-N(1)-C(15)-C(20)	-14.2(5)
Mn(1)-N(1)-C(15)-C(20)	168.7(2)
C(8)-N(2)-C(16)-C(17)	-42.8(4)
Mn(1)-N(2)-C(16)-C(17)	148.3(3)
C(8)-N(2)-C(16)-C(15)	-166.7(3)
Mn(1)-N(2)-C(16)-C(15)	24.4(3)
N(1)-C(15)-C(16)-N(2)	-42.9(3)
C(20)-C(15)-C(16)-N(2)	-170.9(3)
N(1)-C(15)-C(16)-C(17)	-170.5(3)
C(20)-C(15)-C(16)-C(17)	61.5(4)
N(2)-C(16)-C(17)-C(18)	177.0(3)

C(15)-C(16)-C(17)-C(18)	-60.5(4)
C(16)-C(17)-C(18)-C(19)	56.7(4)
C(17)-C(18)-C(19)-C(20)	-54.1(4)
C(18)-C(19)-C(20)-C(15)	52.9(4)
N(1)-C(15)-C(20)-C(19)	-177.8(3)
C(16)-C(15)-C(20)-C(19)	-56.3(4)
C(5)-C(4)-C(21)-C(22)	-123.6(4)
C(3)-C(4)-C(21)-C(22)	58.0(5)
C(5)-C(4)-C(21)-C(23)	-2.3(6)
C(3)-C(4)-C(21)-C(23)	179.3(4)
C(5)-C(4)-C(21)-C(24)	115.2(4)
C(3)-C(4)-C(21)-C(24)	-63.2(5)
C(7)-C(6)-C(25)-C(27)	110.0(4)
C(5)-C(6)-C(25)-C(27)	-67.5(4)
C(7)-C(6)-C(25)-C(26)	-9.6(5)
C(5)-C(6)-C(25)-C(26)	172.9(3)
C(7)-C(6)-C(25)-C(28)	-130.4(4)
C(5)-C(6)-C(25)-C(28)	52.0(5)
C(12)-C(11)-C(29)-C(30)	127.5(4)
C(10)-C(11)-C(29)-C(30)	-54.9(5)
C(12)-C(11)-C(29)-C(31)	-110.9(4)
C(10)-C(11)-C(29)-C(31)	66.7(4)
C(12)-C(11)-C(29)-C(32)	7.7(5)
C(10)-C(11)-C(29)-C(32)	-174.7(3)
C(14)-C(13)-C(33)-C(35)	-98.0(4)
C(12)-C(13)-C(33)-C(35)	75.5(4)
C(14)-C(13)-C(33)-C(36)	21.0(5)
C(12)-C(13)-C(33)-C(36)	-165.5(4)
C(14)-C(13)-C(33)-C(34)	141.8(4)
C(12)-C(13)-C(33)-C(34)	-44.7(5)
C(51)-N(6)-C(37)-C(38)	-179.4(4)
Mn(2)-N(6)-C(37)-C(38)	10.2(6)
N(6)-C(37)-C(38)-C(43)	-175.7(4)
N(6)-C(37)-C(38)-C(39)	5.5(6)
Mn(2)-O(3)-C(39)-C(38)	-13.3(5)
Mn(2)-O(3)-C(39)-C(40)	166.2(3)
C(43)-C(38)-C(39)-O(3)	176.5(3)
C(37)-C(38)-C(39)-O(3)	-4.7(6)
C(43)-C(38)-C(39)-C(40)	-3.1(5)
C(37)-C(38)-C(39)-C(40)	175.7(4)
O(3)-C(39)-C(40)-C(41)	-176.6(3)
C(38)-C(39)-C(40)-C(41)	3.0(5)
O(3)-C(39)-C(40)-C(57)	1.9(5)
C(38)-C(39)-C(40)-C(57)	-178.5(3)
C(39)-C(40)-C(41)-C(42)	-0.9(6)
C(57)-C(40)-C(41)-C(42)	-179.3(4)
C(40)-C(41)-C(42)-C(43)	-1.3(6)
C(40)-C(41)-C(42)-C(61)	174.6(4)
C(41)-C(42)-C(43)-C(38)	1.2(6)
C(61)-C(42)-C(43)-C(38)	-174.5(4)
C(39)-C(38)-C(43)-C(42)	1.0(6)
C(37)-C(38)-C(43)-C(42)	-177.9(4)
C(52)-N(7)-C(44)-C(45)	-169.6(3)
Mn(2)-N(7)-C(44)-C(45)	10.4(5)
N(7)-C(44)-C(45)-C(50)	-179.8(4)
N(7)-C(44)-C(45)-C(46)	7.3(6)
Mn(2)-O(4)-C(46)-C(45)	-14.3(5)
Mn(2)-O(4)-C(46)-C(47)	169.4(3)
C(50)-C(45)-C(46)-O(4)	-178.9(3)
C(44)-C(45)-C(46)-O(4)	-6.2(6)
C(50)-C(45)-C(46)-C(47)	-2.6(5)
C(44)-C(45)-C(46)-C(47)	170.2(3)
O(4)-C(46)-C(47)-C(48)	178.7(3)
C(45)-C(46)-C(47)-C(48)	2.3(5)
O(4)-C(46)-C(47)-C(65)	2.6(5)
C(45)-C(46)-C(47)-C(65)	-173.8(3)

C(46)-C(47)-C(48)-C(49)	0.2(6)
C(65)-C(47)-C(48)-C(49)	176.2(4)
C(47)-C(48)-C(49)-C(50)	-2.5(6)
C(47)-C(48)-C(49)-C(69)	-174.6(4)
C(48)-C(49)-C(50)-C(45)	2.2(6)
C(69)-C(49)-C(50)-C(45)	174.0(4)
C(46)-C(45)-C(50)-C(49)	0.2(6)
C(44)-C(45)-C(50)-C(49)	-172.8(4)
C(37)-N(6)-C(51)-C(52)	-126.2(4)
Mn(2)-N(6)-C(51)-C(52)	45.4(3)
C(37)-N(6)-C(51)-C(56)	-2.8(5)
Mn(2)-N(6)-C(51)-C(56)	168.7(3)
C(44)-N(7)-C(52)-C(51)	-155.6(3)
Mn(2)-N(7)-C(52)-C(51)	24.4(3)
C(44)-N(7)-C(52)-C(53)	-31.3(5)
Mn(2)-N(7)-C(52)-C(53)	148.7(3)
N(6)-C(51)-C(52)-N(7)	-43.4(3)
C(56)-C(51)-C(52)-N(7)	-170.3(3)
N(6)-C(51)-C(52)-C(53)	-171.5(3)
C(56)-C(51)-C(52)-C(53)	61.6(4)
N(7)-C(52)-C(53)-C(54)	178.9(3)
C(51)-C(52)-C(53)-C(54)	-58.4(4)
C(52)-C(53)-C(54)-C(55)	55.8(4)
C(53)-C(54)-C(55)-C(56)	-55.2(4)
N(6)-C(51)-C(56)-C(55)	-179.9(3)
C(52)-C(51)-C(56)-C(55)	-58.9(4)
C(54)-C(55)-C(56)-C(51)	55.6(4)
C(41)-C(40)-C(57)-C(60)	117.5(4)
C(39)-C(40)-C(57)-C(60)	-60.9(4)
C(41)-C(40)-C(57)-C(58)	-121.6(4)
C(39)-C(40)-C(57)-C(58)	60.0(5)
C(41)-C(40)-C(57)-C(59)	-2.1(5)
C(39)-C(40)-C(57)-C(59)	179.5(3)
C(43)-C(42)-C(61)-C(62)	-134.1(4)
C(41)-C(42)-C(61)-C(62)	50.4(5)
C(43)-C(42)-C(61)-C(63)	-12.7(6)
C(41)-C(42)-C(61)-C(63)	171.8(4)
C(43)-C(42)-C(61)-C(64)	106.8(4)
C(41)-C(42)-C(61)-C(64)	-68.7(5)
C(48)-C(47)-C(65)-C(67)	-113.7(4)
C(46)-C(47)-C(65)-C(67)	62.2(4)
C(48)-C(47)-C(65)-C(68)	5.3(5)
C(46)-C(47)-C(65)-C(68)	-178.7(4)
C(48)-C(47)-C(65)-C(66)	123.7(4)
C(46)-C(47)-C(65)-C(66)	-60.4(4)
C(50)-C(49)-C(69)-C(72)	22.1(5)
C(48)-C(49)-C(69)-C(72)	-166.4(4)
C(50)-C(49)-C(69)-C(70)	142.8(4)
C(48)-C(49)-C(69)-C(70)	-45.7(5)
C(50)-C(49)-C(69)-C(71)	-97.6(4)
C(48)-C(49)-C(69)-C(71)	73.9(4)

Symmetry transformations used to generate equivalent atoms

APPENDIX B

DATA PERTAINING TO THE PRODUCTION OF PCHC *VIA* AN *IN SITU* CHROMIUM(III) ACACEN CATALYST

Table B-1. Summary of Catalytic Activity of a Chromium(III) Acacen Catalyst Formed *in situ.*

entry[a]	equiv (^{n}Bu)$_4$NN$_3$	rxn time (h)	Yield (%)[g]	TON[e]	TOF (h^{-1})[e]
1[b,f]	0.50	1.17	36.9	452.0	387.0
2[c,f]	1.00	0.83	46.9	575.0	690.0
3	1.00	2.50	38.9	477.0	191.0
4[d]	2.00	3.80	57.4	705.0	186.0

[a] Conditions: 20 mL CHO *in situ* cat. solution, 80 ºC, 34 bar CO_2

[b] M_n = 8,188, PDI = 1.097. c M_n = 7,592, PDI = 1.105. d M_n = 7,957, PDI = 1.085.

[e] TOF = TON/h. TON = (moles epoxide consumed/moles cat).

[f] Reactions terminated at maxium rate [g] Estimated from polymer yield

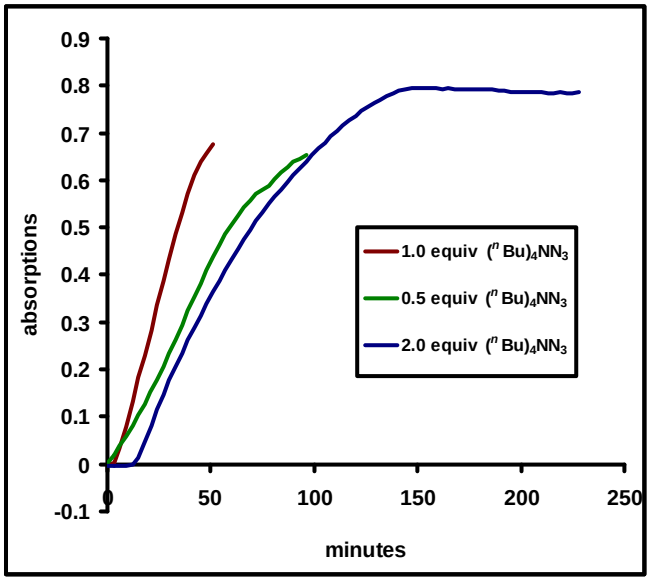

Figure B-1. Three *in situ* IR FTIR spectra profiling the formation of PCHC by tracking the asymmetric carbonyl stretch at 1750 cm^{-1}. The three spectra correspond to entries 1, 2, and 4 of Table B-1.

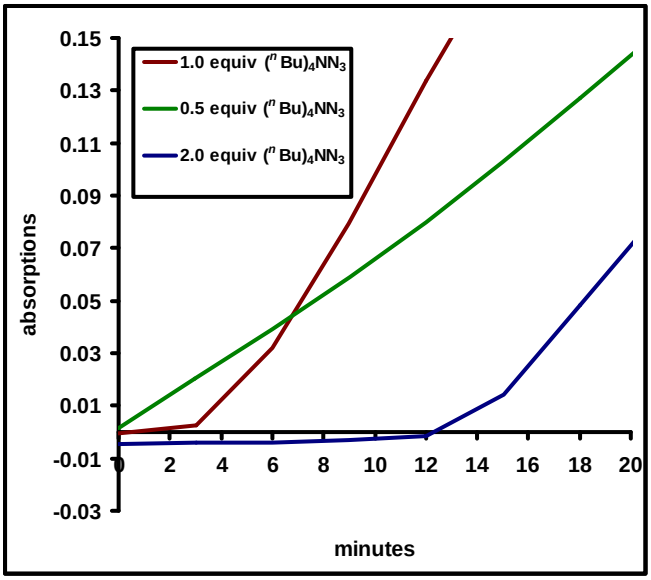

Figure B-2. Profile of the induction periods observed for entries 1, 2 and 4 of Table B-1.

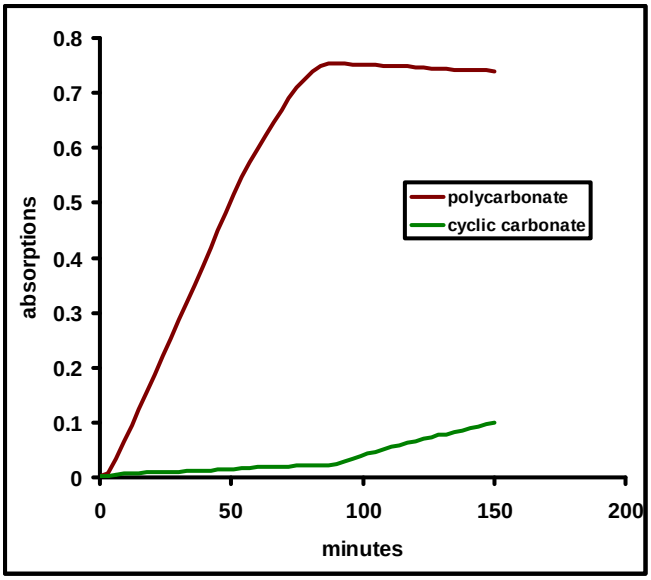

Figure B-3. Profile of polycarbonate and cyclic carbonate formation during a reaction of the *in situ* chromium(III) acacen catalyst with 1 equiv (^{n}Bu)$_4$NN$_3$ (Entry 3 of Table B-1).

VITA

Eric Benjamin Frantz was born in Pasadena, TX. He grew up living on the grounds of the San Jacinto Battleground State Park where his father was chief superintendent. After graduating from Deer Park High School he attended San Jacinto Junior College until transferring to and graduating from the University of Houston with a Bachelor of Science in chemistry in 1999. That same year he went to work as a chemist for Schlumberger Oilfield Services in Houston and later Rock Springs, WY. From 2002 to 2003, he worked for Benchmark Research and Technology in both Manvel and Midland, TX. In the fall of 2003 he returned to school at Texas A&M University, College Station and joined the research group of Professor Donald J. Darensbourg. Further questions and comments may be directed to Texas A&M University, Department of Chemistry, MS 3255, College Station, TX 77842-3012.